

THESIS ON CIVIL ENGINEERING F49

# **Quantification of Spontaneous Current-Induced Patch Formation in the Marine Surface Layer**

ANDREA GIUDICI

**TUT**  
**PRESS**

TALLINN UNIVERSITY OF TECHNOLOGY  
Institute of Cybernetics  
Laboratory of Wave Engineering

**The thesis was accepted for the defence of the degree of Doctor of Philosophy  
in Engineering on 17 December 2014**

**Supervisor:** Prof. Tarmo Soomere  
Institute of Cybernetics, Tallinn University of Technology, Estonia

**Opponents:** Prof. Steven Bishop  
Faculty of Mathematics and Physical Sciences  
University College London, UK

Prof. Kristofer Döös  
Department of Meteorology, Stockholm University, Sweden

**Defence of the thesis:** 27 January 2015

Declaration:

*Hereby I declare that this doctoral thesis, my original investigation and achievement, submitted for the doctoral degree at Tallinn University of Technology, has not been submitted for a doctoral or an equivalent academic degree.*



/Andrea Giudici/

Copyright: Andrea Giudici, 2015  
ISSN 1406-4766  
ISBN 978-9949-23-726-5 (publication)  
ISBN 978-9949-23-727-2 (PDF)

EHITUS F49

**Spontaanne laikude formeerumine  
mere pinnahoovuste mõjul**

ANDREA GIUDICI



## Contents

<b>List of publications constituting the thesis .....</b>	<b>6</b>
<b>List of figures .....</b>	<b>6</b>
<b>Introduction .....</b>	<b>9</b>
Surface transport in the ocean: a global problem with local implications .....	9
Heterogeneity and patchiness of water masses .....	11
Velocity fields naturally generate patches at the sea surface .....	13
The objectives and outline of the thesis .....	16
Approbation of the results .....	17
<b>1. Flow compressibility of surface currents .....</b>	<b>19</b>
1.1. Divergence of velocity and flow compressibility .....	19
1.2. Compressibility of velocity fields in the ocean .....	23
1.3. Finite-time compressibility .....	25
1.4. Classical flow compressibility and finite-time compressibility .....	27
<b>2. Simulation of the dynamics of the Gulf of Finland .....</b>	<b>31</b>
2.1. Surface dynamics in the Baltic Sea and the Gulf of Finland .....	31
2.2. The Rossby Centre Ocean model .....	34
2.3. The OAAS circulation model .....	36
2.4. Statistics of Lagrangian motions of selected water parcels .....	38
<b>3. Calculations of compressibility .....</b>	<b>43</b>
3.1. The QTRAC Simulation Suite .....	43
3.2. Flow compressibility, divergence and concentration field .....	47
3.3. Calculation of finite-time compressibility .....	49
3.4. Spatial distribution of finite-time compressibility .....	52
<b>4. Quantification of spontaneous patch generation .....</b>	<b>55</b>
4.1. Temporal course of high finite-time compressibility .....	55
4.2. Persistency of high values of finite-time compressibility .....	57
4.3. Potential regions of spontaneous patch formation .....	59
4.4. Seasonality of areas hosting high finite-time compressibility .....	61
<b>Conclusions .....</b>	<b>65</b>
Summary of the results .....	65
Main conclusions proposed to defend .....	67
Recommendations for further work .....	68
<b>Bibliography .....</b>	<b>69</b>
Acknowledgements .....	80
<b>Abstract .....</b>	<b>81</b>
<b>Resümee .....</b>	<b>82</b>
<b>Appendix A: Curriculum Vitae .....</b>	<b>83</b>
<b>Appendix B: Elulookirjeldus .....</b>	<b>86</b>

## List of publications constituting the thesis

The thesis is based on five academic publications which are referred to in the text as Paper I, Paper II, Paper III, Paper IV and Paper V.

- Paper I     **Giudici A.**, Kalda J., Soomere T. 2012. On the compressibility of surface currents in the Gulf of Finland, the Baltic Sea. In: *IEEE/OES Baltic 2012 International Symposium, 8–11 May 2012, Klaipėda, Lithuania*. Proceedings. IEEE, 8 pp.
- Paper II     **Giudici A.**, Soomere T. 2013. Identification of areas of frequent patch formation from velocity fields. *Journal of Coastal Research*, Special Issue 65, vol. 1, 231–236.
- Paper III    Kalda J., Soomere T., **Giudici A.** 2014. On the finite-time compressibility of surface currents in the Gulf of Finland, the Baltic Sea. *Journal of Marine Systems*, 129, 56–65.
- Paper IV     **Giudici A.**, Soomere T. 2014. Finite-time compressibility as an agent of frequent spontaneous patch formation in the surface layer: a case study for the Gulf of Finland, the Baltic Sea. *Marine Pollution Bulletin*, 89(1–2), 239–249.
- Paper V     **Giudici A.**, Soomere T. 2014. On the possibility of spontaneous patch formation in the Gulf of Finland. In: *IEEE/OES Symposium “Measuring and Modeling of Multi-scale Interactions in the Marine Environment,” 26–29 May 2014 Tallinn, Estonia*. Proceedings. IEEE, 6 pp., accepted.

## List of figures

<b>Figure 1.</b> Bathymetry and geometry of the Baltic Sea and the Gulf of Finland (Paper IV). .....	14
<b>Figure 2.</b> Divergence of the 2D flow on the sea surface, integrated over the entire Gulf of Finland in 1991 (Paper III). The underlying simulations have been performed using the Rossby Centre Ocean model with a resolution of 2 nautical miles (Section 2.2). .....	20
<b>Figure 3.</b> Scheme of the selection stencil of a triangular surface element and its evolution through time. ....	25
<b>Figure 4.</b> The distortion of a surface element by the velocity field at two infinitely close time intervals. The translation of the element is ignored (Paper I). .....	27
<b>Figure 5.</b> Finite-time compressibility $C_{ftc}$ as a function of classical flow compressibility (Paper I). .....	29

<b>Figure 6.</b> Definition sketch of splitting the simulation period into time windows in Papers I and III. ....	39
<b>Figure 7.</b> A sketch of the QTRAC calculation pipeline.....	40
<b>Figure 8.</b> An instantaneous $C_{ftc}$ map calculated for 01 March 1987 with $SIM_{Length} = 24$ h based on the OAAS model data.....	41
<b>Figure 9.</b> The QTRAC suite, running in the GUI mode. ....	44
<b>Figure 10.</b> Special cases requiring attention. (A) vertices of a triangular element tend to align, yielding a null area; (B) one of the vertices hits the coast (Paper II). ....	46
<b>Figure 11.</b> Dependence of $C_{ftc}$ values initially $>1$ on the number of time steps in a calculation that started on 01 January 1987 (time step of 30 min) (Paper II). ....	47
<b>Figure 12.</b> Classical flow compressibility of the surface velocity field in the Gulf of Finland on 01 April 1991 based on velocity fields from the RCO model (Paper I).....	48
<b>Figure 13.</b> Average divergence (1/s; negative values indicate convergent flow) of the water surface (upper panel) and concentration of floats (per grid cell) in the Gulf of Finland for 01–07 April 1991 (lower panel) (Paper III). ....	49
<b>Figure 14.</b> Average finite-time compressibility of the water surface in the Gulf of Finland for one week (01–07 April 1991), calculated using the time window of 24 h (upper panel), 48 h (middle panel) and 72 h (lower panel) (Paper III). ....	51
<b>Figure 15.</b> Average finite-time compressibility of the water surface in the Gulf of Finland for one week in November 1991, calculated using the time window of 48 h (Paper I).....	53
<b>Figure 16.</b> Spatial distribution of finite-time compressibility (colour code) for the Gulf of Finland in December 1987 (upper panel) and February 1988 (lower panel) (Paper II).....	54
<b>Figure 17.</b> Temporal course of finite-time compressibility at six grid cells in the area of relatively high values of $C_{ftc}$ located outside the Neva Bight, for the first three months of the windy season (October 1987–March 1988, upper panel) and the calm season (April–September 1987, lower panel) (Paper II).....	56
<b>Figure 18.</b> Map of the count of days, during which single values of $C_{ftc}$ exceed the threshold of $\sqrt{1/2}$ within a batch of length $\delta_{FTC} = 30$ days. This map was calculated with $START_{TOT} = 01$ December 1987, $SIM_{STEP} = 3$ h (Paper IV). ....	57
<b>Figure 19.</b> Maps of the average count of the over-threshold FTC values for 180-day-long (upper panel) and 90-day-long (lower panel) batches calculated using the following parameters: $\delta_{SIM} = 24$ h, $SIM_{Length} = 12$ h, $SIM_{Step} = 1.5$ h. The colour coding shows how many times in total the values of $C_{ftc}$ exceed the clustering threshold 0.7 in total of 16 maps for 90-day-long batches or 8 similar maps for 180-day-long batches (Paper IV). ....	58

**Figure 20.** The set of persistent high- $C_{ftc}$  regions in the Gulf of Finland in 1987–1991 (Paper IV). .....60

**Figure 21.** Annual average of the maximum duration of consecutive events of  $C_{ftc}$  within single 30-day-long batches in locations of the highest counts of the over-threshold FTC values in areas 1–9 (Figure 20) in the Gulf of Finland in 1987–1991 (Paper IV). .....61

**Figure 22.** Maps of the average count of the over-threshold FTC values for season-long batches (Paper V). .....62

**Figure 23.** The presence of areas with frequent over-threshold values of FTC in different seasons in the Gulf of Finland for the time windows of 24 h and 48 h. (1) Data not available (Paper V). .....63

## Introduction

### Surface transport in the ocean: a global problem with local implications

The surface layer of the sea plays a core role in a number of oceanic and atmospheric processes. Water parcels, various substances and items located in this layer are often strongly impacted by various drivers and forces and may be carried by surface currents over great distances (Maximenko et al., 2012). In particular, items and substances that are lighter than sea water may stay in the surface layer for a long time and may be relocated, redistributed or mixed over the entire surface of the World Ocean (Maximenko et al., 2013). The processes in the surface layer thus serve as a connecting link between greatly different regions of the ocean (Simpson et al., 2014).

On 11 March 2011, an earthquake with a magnitude of 9.0 on the Richter scale took place off the coast of Sendai, Japan. The generated tsunami wave severely hit the northern coastline of Honshu Island (Mori et al., 2011). It caused widespread disaster on land and took the lives of more than 18 000 people (Yun and Hamada, 2014). When water was flowing back to the sea, it resulted in a large-scale discharge of debris into the ocean (Lebreton and Borrero, 2013). At the time of the event it was impossible to control or collect the flow of this debris and much of it probably is still at sea. Part of the debris may have been pushed back to the coast under the effect of winds, waves and currents. Some of it may have sunk to the bottom of the ocean. A large part of the debris, however, was transported towards the open ocean and may still be floating today. Some specific items crossed the entire Pacific and reached the coasts of the U.S.A. within a year (Wilson et al., 2012)

The processes of redistribution of mass, nutrients, heat or various items that have been released to the sea by natural processes have been an intrinsic element of the functioning of the entire Earth system for millions of years. Human activities have added new and important constituents to this system. Some of them are probably neutral for the environment but some may have massive adverse impact. One of the largest concerns is the potential release of oil products into the marine environment. In a different part of the world, in the Gulf of Finland in the Baltic Sea, Finnish authorities have been monitoring the quantity and properties of oil spills during the years. In 2012, 54 events of this type were recorded, 47 of which were observed in the Finnish sea area<sup>1</sup>, six in Estonian waters and one in Swedish waters. While the majority of these events were registered within coastal areas and inside ports, aerial surveillance planes detected several spills nearby the major shipping lanes. Although the magnitude and frequency of spills have been gradually reduced, partially thanks to active legislation intervention, the typical

---

<sup>1</sup> [http://www.syke.fi/en-US/SYKE\\_Info/Communications\\_material/Press\\_releases/Number\\_of\\_oil\\_spills\\_reduced\\_by\\_50\\_per\\_c%283374%29](http://www.syke.fi/en-US/SYKE_Info/Communications_material/Press_releases/Number_of_oil_spills_reduced_by_50_per_c%283374%29)

evolution and destiny of the resulting oil patches are still quite unclear (Soomere and Quak, 2007; Delpeche-Ellmann, 2014; Viikmäe, 2014). Another kind of a “ticking time bomb” is radioactive pollution that often has a tendency to stay in the uppermost layer of the sea (Periáñez, 2004). An increased knowledge on this topic is of great importance (Còzar et al., 2014).

These are just a few examples of the occurrences of floating matter being released at sea, which possibly endanger or deeply affect the marine ecosystem. In recent times the scientific community has paid increasing attention to the topic of floating debris. Studies have been focused on a number of different direct implications, such as the entanglement of marine mammals and other species (Laist, 1997; Erikson and Burton, 2003) or the ingestion of debris by birds and turtles (Bugoni and Krause, 2001; Cadee, 2002; Mallory, 2008). A closely related challenge is the quantification of the immediate threat to marine safety created by large dense patches of floating debris. Such patches of debris may also provide a shelter for different species. For example, species that are characteristic of the coastal waters of Japan may survive a trans-Pacific voyage towards the U.S. West Coast (Barnes et al., 2009).

A notable type of floating pollution is plastic litter in the oceans, which has been reported as early as in the 1970s (Carpenter et al., 1972; Carpenter and Smith, 1972; Colton and Knapp, 1974; Fowler, 1987; Coe and Rogers, 1996). Minuscule fragments of plastic debris are found in the oceans worldwide. The major carriers of their relocation are surface currents. It is well known that large quasi-stationary currents such as the Gulf Stream in the Atlantic or Kuroshio in the Pacific carry large water masses stemming from coastal areas across oceans to distances of many thousands of kilometres. The impact of ocean currents renders the problem of propagation and fate of debris and pollution to a fairly general and intrinsically global one. Various items and substances found in the surface layer are often carried to very remote locations also over such areas that do not host strong jet-like currents (Froyland et al., 2014). For example, debris originating from various parts of South America is often found on beaches of remote Pacific Islands (Richards, 2011). Extensive transport may also occur in sea areas such as the Gulf of Finland where surface currents are often interpreted as highly chaotic (Soomere et al., 2011; Delpeche-Ellmann, 2014). This importance of the related effects and the necessity to understand the associated mechanisms have been reflected, for example, by defining the topic of floating pollution as a high-priority research area in marine biology (Derraik, 2002; Page and McKenzie, 2004).

The described material suggests that the knowledge of fundamental features of debris and pollution behaviour, fate of various items and impacts of these on the marine environment is crucial for sustainable management of vulnerable sea areas. It plays a key role not only in terms of a better understanding of the environmental responses to pollutants but also for the development of efficient prevention measures. Despite the research efforts done so far, this knowledge is still generally sparse and many factors are yet to be taken into account (Andrady, 2011; Schilling and Zessner, 2011; Froyland et al., 2014).

## Heterogeneity and patchiness of water masses

One of the most important questions is how and where dangerous concentrations of various items or adverse impacts (e.g., harmful algal blooms, patches of microplastics, etc.), frequently observed in natural conditions in the surface layer, develop from seemingly favourable background conditions. The motion of different substances within the ocean water column is governed by the three-dimensional (3D) system of currents. Such motions generally result in the spreading of initially closely located particles (Richardson, 1926; Ollitrault et al., 2005). It is thus reasonable to assume that the concentration of different substances is the largest near their release locations and that remote areas are likely affected by much lower (and usually harmless) concentrations.

A fascinating ability of floating marine debris is that it may occasionally be collected into high concentration areas. The most well-known such area is located in the North Pacific Subtropical Convergence Zone and is sometimes referred to as the Great Pacific Ocean Garbage Patch (Pichel, 2007). Therefore, even remote offshore locations are not immune from the implications related to high concentrations of pollution or litter in the surface layer.

Similarly, the water masses in the World Ocean are often highly heterogeneous, whereas variations in their properties occur over a wide range of temporal and spatial scales. Several variations in different biogeochemical variables (such as salinity or temperature) are an intrinsic part of the functioning of the entire ocean, while variations in the availability of, e.g., nutrients, oxygen or optically active substances are decisive for the marine ecosystem.

This intrinsic feature of the ocean is discussed from the viewpoint of the thesis in Paper IV. A localized increase or decrease in the concentration of any of the listed items or substances from ambient levels is commonly referred to as a *patch* in the literature. The presence of patches is sometimes termed *patchiness* (Brentnall et al., 2003) or more frequently *patchiness* (e.g., Kononen et al., 1992; Levin, 1994; Grünbaum, 2012). This property is not just a feature of the marine environment (Kononen et al., 1992; Granskog et al., 2005). More importantly, it is also a principal driver of interactions between the physical variables and living organisms and in this way serves as a fundamental support of the marine ecosystem (Levin et al., 2001; Chelton et al., 2011; Gruber et al., 2011; Grünbaum, 2012).

The property of patchiness is not always positive for the marine life. Some of the variations in the properties of water masses support the life (e.g., by providing more oxygen or light), while others (such as pollution or marine litter) may lead to degradation of life in the sea. It is well known that patches of various substances (e.g., oil or chemical or radioactive pollution) may totally destroy the ecosystem (Kachel, 2008), while other (naturally generated) patches, such as those occurring during algal blooms, are highly inconvenient for the users of the sea and coasts.

A multitude of natural mechanisms may create patches of different magnitude and extension in the open ocean (Paper IV). The list of such mechanisms includes (but is not limited to) mesoscale eddies (Samuelson et al., 2012), upwelling and

downwelling phenomena, the internal dynamics of the ocean currents, the impact of surface and internal waves (Kahru, 1983; Lennert-Cody and Franks, 2002), or interplay between waves and currents (e.g., Powell and Okubo, 1994; Leichter et al., 2005; Vucelja et al., 2007). This pool of natural mechanisms and drivers also involves the situations when a horizontal density gradient is present (Burchard et al., 2008) and processes created within the classical estuarine circulation (Burchard et al., 2004). On smaller scales and mostly acting on the sea surface, Langmuir circulation often collects various items floating on the sea surface (called surface floats below) into long windrows (Alldredge et al., 2002; Dethleff et al., 2009; Thorpe, 2009; Akan et al., 2013).

The interaction of physical and chemical fields with biological activity may lead to other types of patch generation (Paper IV). For example, algal blooms are typical examples of “hot spots” of bioproduction (Strass, 1992; Calil and Richards, 2010). In some occasions the ocean environment functions as an excitable medium (Brentnall et al., 2003). In such environments the signal or wave (e.g., a forest fire in the mainland) may propagate through the medium only once, after which the environment cannot support the passing of a similar signal for some time.

The nearshore area is usually particularly rich in patches. Inhomogeneities of different magnitude and extension are often created as filaments of almost fresh water near river mouths, via differential heating by the Sun or resuspension of bottom sediments owing to wave impact (Abraham, 1998). In particular, filament generation in quasi-two-dimensional velocity fields (Held et al., 1995) naturally leads to an extremely complicated spatial structure of concentrations of various properties (Kalda, 2000). This process often causes local accumulation of particles that are locked in the surface layer and is frequently responsible for well-defined turbidity maxima.

In the recent past various human activities (e.g., dredging, dumping, land reclamation or aquafarming) have been responsible for an increasing number of patches with mostly negative impact on the ecosystem. Such patches are often generated on the sea surface or in the coastal areas through river discharge of nutrients and chemicals, or release of oil. Quite recently, patches of turbidity resulting from dredging (Erftemeijer and Robin Lewis, 2006), deep-water trawling (Martin et al., 2008) and mining (Jankowski et al., 1996) or deep-water oil discharges from pipelines (Burgherr, 2007) or platforms (Klemas, 2010; Liu et al., 2011) have become a part of the functioning of the ocean.

The focus in this thesis is on items and substances (such as the mentioned oil pollution or (micro)plastic debris (Cole et al., 2011)) that are locked at or near the sea surface. Their behaviour (as well as the behaviour of the entire surface layer) is additionally modified by the impact of wind and waves. The resulting relocation of items and substances mostly mimics the behaviour of the wind and wave patterns, which can be replicated (forecast or hindcast) with a reasonable accuracy (Arduin et al., 2009). Since spatial variations in the properties of these factors are often fairly limited, the induced transport in open sea areas normally does not cause substantial changes in the concentration of different substances in the surface layer.

Although surface wave fields usually do not lead to changes in concentrations in the surface layer, extreme events of edge waves (Averbukh et al., 2014) may affect surfactant films and substances (e.g., litter, biomass) which are either locked onto the surface or freely moving within the uppermost layer.

### **Velocity fields naturally generate patches at the sea surface**

An often overlooked driver of the patch formation is a system of 3D motions in the water column, underlying a two-dimensional (2D) field of substances which are concentrated in the surface layer or locked at the surface (Lee, 2010; Froyland et al., 2014). Such a layered structure in which the uppermost layer has limited interaction with the underlying layers often occurs in strongly stratified environments. For example, buoyancy effects keep substances and contaminants in the relatively fresh surface layer in microtidal shelf areas near large river mouths. In such occasions convergence or divergence of the (velocity field of) local currents in the surface layer (of possibly varying thickness) may result in extensive contraction or expansion of the surface layer (Paper III).

The convergence and divergence regions are usually very variable and thus normally not able to produce extensive patches (understood here as changes in the concentrations) of floats or substances locked in the surface layer of the sea. A generalization of the notion of divergence is the concept of (flow) compressibility of the velocity field (Section 1.1). If the velocity field in a particular layer of the 3D environment exhibits high compressibility, the formation of high-concentration regions of passive tracers is likely (De Pietro et al., 2014). This phenomenon, if occurring in the surface layer, intrinsically leads to certain changes in the total amount of the items or substances in question per unit of surface. The “ability” of certain marine areas to serve as a gathering place of floating debris (Pichel et al., 2007) is often a direct result of this mechanism.

The definition of the classical measure of flow compressibility of the velocity field (Section 1.1) relies on instantaneous properties of the flow field and does not take into account the history of motions. In reality, the history of interactions between the divergence field and the Lagrangian transport of parcels of the medium plays a large role in the gathering of floating particles into clusters (Samuelson et al., 2012). As discussed in Papers I and III, it is likely that the most systematic and rapid, effectively spontaneous formation of patches occurs when a localized convergence zone moves together with the surface current (Samuelson et al., 2012). This process is, in essence, a mirror phenomenon of a transient upwelling (Fennel et al., 2010). Very little is known about its qualitative and quantitative details, although this and similar mechanisms (often associated with so-called basins of attraction, Froyland et al., 2014) are frequently active in strongly stratified environments.

Many strong and long-living divergence and convergence zones are formed due to the interaction of marine currents and internal waves with coasts or with a sloping bottom. The presence of such zones is a frequent feature in semi-enclosed

seas that host highly variable forcing patterns and a complicated regime of currents. The typical consequences of the presence of such zones are upwelling and downwelling phenomena (Leppäranta and Myrberg, 2009). The focus of this study is on the Baltic Sea (Figure 1) which is famous for the complexity of its dynamics, including the frequent presence of up- and downwellings (Myrberg and Andrejev, 2003; Lehmann et al., 2012).

The field of currents (incl. surface currents) is particularly complicated in the Gulf of Finland (Figure 1), an elongated basin in the easternmost part of the Baltic Sea. Similarly to the rest of this sea, the system of currents in this gulf often contains a substantial vertical component (Alenius et al., 1998; Andrejev et al., 2004) that becomes evident in the form of frequent up- and downwellings (Myrberg and Andrejev, 2003). This gulf is thus a likely place for frequent patch generation.

The resulting sea surface temperature fronts (Kahru et al., 1995) are typically aligned to the coast or the isobaths. If a convergence zone, either stationary or

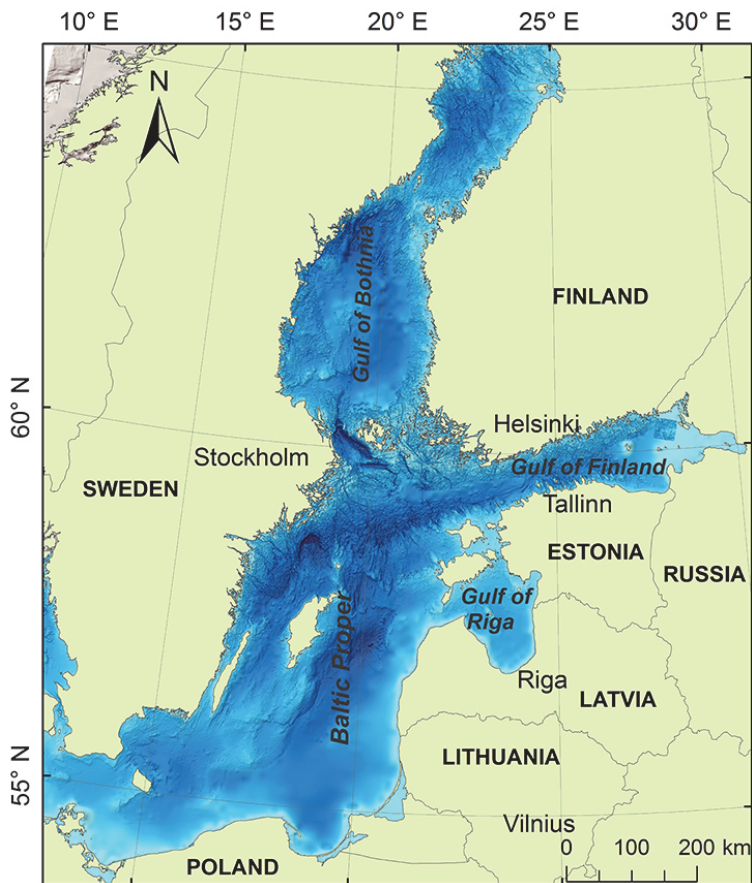


**Figure 1.** Bathymetry and geometry of the Baltic Sea and the Gulf of Finland (Paper IV).

moving together with water masses, affects a certain sea area, the result usually is a downwelling. Compared with the massive pool of information about upwellings (e.g., Myrberg and Andrejev, 2003; Lehmann et al., 2012), the research into downwellings has been very limited (Kowalewski and Ostrowski, 2005; Golenko and Golenko, 2012). A possible reason is that an upwelling can be easily quantified, e.g., from the sea surface temperature (Myrberg and Andrejev, 2003; Lehmann et al., 2012) or from consequences to the biological fields (Uiboupin et al., 2012) but identification of a downwelling often requires measurements in the water column that are costly and time-consuming. As a result, most of the existing means of remote detection of downwellings are implicit and not particularly reliable (Chubarenko, 2010). The analysis of the history of the divergence field eventually provides a more reliable option to identify and predict downwellings, and to build their climatology.

In this thesis, I employ the concept of finite-time compressibility (FTC, Paper I) to identify and quantify the joint impact of convergence of the surface velocity field and the underlying current (more generally, the Lagrangian transport). The major assumption is that the strongest changes in the surface concentrations occur if the relocation of a convergence area is synchronized with the surface current. The introduction of the FTC as an extension of the classical measure of flow compressibility of velocity fields makes it possible to systematically quantify the joint impact of such synchronization on the concentration of floats. High values of FTC reflect a match between convergence fields that move along the sea surface and the Lagrangian transport in the surface layer (Samuelson et al., 2012). The calculation of FTC integrates a certain segment of the history of the surface flow and thus takes into account long-term correlations between an emerging patch, its Lagrangian transport and the displacement of the convergence field.

Both experimental and numerical results indicate that the time correlations (which are always present for real hydrodynamic flows) can either inhibit or catalyse the process of rapid clustering of various floats (Boffetta et al., 2004; Samuelson et al., 2012). This phenomenon is equivalent to a rapid increase in the concentrations of surface floats, equivalently, to *spontaneous* formation of patches of these floats. Importantly, certain sufficiently large values of FTC (that exceed a certain threshold) are equivalent to the levels of the classical flow compressibility at which rapid clustering of items floating on the sea surface may occur (Papers I and IV).

Based on this parallel and using the concept of FTC, I study the appearance, magnitude, persistence and seasonal variations of areas that regularly exhibit favourable conditions for a rapid increase in the surface concentrations of various items and substances. The results shed light onto how various kinds of pollution, adverse impacts or contaminants that are either floating on the sea surface or are locked in the surface layer may spontaneously form patches of increased concentrations.

## The objectives and outline of the thesis

The analysis presented in this thesis demonstrates the existence of regions which exhibit very high instantaneous values of FTC. Further inspection highlights areas in the Gulf of Finland where such high values may regularly occur over certain time intervals. Heuristically, such areas are expected to often host downwelling events. During such events a certain amount of water parcels that originally reside near the surface sink into deeper layers whereas lighter additives (debris, microplastic, oil spills, polluted or nutrient-rich fresh water from rivers) remain in the uppermost layer. This process naturally leads to an increase in the concentration of additives per unit of the sea area. It may be greatly augmented if the classical flow compressibility or FTC exceeds a certain value, after which rapid clustering of floats may be triggered (Falkovich et al., 2001). A major goal of the analysis is to highlight the areas where augmentation of the clustering phenomenon is frequent.

The main objectives of this thesis are as follows:

- to introduce an easily employable measure for quantifying the ability of spontaneous formation of high concentrations of various items and substances in the surface layer;
- to relate the properties of this measure with those of the classical measures of compressibility of the velocity field;
- to verify whether this measure is applicable to the analysis of properties of surface flows in semi-enclosed seas hosting complicated flow patterns such as the Gulf of Finland, the Baltic Sea;
- to identify areas of enhanced probability of spontaneous patch formation and to provide a first-order estimate of their appearance pattern and persistency in time and space.

To fulfil these objectives, Chapter 1 provides an insight into the efforts towards a proper definition of a measure that is able to systematically quantify the likelihood of patch formation in a formal manner. The formation of patches, heuristically, means that the distance between single parcels decreases. This process is generally characteristic of the phenomenon of compressibility and can be quantified as a change in the concentration of some items owing to the relative volume change of the environment. As sea water is an almost incompressible medium, the classical notion of compressibility is not applicable for the described purposes. A feasible solution, described in Chapter 1, is to employ a measure of the so-called flow compressibility of the “volume” of velocities of water parcels at the sea surface. This measure is a natural generalization of the divergence or convergence of the flow field.

The central concept addressed in this thesis is an extension of the classical flow compressibility. This relevant measure of FTC is defined based on tracking changes in simple surface elements carried by surface currents during a certain time interval and thus is able to take into account a part of the time history of surface motions. Following Papers I and II, Chapter 1 presents a short insight into

how to frame such a measure in the landscape of existing measures and how to elicit a direct relationship between the newly introduced measure and the classical flow compressibility.

This theoretical framing is followed by a description of the study area in Chapter 2. The test area is the Gulf of Finland (Figure 1) that hosts not only an extremely complicated regime of surface currents but also frequent upwelling and downwelling events. It is thus likely that large levels of classical flow compressibility and FTC may occur in this water body and that spontaneous patch generation is a frequent phenomenon. After a short insight into the major forcing factors and known properties of the complex dynamics of the Gulf of Finland, an introduction is provided about the main features of the employed Rossby Centre Ocean model (Section 2.2) and OAAS circulation models (Section 2.3), together with their forcing data and parameters of their output information, and about the technique of replication of Lagrangian trajectories of passive floats or selected water parcels at the sea surface. The material mostly follows the presentation in Papers II and III.

Chapter 3 starts from a description of the specifically developed simulation environment QTRAC. The simulations involve several measures for the spatial quantification of the processes on the sea surface such as the divergence field, flow compressibility and FTC. The calculations are based on the moderate resolution (2 nautical miles and 6 h) velocity fields from the Rossby Centre Ocean model. A few intermediate results detail the main steps on the way towards the identification of those areas that may systematically host patch formation. The main outcome of this chapter is a demonstration (presented in Papers III and IV) of the applicability of the concept of FTC for providing interesting information about processes in the surface layer of the Gulf of Finland.

Chapter 4 explores the idea that the most rapid patch formation is likely in areas where flow compressibility or FTC exceed a certain threshold, after which floats may start to cluster together (Falkovich et al., 2001). This possibility is associated with a high likelihood for spontaneous patch formation. The relevant analysis is carried out in Papers IV and V using velocity fields with a finer spatial resolution of 1 nautical mile from the OAAS model. The qualitative and quantitative analysis of the areas of large FTC addresses their location, temporal course, seasonal variation and persistency.

## **Approbation of the results**

The basic results described in this thesis have been presented by the author at the following international conferences:

**Giudici A.**, Soomere T. 2014. Finite-time compressibility as a measure of likelihood of spontaneous patch formation in the Gulf of Finland. Oral presentation at the *International Union of Theoretical and Applied Mathematics Symposium* (8–12 September 2014, Tallinn, Estonia).

**Giudici A.**, Soomere T. 2014. Quantification of spontaneous patch generation in the marine surface layer. Oral presentation at the *1st International Conference on Mathematics and Engineering in Marine and Earth Problems* (22–25 July 2014, Aveiro, Portugal).

**Giudici A.**, Soomere T. 2014. Measuring finite time compressibility from large simulated datasets: Towards identification of areas of spontaneous patch formation in the Gulf of Finland. Oral presentation at the *11th International Baltic Conference on DB and IS* (8–11 June 2014, Tallinn, Estonia).

**Giudici A.**, Soomere T. 2014. On the possibility of spontaneous patch formation in the Gulf of Finland. Oral presentation at the *6th IEEE/OES Baltic International Symposium* (26–29 May 2014, Tallinn, Estonia).

**Giudici A.**, Soomere T. 2014. Highly persisting patch formation areas and their interannual variability in the Gulf of Finland. Oral presentation at the *2nd International Conference on Climate Change – The Environmental and Socio-Economic Response in the Southern Baltic Region* (12–15 May 2014, Szczecin, Poland).

**Giudici A.**, Soomere T. 2013. In search for the areas of natural patch generation in the Gulf of Finland. Oral presentation at the *9th Baltic Sea Science Congress* (26–30 August 2013, Klaipėda, Lithuania).

**Giudici A.**, Soomere T. 2013. Identification of areas of frequent patch formation from velocity fields. Oral presentation at the *12th International Coastal Symposium* (8–12 April 2013, Plymouth, United Kingdom).

**Giudici A.**, Soomere T. 2012. Compressibility of surface currents analysis in the Gulf of Finland, the Baltic Sea. Oral presentation at the *International Student Conference on Aquatic Environmental Research* (17–19 October 2012, Palanga, Lithuania).

**Giudici A.**, Soomere T. 2012. On the compressibility of surface currents in the Gulf of Finland, the Baltic Sea. Oral presentation at the *5th IEEE/OES Baltic International Symposium* (08–11 May 2012, Klaipėda, Lithuania).

Kalda J., Soomere T., **Giudici A.** 2011. Compressibility of the surface currents created by nonlinear waves. Oral presentation at the *8th Baltic Sea Science Congress* (22–26 August 2011, St. Petersburg, Russian Federation).

## **1. Flow compressibility of surface currents**

The underlying idea of the analysis in this thesis is to link the potential of the formation of patches on the sea surface with certain properties of surface currents. When talking about patches, I have in mind any inhomogeneities (usually increased concentrations) in initially homogeneous fields of various items and substances that are locked in the surface layer of the sea. For simplicity, these items and substances are at times called passive tracers.

A change in the concentration of tracers on the sea surface can be characterized in terms of the relative volume change of the water mass that contains a fixed amount of tracers. An increase in the concentration of tracers is a natural outcome of a converging flow or a compression of the medium. As sea water is an almost incompressible medium, the classical notion of compressibility as a measure of the relative volume change of a fluid as a response to pressure variations cannot be used to quantify these changes. For this reason, these changes are commonly expressed by means of the compressibility of the “volume” of velocities of water parcels. This quantity, called flow compressibility, relies on the instantaneous difference between the motion of water particles and tracers (Falkovich et al., 2001) and is a natural generalization of the divergence or convergence of the flow field. The central quantity addressed in this thesis is the finite-time flow compressibility (FTC), an extension of the concept of flow compressibility that is able to take into account a part of the time history of surface motions.

The presentation in this chapter largely follows Papers I and II. It starts from a formal definition of the flow compressibility, followed by a discussion of its properties in the surface layer of seas and oceans (Sections 1.1 and 1.2). Section 1.3 introduces the generalization of this measure that is able to take into account some parts of the time history of the flow and Section 1.4 analyses the interrelations between these two measures.

### **1.1. Divergence of velocity and flow compressibility**

The “ability” of the field of various substances and items on the sea surface to exhibit extensive variations in the concentration (or to gather into patches) is one of the most important factors which control the behaviour of pollution and other adverse impacts. In extreme situations this ability may naturally lead to the formation of high concentrations in different adverse impacts or marine litter. This feature expresses the potential of the compressibility of certain fields even if the medium containing these substances or items (e.g., sea water) is almost incompressible. The compressibility of the field of tracers is obviously connected with various motions of water parcels. In essence, nonzero compressibility of this field expresses the systematic difference between the relocation of water parcels and substances or items in question. For example, if water parcels dive during a downwelling event, items floating on the sea surface cannot follow the vertical

motions. They are carried by water to the region of downwelling and naturally gather there.

The described difference in the velocities of water parcels and buoyant tracers can be characterized using so-called flow compressibility. Importantly, this measure exclusively characterizes the *velocity field* of the medium, equivalently, the motion of water particles. It is thus substantially different from the common concept of compressibility of the medium (sea water or air) that is understood as a measure of the relative volume change. For simplicity, I use the term flow compressibility (of the sea surface) as a synonym to the flow compressibility of the field of surface velocities.

This measure is often used to characterize the generation of inhomogeneities in various environments (Falkovich et al., 2001). Inhomogeneities are naturally produced if the surface flow has nonzero divergence (or convergence). Since the total surface of an enclosed sea area does not significantly change in time, the average flow divergence over the entire sea surface is almost zero. This assertion has been validated in Paper III for the Gulf of Finland (Figure 1). The magnitude of average flow divergence thus provides an implicit way to judge to a certain degree over the correctness of the calculations of the divergence and its generalizations from discrete velocity fields.

Figure 2 presents the average divergence over the entire Gulf of Finland and calculated over a set of 4 h long time slices (Section 2.2). The maximum absolute values of divergence reach 0.8 1/s in single locations of the gulf. However, the average divergence over the entire surface of this gulf has typical values of the order of 0.01 1/s for single calendar days throughout the year 1991 (Figure 2). Such small values signal that the implementation of the calculations (Chapter 2) is reliable and that the velocity fields used in the study are, technically, adequate for

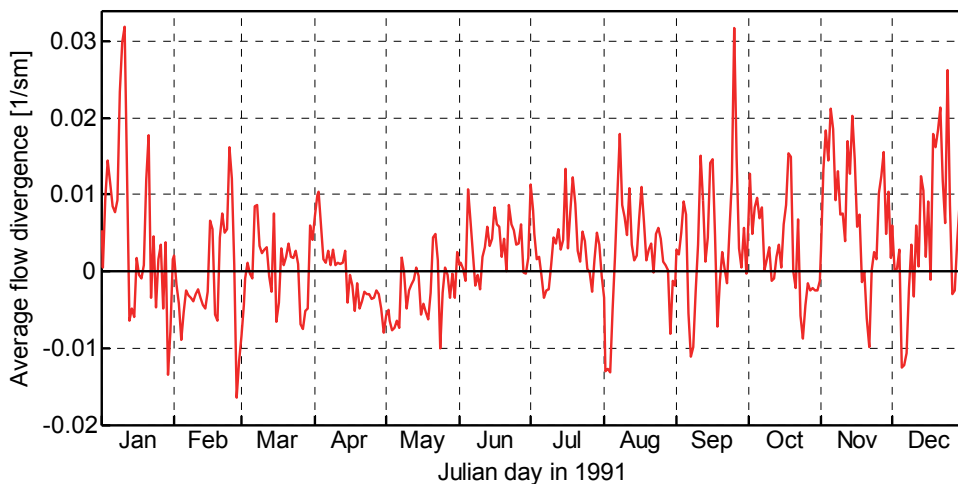


**Figure 2.** Divergence of the 2D flow on the sea surface, integrated over the entire Gulf of Finland in 1991 (Paper III). The underlying simulations have been performed using the Rossby Centre Ocean model with a resolution of 2 nautical miles (Section 2.2).

the purposes of this thesis.

Part of the small variations in the overall average divergence apparently reflect inaccuracies of the discrete approximation of the velocity field. Some variations, however, may also reflect the surface water exchange between the Gulf of Finland (over which the divergence is calculated) and the rest of the Baltic Sea. The mostly positive values and the overall annual average of 0.0025 1/s seemingly reflect the excess of freshwater inflow in this area (Leppäranta and Myrberg, 2009). Some negative values are explained with a surface water inflow owing to specific wind events.

There is a certain asymmetry between the contraction and expansion of the water surface. Floating substances tend to spend more time in contracting regions than in expanding ones. The expanding flows tend to push substances away from their virtual centres, while contracting ones tend to attract and keep such substances within their areas of influence. This simple asymmetry generally gives rise to a certain inhomogeneity in the concentrations of substances or items in flows with nonzero divergence.

The classical definition of flow compressibility is based on the fundamental theorem of vector calculus, Helmholtz's theorem (Bladel, 1959). It states that any sufficiently smooth (in terms of the existence of derivatives) and reasonably rapidly decaying vector field  $\vec{v}$  (whose velocity values decrease in all directions) can be expressed as the sum of an irrotational (curl-free, also called potential) vector field  $\vec{U} = \nabla\varphi$  (where  $\varphi$  is a scalar potential) and a solenoidal (divergence-free) vector field  $\vec{V} = \nabla \times \vec{\psi}$  (where  $\vec{\psi}$  is a vector potential):

$$\vec{v} = \nabla\varphi + \nabla \times \vec{\psi} . \quad (1)$$

This way of separating the components of a velocity field is known as the Helmholtz decomposition.

The water mass in the ocean is limited in space and the local changes in its velocities are limited by viscosity. Therefore, virtually every realistic field of motions in the ocean is, formally, defined everywhere in space, has smooth second-order derivatives and definitely vanishes at infinity together with its first derivatives. Consequently, it can be decomposed, to a first approximation, into its solenoidal  $\vec{V} = \nabla \times \vec{\psi}$  and potential  $\vec{U} = \nabla\varphi$  components. These components have zero divergence and curl, respectively.

The flow compressibility  $C_c$  is defined as the relative weight of the divergence of the irrotational component  $\vec{U} = \nabla\varphi$  of the velocity field (Falkovich et al., 2001). In 2D environment the potential  $\vec{\psi}$  is a scalar and

$$C_c = \frac{\langle (\Delta\varphi)^2 \rangle}{\langle (\Delta\varphi)^2 + (\Delta\psi)^2 \rangle} . \quad (2)$$

A fully solenoidal flow has compressibility  $C_c = 0$  and a purely potential flow has compressibility  $C_c = 1$ . Therefore, the flow compressibility is a naturally normalized generalization of the divergence of this flow.

Another widely used definition of flow compressibility expresses this measure directly from the properties of the vector field of velocity as the ratio of the squared velocity divergence to the squared norm of the velocity gradient tensor (Falkovich et al., 2001):

$$C_2 = \frac{\langle (\text{div } \vec{v})^2 \rangle}{\langle \|\partial v_i / \partial x_j\|^2 \rangle}. \quad (3)$$

Here  $\vec{v} = (v_1, v_2, v_3)$  is the velocity field,  $(x_1, x_2, x_3)$  are spatial coordinates and  $i, j = 1, 2, 3$ .

The two measures  $C_c$  and  $C_2$  appear to be the same if the vector field is bounded in the entire (e.g., very large but still finite) domain. This assumption is intuitively obvious in the marine environment where the velocities of single water parcels are always finite. Technically, this assertion guarantees that the velocity values do not grow indefinitely in any location even infinitely far from the area of interest, and that we can neglect the contributions from the boundary, when integrating by parts.

To show that these two definitions (Eq. (2) and Eq. (3)) are equivalent under this assumption, it is convenient to express first the divergence of the vector field  $\vec{v}$  in terms of its potential component. I restrict this derivation to the 2D case for simplicity, but it can be extended to an arbitrary number of dimensions (Falkovich et al., 2001). In this case the spatial coordinates are  $(x, y)$ , the velocity can be expressed as  $\vec{v} = (u, v)$  and the numerator in Eq. (3) can be expressed as follows:

$$\langle (\text{div } \vec{v})^2 \rangle = \langle (\varphi_{xx} + \varphi_{yy})^2 \rangle = \langle (\Delta \varphi)^2 \rangle, \quad (4)$$

where the subscript has the meaning of partial derivative along the respective coordinate axis. The operator of averaging in Eqs. (2)–(4) has the meaning of averaging both over space and over an ensemble of different realizations of the vector field. The order is arbitrary, so the space average can be addressed first. For the finite ocean it is sufficient to integrate over the entire surface and to divide the result by the surface area.

The denominator of Eq. (3) can also be rewritten in terms of potential and solenoidal components of the velocity field  $\vec{v} = (u, v)$ :

$$\begin{aligned} \langle \|\partial v_i / \partial x_j\|^2 \rangle &= \langle (\varphi_{xx} + \psi_{xy})^2 + (\varphi_{xy} + \psi_{yy})^2 + (\varphi_{xy} - \psi_{xx})^2 + (\varphi_{yy} - \psi_{xy})^2 \rangle \\ &= \langle (\varphi_{xx})^2 \rangle + 2\langle \varphi_{xx}\psi_{xy} \rangle + \langle (\psi_{xy})^2 \rangle + \langle (\varphi_{xy})^2 \rangle + 2\langle \varphi_{xy}\psi_{yy} \rangle + \langle (\psi_{yy})^2 \rangle \\ &\quad + \langle (\varphi_{xy})^2 \rangle - 2\langle \varphi_{xy}\psi_{xx} \rangle + \langle (\psi_{xx})^2 \rangle + \langle (\varphi_{yy})^2 \rangle - 2\langle \varphi_{yy}\psi_{xy} \rangle + \langle (\psi_{xy})^2 \rangle. \end{aligned} \quad (5)$$

From the right hand side of Eq. (5), the additives  $2\langle \varphi_{xx}\psi_{xy} \rangle$  and  $-2\langle \varphi_{xy}\psi_{xx} \rangle$ , and  $2\langle \varphi_{xy}\psi_{yy} \rangle$  and  $-2\langle \varphi_{yy}\psi_{xy} \rangle$ , have opposite signs and cancel out pairwise when

integrating by parts. Collecting together the equivalent terms and integrating by parts yields

$$\left\langle \left\| \partial v_i / \partial x_j \right\|^2 \right\rangle = \left\langle \varphi_{xx}^2 + 2\varphi_{xx}\varphi_{yy} + \varphi_{yy}^2 + \psi_{xx}^2 + 2\psi_{xx}\psi_{yy} + \psi_{yy}^2 \right\rangle = \left\langle (\Delta\varphi)^2 + (\Delta\psi)^2 \right\rangle. \quad (6)$$

Comparison of Eqs. (4) and (6) with Eq. (2) reveals that  $C_2 \equiv C_c$  under the discussed assumption.

## 1.2. Compressibility of velocity fields in the ocean

Three-dimensional geophysical flows in the atmosphere and in the ocean (as well as the flows in lakes and rivers) are usually almost incompressible in this context. The situation is often completely different for 2D slices of the medium (De Pietro et al., 2014). As described above, the 3D motions of water parcels may be considerably different from the motions of items that are locked on the surface. As a consequence, the average flow compressibility of a 2D velocity field on the sea surface may largely exceed the analogous values for the overall 3D motion. In other words, nonzero flow compressibility is characteristic of many examples of 2D velocity fields that consist of horizontal components of water parcels at the sea surface.

A 2D velocity field that characterizes velocities averaged over a certain surface layer can be compressible even when water particles, initially located at the surface, are confined to stay at the surface. This is also the case in a discrete representation of circulation patterns in numerical ocean models. For example, the free-slip surface of fully turbulent water volumes is characterized by  $C_c \approx 0.5$  (Schumacher and Eckhardt, 2002). This observation suggests that flow compressibility (the compressibility of the sea surface) can be interpreted as an indicator of the impact of 3D motions on the concentrations of different substances at a particular location of the surface, equivalently, as a measure of the likelihood of a marine surface region to host patch-formation processes.

As discussed in Papers I–III, different properties of the fluid motion and associated transport of fluid parcels and various substances have been related to the effects of flow compressibility within various theoretical and experimental approaches (Falkovich et al., 2001; Boffetta et al., 2004; Cressman et al., 2004; Kalda, 2007). An attempt is made in this thesis to clear up what role does flow compressibility play in terms of affecting the marine environment.

The systematic formation of areas with higher or lower concentration of tracers than the average one is possible only if the potential flow component dominates (Falkovich et al., 2001). Moreover, the impact of the presence of large values of flow compressibility may be highly augmented whenever its local values exceed a certain threshold. This feature can be exemplified for so-called ideal Kraichnan flows. This class denotes flows in 3D ideal fluids in which instantaneous velocities form a random dynamical system (Kraichnan, 1968). Although this idealization does not exactly replicate the properties of realistic dynamics of seas and oceans, it

is often used as a convenient (accessible to an exact analysis) and rich in content framework to study fundamentals of ocean motions (Chetrite et al., 2007). This definition implies that the local properties of ideal Kraichnan flows do not depend on the history of the flow. Mathematically, it means that such flows are delta-correlated in time.

The analysis of the behaviour of such flows has shown that nonzero values of flow compressibility can dramatically affect the behaviour of the floating particles. Namely, extensive formation of clusters and development of fractal structures (Bec et al., 2004; Perlekar et al., 2010) may occur when the flow compressibility exceeds a certain threshold. If the flow contains a large number of items floating on the surface, enhanced formation of clusters (equivalently, an increase in the relevant concentration) may occur if the flow compressibility exceeds the critical value of  $C_c = 0.5$  (Falkovich et al., 2001). The highest values of flow compressibility at the sea surface can thus be naturally associated with areas prone to spontaneous development of patches of floating matter.

Offshore areas systematically showing values  $C_c > 0.5$  on the sea surface are good candidates in terms of regions of reduced risk of pollution transport towards the coasts (Soomere et al., 2010). Such areas implicitly attract various items and substances that are located in the surface layer (Froyland et al., 2014). Environmental management policies could potentially benefit from both the decreased probability of coastal hits by current-driven adverse impacts released in such regions and the increased propagation time of adverse impacts originating from such patch-gathering areas (Soomere and Quak, 2013).

As 3D ocean flows are usually almost incompressible in this framework (Fine and Millero, 1973), they are incapable of producing favourable conditions for the formation of clusters. The impact of linear and weakly nonlinear surface waves also does not contribute to flow compressibility because an increase in the values of  $C_c$  owing to surface wave trains is almost negligible in the marine environment (Vucelja et al., 2007). It is, however, likely that specific edge wave events may still contribute to the patch-formation process (Averbukh et al., 2014).

A notable exception which may show significant levels of flow compressibility is the marine surface layer. This part of the marine environment often hosts an almost 2D velocity field. Surface currents often have a very low level of persistency (Andrejev et al., 2004) and the related velocity field therefore can be interpreted as a Kraichnan flow. The specific feature of this uppermost layer of the sea that allows large values of  $C_c$  is the capacity of the water particles located at the surface to dive into the third, vertical dimension (Garrison, 2011). Such motions are intrinsic to upwelling or downwelling phenomena that are frequent in the Baltic Sea (Lehmann et al., 2012). Importantly, these processes leave the floats locked onto the surface and evidently are able to modify their local concentrations. An increase in the concentration is likely to occur in the downwelling regions and a decrease in the upwelling areas.

For this reason, the average flow compressibility of such a 2D velocity field at the sea surface may largely exceed the similar values related to the overall 3D

motion. The underlying mechanism could then explain, at least partially, the process of development of patches of floating substances in the marine environment. It is important to emphasize the role of 3D effects on the large values of  $C_c$ . Since mesoscale (see Cushman-Roisin and Beckers, 2011) and large-scale flows in marine environments are often quasi-2D (Rhines, 1979; Kraichnan and Montgomery, 1980), the observed “large-scale” values of flow compressibility at the surface are usually relatively low.

### 1.3. Finite-time compressibility

The practical evaluation of flow compressibility discussed in Sections 1.1 and 1.2 is fairly complicated as it is necessary to perform averaging over the entire area filled by the fluid and possibly over many realizations. It is thus desirable to introduce a measure that would be similarly able to quantify the likelihood of the patch-formation process but would also be able to evaluate this likelihood based on certain local quantities (or at least on a set of quantities in a limited sea area). This quantity should also include some part of the history of the motions (equivalently, finite-time correlations within the velocity field) that may enhance the patch-generation process (Samuelson et al., 2012). The goal is to have a measure which is directly linked with the physical formation of patches and allows for an easy calculation starting from simulated or experimental data.

The main idea of the modification of the concept of flow compressibility, first introduced in Paper I, is to relate finite-time changes in the material volumes (2D surface areas overlying 3D circulation) with those in the distance that separates material parcels. This modification accounts for certain amount of finite-time correlations and is consistent with the existing measure of flow compressibility as it coincides with it at the limit of infinitesimally small time windows and Kraichnan flows (Paper I). Moreover, it is designed in such a way that its values are directly related to the ability of a medium to gather the floats into patches.

The calculation of this modified measure, called finite-time compressibility (FTC), is performed by tracking changes of small conveniently defined elements on the sea surface. The technology developed in Paper I (and used in all papers constituting the thesis) considers triangular elements (Figure 3). Specifically, let  $(x'_1, y'_1)$ ,  $(x'_2, y'_2)$  and  $(x'_3, y'_3)$  be the coordinates of the vertices of an arbitrary

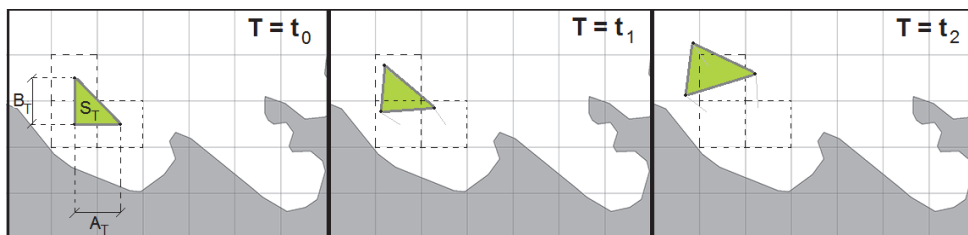


**Figure 3.** Scheme of the selection stencil of a triangular surface element and its evolution through time.

triangular element, at time instant  $t$ . Let us then consider the quantity of twice its surface area  $S_t$ :

$$2S_t = \left| (x_1^t - x_2^t) \cdot (x_1^t - x_3^t) \cdot (y_1^t - y_3^t) \cdot (y_1^t - y_2^t) \right|. \quad (7)$$

The relative change in this quantity between two consecutive time instants  $t-1$  and  $t$  is  $dS_t = (S_t - S_{t-1})/S_t$ .

The other constituents of the modified measure of flow compressibility are the squared lengths of two arbitrary edges of the triangular element, say,  $A_t$  and  $B_t$  (Figure 3):

$$A_t = (x_1^t - x_2^t)^2 + (y_1^t - y_2^t)^2; \quad B_t = (x_1^t - x_3^t)^2 + (y_1^t - y_3^t)^2. \quad (8)$$

The relative change in these two measures between two consecutive time steps is expressed as  $dA_t = (A_t - A_{t-1})/A_t$  and  $dB_t = (B_t - B_{t-1})/B_t$ . An estimate of FTC is calculated from the following expression:

$$C_{ftc} = \frac{2dS_{rms}}{dA_{rms} + dB_{rms}}. \quad (9)$$

The subscripts  $rms$  at the right-hand side of Eq. (9) have the meaning of root mean square values of the relevant quantities:

$$dS_{rms} = \sqrt{\frac{1}{n} \sum_i^n dS_i^2}, \quad dA_{rms} = \sqrt{\frac{1}{n} \sum_i^n dA_i^2}, \quad dB_{rms} = \sqrt{\frac{1}{n} \sum_i^n dB_i^2}, \quad (10)$$

where  $i$  indicates a particular time step within the simulation.

The quantities in Eqs. (9) and (10) are usually calculated from a set of instantaneous values of  $S_t$ ,  $A_t$  and  $B_t$  over a realistic time interval. They are therefore single samples of the “true” values of  $C_{ftc}$ . It is however clear that under the assumption that the input velocity field models a stochastic stationary process (whose probability distribution does not change when shifted in time), the lengthening of the sequence of instants involved into Eq. (9) and/or increasing the number of realizations of the process would lead to even better estimates of the values of  $C_{ftc}$ .

From Eqs. (7)–(9) it follows that for a purely incompressible flow ( $C_c = 0$ ), the triangular elements’ surface areas remain unchanged between consecutive time steps. Thus their relative change is zero  $dS_{rms} = 0$ , and hence FTC would be  $C_{ftc} = 0$  as well, in the entire volume (or overlying the area) covered by such a flow. In the opposite situation of a purely contracting or expanding flow, the squared lengths of two of the edges of each triangular element would change with the same relative rate as the element’s surface, therefore yielding  $C_{ftc} = 1$ . This value thus characterizes a purely compressible flow.

#### 1.4. Classical flow compressibility and finite-time compressibility

An explicit comparison of the measure of FTC (Eq. (9)) introduced in Section 1.3 and the classical flow compressibility  $C_c$  is provided in Paper I. The idea behind the derivation is to replace the expressions  $dS_{rms}$  and  $dA_{rms} + dB_{rms}$  present in the definition of FTC (Eq. (9)) in terms of the averaged velocities and the classical flow compressibility.

The presentation in this section follows the material from Paper I. It is convenient to provide the derivation using discrete representation of velocities of floating water parcels. The resulting estimates of FTC may slightly deviate from the theoretical ones owing to the use of finite-difference representation of the velocity field. Doing so, however, follows the algorithm of numerical simulations where the velocity vector field used in calculations is a discrete approximation of the actual velocity field along the trajectory of the selected parcels. The relevant details of the comparison for the case when only a finite set of trajectories of tracers are available (and not the entire velocity field) are provided in Paper I.

The starting point is a single surface element carried and possibly deformed by the velocity field at two infinitely close time instants  $t$  and  $t+1$  (Figure 4) separated by  $\Delta t$ . Let us consider the flux of the vector field of the velocity  $\vec{v} = (u, v)$  through the contour of a chosen surface element. This flux is related to the behaviour of the vector field inside that element by Ostrogradsky's theorem:

$$\Delta S = \int_S \nabla \cdot \vec{v} dt. \quad (11)$$

If the two time instants are infinitesimally close (Figure 4), it is safe to assume that the floating element's surface area does not change significantly over  $\Delta t$ , and therefore the integral in Eq. (11) can be approximated as  $\Delta S = \nabla \cdot \vec{v}(S\Delta t)$ . From this relation it follows that

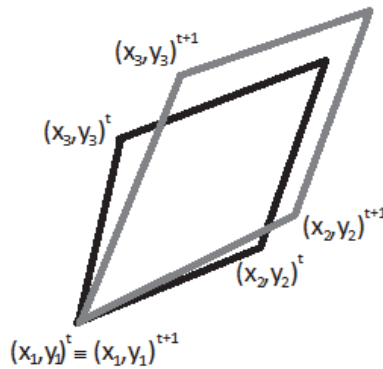


**Figure 4.** The distortion of a surface element by the velocity field at two infinitely close time intervals. The translation of the element is ignored (Paper I).

$$dS = \frac{\Delta S}{S} = \nabla \cdot \vec{v} \Delta t \text{ or } (dS_{rms})^2 = \langle (\nabla \cdot \vec{v})^2 \rangle (\Delta t)^2, \quad (12)$$

where the angle brackets denote the root mean square.

To express the sum  $dA_{rms} + dB_{rms}$  in terms of discrete velocities, let us now consider a moving frame of reference  $(\xi, \eta)$ , centred at the vertex  $(x_1^t, y_1^t)$  of the triangular floating element (Figure 3). One of its axes, let it be  $\zeta$ , is parallel to the edge vector  $\vec{a}_3^t = (x_3^t - x_1^t, y_3^t - y_1^t)$ . In the coordinates  $(\xi, \eta)$  vector  $\vec{a}_3$  has components  $(L_B, 0)$  and represents the length  $|\vec{a}_3^t| = \sqrt{B} = L_B$  of the corresponding edge. At the time instant  $t+1$ , vector  $\vec{a}_3^{t+1}$  becomes

$$\vec{a}_3^{t+1} = (L_B + U_\xi L_B \Delta t, V_\xi L_B \Delta t), \quad (13)$$

where  $\vec{V} = (U, V)$  is the velocity in the  $(\xi, \eta)$ -coordinates. The change in the length of this vector is therefore

$$\Delta(\vec{a}_3)^2 = |\vec{a}_3^{t+1}|^2 - |\vec{a}_3^t|^2 \approx 2U_\xi L_B^2 \Delta t, \quad (14)$$

where the terms  $O((\Delta t)^2)$  have been ignored. If the averaging operator has the meaning of calculation of the root mean square value over a number of short time intervals, this construction leads to the following expression for  $dB_{rms} = \langle d(L_B^2) \rangle = \langle dB \rangle$ :

$$dB_{rms} = \langle d(L_B^2) \rangle = \left\langle \frac{\Delta(\vec{a}_3)^2}{(\vec{a}_3)^2} \right\rangle \approx \langle 2U_\xi \Delta t \rangle = 2\sqrt{\langle U_\xi^2 \rangle} \Delta t. \quad (15)$$

If the vector field of velocity is statistically isotropic, Eq. (15) can be reduced to

$$dB_{rms} \approx 2\sqrt{\langle U_\xi^2 \rangle} \Delta t = 2\sqrt{\langle u_x^2 \rangle} \Delta t = 2\sqrt{\langle v_y^2 \rangle} \Delta t. \quad (16)$$

Similarly, it can be written:

$$dA_{rms} \approx 2\sqrt{\langle u_x^2 \rangle} \Delta t. \quad (17)$$

For the 2D motions the velocity field is  $\vec{v} = (u, v)$  and the flow compressibility (expressed as the square ratio of the velocity divergence to the norm of the velocity gradient tensor) is presented by Eq. (2):

$$C_c = \frac{(u_x + v_y)^2}{u_x^2 + u_y^2 + v_x^2 + v_y^2}. \quad (18)$$

Here subscripts indicate differentiation along the corresponding coordinate. As demonstrated in Section 1.1 and Paper I, for ideal Kraichnan flows this definition coincides with the classical one. Using the above-derived expressions for velocity components, Eqs. (9) and (18) can be rewritten as

$$C_c = \frac{\langle (\nabla \cdot \bar{v})^2 \rangle}{2\langle u_x^2 \rangle + 2\langle v_y^2 \rangle}, \quad C_{fic}^2 = \frac{4(dS_{rms})^2}{(dA_{rms} + dB_{rms})^2} = \frac{\langle (\nabla \cdot \bar{v})^2 \rangle}{4\langle u_x^2 \rangle}. \quad (19)$$

Therefore, the classical flow compressibility and the FTC are interrelated as follows:

$$C_{fic}^2 = \frac{\langle u_x^2 \rangle + \langle v_y^2 \rangle}{2\langle u_x^2 \rangle} C_c. \quad (20)$$

For ideal Kraichnan flows, in Eq. (20) the average velocity components can be expressed in terms of  $C_c$  (Falkovich, 2001, Eq. (58)) as follows:

$$\begin{aligned} \langle u_x^2 \rangle &= K[(3 - 2C_c) + 2(2C_c - 1)] = K(2C_c + 1), \\ \langle v_y^2 \rangle &= K(3 - 2C_c). \end{aligned} \quad (21)$$

Substituting Eq. (22) into Eq. (21) produces the following simple relationship in which the constant  $K$  cancels out:

$$C_{fic}^2 = \frac{2C_c}{2C_c + 1}. \quad (22)$$

From this relationship it is clear that both measures  $C_c$  and  $C_{fic}$  simultaneously tend to zero (Figure 5). At the critical threshold  $C_c = 0.5$  for the clustering process to appear, the corresponding value of FTC is  $C_{fic} = \sqrt{1/2} \approx 0.7071$ . For moderate levels of compressibility in terms of  $C_c$  the values of FTC always exceed those of classical flow compressibility ( $C_{fic} > C_c$ ). The two measures only coincide for

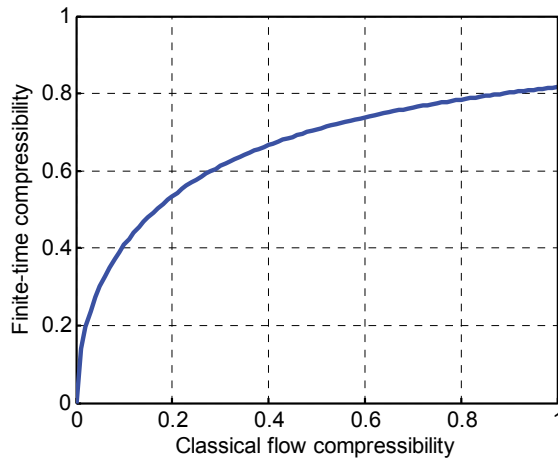


**Figure 5.** Finite-time compressibility  $C_{fic}$  as a function of classical flow compressibility (Paper I).

$$C_{f_{tc}} = C_c = \frac{\sqrt{17}-1}{4} \approx 0.781. \quad (23)$$

For larger values of  $C_c$ , the measure of flow compressibility exceeds that of FTC.

When  $C_c = 1$ , FTC measures  $C_{f_{tc}} = \sqrt{2/3}$ . This implies that for  $\sqrt{2/3} < C_{f_{tc}} \leq 1$  there are no corresponding values of flow compressibility. It is, however, straightforward to show a plausible set of conditions under which the value of FTC may reach  $C_{f_{tc}} = 1$ . The classical flow compressibility, according to the relationship expressed in Eq. (22), is not capable of properly describing such situations.

Let us consider a triangular element, whose edges are perpendicular to each other (Figure 3), and whose vertices are moving apart from each other alongside its edges. Let the squared lengths of the edges  $A$  and  $B$  be respectively  $L_A^2$  and  $L_B^2$  at time step  $t$  and  $L_A^2(1-\varepsilon)^2$  and  $L_B^2(1-\varepsilon)^2$  at time step  $t+1$ , where  $\varepsilon$  is an arbitrarily small value. Furthermore, the measure of the surface area of the element is  $S^t = L_A L_B$  at time step  $t$  and  $S^{t+1} = L_A L_B (1-\varepsilon)^2$  at time step  $t+1$ . Therefore,  $dS \approx -2\varepsilon L_A L_B$  and  $dA \approx dB \approx -2\varepsilon L_A^2$  provided  $L_A \approx L_B$ . Substituting these values into the definition of  $C_{f_{tc}}$  (Eq. (9)) gives

$$C_{f_{tc}} = \frac{2\langle dS \rangle}{\langle dA \rangle + \langle dB \rangle} = \frac{2 \cdot (-2\varepsilon)}{-2\varepsilon - 2\varepsilon} = 1. \quad (24)$$

## **2. Simulation of the dynamics of the Gulf of Finland**

The test area addressed in this study is the Gulf of Finland in the eastern part of the Baltic Sea (Figure 1). This water body hosts an extremely complicated regime of currents (Alenius et al., 1998; Andrejev et al., 2004) and frequent upwelling and downwelling (Myrberg and Andrejev, 2003). It is thus a likely place for large levels of classical flow compressibility, FTC and spontaneous patch generation. Section 2.1 provides a short insight into the major features of circulation and surface dynamics of this water body.

The calculations of FTC performed in this thesis rely on the outcome of contemporary ocean circulation models. The key input for the calculations is the 3D velocity data for the entire Gulf of Finland from two ocean models. Such fields, calculated in a moderate resolution ( $2 \times 2$  nautical miles) for the years 1987–1991 at the Swedish Meteorological and Hydrological Institute, using the Rossby Centre Ocean (RCO) model, were made available in the framework of the BONUS+ BalticWay Cooperation (Soomere et al., 2014). The basic features of this model are described in Section 2.2. This data set was used in the early stage of the presented studies to check the applicability of the concept of FTC. As discussed in Paper III, the time interval of 1987–1991 was chosen to make the results of this study comparable with those obtained within the framework of studies of the quantification of offshore areas in terms of their capacity to serve as sources of environmental risk to the coastal areas due to current-induced transport of floating pollution (Soomere et al., 2011; Delpeche-Ellmann, 2014; Viikmäe, 2014).

The resolution of  $2 \times 2$  nautical miles (about  $5.5 \times 5.5$  km) is considered acceptable in terms of resolving mesoscale dynamics in the open part of the Baltic Sea (Meier et al., 2003; Meier, 2007). Adequate modelling of the dynamics of the Gulf of Finland requires a model with a better horizontal resolution. Velocity fields with enhanced resolution of  $1 \times 1$  nautical miles were calculated using the OAAS model and kindly provided by Oleg Andrejev for the same years 1987–1991. The main features of this model are presented in Section 2.3.

Throughout this work I employed surface velocity fields which were used within two trajectory models (TRACMASS and QTRAC) to evaluate the transport paths of water parcels and simulated floats. Section 2.4 provides a short overview of these models.

### **2.1. Surface dynamics in the Baltic Sea and the Gulf of Finland**

The Gulf of Finland is an elongated relatively shallow sub-basin (mean depth around 37 m) in the eastern part of the Baltic Sea (Alenius et al., 1998; Soomere et al., 2008; Leppäranta and Myrberg, 2009). This gulf has a length of about 400 km and its width ranging from about 50 to 125 km. The gulf is a semi-enclosed water body that has no sill between its waters and the central part of the Baltic Sea (called

Baltic Proper). Therefore, the main atmospheric, hydrodynamic and oceanographic driving forces of the gulf are essentially the same as for the Baltic Proper and the circulation in the gulf experiences extensive impact from the open Baltic Sea.

As the analysis in this thesis addresses exclusively motions in the uppermost layer, I present only a short introduction to the forcing factors and overall properties of surface currents and leave out discussion of other hydrographic properties of this gulf.

The atmospheric forcing in the northern Baltic Proper and in the Gulf of Finland is highly variable on seasonal, interannual and decadal scales. The common understanding is that the most frequent wind directions are south-west and north-north-west (Soomere and Keevallik, 2003). A specific feature of the Gulf of Finland is that the directions of the strongest winds do not necessarily coincide with the most frequent wind directions. The reason is the mismatch of the geometry of the Gulf of Finland (it is elongated in the east–west direction), so that the predominant strong winds blow obliquely to this basin.

The wind conditions in the entire Baltic Sea show a strong seasonal variation. The wind speed is usually strongest (monthly average 8–10 m/s, Niros et al., 2003) in later autumn and winter (October–February) and weakest (5–6 m/s) in early spring and summer (April–June). The predominant wind directions show a similar but less clear seasonal pattern. The described variability naturally generates a remarkable variability in the patterns of Lagrangian surface transport (Soomere et al., 2011) and in the associated probabilities of transport of various items and substances driven by surface currents (Andrejev et al., 2011).

Depending on the value of the so-called North Atlantic Oscillation (NAO) index (Visbeck et al., 2001), two different wind regimes may be present. In essence, this index characterizes the intensity of westerlies in the entire region. If the NAO index is positive, relatively mild westerly winds prevail. When this index is negative, a substantial part of the winds blow from northerly and easterly directions (Lehmann et al., 2002).

The key parameter that describes the typical size of mesoscale or synoptic eddies is the so-called baroclinic or internal Rossby radius. Its values are about 10 km in the Baltic Proper and even smaller, a few kilometres in the Gulf of Finland (Leppäranta and Myrberg, 2009). These values are by several times smaller than in the open ocean (Cushman-Roisin and Beckers, 2011). This is one of the reasons behind extensive variability and largely unordered nature of surface currents in which the overall cyclonic circulation only becomes evident on average (Lehmann et al., 2002). Small values of the Rossby radius make the modelling of the dynamics of the Baltic Sea and especially of the Gulf of Finland a great challenge. Namely, in order to resolve the impact of mesoscale eddies on current-driven transport, the circulation model grid size should not exceed about 50% of this radius (Myrberg and Soomere, 2013).

The presence of strong stratification substantially affects the dynamics of the Baltic Sea and the Gulf of Finland. The deeper parts of both water bodies normally have an almost permanent two-layer structure. Lighter water in the about 40–80 m

thick surface layer is formed owing to river runoff and precipitation. More saline and denser water partially stems from water inflow from the North Sea. As a result, the atmospheric forcing directly affects the upper layer and only indirectly the processes in the bottom layer. The vertical structure may be more complicated in summer and early autumn when a well-mixed surface layer (typical thickness 15–20 m) is formed (Leppäranta and Myrberg, 2009).

The described hydrographic features suggest that the motions in the uppermost layer of the Baltic Sea and the Gulf of Finland are particularly strongly affected by atmospheric forces. The presence of strong stratification in the deeper western part of the gulf leads to the decoupling of the motions in the bottom layers from the direct atmospheric forcing. The impact of winds often leads to Ekman transport in the surface layer and drives coastal upwellings and downwellings (Lehmann et al., 2012). Similarly to the Baltic Proper, the overall circulation scheme of the Gulf of Finland water masses is quite complicated and contains many mesoscale features (Andrejev et al., 2004). Numerical simulations suggest that the inflow into the gulf is frequent along the southern (Estonian) coast of the gulf and outflow mostly occurs adjacent to the northern (Finnish) coast. The idealized cyclonic circulation pattern, characteristic of water bodies on the northern hemisphere, becomes evident only as a long-term average (Myrberg and Soomere, 2013).

The circulation patterns may be radically different in different layers of the Gulf of Finland (Andrejev et al., 2004). These patterns are most complicated in the uppermost layer. According to numerical simulations (e.g., Andrejev et al., 2004), a thin layer (0–2.5 m) on the sea surface is mainly wind-driven. The instantaneous surface currents often represent Ekman-like drift and are usually deflected to the right from the wind direction owing to Coriolis force. The typical current velocities are 5–10 cm/s. As wind is often blowing obliquely with respect to the coast, up- and downwellings frequently occur along the coast of the Gulf of Finland (Myrberg and Andrejev, 2003).

Surface currents are highly variable in the entire Gulf of Finland. Their long-term directional persistency is between 6% and 26% (Leppäranta and Myrberg, 2009). Therefore, statistically, the surface-layer flow is fairly chaotic, particularly in the central part of the gulf. This feature partially justifies the applicability of the concept of ideal Kraichnan flows as the basic assumption in the derivation of the measure of FTC. Another aspect of this feature is that most circulation studies of the Gulf of Finland require some degree of averaging to highlight the mean or residual flow and frequently repeating patterns. The resulting pattern may strongly depend on the choice of the averaging interval (Delpeche-Ellmann, 2014).

Many authors emphasize that the mean circulation in the Gulf of Finland is not a permanent feature and generally represents a statistical property of the flow (Alenius et al., 1998; Myrberg and Soomere, 2013). Somewhat counter-intuitively, Soomere et al. (2011) demonstrated that even an anticyclonic gyre may occur in the central part of the gulf. This result once more underlines that the effect of the wind-driven drift is of great importance in the surface layer of this water body.

The presented features do not exclude the occurrence of certain regularly occurring flow features and transport patterns at certain time scales. A frequently considered time scale in the context of transport of various items on the sea surface is the weekly scale (Delpeche-Ellmann, 2014; Viikmäe 2014). Recent studies have indicated the frequent presence of surface current and transport patterns with a lifetime of about a week (Soomere et al., 2011). Their existence has a high potential for the systematic transport of various substances and items on the sea surface and thus serves as an important precondition, additionally to the frequent presence of downwellings, for the formation of areas hosting high values of FTC.

As mentioned above, seasonal and interannual variations in the wind forcing eventually have considerable impact on both local dynamical processes (such as upwelling or downwelling) and patterns of transport (Myrberg and Andrejev, 2003; Soomere et al., 2011). This seasonality becomes vividly evident in the radical difference in the environmentally optimized fairways that minimize the possibility of the transport of potential pollution from the major fairway to the coastal areas (Murawsky and Woge Nielsen, 2013). It is likely that this variation gives also rise to extensive seasonal and interannual variability of the level of FTC and the entire potential for spontaneous patch formation in the uppermost layer of the Gulf of Finland as discussed in Paper V.

## **2.2. The Rossby Centre Ocean model**

The initial phase of the studies presented in this thesis (Papers I and III) was performed based on velocity information calculated using a moderate resolution version of the RCO model. As this model has been extensively described in the scientific literature (see Meier and Höglund, 2013 for the set-up of the model in detail) and was run in the Swedish Meteorological and Hydrological Institute by the authors of the model, I present here only a brief description of its basic features. The presentation largely follows the material of Paper III. The information about extensive validation of this model against measured data is provided in Meier et al. (2003) and Meier (2007).

The RCO model is a 3D coupled ice-ocean model of the Baltic Sea based on so-called primitive equations. It is intended for simulating physical processes on a wide range of scales, from hours to many decades. The main aim of its development was to produce a tool for reliable analysis of the variability of the marine climate in the Baltic Sea region (Meier, 1999; Meier et al., 2003).

The model depths are based on the so-called Warnemünde digital bottom topography (Seifert et al., 2001). The resolution of the topography data set is 2' along longitudes and 1' along latitudes. The model uses 41 vertical levels in  $z$ -coordinates (Meier et al., 2003; Meier, 2007). The thickness of the vertical layers ranges from 3 m below the surface to 12 m at 250 m depth. The uppermost layer includes depths in the range 0–3 m. It properly accounts for the region's significant driving forces (atmospheric conditions, forcing from boundary sea regions, river discharge), for the underlying bathymetry, and it acceptably resolves the

fundamental hydrodynamic processes in this basin (Meier et al., 2003; Meier, 2007).

The RCO model is, in essence, a variation of the Bryan–Cox–Semtner primitive equation model following Webb et al. (1997), with free surface (Killworth et al., 1991) and open boundary conditions (Stevens, 1991) in the northern Kattegat. In case of outflow, it uses a modified Orlanski radiation condition (Orlanski, 1976). In case of inflow, the temperature and salinity values at the boundaries are smoothed towards observed climatological profiles. The sea level elevation at the boundary is prescribed from hourly tide gauge data. The employed monthly river runoff data originated from the Baltic Sea Experiment (BALTEX) Hydrological Data Centre (BHDC) and SMHI (Bergström and Carlsson, 1994).

The model involves algorithms to replicate the most important dynamic processes in the water column (Meier and Höglund, 2013). For example, subgrid-scale mixing (that is, processes that have scales smaller than the resolution of the model) is parameterized using a turbulence closure scheme of the  $k$ – $\epsilon$  type. This scheme is complemented with flux boundary conditions to include the effect of a turbulence-enhanced layer due to breaking surface gravity waves (Meier, 2001). A flux-corrected, monotonicity-preserving transport scheme following Gerdes et al. (1991) is embedded. No explicit horizontal diffusion is applied. A time step splitting scheme is used, with 150 s for the baroclinic and 15 s for the barotropic timestep. The output is stored once in every 6 h.

The atmospheric forcing used to run the model is based on 3-hourly observations of the sea level pressure, geostrophic wind components, 2 m air temperature, 2 m relative humidity, precipitation, total cloudiness and sea level pressure fields from a regionalization of the ERA-40 re-analysis (Uppala et al., 2005) over Europe, using a regional atmosphere model with a horizontal resolution of 25 km (Samuelsson et al., 2011). Data from all available synoptic stations (about 700 to 800) covering the entire Baltic Sea drainage basin were interpolated on a regular horizontal grid. A boundary layer parameterization was utilized to calculate wind speeds at 10 m height above sea level from the geostrophic wind data (Bumke et al., 1998). Since the atmospheric model tends to underestimate wind speed extremes, the wind regime is adjusted employing simulated gustiness to improve the wind statistics (Samuelsson et al., 2011). The model is coupled with a Hibler-type sea ice model (Hibler, 1979) with elastic-viscous-plastic rheology. It does not account for the roughness of the bottom surface of the ice cover (e.g., ridging).

While the model seems to resolve all the major dynamics of water masses in the Baltic Proper, the gridded representation of the reality evidently does not replicate perfectly all the multitude of processes in the Gulf of Finland. The biggest sources of uncertainties are the inexact parameterizations of the subgrid-scale processes, the inaccuracies of the forcing fields and the spatial resolution. The most significant deviations from reality occur within the internal fields of water masses: the main halocline is often found in the model at a greater height than the real one (Meier, 2007), mixing during salt water inflow is not correctly described (Meier et al., 2003) and the sea surface temperature is subject to sporadic computational

noise (Löptien and Meier, 2011). All these deviations seem to be common to all the contemporary circulation models employed in the Baltic Sea (Lagemaa et al., 2011).

There is ongoing discussion whether the employed spatial resolution (about 2 nautical miles) is sufficient for the replication of the dynamic processes in the Gulf of Finland, where typical values of the baroclinic Rossby radius are 2–4 km (Alenius et al., 2003). Moreover, the output of the RCO model has a relatively large bias for several Lagrangian properties of passive tracers (Kjellsson and Döös, 2012). It has been shown (Andrejev et al., 2011; Viikmäe et al., 2013) that many important statistical properties of current-driven transport are almost invariant with respect to the model resolution and with respect to a particular way of inclusion of subgrid-scale processes. It is therefore acceptable to assume that the RCO model replicates the major statistical properties of the Lagrangian transport in the area of interest, as the effect of mesoscale motions is partially accounted for through parameterization of the subgrid processes.

### **2.3. The OAAS circulation model**

A reasonable way to improve the quality of numerical replication of the properties of velocity fields and an implicit method to validate the results of calculations performed using moderate-resolution data sets is to increase the resolution of the ocean model. The results presented in Andrejev et al. (2011) suggest that the use of spatial resolution of about 1 nautical mile is generally sufficient to appropriately replicate the main features of statistics of Lagrangian transport in the Gulf of Finland. This resolution is supposedly high enough to properly resolve most of the mesoscale dynamics in the Gulf of Finland (Andrejev et al., 2010), which may have been missed in lower-resolution models such as the RCO model.

More specifically, 2D surface velocity fields with a resolution of 1 nautical mile were employed in the latter stage of this study. This data set was extracted from long-term numerical simulations using the so-called OAAS hydrodynamic model. The simulations were also performed within the framework of BONUS+ BalticWay cooperation and provided kindly by the authors of the model. The OAAS model is named after Oleg Andrejev and Aleksander Sokolov (Andrejev and Sokolov, 1989, 1990). This model, according to the comments of the authors, was developed specifically for use in basins with complicated bathymetry and hydrography, such as the Gulf of Finland. It has shown excellent results in replication of the local dynamics of this water body (Gästgifvars et al., 2006). As the model was run by the authors and its extensive description is available in the scientific literature (e.g., Andrejev et al., 2010), I describe only shortly its main features as presented in Papers II and IV.

The OAAS model follows the structure of the Princeton Ocean Model (Bryan, 1969). Similarly to the RCO model, the OAAS model is based on the system of primitive horizontal momentum balance equation, continuity equation, state equation, hydrostatic equation and heat- and salt-transport equations. The model

employs standard simplifications of large-scale circulation models such as the incompressibility of the flow (which has the effect of filtering out acoustic waves, which do not significantly contribute to the circulation) and the Boussinesq and hydrostatic approximation (implying that vertical density gradients are ignored in the equations of horizontal momentum balance and are accounted for only in terms of buoyancy). The equation of state is employed using its implicit formulation, adjusted for the Baltic Sea conditions (Millero, 1976).

In its latest version, the model embeds the classical Smagorinsky scheme (Smagorinsky, 1963) to approximately represent the impact of horizontal turbulence on the gridded velocity field, while vertical small-scale motions are modelled using the so-called Prandtl–Obukhov formula (Kochergin, 1987).

Similarly to the RCO model, the OAAS model deals with time-dependent, free-surface conditions and takes into account baroclinic effects and variations in the Coriolis effect due to latitude changes (using the exact value of the corresponding parameter for each latitude). The finite difference scheme uses Arakawa staggered C-grid (Arakawa and Lamb, 1977) and the method of time-step splitting (Liu, 1978). The bottom friction is introduced by means of the no-slip (first-type Dirichlet) boundary condition for all velocity components. At the sea surface the typical kinematic boundary condition is applied: it is assumed that particles that were initially at the surface shall remain there forever (which is typical for boundary problems in circulation modelling).

The bathymetry implemented in the OAAS model is provided in a regular rectangular coordinate system (equivalent to the Mercator projection) with the original resolution of 1/2' along longitudes and 1/4' along latitudes (¼ nautical mile) for most of the Gulf of Finland. For the central part of the gulf the above-mentioned Warnemünde data set was used. The dynamical and state equations are discretized using a spherical set of coordinates (Andrejev et al., 2010). This is an acceptable practice in simulations of the Gulf of Finland as this narrow water body is elongated in the east–west direction and therefore the deviations of the representation in spherical and rectangular coordinates are minor. The error, associated with the difference in the approximations for bathymetry and dynamical features (~3%), is smaller than the typical uncertainty of the bathymetry (Andrejev et al., 2010).

In this thesis I use surface-layer velocity fields from a model run that was forced with the same river runoff data (Bergström and Carlsson, 1994) and meteorological forcing (a regionalization of the ERA-40 reanalysis over Europe using a regional atmosphere model with a horizontal resolution of 25 km; Samuelsson et al., 2001; Höglund et al., 2009) employed in the RCO model described in Section 2.2. The simulations were performed using bathymetric data with a resolution of 1 nautical mile that was obtained by means of averaging the gridded data set with a resolution of ¼ nautical mile (about 470 m) (Andrejev et al., 2010). The model has a vertical resolution of 1 m (whereas only the uppermost layer is assumed to be 2 m thick). This resolution apparently much better reproduces the 3D variability of the hydrographic and kinematic parameters than the simulations using the RCO model.

The information about extensive validation of this model against measured data in the Gulf of Finland is provided in Myrberg et al. (2010).

As detailed in Paper IV, the OAAS model was run for the interior of the Gulf of Finland to the east of longitude 23°27' E. At this boundary, the OAAS model uses 3D information about hydrographic and hydrodynamic fields calculated using the RCO model for the entire Baltic Sea. The surface velocity data produced using the OAAS model and employed in this work cover the area of interest for the time interval of 1987–1991, with a temporal resolution of 3 h. The data set thus contains 161 600 velocity vectors per day for the entire Gulf of Finland.

#### **2.4. Statistics of Lagrangian motions of selected water parcels**

The calculations of flow compressibility and FTC are based on tracking the paths of selected parcels on the water surface. Such a path is, in essence, a Lagrangian trajectory of the parcel. These trajectories can be easily calculated if the underlying Eulerian surface velocity field is known and if the parcels are passively advected with the flow. I used two techniques to evaluate the Lagrangian trajectories of the vertices of selected triangular surface elements (Figure 3). Firstly, the simulation package TRACMASS (Döös, 1995) was used to track the virtual parcels. This software was used in Paper I based on precomputed Eulerian velocity data extracted from the output of the RCO model.

The TRACMASS code is a widely used tool for global (Döös and Coward, 1997; Döös et al., 2013) and regional (Döös et al., 2004; Engqvist et al., 2006; Soomere et al., 2011) studies of Lagrangian trajectories and transport in various water bodies. It has also been successfully used in research into large-scale atmospheric motions (Kjellsson and Döös, 2012; Kjellsson et al., 2013).

The TRACMASS model first recalculates the RCO model output (that is stored using the so-called Arakawa B-grid cell staggering technique at the corners of each cell, see, e.g., Torsvik, 2013) into another format (so-called C-grid at the walls of each grid cell) by simple linear interpolation. The path of a parcel through each grid cell is evaluated using an analytical solution of a differential equation which depends on the resulting velocities (de Vries and Döös, 2001; Döös et al., 2013).

Alternatively, the trajectories of the simulated parcels were evaluated through an Euler-type Runge–Kutta procedure in Papers II, IV and V. To keep the technique as simple as possible, I used a first-order method. This method yields a global error which is proportional to its time step (Kloeden and Platen, 1999). Whilst higher-order schemes should be implemented to properly calculate the vertical motions of 3D trajectories in strongly stratified environments (Gräwe et al., 2012), surface trajectories are locked in the uppermost layer where the Euler-type scheme apparently gives proper results.

In both versions of the evaluation of Lagrangian trajectories it was assumed that the modelled surface velocities adequately represent the motions in the surface layer of the Gulf of Finland. An exact replication of such trajectories cannot be expected because even small errors in the estimation of Eulerian velocities may

considerably change single trajectories (Vandenbulcke et al., 2009). The modelled velocities obviously include, along with numerical and discretization errors, also uncertainties in forcing data. It is generally expected that various small-scale processes in the real marine environment will lead to a certain spreading of trajectories of initially closely located parcels. The experience with the TRACMASS code reveals that the spreading of the numerically evaluated calculated trajectories is, on average, much slower than the spreading of real drifters (Kjellsson and Döös, 2012; Kjellsson et al., 2013). This issue evidently results from the ignoring of sub-grid processes in the marine environment.

It has recently been demonstrated that even if single trajectories are not represented correctly, several key properties of the statistics of Lagrangian trajectories (e.g., the most likely coastal areas being hit by the parcels released along the major fairway and further driven by currents) are invariant with respect to even substantial modifications of the input velocity fields (Viikmäe et al., 2013). It is thus likely that the outcome of the presented analysis (that relies on a large number of properties of single trajectories) properly reflects the major statistical features of the flow compressibility and FTC.

The entire scheme of calculations in this thesis resembles a similar scheme used for the identification of semi-persistent surface flow patterns (Soomere et al., 2010). An extended time interval  $t_D$  of interest (year 1991 in the calculations performed in Papers I and II) was divided into time intervals (windows) of length  $t_W = 4\text{--}96$  hours (Figure 6).

At the beginning instant of each time window, one virtual floating parcel was seeded into the centre of each wet grid cell of the RCO model. The distance between two neighbouring parcels along latitudes and along longitudes is therefore about 2 nautical miles. The parcels placed at the centres of three adjacent wet grid cells were assigned to a single triangular surface element. The stencil for each grid cell involved the bordering cells in the northern and eastern direction (Figure 3). The motion of the parcels was tracked using either the TRACMASS code or the above-described Runge–Kutta procedure over the time window. Calculations of a subsequent realization were started from the same pattern of parcels' positions with

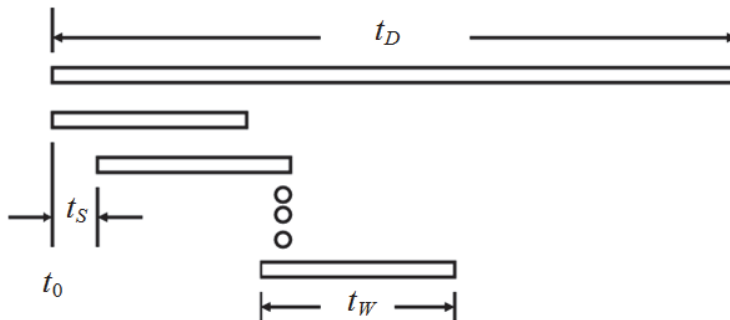


**Figure 6.** Definition sketch of splitting the simulation period into time windows in Papers I and III.

a time lag of  $t_s = 1$  day. Longer realizations thus overlap to some extent.

The set of calculations over single time windows forms an ensemble of realizations of the changes in the surface elements. The outcome of simulations over single time windows was averaged for each wet point of the circulation model over time interval  $t_D$ . The central quantity was a displacement vector field of all the parcels' positions. It was straightforward to calculate the properties of the surface elements to be used to evaluate flow compressibility, FTC as well as the divergence of the surface velocity field from this set of displacements. An example of calculations of the divergence of surface velocity fields from the RCO model, performed as described here with  $t_w = 1$  day, is presented in Section 1.1.

After performing the simulations of the entire pool of realizations, the values of the quantities of interest (flow compressibility or FTC) for each grid cell were pointwise averaged over different time spans on a daily, monthly, seasonal and yearly basis. The resulting distributions characterize the spatial variations in the field of compressibility for different time intervals. Given the nature of the measure, and as described above, high values of FTC in these distributions highlight an increased likelihood for the corresponding grid cells to show patch-formation characteristics.

Papers III and IV introduce a more elaborated and flexible version of the organization of calculations (Figure 7). Similarly to the scheme in Figure 6, the input for the calculations is 2D horizontal velocity components at the sea surface, extracted from any ocean circulation model for a certain sea area and a time

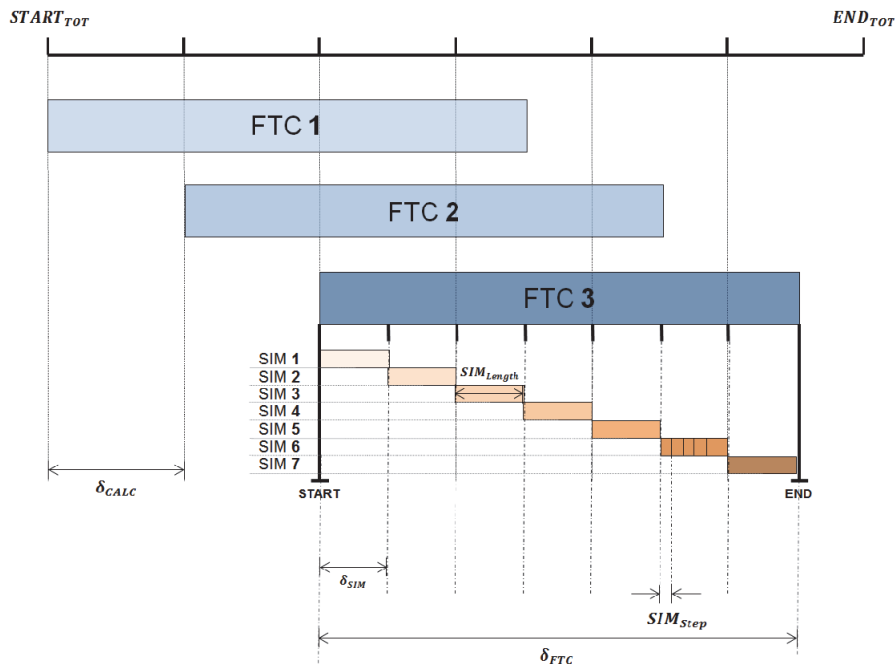


**Figure 7.** A sketch of the QTRAC calculation pipeline.

interval  $[START_{TOT}, END_{TOT}]$ . The temporal resolution of the available velocity fields is  $SIM_{Step}$ .

One virtual passive parcel is then placed at the centre of each wet grid cell of the employed model. Since the ocean models, the velocities from which are used in this study, employ regular rectangular grids with an almost constant step along latitudes and longitudes (Meier, 2001; Meier et al., 2003; Andrejev et al., 2010; 2011), the chosen surface elements uniformly cover the sea area in question.

The simulation interval  $[START_{TOT}, END_{TOT}]$  is then divided into fixed-length time windows. The motion of all the surface elements and their vertices is tracked over these time windows. Their length  $SIM_{Length}$ , in essence, represents the correlation length during which the local properties of flow divergence (convergence) and underlying Lagrangian transport are tracked. As above, the trajectories of the parcels and the evolution of surface elements are resolved and composed according to the triangular stencil (Figure 3). The instantaneous variations in the area of the elements, and of the (squared) lengths of two of its edges ( $dS_t$ ,  $dA_t$  and  $dB_t$ , respectively) are evaluated at each time step of the relevant time window.

After performing the necessary number (as described in Section 3.1) of steps over the particular time window, the respective averages (root mean squares  $dS_{rms}$ ,  $dA_{rms}$  and  $dB_{rms}$ ) are calculated using Eq. (10). The result of each slice of calculations for the surface element, associated with the starting point of the parcel at the right angle of the stencil (Figure 3) over a time window with the length of  $SIM_{Length}$ , is an approximate value of FTC for this point and time window. The set of such values for the entire sea domain (or for some area of interest) is an approximate spatial distribution (realization) of the FTC. Such sets are referred to as instantaneous FTC ( $C_{fic}$ ) maps (Figure 8).

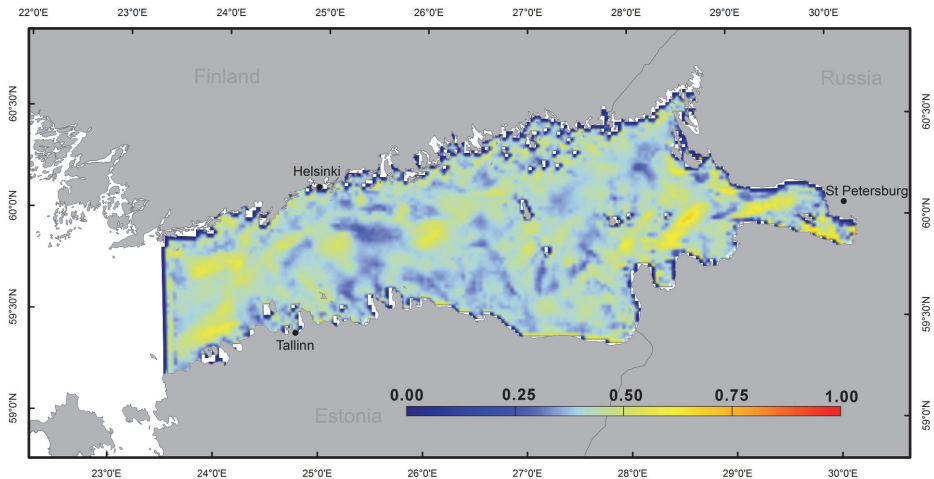


**Figure 8.** An instantaneous  $C_{fic}$  map calculated for 01 March 1987 with  $SIM_{Length} = 24$  h based on the OAAS model data.

The instantaneous FTC maps are generally quite noisy and pixelated as expected for a single realization of a complicated process or measure. To reduce noise and to highlight physically meaningful features, it is necessary to produce and analyse a large number of independent instantaneous  $C_{ftc}$  maps. This is organized by means of performing a series of similar calculations using different starting instants separated by the time lag  $\delta_{calc}$ . The initial set of virtual parcels and surface elements is the same for each subsequent calculation. This results in a set of instantaneous  $C_{ftc}$  maps, each of which represents the chosen time window (and thus a fixed correlation length) but a different starting instant and therefore a different example of the dynamics of the velocity field.

The instantaneous  $C_{ftc}$  maps are collected together into so-called  $C_{ftc}$  batches (denoted as FTC1, FTC2, etc. in Figure 7). These batches typically have a length of one month or one season. Similarly to recent studies of semi-persistent patterns of Lagrangian transport (Soomere et al., 2011) and fairway design (Andrejev et al., 2011; Lu et al., 2012), these batches of a certain length are further processed by means of pixel-wise (grid cell-wise) averaging of the values in similar distributions over a certain set of time windows.

### 3. Calculations of compressibility

The key outcome in Chapter 1 is a simple proof that under reasonable assumptions and short time intervals FTC is a direct extension of the classical flow compressibility. Section 3.1 details the calculation scheme of this measure that has been implemented in Paper II and further used in Papers IV and V. The relevant software (called QTRAC suite) performs all steps starting from the extraction of the input velocity data up to visualization of the FTC distributions.

This chapter provides an insight into the results of calculations of various measures of flow compressibility based on the moderate resolution (2 nautical miles and 6 h) velocity fields from the RCO model. Section 3.2 presents a comparison of the divergence and flow compressibility fields with the changes in the distribution of an initially homogeneous field of virtual parcels on the sea surface based on material from Paper III. A short overview of the calculations of FTC and the dependence of this measure on the parameters of the scheme (most importantly, on the correlation length) is presented in Section 3.3. Finally, Section 3.4 provides a discussion of the basic features of spatial and temporal variability of the FTC in the Gulf of Finland. The main outcome is a demonstration that the concept of FTC is able to provide some essential new information about the structure of surface currents in the Gulf of Finland even if the underlying velocity fields have only moderate resolution.

#### 3.1. The QTRAC Simulation Suite

In order to effectively handle the large number of simulations of various properties of surface velocity fields, I developed a simulation environment (called QTRAC, Quick Tracking for Compressibility) to calculate and analyse spatial distributions of  $C_{ftc}$ . This environment was specifically implemented for the use of higher-resolution (1 nautical mile) velocity fields from the OAAS model, as detailed in Paper II. Its early version was also used to analyse the output of the RCO model.

The basic advantage of the QTRAC suite (Figure 9) is the simplicity of storing internal data used for calculations in a query-oriented set of specifically developed data structures. Similarly to the well-known Matlab environment, this allows for the possibility of querying the calculation pipeline at any stage for intermediate results. This property is useful for performing intermediate consistency (so-called debug/profile) checks, as well as for ensuring the possibility of direct implementation of constraints on the on-going calculations, in order to minimize the chance of unforeseen numerical errors. It also allows for an approach of unit-testing with customizable granularity. This helps to manage the algorithm throughout its evolution.

The QTRAC software was developed using C# in Microsoft Visual Studio 2010 Professional, and it extends across roughly 10 kloc. It can be operated using two different interfaces: command-line and graphical (Figure 9). Through the graphical

user interface (GUI), it is possible to load input vector fields from external models for an arbitrary time span (Figure 6), and to visualize the intermediate results for each individual calculation step as an interactive model map. Through this interface it is also possible to create, configure and run tracking simulations and to calculate various characteristics of compressibility over the area of interest or over subsets of certain regions.

The set of graphical tools and utilities to pack, analyse and process the produced data can be used for other purposes. The current core of the QTRAC suite is the pipeline of calculations of FTC maps starting from velocity fields, tightly lined up with the purpose of this work.

The pipeline (Figure 7) starts with loading the surface velocity information. The first step is to run a parser algorithm over the input information (2D vectors representing velocity fields). The parser at the moment supports and parses all the information contained within the OAAS model's ASCII encoded output files. This information is stored for the use with a staggered Arakawa B-grid (Arakawa and Lamb, 1997). An (offline) interpolation in time is then optionally performed to fit the data with any resolution chosen for the simulations, thus enabling the emulation of sub-model time resolution. The velocities are assumed to vanish at dry grid cells and outside the boundaries of the model.

The displacement of the simulated parcels from their initial position is tracked throughout the chosen time span  $SIM_{Length}$ . It is assumed that parcels are passively carried by the currents that exactly match the modelled velocity field as described in Section 2.4. The used version of QTRAC does not implement any means to replicate the effect of subgrid-scale motions. The coordinates of the resulting trajectories are sampled at a custom rate. The position of the parcels is then reset and started again, typically one day ( $\delta_{SIM} = 24$  h) after the previous simulation's starting instant.

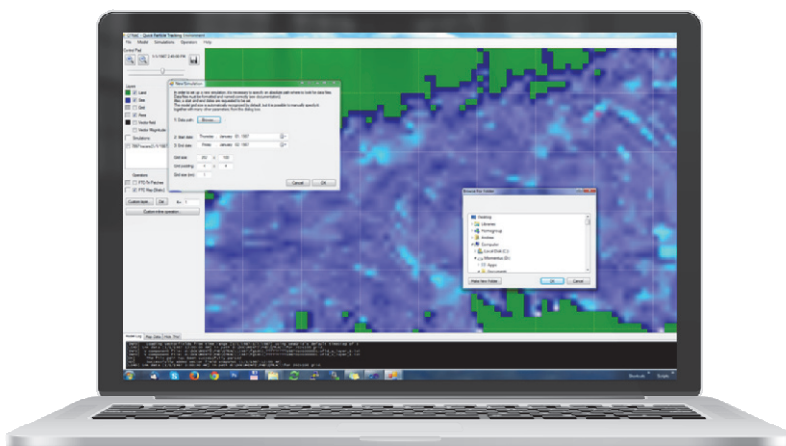


**Figure 9.** The QTRAC suite, running in the GUI mode.

The components of the velocity field at the points of the sea surface that do not coincide with the locations of the model grid points (or their walls) are calculated via a double linear interpolation from the modelled velocity components at the four closest grid points to the current location of the trajectory. The resulting displacement vectors are applied to the parcels component-wise.

At the completion of each simulation over the chosen time span, its results are stored in volatile memory using double-linked lists. The trajectory of each simulated parcel is then matched with the trajectories of its neighbours according to the triangular stencil (Figure 3). This produces linked-lists of triplet-like data structures that represent synchronized sequences of positions of each individual triangular element on the surface, throughout the simulation time span  $SIM_{Length}$ . A value of the FTC for a single realization of the flow is then associated with each grid cell and the initial time of each time span using Eq. (11).

The overall time complexity  $C_{Time}$  of the calculation pipeline may be expressed as a function of the size of the input data set  $N$  and the resolution of the desired output. This measure is asymptotically proportional to

$$C_{Time} = O(N \times T_1 \times T_2), \quad (25)$$

where the terms  $N$ ,  $T_1$  and  $T_2$  refer to the size of the domain (expressed in the number of model grid cells), the overall time span to cover (more specifically, the number of single simulations  $(END_{TOT} - START_{TOT})/SIM_{Length}$ ) and the resolution at which running the simulations (which is a function of  $SIM_{Length}$  and  $SIM_{Step}$ ).

The initial data-loading step deserves particular attention in terms of time complexity presented by Eq. (25). As its time complexity is proportional to  $C_{Time}^{(1)} = O(N \times T_1)$ , in many realistic situations (of sub-asymptotic dataset sizes) its contribution may substantially affect the overall computation time.

The overall space complexity  $C_{Space}$  for the calculation pipeline can be expressed similarly as a function of  $N$ ,  $T_1$  and  $T_2$ . It is bounded asymptotically by

$$C_{Space} = O(N^2 \times T_1 \times T_2). \quad (26)$$

The calculation pipeline has not been deeply optimized for space (understood here as volatile computer memory) consumption. This is intentional, with the main purpose of allowing the possibility of maintaining control structures along with the core data. Keeping this option generally leads to an increased space occupation on the computer. Strictly speaking, the same calculation pipeline could be run at a much lower space complexity if the control structures are ignored.

Certain control structures are definitely necessary because several types of singular situations may occur in the simulations. Their possibility renders any attempt at further optimizing the space complexity (Eq. (26)) risky.

For low-vorticity flows in offshore domains the distortions to the triangular elements normally remain modest. Although the Gulf of Finland is usually thought to have a number of mesoscale eddies (Andrejev et al., 2004), there is evidence that the vorticity field is relatively volatile and only a few more or less circular eddies are present (Viikmäe and Torsvik, 2013). This suggests that, in general, different

parcels are mostly carried in a more or less uniform way by the surface currents. However, in several cases of realistic flows particular attention is needed (Figure 10).

As described in Paper II, QTRAC takes care of three main singular cases which may potentially disrupt the normal path of the calculations. Firstly, whenever a simulated parcel drifts outside the Gulf of Finland, or reaches a dry grid cell of the model (where the velocity is zero), its position is steady and its further behaviour represents neither the properties of surface currents nor the compressibility of surface currents. To remove the associated non-physical values in Eq. (9), the further evolution of such triplets is discarded, starting from the instant when the simulated particle first hits a boundary cell of any kind.

Secondly, it may happen that the three vertices of a particular triplet line up or merge so that the surface area vanishes (with computing precision). This would result in divide-by-zero errors due to machine limitations rather than physical singularities. From a physical viewpoint, this case mirrors strong stretching or deformation in the relevant area, and the evolution of the triangular element no longer adequately characterizes the compressibility. Similarly to the above case, the evaluation of compressibility according to Eq. (9) is interrupted whenever the three triangular elements become too closely aligned or nearly coincident. The further behaviour of such triplets is ignored.

Thirdly, while the expected values of  $C_{fic}$  for each point must be  $\leq 1$ , there still is a possibility for single larger values of this measure at the first steps of the calculation (Figure 11). Such values may appear in quite diverse locations basically

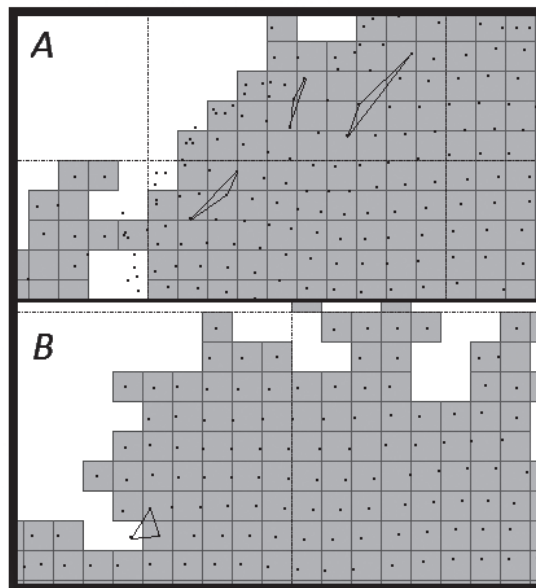


**Figure 10.** Special cases requiring attention. (A) vertices of a triangular element tend to align, yielding a null area; (B) one of the vertices hits the coast (Paper II).

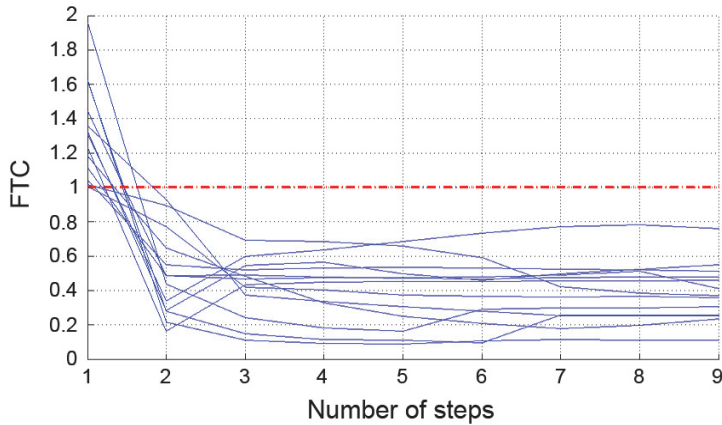


**Figure 11.** Dependence of  $C_{ftc}$  values initially  $>1$  on the number of time steps in a calculation that started on 01 January 1987 (time step of 30 min) (Paper II).

owing to discretization or interpolation errors at the very first internal time steps  $SIM_{Step}$  (Figure 7). Such initial estimates of  $C_{ftc}$  always decrease rapidly, normally within one time step, into the expected range  $[0,1]$  (Figure 11). As a rule, the pointwise values of  $C_{ftc}$  relax to the level close to their final values within 2–3 steps. For this reason, QTRAC is designed to execute a verification of the constraint  $C_{ftc} \leq 1$  for segments of simulations that are five steps long. The code issues a warning when this constraint is violated anywhere within the domain.

Additionally to the routine control of the described singular or clearly erroneous situations, the accuracy of the calculation of classical flow compressibility is implicitly validated by means of verifying whether the basin-wide average 2D flow divergence remains on a low level as discussed in Section 1.1.

### 3.2. Flow compressibility, divergence and concentration field

The major difference between the two measures of compressibility of sea surface (classical flow compressibility  $C_c$  and finite-time compressibility  $C_{ftc}$ ) is that  $C_c$  is a measure of instantaneous properties of the velocity field, whereas  $C_{ftc}$  always involves integration over a certain time interval. This feature of the classical flow compressibility  $C_c$  becomes vividly evident in spatial maps of this quantity (Figure 12). This measure is, in essence, equivalent to a limiting value of FTC if only one time step is taken into account.

As discussed above, the high pointwise values of classical flow compressibility offer some indication about areas where floating items are likely to gather and its low pointwise values indicate areas where concentrations of various items or substances located in the surface layer are likely to decrease. In general these maps are quite pixelated, show very large contrasts and change in time quite rapidly (Paper I). These properties signal that a grid cell characterized by high flow

compressibility does not necessarily mean a high likelihood of that cell to develop patches of floating items during a longer time interval.

Paper III provides further analysis of the potential of the divergence field to represent and characterize the likelihood of patch generation (Figure 13). The instantaneous divergence field is purely local and has essentially no correlation with the long-term flow properties or with flow properties in neighbouring areas. Importantly, large pointwise values of classical flow compressibility mirror high instantaneous local values of divergence or convergence.

Similarly to the classical flow compressibility, the instantaneous maps of divergence and concentration of tracers (Figure 13) are highly pixelated and contain strong gradients. These features are apparently caused by the joint impact of the combination of the discrete nature of the initial field of parcels (one parcel inserted into each wet grid cell of the ocean model) and the highly rotational character of the circulation field in the Gulf of Finland (Lilover et al., 2011). This combination frequently causes a synchronous rotation and advection of the virtual tracers in adjacent model grid cells. While their mutual distance may be almost constant, they may still appear in the same grid cell, for instance, if being aligned along its diagonal (see the middle panel of Figure 1 in Paper I). This process leads to large (by a factor of two) but essentially random local and short-time fluctuations of the instantaneous concentration of tracers. These contrasts are to some extent smoothed by means of averaging these maps over longer time intervals (Figure 13). It is natural that both distributions represented in Figure 13 reveal qualitatively overlapping deviations from the zero mean at the same locations.

As discussed above, the distribution of average divergence, although it is capable of identifying short-term changes in the concentration of floats, is not always suitable to highlight areas of patch generation in the long-term run. The reason is that currents generally carry the emerging patches away from the regions of high convergence.

This feature has been exemplified in numerical simulations of particle

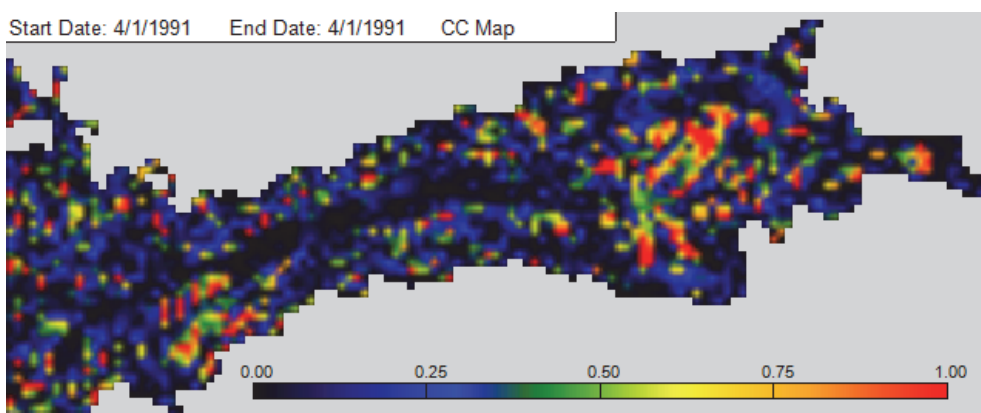


**Figure 12.** Classical flow compressibility of the surface velocity field in the Gulf of Finland on 01 April 1991 based on velocity fields from the RCO model (Paper I).

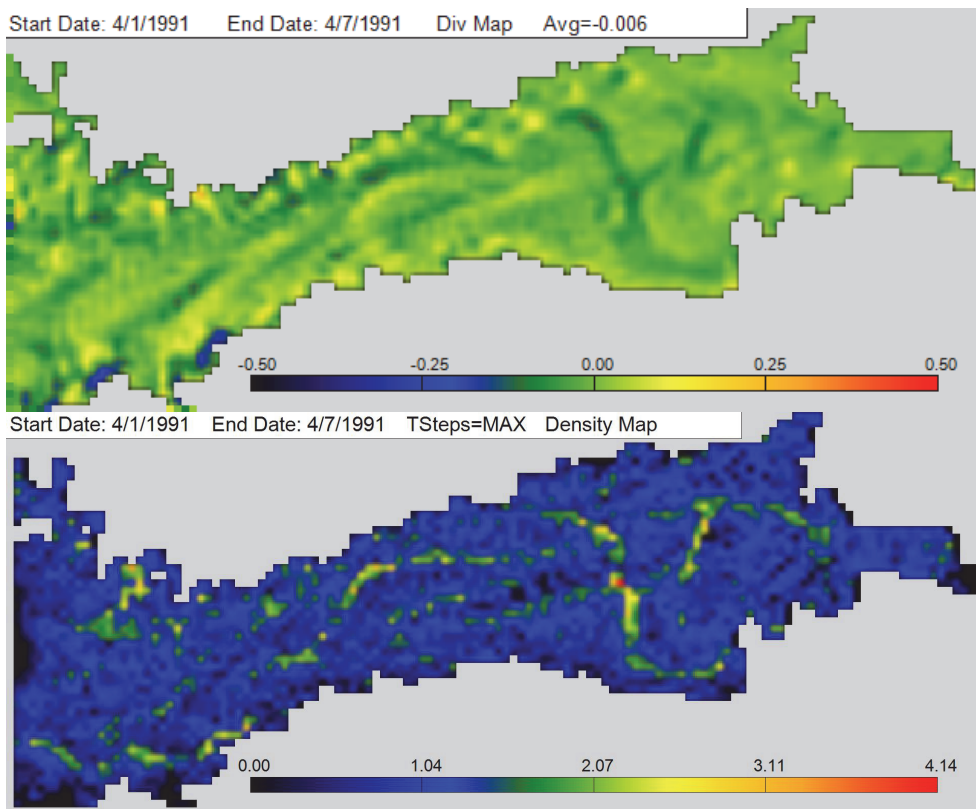


**Figure 13.** Average divergence (1/s; negative values indicate convergent flow) of the water surface (upper panel) and concentration of floats (per grid cell) in the Gulf of Finland for 01–07 April 1991 (lower panel) (Paper III).

aggregation in the boundary region of an anticyclonic eddy. The core result was that the highest particle concentration coincided with the vorticity patterns, but not with the high-convergence area. A probable reason for such an effect was spatial de-correlation between the divergence field and the areas of high concentration. Namely, the areas hosting high convergence were spatially associated with the eddy, while the simulated parcels were carried with the surface currents (Samuelson et al., 2012).

### 3.3. Calculation of finite-time compressibility

An attempt to qualitatively link the concentration field of virtual tracers with the properties of the FTC field has been made in Papers II and III based on the RCO velocity fields with a moderate spatial resolution. The maps of FTC account for changing flow properties over longer time windows and therefore are better candidates for indicating enhanced likelihood of the development of patches than the divergence field or the distribution of classical flow compressibility.

The analysis in Paper I demonstrates that the FTC values tend to behave qualitatively similarly to the classical flow compressibility, although the particular values of these two quantities are generally different (Figure 5). The properties of the FTC maps obviously depend on the averaging interval used in their calculation. The parameters of the calculation scheme depicted in Section 2.4 may have a major effect on the results of the calculation, similarly to the analogous parameters in the calculation of the statistics of Lagrangian transport of pollution by surface currents (Viikmäe et al., 2010; Viikmäe, 2014).

A qualitative overview of the role of different parameters in Figures 6 and 7 in the FTC calculations is provided in Papers IV and V. Three parameters indicated in these figures can be adjusted only by rerunning the ocean model. These are  $START_{TOT}$  and  $END_{TOT}$  (that define the entire time interval for which velocity data are available) and the temporal resolution of this data set  $SIM_{Step}$ . The presence of high seasonal variations in the forcing and dynamics of the Gulf of Finland suggest that the FTC calculations should cover at least one year. The analysis in Andrejev et al. (2011) signals that in order to obtain climatologically valid FTC distributions, the calculation should cover at least 3–5 years.

The level of representation of details of the velocity field in the input data for the FTC calculations substantially depend on the time step of the available velocity data. It is, however, customary that in order to keep the data set within a reasonable size, the output of ocean models is saved and/or provided to the user only once in several hours. For example, the RCO data were only available once in 6 h. Such large values of the  $SIM_{Step}$  parameter may smooth out high local instantaneous  $C_{fic}$  values. In general, the longer the simulation step is, the greater is the chance to overlook small-scale or short-lived processes which may affect high  $C_{fic}$  counts. While the values of  $C_{fic}$  highly depend on time correlations, it is not known beforehand for how long such correlations exist. However, as the patch-formation process at the scales comparable with the grid size of the ocean model usually takes several days, the values of  $SIM_{Step}$  on the order of a few hours are acceptable.

The calculation scheme (Figure 7) contains several other adjustable parameters that can be varied in order to properly highlight phenomena with specific time scales. An in-depth analysis of the reasonable choice of these parameters for the Gulf of Finland conditions was performed in the context of semi-persistent patterns of Lagrangian transport (Viikmäe et al., 2010; Soomere et al., 2011). The key parameter is the length of each parcel tracking  $SIM_{Length}$ , called time window by Viikmäe (2014). It defines the length of the time interval over which the correlation between the convergence field and the Lagrangian transport of the emerging patch is considered.

Based on the concept presented in Samuelson et al. (2012), the formation of high concentrations in the marine surface layer apparently is strongest and most evident when a domain of convergence of the surface velocity field moves together with the underlying currents. It is thus natural to assume that high values of  $C_{fic}$  emerge at time scales that roughly match the persistency of the local Lagrangian transport.

Semi-persistent patterns of Lagrangian flows have a typical time scale of a few days in the Gulf of Finland (Soomere et al., 2011). Based on this result, the values of  $SIM_{Length}$  up to 3 days have been used in this thesis (Figure 14). The use of very short windows leads, as expected, to maps that are qualitatively similar to the maps of average divergence or classical flow compressibility (Paper III).

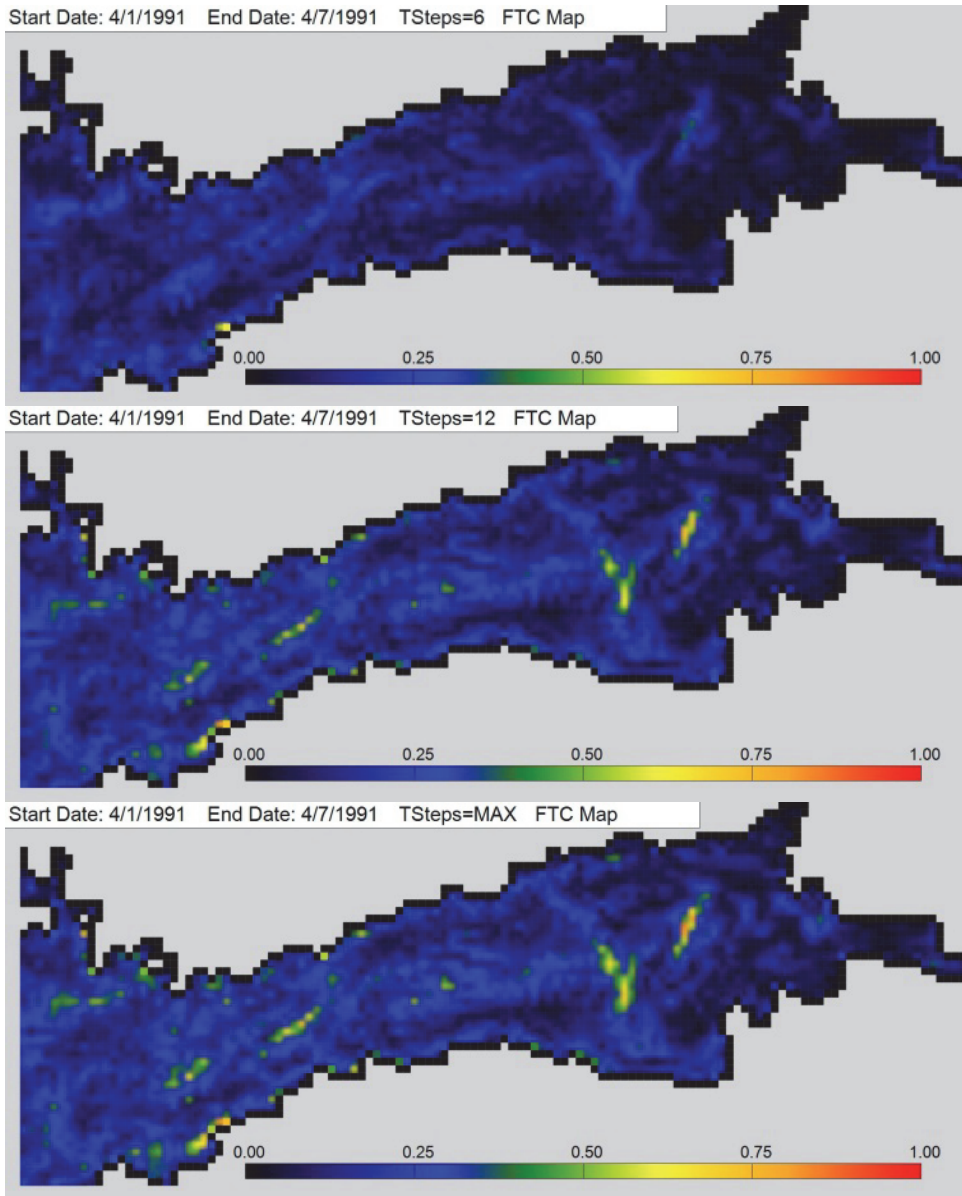


**Figure 14.** Average finite-time compressibility of the water surface in the Gulf of Finland for one week (01–07 April 1991), calculated using the time window of 24 h (upper panel), 48 h (middle panel) and 72 h (lower panel) (Paper III).

The gradual lengthening of the time window allows for tracking the distortions of the surface elements over a certain time and thus makes it possible to identify areas over which the concentrations are likely to increase cumulatively. The relevant maps are often much richer in content than similar maps of average divergence. The use of very large time windows tends to gradually smooth out many features.

Another key parameter is the batch length  $\delta_{FTC}$ . It defines the characteristic time scale (weekly, seasonal, annual, etc.), during which the frequent patch formation areas are expected to exist. An average over the instantaneous FTC maps evidently suppresses noise and contrasts in single maps but may also smooth out processes and phenomena that occur during shorter time intervals. A proper choice of  $\delta_{FTC}$  plays a particular role in the calculations of certain over-threshold values of FTC as discussed below.

The role of the temporal distance (time lag)  $\delta_{SIM}$  between two consecutive calculations of instantaneous  $C_{fic}$  values is less obvious. Formally, it defines the total number of  $C_{fic}$  calculations to be performed based on the existing velocity data. A much more important request is to ensure that subsequent realizations of the trajectories of parcels that form the triangular elements (Figure 3) are uncorrelated.

As discussed above, the trajectories of initially closely located virtual tracers, calculated with the TRACMASS code from the RCO velocities, tend to stay together. This means that the trajectories of parcels that start their drift from the same model grid cell, either simultaneously or with a small time lag, are strongly correlated. To avoid such correlations, the subsequent calculation should only start after the majority of parcels have drifted to the neighbouring cells.

Given the typical surface velocities in the Gulf of Finland 10–20 cm/s (Alenius et al., 1998), it would take about 6–10 h for the selected parcels to enter the neighbouring RCO model grid cell. The analysis in Viikmäe et al. (2010) suggests that the statistics of Lagrangian transport only weakly depends on the particular value of the time lag and reasonable results can be obtained for as large values of  $\delta_{SIM}$  as 10 days. Based on this observation, in the analysis of this thesis always  $\delta_{SIM} \geq SIM_{Length}$  to prevent the produced results from being serially correlated.

### 3.4. Spatial distribution of finite-time compressibility

The results of several series of calculations of spatio-temporal distributions of FTC based on the RCO velocity data with a moderate spatial resolution (2 nautical miles) are reported in Papers I and III. Spatial distributions of the FTC for single weeks and months revealed comparatively large variability for this measure, both in space and time. The contrasts were, as expected, the largest for maps averaged over relatively small time intervals (weeks, Figures 14 and 15) whereas averaging over several months resulted in maps that contained much less details (Figure 16).

High values of FTC are spotted at different locations in the Gulf of Finland. The patterns of high and low FTC levels vary considerably in different months and

seasons. Some of these areas have an elongated stripe-like shape and are located close to the shore and most likely coincide with regions hosting intense vertical motions (coastal downwelling or upwelling, respectively) (Myrberg and Andrejev, 2003; Lehmann et al., 2012). Other areas of high values of FTC may mirror the regions between upwelling filaments that have reached the offshore, or convergence zones between coastal currents and offshore mesoscale circulation (cf. Andrejev et al., 2004; Soomere et al., 2011).

Some elongated areas of high FTC become visible across the central and eastern sections of the Gulf of Finland. Their presence may be associated with regions where Lagrangian surface transport is accompanied by gradual contraction of the surface area. These offshore areas may also be considered as likely regions to host patch formation.

The overall average level of  $C_{ftc}$  across the whole Gulf of Finland is around 0.4 during the windy season (October–March) when the values are generally the highest. A similar analysis using the velocity data from the OAAS model with a finer resolution of 1 nautical mile (Paper II) reveals that the FTC maps for single weeks and months still contain a relatively high variability both in space and time. While for some periods the average FTC maps hardly show any recognizable features, during other intervals they contain a number of clearly defined areas with high values of  $C_{ftc}$ . The typical maxima of  $C_{ftc}$  for single month-long batches are around 0.6 (Paper II), that is, below the threshold  $C_{ftc} = \sqrt{1/2}$  for the clustering process (Section 1.3) to become effective. The largest values of  $C_{ftc}$  are usually found (i) in the nearshore of the southern coast of the Gulf of Finland and (ii) in the north-western and (iii) easternmost regions of the gulf.

Offshore areas hosting the largest monthly average values of  $C_{ftc} > 0.5$  are normally different in different months (Figure 16). One area at the mouth of the River Neva in the easternmost part of the gulf shows regularly large values of  $C_{ftc}$ . This region is characterized by a very small internal Rossby radius (Soomere et al., 2008). It hosts a complicated flow pattern driven by the interaction of basin-wide

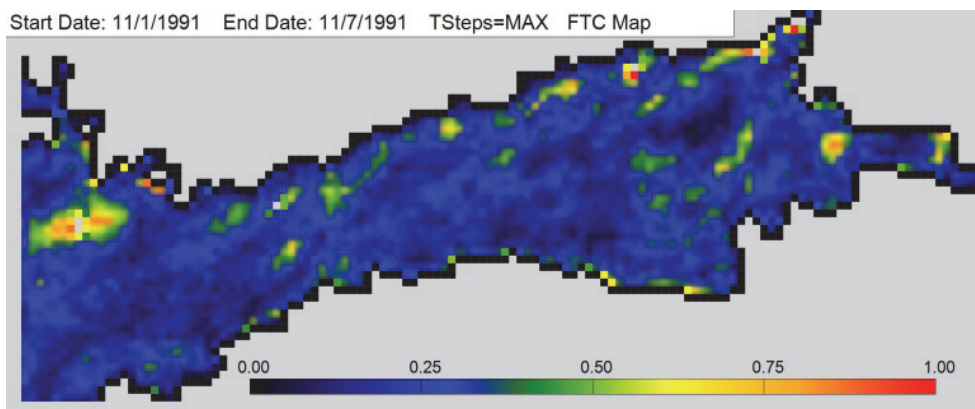


**Figure 15.** Average finite-time compressibility of the water surface in the Gulf of Finland for one week in November 1991, calculated using the time window of 48 h (Paper I).

circulation of water masses (incl. an optional anticyclonic gyre in the surface layer (Soomere et al., 2011)) with the large runoff of the River Neva (Leppäranta and Myrberg, 2009). Another relatively persistent area of high values of  $C_{ftc}$  is located in the middle of the widest part of the Gulf of Finland.

The maps presented in Figure 16 give a flavour of the spatial distribution of areas with high FTC for limited time intervals. Owing to extensive variability of these maps for different months and seasons, they fail to deliver a proper representation of areas where the clustering of particles or formation of high concentrations is likely to occur in long-term run. An extension of either of the time window or the averaging (batch) length does not lead to a more advanced understanding of the situation as the average  $C_{ftc}$  tends to fade towards lower values when considering longer intervals (Paper I). A basin-wide type of pointwise averaging would likely smoothen out such features, with an intensity which is proportional to the size of  $\delta_{FTC}$ .

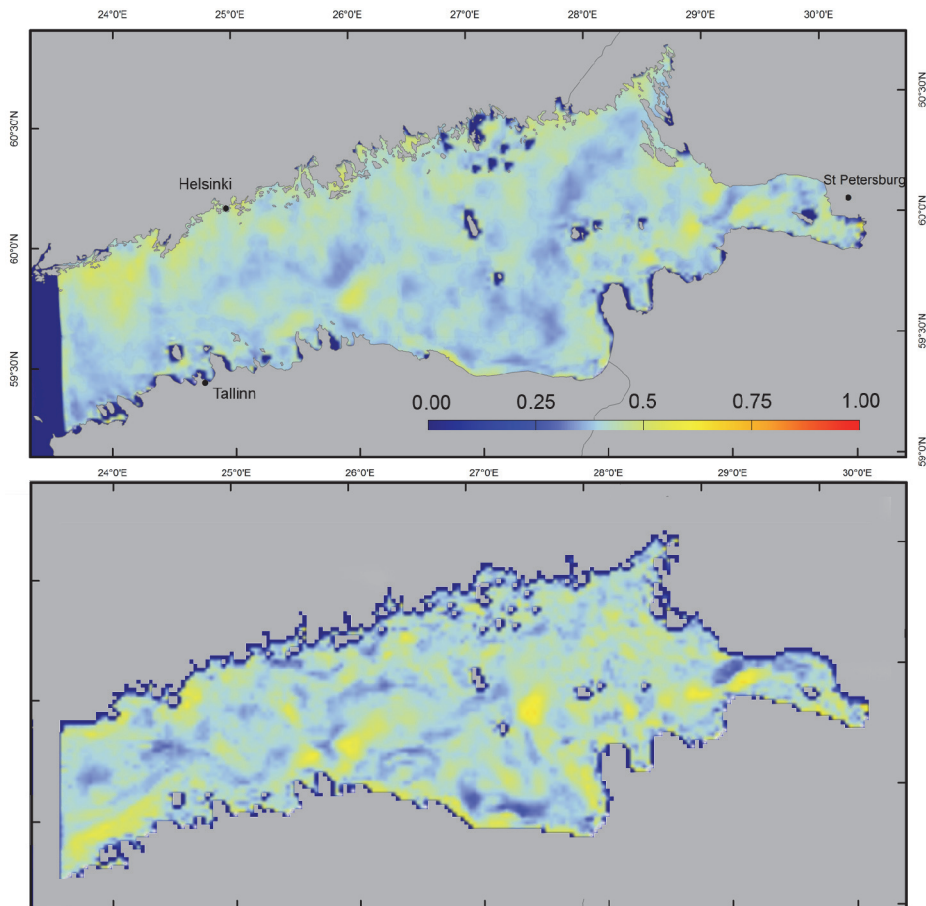


**Figure 16.** Spatial distribution of finite-time compressibility (colour code) for the Gulf of Finland in December 1987 (upper panel) and February 1988 (lower panel) (Paper II).

## 4. Quantification of spontaneous patch generation

The definition of FTC (Section 1.3) suggests that certain changes in the surface concentrations may occur already at moderate average levels of  $C_{ftc}$ . As discussed in Section 1.4, a much faster process of changes in the concentration of floats may start if these items start to cluster together (Falkovich et al., 2001). Rapid formation of clusters is likely to occur if the threshold  $C_{ftc} = \sqrt{1/2}$  is exceeded in some sea area for a relatively long time. In other words, systematic spontaneous patch formation eventually occurs in such areas when this threshold is exceeded.

This chapter is dedicated to the analysis of this possibility. The relevant efforts were started in Paper II and continued in Papers IV and V based on the calculations using velocity fields with a spatial resolution of 1 nautical mile. Section 4.1 starts this analysis from considering the temporal course of FTC based on material from Paper II. The idea of looking only at these values of FTC that exceed the threshold for the clustering is presented in Section 4.2 following the material from Paper IV. A more detailed analysis of areas in which this threshold is often exceeded (Section 4.3, Paper IV) leads to the identification of nine clearly distinguishable regions in the Gulf of Finland where spontaneous patch formation via the clustering phenomenon is likely to occur during an appreciable time each year. Seasonal variations in the location and magnitude of these areas are addressed in Section 4.4 based on the material from Paper V.

### 4.1. Temporal course of high finite-time compressibility

The analysis of the frequency and timing of events in which  $C_{ftc} > \sqrt{1/2}$  has been started in Paper II based on the velocity fields from the OAAS model with a resolution of 1 nautical mile. The use of better-resolution data compared to simulations performed based on RCO data in Papers I and III revealed many more details in spatial distributions of FTC.

Figure 17 illustrates the temporal course of FTC at six grid cells in the easternmost part of the Gulf of Finland, in an area where the monthly average FTC values are relatively large. The typical levels of FTC at these points were 0.4 during the calm season in 1987 and only slightly higher during the windy season in 1987–1988. Importantly, the threshold  $C_{ftc} = \sqrt{1/2}$  was exceeded at several points during a week also in the calm season. This feature suggests that simple averaging of the FTC values (even over batches of variable length) is generally not able to reveal the locations and time intervals of spontaneous patch generation.

For this reason, Papers IV and V focus on the frequency at which  $C_{ftc}$  exceeds the threshold  $C_{ftc} = \sqrt{1/2}$  for clustering and possibly associated spontaneous formation of patches of floating tracers. The course of  $C_{ftc}$  presented in Figure 17 suggests that this threshold may be exceeded in all seasons and possibly even in locations where the average values of  $C_{ftc}$  are not exceptionally large.

To identify and highlight those grid cells whose values of  $C_{fic}$  often exceed the threshold, a different way to extract relevant information from the instantaneous  $C_{fic}$  maps has been introduced in Paper IV. Namely, the temporal behaviour of single  $C_{fic}$  values for all wet grids of the circulation model and inside each calculation batch is analysed using a method similar to the peak-over-threshold approach. This approach is widely used in various fields of physical oceanography (e.g., in Holthuijsen, 2007).

The method employed in Papers IV and V relies on a simple count for each wet grid cell of the model of how many instantaneous values of  $C_{fic}$  exceed the threshold of  $\sqrt{1/2}$  at which clustering is likely to start. This count is performed during the time interval covered by a single batch in Figure 7, or for a selection of batches grouped together. The result is a map of the total count (equivalently, the frequency of occurrence) of over-threshold values of  $C_{fic}$  within a single batch (Figure 18) or a group of batches.

Finally, the total number of such values (for example, for specific seasons) is counted for each wet grid point over a set of batches of a fixed length. This procedure is equivalent to calculating the average number of occasions of  $C_{fic} > \sqrt{1/2}$  for each cell. To some extent, it reduces the numerical noise associated with the moderate temporal and spatial resolution of the input data. The actual variations in the  $C_{fic}$  values are ignored in the count of the total number of

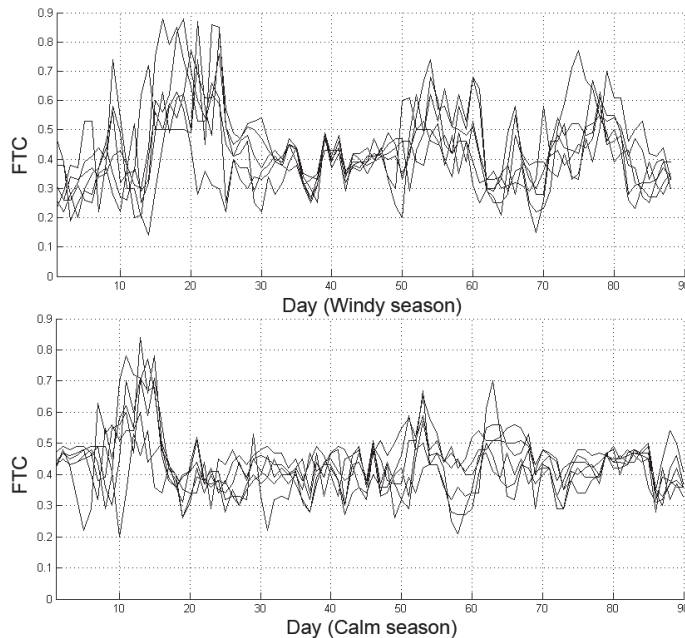


**Figure 17.** Temporal course of finite-time compressibility at six grid cells in the area of relatively high values of  $C_{fic}$  located outside the Neva Bight, for the first three months of the windy season (October 1987–March 1988, upper panel) and the calm season (April–September 1987, lower panel) (Paper II).

over-threshold values. The resulting maps of average counts of above-threshold values of  $C_{ftc}$  (optionally over a set of batches) eventually highlight the areas hosting most frequent (or persistent) spontaneous patch generation.

## 4.2. Persistency of high values of finite-time compressibility

The areas that occasionally host high FTC in the instantaneous maps (Figure 16) as well as in the counts of over-threshold values of  $C_{ftc}$  in single batches (Figure 18) are quite variable in space and time. Moreover, the process of constructing the maps of frequency of occurrence of over-threshold FTC values ignores part of the variability: even if a single FTC value is exceptionally high, its actual value is ignored and only the event  $C_{ftc} > \sqrt{1/2}$  is counted. It is therefore not unexpected that the presence of above-threshold instantaneous values of  $C_{ftc}$  are smoothed out already for relatively short batches (Figure 18).

Subsequent integration of the count of over-threshold  $C_{ftc}$  values over longer sets of simulations generally smoothens out details and contrasts of single maps and their averages for shorter time intervals. Interestingly, some features are very persistent. Figure 19 demonstrates that certain areas of the Gulf of Finland often host above-clustering-threshold values of FTC in 90-day-long and 180-day-long averages.

The overall average count of  $C_{ftc} > \sqrt{1/2}$  is generally fairly small: around 0.93 days for 90-day-long batches and 1.91 days for 180-day-long batches (Paper IV). A few clearly distinguishable regions show such counts of up to 30 and 60 days, respectively. In other words, in these regions the phenomenon of spontaneous

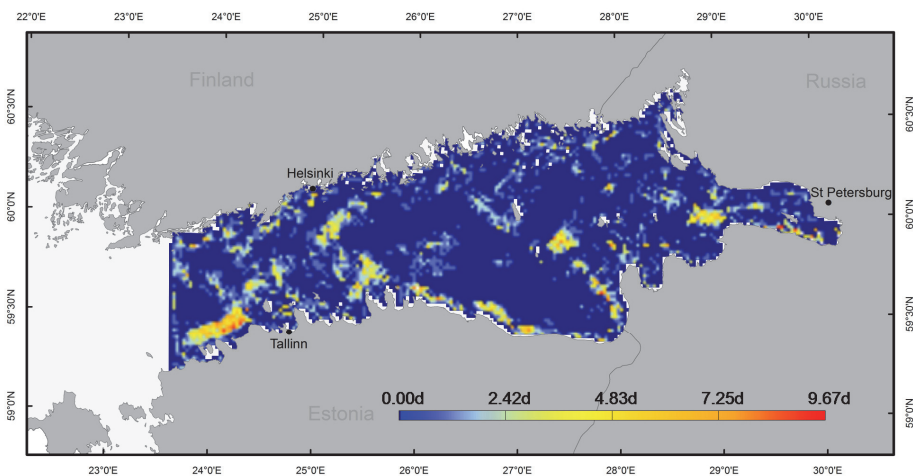


**Figure 18.** Map of the count of days, during which single values of  $C_{ftc}$  exceed the threshold of  $\sqrt{1/2}$  within a batch of length  $\delta_{FTC} = 30$  days. This map was calculated with  $START_{TOT} = 01$  December 1987,  $SIM_{STEP} = 3$  h (Paper IV).

patch formation is likely to take place for over one third of the time. This count only characterizes the frequency of potential occurrence of clustering but does not indicate how persistent this phenomenon is. Although the results averaged over 180 days reveal clearly less spatial variability of the high- $C_{ftc}$  count, Figure 19 suggests that the maximum relative frequency of the occurrence of above-threshold values of  $C_{ftc}$  is almost the same for 90-day-long and 180-day long batches. A natural conjecture is that some areas of the Gulf of Finland may host intense patch generation during substantial time intervals.

The most remarkable coastal areas where over-threshold values of FTC often

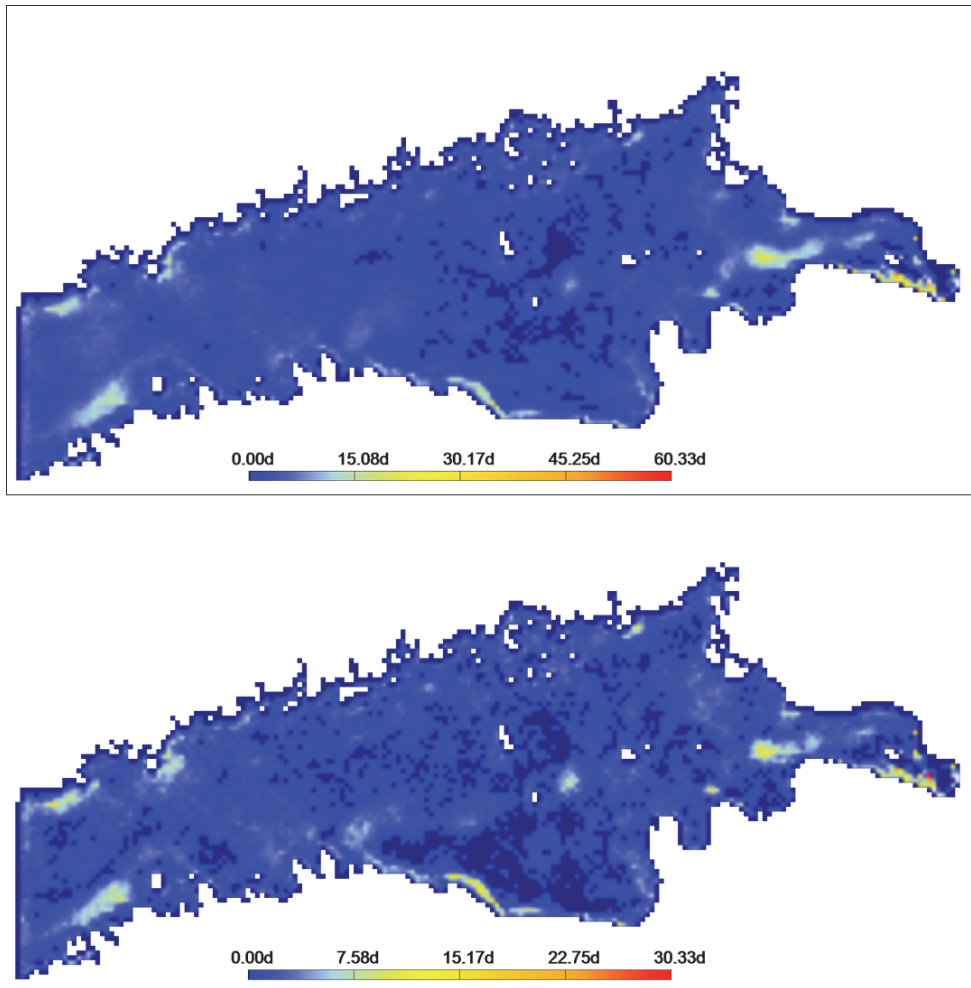


**Figure 19.** Maps of the average count of the over-threshold FTC values for 180-day-long (upper panel) and 90-day-long (lower panel) batches calculated using the following parameters:  $\delta_{SIM} = 24$  h,  $SIM_{Length} = 12$  h,  $SIM_{Step} = 1.5$  h. The colour coding shows how many times in total the values of  $C_{ftc}$  exceed the clustering threshold 0.7 in total of 16 maps for 90-day-long batches or 8 similar maps for 180-day-long batches (Paper IV).

occur are located along the north-eastern coast of Estonia, between the islands of Naissaar and Pakri, and near the northern coast of the gulf (Figure 19). The most contrast offshore areas highlighted in Figure 19 are located at the entrance to the Neva Bight and in the widest part of the gulf. As explained in Paper V, a similar area next to Saint Petersburg may reflect the inability of the model to properly resolve the impact of the Saint Petersburg Flood Protection Facility.

The long-term average pointwise values of frequent occurrence of the values  $C_{fic} > \sqrt{1/2}$  vary considerably along the gulf (in the east–west direction, Paper V). The southern regions host systematically more frequent occurrence of  $C_{fic} > \sqrt{1/2}$  than the northern parts. The central part of the gulf has an overall low level of this measure. The easternmost part of the gulf hosts several high peaks of  $C_{fic}$ , which apparently reflect frequent convergence of the overall circulation of water masses with the voluminous freshwater discharge into this region.

### 4.3. Potential regions of spontaneous patch formation

As the over-threshold values of FTC support the possibility of the clustering of floating items on the sea surface, it is natural to assume that the spatial maxima of the frequency of occurrence of such values indicate the areas in which spontaneous patch formation is likely. In other words, spontaneous increase in the concentration of surface floats, pollution or contaminants locked in the surface layer is much more likely in these areas than in other sea regions.

An attempt to locate such areas is undertaken in Papers IV and V by means of an analysis of the temporal persistency of regions of the frequent occurrence of over-threshold values of FTC for single batches. Each of such areas highlighted in a certain batch has been associated to an oval-shaped region. This oval roughly matches the orientation and appearance of each area. The centre of the oval is associated with the location of the relevant local maximum count of over-threshold values of FTC.

The areas of likely and frequent patch generation were selected according to the persistency of their appearance in the maps of counts of over-threshold FTC values. Only those areas were selected, for which a clearly identifiable local maximum was present within at least 80% of the total amount of single batches. As the duration of the batches used in this procedure was 90 and 180 days and the simulations covered the time interval 1987–1991, the selected areas were apparently present in all seasons. Therefore, they serve as a first approximation of the “climatologically” valid specification of likely spontaneous patch-generation regions.

The described procedure highlighted nine clearly separated regions where high values of  $C_{fic}$  regularly occur (Figure 20). The majority of such areas (3, 4, 5, 7, 9; also area 8 to some extent) are located near the southern coast of the gulf at more or less regular spatial intervals. Only two such regions became evident near the north-western coast of the gulf, to the west of Helsinki. As discussed above, area 9 near Saint Petersburg may be an artefact of the model. The existence of area 8

apparently reflects the convergence of the runoff of the River Neva with the overall circulation in the gulf (Leppäranta and Myrberg, 2009). The most interesting finding is the existence of area 6 in the middle of the widest part of the gulf.

A comparison of Figure 20 with the maps presented in Figures 14–16 demonstrate that several areas highlighted in Figure 20, most notably areas 5, 8 and 9, were already occasionally visible (although not identified) in the results of calculations that employed lower-resolution velocity data. This (at least partial) invariance of persistent high-FTC areas signals that this measure is able to reveal certain interesting feature of the structure of surface currents even if only moderate-resolution data are available.

The long-term persistency of the areas highlighted in Figure 20 can be to some extent quantified by means of the maxima in the count of over-threshold FTC values for single batches (Paper IV). The standard deviation of these maxima is generally well below half (and often 20–30%) the relevant average value. This signals that the selected areas are fairly persistent. Area 6 has the smallest persistency and strength (defined as the average of the maxima in question). It is likely that this area may be present only during particular seasons (Section 4.4).

As discussed above, the patch generation process is generally slow and requires several consecutive days of high correlation between the convergence field and the underlying Lagrangian transport. The results of FTC analysis, including the count of over-threshold values of FTC, reflect the overall frequency of high-FTC events but do not reveal whether such events occur separately or in sequence. The possibility of long sequences of high FTC values in certain locations can be to some extent characterized by means of the longest continuous time interval during which  $C_{ftc} > \sqrt{1/2}$ . This analysis has been presented in Paper IV for each batch in each of areas 1–9 (Figure 20).

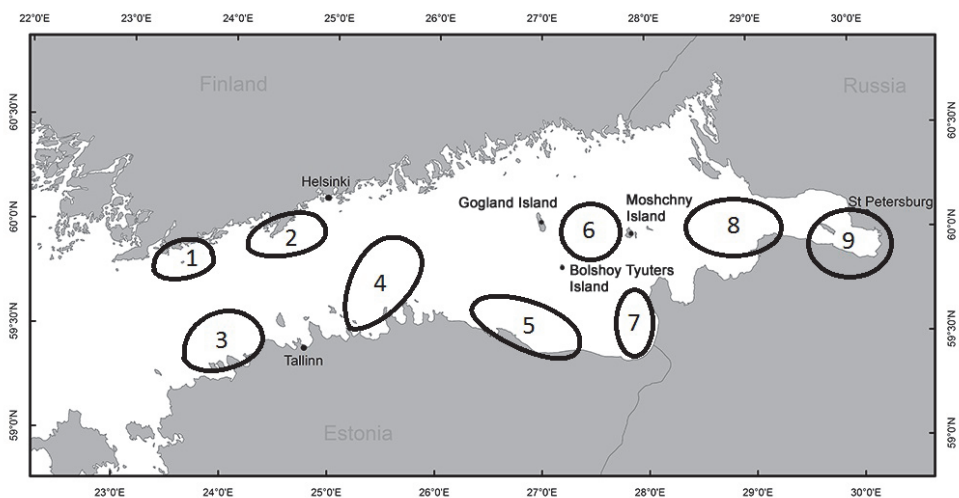


**Figure 20.** The set of persistent high- $C_{ftc}$  regions in the Gulf of Finland in 1987–1991 (Paper IV).

The average length of the time interval defined in this manner for single years and areas was mostly between 2 and 3 days (Figure 21). This time interval is apparently long enough for patch formation. Its smallest values were found for area 6. It is thus natural to conclude that the overall pattern of currents in this offshore region is more variable than in other areas presented in Figure 20.

#### 4.4. Seasonality of areas hosting high finite-time compressibility

A well-known feature of atmospheric forcing of the Baltic Sea and the Gulf of Finland is its strong seasonal pattern (Leppäranta and Myrberg, 2009). This feature is clearly reflected in seasonal variations in currents and associated Lagrangian transport (Soomere et al., 2010; Andrejev et al., 2011; Viikmäe and Soomere, 2014). Potential implications of this pattern are briefly analysed in Paper V.

Based on the analysis of the seasonal course of wave heights in the Gulf of Finland (Zaitseva-Pärnaste, 2013), the following representation of seasons was chosen in Paper V: May, June and July formed the calm spring–summer season, August, September and October belonged to the transitional autumn season, November, December and January were associated with the windy autumn–winter season and February, March and April with the transitional spring season. Similarly to the analysis in Section 4.3, for each wet grid point it was counted how many times the instantaneous values of  $C_{ftc}$  exceeded the threshold for the rapid formation of clusters in each season.

The seasonal areas of high values of  $C_{ftc}$  (Figure 22) are, as expected for shorter averaging intervals, more concentrated than similar areas in Figure 20. Some areas are evident only during certain seasons. For example, area 4 is clearly distinct during spring and area 2 during autumn. Somewhat unexpectedly, area 6 is prominent in spring and winter.

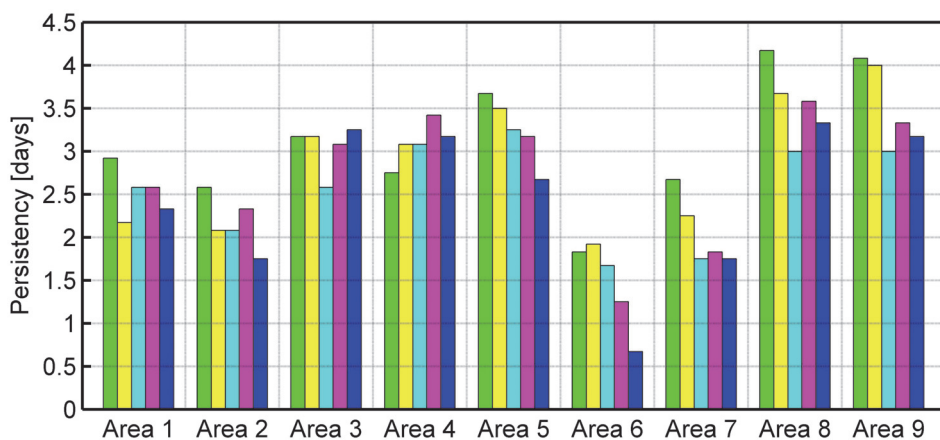


**Figure 21.** Annual average of the maximum duration of consecutive events of  $C_{ftc}$  within single 30-day-long batches in locations of the highest counts of the over-threshold FTC values in areas 1–9 (Figure 20) in the Gulf of Finland in 1987–1991 (Paper IV).

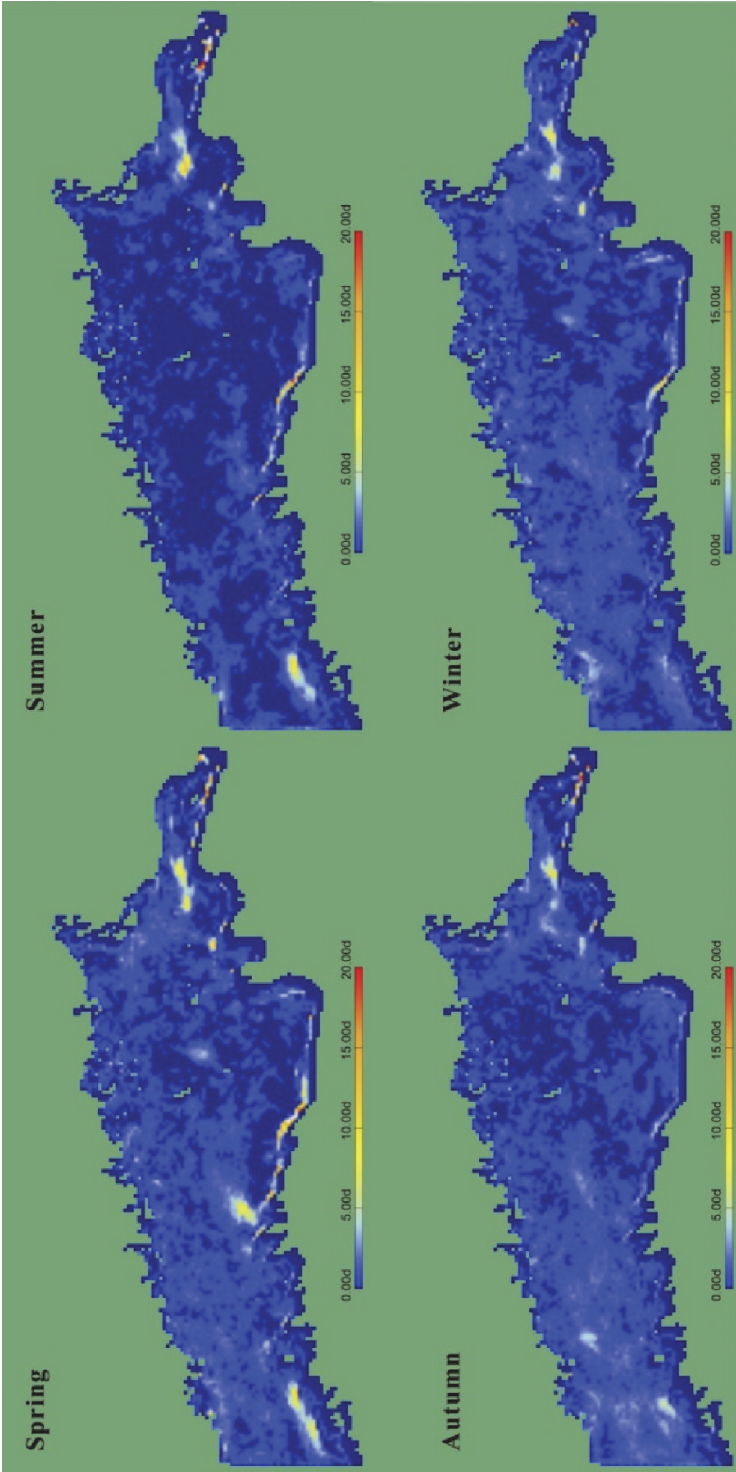


**Figure 22.** Maps of the average count of the over-threshold FTC values for season-long batches (Paper V).

This variability may be related to the presence of sea ice during a large part of the year in this region of the Gulf of Finland.

Although other areas are evident in all seasons, the count of over-threshold occurrences of  $C_{fc}$  varies substantially in different seasons. For example, area 3 is clearly defined during spring and summer but almost disappears in winter. Similarly, this count substantially varies for area 7 in Narva Bay and for area 5 along the north-eastern coast of Estonia, whereas their shape and position hardly change. The most persistent is the relatively large area 8. This area in the eastern part of the gulf also hosts high flow compressibility and convergence (Chapter 3). High FTC levels in this region are not unexpected because the overall circulation of water masses of the Gulf of Finland merges here with the voluminous runoff of the River Neva. It is thus likely that the established feature reflects a long-term property of the dynamics of the Gulf of Finland.

A schematic representation of the seasonal appearance pattern of the areas of high FTC (Figure 23) is available in Paper V. Such representation also confirms that some areas (e.g., areas 3 and 8) are present in almost all seasons of the years 1987–1991. Most of the areas are present during spring but they are relatively rare during summer. This pattern could possibly reflect seasonal variations in the directional structure of winds (and the associated seasonal relocation of downwelling areas) in the Gulf of Finland (Paper IV), even though no clear

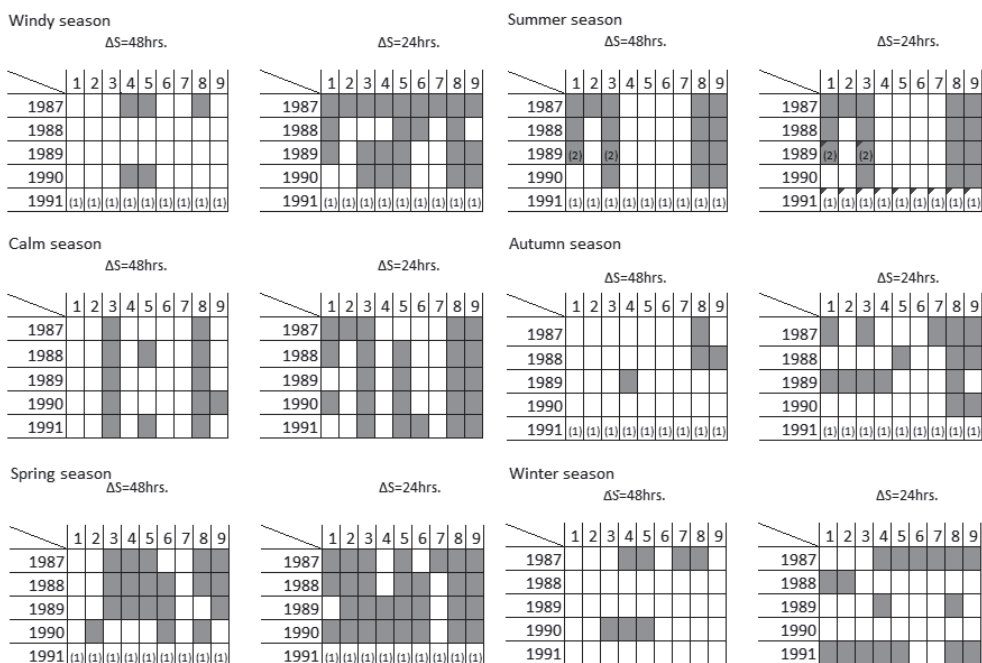


**Figure 23.** The presence of areas with frequent over-threshold values of FTC in different seasons in the Gulf of Finland for the time windows of 24 h and 48 h. (1) Data not available (Paper V).

relationship has been established yet between these phenomena and areas of likely patch formation.

To summarize, the approach presented and discussed in this thesis is targeted to quantify the potential of different sea areas to serve as locations of spontaneous formation of patches of various items and substances locked in the uppermost layer of the sea. The implemented technique exclusively relies on the standard output of contemporary 3D ocean models. The calculations use a set of simple geometric elements to detect the areas where high flow compressibility of the surface velocity field is synchronized with the local Lagrangian transport.

The material presented demonstrates that this fairly elementary approach of tracking triangular elements on the sea surface and counting the occurrences of high values of a certain measure has the capacity to highlight clearly defined areas where the joint impact of the convergence of surface flow and the current-driven Lagrangian transport of the emerging patches may often lead to considerable increase in concentrations of surface floats, contaminants or pollution in the surface layer, surfactant films, or other items of substances that are locked in the water column near the sea surface.

# Conclusions

## Summary of the results

The interplay of ocean currents and items floating on the sea surface or substances locked in the uppermost layer of the sea often naturally leads to changes in the concentration of these items or substances. During downwelling events the surface currents converge and water parcels sink into deeper layers, whereas lighter additives (debris, microplastic, oil, polluted or nutrient-rich fresh water from rivers) remain in the uppermost layer and their concentration increases. This process may be greatly accelerated by rapid clustering of floats. It is likely that the most systematic, rapid and spontaneous formation of patches occurs when a localized convergence zone (a transient downwelling) moves together with the underlying surface current. The test area (the Gulf of Finland in the Baltic Sea) hosts an extremely complicated, often almost chaotic system of currents which generally contains a substantial vertical component. The common presence of upwelling and downwelling suggests that the described mechanism is frequently active.

The main target of this thesis was to quantify this natural patch formation mechanism. Its intensity and persistency were investigated by means of the newly introduced measure of finite-time compressibility (FTC). This measure is designed to take into account the time correlations of realistic flows on the sea surface and to link these with the phenomenon of clustering of floating parcels into patches in certain surface regions. A method of calculation of FTC was implemented based on geometrical properties of surface elements formed by passively carried triplets of surface floats.

The properties of FTC were first validated from a theoretical viewpoint and compared to those of other existing measures of compressibility. It was shown that FTC was a direct extension of the classical flow compressibility of velocity fields. The two measures are equivalent when the length of accounted-for time correlations tends to zero. For ideal Kraichnan flows these measures have a simple quadratic relationship. The threshold 0.5 for the classical flow compressibility to support the clustering of surface floats corresponds to a similar threshold  $\sqrt{1/2}$  of FTC. The flows characterized by the values of FTC exceeding this threshold are likely to host spontaneous patch formation.

Spatio-temporal distributions of FTC were calculated for the Gulf of Finland based on surface velocity fields for 1987–1991 from two different ocean models and using two methods of the evaluation of Lagrangian trajectories of selected water parcels. Simulations using surface velocities with a horizontal resolution of 2 nautical miles from the Rossby Centre Ocean model and the TRACMASS code to build the trajectories revealed that the overall average level of FTC in the whole gulf was usually well below the threshold for clustering to occur. In particular, the average value of FTC is around 0.4 during the windy season, when its values are generally the highest.

A simulation environment QTRAC (Quick Tracking for Compressibility) was developed to calculate and analyse spatial distributions of FTC based on a higher-resolution (1 nautical mile) velocity data set produced by the OAAS model (Oleg Andrejev and Aleksander Sokolov, 1989). This environment performs an Euler-type tracking of parcels on the surface and handles a set of singular cases that may happen during the transport and distortion of the triangular surface elements. The parameters of calculations were optimized for the purpose of this study.

Distributions of instantaneous values of FTC as well as FTC maps for single weeks and months, calculated using higher-resolution (1 nautical mile) velocity data, also have a large variability both in space and time. These maps qualitatively coincide with those obtained using velocity data of moderate resolution (2 nautical miles). While for some periods the average FTC maps hardly show any recognizable features, during other intervals they contain clearly defined areas characterized by high FTC values. The typical maxima of FTC for single month-long batches around 0.6 are usually found in the nearshore of the southern coast of the Gulf of Finland and in the north-western and easternmost regions of the gulf. Offshore areas hosting the largest monthly average values  $>0.5$  are normally different in different months. Only one area at the mouth of the River Neva in the easternmost part of the gulf and another region in the middle of the widest part of the gulf show regularly large values of FTC.

To better quantify the potential of spontaneous patch generation, a method (similar to the peak-over-threshold method) was introduced to highlight areas where the critical value of  $\text{FTC} = \sqrt{1/2}$  is exceeded for a relatively long time. It calculates for each wet grid cell of the ocean model the number of occurrences of above-threshold values of FTC. The overall average relative count of  $\text{FTC} > \sqrt{1/2}$  is fairly small ( $\sim 1\%$ ) but in some areas up to 30%. In these areas spontaneous patch formation is likely owing to high correlation of the convergence of the velocity field and the underlying Lagrangian transport.

High values of this count regularly occur in nine clearly distinguishable areas of the Gulf of Finland. These areas are present for over 80% of the total amount of single seasons. Five of these areas are found near the southern coast of the gulf, but only two are evident in the northern part of the gulf, to the west of Helsinki. One of the latter is located in the middle of the widest part of the gulf. One such area near Saint Petersburg may be related to artefacts of the model because its forcing data resolution is not fine enough to resolve the dynamics of the narrow easternmost sector of the gulf. An “index of persistency” was introduced and calculated for each of the found areas to characterize the number of consecutive days of over-threshold FTC levels (equivalently, high correlation between the convergence field and the underlying transport). The average length for this index for single years and areas is between 2 and 3 days. The appearance of the areas which often host over-threshold FTC levels has large seasonal variability. Some of these areas are detected only during certain seasons. Most of the areas are present during spring, but they are generally rare during the summer. No evident patterns were identified at this stage across the overall yearly appearance distribution.

## **Main conclusions proposed to defend**

1. Finite-time compressibility is introduced as a new measure of properties of surface velocity fields, designed to account for time correlations of realistic flows on the sea surface based on deformations of triangular elements floating on it over a certain time interval
2. The values of finite-time compressibility behave qualitatively similarly to the respective values of classical flow compressibility. The particular values of these two quantities are generally different but a quadratic relationship between them exists for ideal Kraichnan flows. The clustering of passive surface tracers may occur if finite-time compressibility exceeds a critical value of  $\sqrt{1/2}$ .
3. Spatial maps of finite-time compressibility are calculated for the Gulf of Finland and the basic properties of this measure are established using Lagrangian trajectories obtained from surface velocity data. These maps qualitatively coincide for velocity data of moderate (2 nautical miles) and enhanced (1 nautical mile) resolution.
4. A method of counting the instantaneous values of finite-time compressibility that exceed the threshold for the clustering of surface floats is introduced. The relevant instantaneous distributions and frequency maps are produced for different seasons.
5. High values of finite-time compressibility regularly occur in nine clearly separated regions of the Gulf of Finland. In these areas spontaneous patch formation is likely owing to high correlation of the convergence of the velocity field and the underlying Lagrangian transport. The majority of such areas are located near the southern coast of the gulf. Two such regions are evident near the north-western coast of the gulf and one is found in the central part of the gulf.
6. The average duration of over-threshold (for clustering) levels of finite-time compressibility for single years is mostly between 2 and 3 days.
7. The areas showing high values of finite-time compressibility and the high count of its over-threshold values exhibit substantial seasonal variations. Most of the areas are present during the spring and are less distinct during the summer.

## Recommendations for further work

The material presented suggests that domains on the sea surface which show enhance potential of patch formation can be systematically highlighted by means of the newly introduced measure of finite-time compressibility. Based on sound assumptions and designed around a pragmatic use-case, this measure seems to produce meaningful results for even modest-resolution velocity data sets.

As a general task for further work on this topic, it would be natural to further increase the resolution of the velocity data on which the calculations are performed. Doing so would allow verifying the reliability of the results obtained in this thesis and to better link the areas of likely patch generation with other features of the dynamics of water masses. Also, enhanced resolution of velocity data would eventually be able to more exactly locate the areas of potential patch formation and/or seasons (or specific wind conditions) in which the patch formation is most active. Application of higher resolution data sets may clear several uncertainties related to the nature of some of the patch formation areas established. For example, the current horizontal resolution of 1 nautical mile is evidently too coarse to resolve the complicated local surface dynamics in the easternmost areas of the gulf.

Another natural but more fundamental improvement to the estimation of areas of potential patch formation would be the introduction of more detailed measures to describe the nature of the identified areas. For instance, the current calculation pipeline only relies on the changes in single surface elements but does not explicitly account for the total distance that each triplet of selected parcels travels. Typical surface velocities (and also the associated velocities of Lagrangian transport) in the Gulf of Finland are relatively low and this issue apparently is not critical here, however, it could add substantially to the measure of compressibility in the open ocean. To understand the impact of the frequent presence of areas where patch formation is likely, it is desirable to verify to which extent the realistic density distributions of various potentially harmful quantities in the surface layer match the predicted patch formation areas, and under which conditions.

A further research subject is to develop a method to validate the results produced using simulated data against an experimentally measured dataset. This issue is particularly challenging due to the highly sophisticated nature of calculations (that involve several major sources of uncertainties) and the scale of phenomena dealt with in this thesis. These aspects would render any small scale localized experimental approach (like the employment of GPS-enabled surface drifters) rather useless for the production of sufficient data to empirically support the claims in this thesis. It seems possible, though, to perform a verification of the results by means of high-resolution airborne or satellite tracking of passive (bio)degradable floating elements, for example, blocks of ice released uniformly across the sea domain from an aircraft.

A broader, longer-term core challenge is the conversion of the outcome of this thesis into supporting material for decision-making in the management and protection of coastal and marine areas.

## Bibliography

- Abraham E.R. 1998. The generation of plankton patchiness by turbulent stirring. *Nature*, 391, 577–580.
- Akan C., Tejada-Martinez A.E., Grosch C.E., Martinat G. 2013. Scalar transport in large-eddy simulation of Langmuir turbulence in shallow water. *Continental Shelf Research*, 55, 1–16.
- Alenius P., Myrberg K., Nekrasov A. 1998. Physical oceanography of the Gulf of Finland: a review. *Boreal Environment Research*, 3, 97–125.
- Alenius P., Nekrasov A., Myrberg K. 2003. The baroclinic Rossby-radius in the Gulf of Finland. *Continental Shelf Research*, 23, 563–573.
- Allredge A.L., Cowles T.J., MacIntyre S., Rines J.E.B., Donaghay P.L., Greenlaw C.F., Holliday D.V., Deksheniaks M.M., Sullivan J.M., Zaneveld J.R.V. 2002. Occurrence and mechanisms of formation of a dramatic thin layer of marine snow in a shallow Pacific fjord. *Marine Ecology Progress Series*, 233, 1–12.
- Andrady A.L. 2011. Microplastics in the marine environment. *Marine Pollution Bulletin*, 62(8), 1596–1605.
- Andrejev O., Sokolov A. 1989. Numerical modelling of the water dynamics and passive pollutant transport in the Neva inlet. *Meteorologia i Hydrologia*, 12, 75–85 (in Russian).
- Andrejev O., Sokolov A. 1990. 3D baroclinic hydrodynamic model and its applications to Skagerrak circulation modelling. In: *Proceedings of the 17th Conference of the Baltic Oceanographers*, Norrköping, Sweden, 38–46.
- Andrejev O., Myrberg K., Alenius P., Lundberg P.A. 2004. Mean circulation and water exchange in the Gulf of Finland – a study based on three-dimensional modeling. *Boreal Environment Research*, 9, 1–16.
- Andrejev O., Sokolov A., Soomere T., Värvi R., Viikmäe B. 2010. The use of high-resolution bathymetry for circulation modelling in the Gulf of Finland. *Estonian Journal of Engineering*, 16(3), 187–210.
- Andrejev O., Soomere T., Sokolov A., Myrberg K. 2011. The role of spatial resolution of a three-dimensional hydrodynamic model for marine transport risk assessment. *Oceanologia*, 53(1-TI), 309–334.
- Arakawa A., Lamb V.R. 1977. Computational design of the basic dynamics processes of the UCLA General Circulation Model. *Methods of Computational Physics*, 17, 173–265.
- Ardhuin F., Marié L., Rascale N., Forget P. 2009. Observation and estimation of Lagrangian, Stokes and Eulerian currents induced by wind and waves at the sea surface. *Journal of Physical Oceanography*, 39, 2820–2838.

- Averbukh E., Kurkina O., Kurkin A., Soomere T. 2014. Edge-wave-driven durable variations in the thickness of the surfactant film and concentration of surface floats. *Physics Letters A*, 378, 53–58.
- Barnes D.K.A., Galgani F., Thompson R.C., Barlaz M. 2009. Accumulation and fragmentation of plastic debris in global environments. *Philosophical Transactions of the Royal Society B*, 364, 1985–1998.
- Bec J., Gawedzki K., Horvai P. 2004. Multifractal clustering in compressible flows. *Physical Review Letters*, 92(22), Art. No. 224501.
- Bergström S., Carlsson B. 1994. River runoff to the Baltic Sea 1950–1990. *Ambio*, 23, 280–287.
- Bladel J. 1959. On Helmholtz's theorem in finite regions. *IRE Transactions on Antennas and Propagation*, vol. 7(5), 119.
- Boffetta G., Davoudi J., Eckhardt B., Schumacher J. 2004. Lagrangian tracers on a surface flow: The role of time correlations. *Physical Review Letters*, 93(13), Art. No. 134501.
- Brentnall S.J., Brindley K.J., Murphy E. 2003. Plankton patchiness and its effect on larger scale productivity. *Journal of Plankton Research*, 25, 121–140.
- Bryan K.A. 1969. A numerical method for the study of the circulation of the World Ocean. *Journal of Computational Physics*, 4, 347–376.
- Bugoni L., Krause L. 2001. Marine debris and human impacts on sea turtles in southern Brazil. *Marine Pollution Bulletin*, 42(12), 1330–1334.
- Bumke K., Karger U., Hasse L., Niekamp K. 1998. Evaporation over the Baltic Sea as an example of a semi-enclosed sea. *Contributions to Atmospheric Physics*, 71(2), 249–261.
- Burchard H., Bolding K., Villarreal M.R. 2004. Three-dimensional modelling of estuarine turbidity maxima in a tidal estuary. *Ocean Dynamics*, 54(2), 250–265.
- Burchard H., Floeser G., Staneva J.V., Badewien T.H., Riethmüller R. 2008. Impact of density gradients on net sediment transport into the Wadden Sea. *Journal of Physical Oceanography*, 38(3), 566–587.
- Burgherr P. 2007. In-depth analysis of accidental oil spills from tankers in the context of global spill trends from all sources. *Journal of Hazardous Materials*, 140, 245–256.
- Cadee G.C. 2002. Seabirds and floating plastic debris. *Marine Pollution Bulletin*, 44(11), 1294–1295.
- Calil P.H.R., Richards K.J. 2010. Transient upwelling hot spots in the oligotrophic North Pacific. *Journal of Geophysical Research–Oceans*, 115, Art. No. C02003.
- Carpenter E.J., Smith Jr. K.L. 1972. Plastics on the Sargasso Sea surface. *Science*, 175, 1240–1241.
- Carpenter E.J., Anderson S.J., Harvey G.R., Miklas H.P., Peck B.B. 1972. Polystyrenespherules in coastal water. *Science*, 178, 749–750.

- Chelton D.B., Gaube P., Schlax M.G., Early J.J., Samelson R.M. 2011. The influence of nonlinear mesoscale eddies on near-surface oceanic chlorophyll. *Science*, 334, 328–332.
- Chetrite R., Delannoy J.-Y., Gawedzki K. 2007. Kraichnan flow in a square: An example of integrable chaos. *Journal of Statistical Physics*, 126(6), 1165–1200.
- Chubarenko I. 2010. Horizontal convective water exchange above sloping bottom: the mechanism of its formation and an analysis of its development. *Oceanology*, 50(2), 166–174.
- Coe J., Rogers D. 1996. *Marine Debris Sources, Impacts, and Solutions*. Springer-Verlag, New York.
- Cole M., Lindeque P., Halsband C., Galloway T.S. 2011. Microplastics as contaminants in the marine environment: A review. *Marine Pollution Bulletin*, 62(12), 2588–2597.
- Colton J.B., Knapp F.D. 1974. Plastic particles in surface waters of the northwestern Atlantic. *Science*, 185, 491–497.
- Cózar A, Echevarría F, González-Gordillo J.I., Irigoien X., Úbeda B., Hernández-León S., Palma Á.T., Navarro S., García-de-Lomas J., Ruiz A., Fernández-de-Puelles M.L., Duarte C.M. 2014. Plastic debris in the open ocean. *Proceedings of the National Academy of Sciences of the United States of America*, 111(28), 10239–10244.
- Cressman J.R., Davoudi J., Goldberg W.I., Schumacher J. 2004. Eulerian and Lagrangian studies in surface flow turbulence. *New Journal of Physics*, 6, Art. No. 53.
- Cushman-Roisin B.J., Beckers J.-M. 2011. *Introduction to Geophysical Fluid Dynamics: Physical and Numerical Aspects*. Elsevier/Academic Press, Amsterdam, San Diego, 828 pp.
- Delpeche-Ellmann N. 2014. *Circulation Patterns in the Gulf of Finland Applied to Environmental Management of Marine Protected Areas*. PhD thesis. Tallinn University of Technology, 143 pp.
- De Pietro M., van Hinsberg M.A.T., Biferale L., Clercx H.J.H., Perlekar P., Toschi F. 2014. On clustering of vertically constrained passive particles in homogeneous, isotropic turbulence. arXiv: 1411.1950v1 [physics.flu-dyn]
- Derraik J.G.B. 2002. The pollution of the marine environment by plastic debris: A review. *Marine Pollution Bulletin*, 44(9), 842–852.
- Dethleff D., Kempema E.W., Koch R., Chubarenko I. 2009. On the helical flow of Langmuir circulation – approaching the process of suspension freezing. *Cold Regions Science and Technologies*, 56, 50–57.
- De Vries P., Döös K. 2001. Calculating Lagrangian trajectories using time-dependent velocity fields. *Journal of Atmospheric and Oceanic Technology*, 18(6), 1092–1101.

- Döös K. 1995. Inter-ocean exchange of water masses. *Journal of Geophysical Research–Oceans*, 100(C7), 13499–13514.
- Döös K., Coward A.C. 1997. The Southern Ocean as the major upwelling zone of the North Atlantic Deep Water. *WOCE Newsletter*, 27, 3–17.
- Döös K., Meier H.E.M., Döscher R. 2004. The Baltic haline conveyor belt or the overturning circulation and mixing in the Baltic. *Ambio*, 33, 261–266.
- Döös K., Kjellsson J., Jönsson B. 2013. TRACMASS—A Lagrangian trajectory model. In: Soomere T., Quak E. (eds.), *Preventive Methods for Coastal Protection*. Springer, Cham, Heidelberg, pp. 225–249.
- Engqvist A., Döös K., Andrejev O. 2006. Modelling water exchange and contaminant transport through a Baltic coastal region. *Ambio*, 35, 435–447.
- Erfteimeijer P.L.A., Robin Lewis III R.R. 2006. Environmental impacts of dredging on seagrasses: A review. *Marine Pollution Bulletin*, 52(12), 1553–1572.
- Erikson C., Burton H. 2003. Origins and biological accumulation of plastic particles in fur seals from Macquarie Island. *Ambio*, 32, 380–384.
- Falkovich G., Gawedzki K., Vergassola M. 2001. Particles and fields in fluid turbulence. *Reviews of Modern Physics*, 73(4), 913–975.
- Fennel W., Radtke H., Schmidt M., Neumann T. 2010. Transient upwelling in the central Baltic Sea. *Continental Shelf Research*, 30, 2015–2026.
- Fine R.A., Millero F.J. 1973. Compressibility of fluids as a function of temperature and pressure. *Journal of Chemical Physics*, 59(10), 5529–5536.
- Fowler C.W. 1987. Marine debris and northern fur seals: A case study. *Marine Pollution Bulletin*, 18(6), 326–335.
- Froyland G., Stuart R.M., van Sebille E. 2014. How well-connected is the surface of the global ocean? *Chaos*, 24, Art. No. 033126.
- Garrison T.S. 2011. *Essentials of Oceanography*, 5th ed. Brooks Cole, Pacific Grove.
- Gästgifvars M., Lauri H., Sarkanen A.-K., Myrberg K., Andrejev O., Ambjörn C. 2006. Modelling surface drifting of buoys during a rapidly-moving weather front in the Gulf of Finland, Baltic Sea. *Estuarine, Coastal and Shelf Science*, 70, 567–576.
- Gerdes R., Köberle C., Willebrand J. 1991. The influence of numerical advection schemes on the results of ocean general circulation models. *Climate Dynamics*, 5, 211–226.
- Golenko M.N., Golenko N.N. 2012. Structure of dynamic fields in the Southeastern Baltic during wind forcings that cause upwelling and downwelling. *Oceanology*, 52(5), 604–616.
- Granskog M., Kaartokallio H., Kuosa H., Thomas D., Ehn J., Sonninen E. 2005. Scales of horizontal patchiness in chlorophyll a, chemical and physical properties of landfast sea ice in the Gulf of Finland (Baltic Sea). *Polar Biology*, 28(4), 276–283.

- Gräwe U., Deleersnijder E., Shah S.H.A.M., Heemink A.W. 2012. Why the Euler scheme in particle tracking is not enough: The shallow-sea pycnocline test case. *Ocean Dynamics*, 62(4), 501–514.
- Gruber N., Lachkar Z., Frenzel H., Marchesiello P., Münnich M., McWilliams J.C., Nagai T., Plattner G.-K. 2011. Eddy-induced reduction of biological production in eastern boundary upwelling systems. *Nature Geoscience*, 4, 787–792.
- Grünbaum D. 2012. The logic of ecological patchiness. *Interface Focus*, 2, 150–155.
- Held I.M., Pierrehumbert R.T., Garner S.T., Swanson K.L. 1995. Surface quasi-geostrophic dynamics. *Journal of Fluid Mechanics*, 282, 1–20.
- Hibler, W., 1979. A dynamic thermodynamic sea ice model. *Journal of Physical Oceanography*, 9, 815–846.
- Höglund A., Meier H.E.M., Broman B. and Kriezi E. 2009. Validation and correction of regionalised ERA-40 wind fields over the Baltic Sea using the Rossby Centre Atmosphere Model RCA3.0. *Rapport Oceanografi*, 97, Norrköping, Sweden: Swedish Meteorological and Hydrological Institute.
- Holthuijsen L.H. 2007. *Waves in Oceanic and Coastal Waters*. Cambridge University Press, 387 pp.
- Jankowski, J.A., Malcherek, A., Zielke, W. 1996. Numerical modeling of suspended sediment due to deep-sea mining. *Journal of Geophysical Research–Oceans*, 101(C2), 3545–3560.
- Kachel M. J. 2008. *Particularly Sensitive Sea Areas: The IMO's Role in Protecting Vulnerable Marine Areas*. Hamburg Studies on Maritime Affairs, 13, Springer, Berlin, 376 pp.
- Kahru M. 1983. Phytoplankton patchiness generated by long internal waves – a model. *Marine Ecology Progress Series*, 10, 111–117.
- Kahru M., Håkansson B., Rud O. 1995. Distribution of the sea surface temperature fronts in the Baltic Sea as derived from satellite imagery. *Continental Shelf Research*, 15(6), 663–679.
- Kalda J. 2000. Simple model of intermittent passive scalar turbulence. *Physical Review Letters*, 84(3), 471–474.
- Kalda J. 2007. Sticky particles in compressible flows: Aggregation and Richardson's Law. *Physical Review Letters*, 98(6), Art. No. 064501.
- Killworth P., Stainforth D., Webb D., Paterson S. 1991. The development of a free-surface Bryan–Cox–Semtner ocean model. *Journal of Physical Oceanography*, 21, 1333–1348.
- Kjellsson J., Döös K. 2012. Surface drifters and model trajectories in the Baltic Sea. *Boreal Environment Research*, 17(6), 447–459.
- Kjellsson J., Döös K., Soomere T. 2013. Evaluation and tuning of model trajectories and spreading rates in the Baltic Sea using surface drifter

- observations. In: Soomere T., Quak E. (eds.), *Preventive Methods for Coastal Protection*. Springer, Cham, Heidelberg, pp. 251–282.
- Klemas V. 2010. Tracking oil spill and predicting their trajectories using remote sensors and models: Case studies of the Sea Princess and Deepwater Horizon oil spills. *Journal of Coastal Research*, 26, 789–797.
- Kloeden P.E., Platen E. 1999. *Numerical Solution of Stochastic Differential Equations*. Springer, Berlin, 632 pp.
- Kochergin V.P., 1987. Three-dimensional prognostic models. In: Heaps N.S. (ed.), *Three-Dimensional Coastal Ocean Models*. American Geophysical Union, Washington, D.C. doi: 10.1029/CO004p0201.
- Kononen K., Nõmmann S., Hansen G., Hansen R., Breuel G., Gupalo E.N. 1992. Spatial heterogeneity and dynamics of vernal phytoplankton species in the Baltic Sea in April–May 1986. *Journal of Plankton Research*, 14(1), 107–125.
- Kowalewski M., Ostrowski M. 2005. Coastal up- and downwelling in the southern Baltic. *Oceanologia*, 47(4), 453–475.
- Kraichnan R.H. 1968. Small scale structure of a scalar field convected by turbulence. *Physics of Fluids*, 11, 945–953.
- Kraichnan R.H., Montgomery D. 1980. Two-dimensional turbulence. *Reports on Progress in Physics*, 43(5), 548–619.
- Lagemaa P., Elken J., Kõuts T. 2011. Operational sea level forecasting in Estonia. *Estonian Journal of Engineering*, 17, 301–331.
- Laist D.W. 1997. Impacts of marine debris: Entanglement of marine life in marine debris including a comprehensive list of species with entanglement and ingestion records. In: Coe J.M., Rogers D.B. (eds.), *Marine Debris: Sources, Impacts and Solutions*. Springer-Verlag, New York.
- Lebreton L.C., Borrero J.C., 2013. Modeling the transport and accumulation floating debris generated by the 11 March 2011 Tohoku tsunami. *Marine Pollution Bulletin*, 66(1–2), 53–58.
- Lee D.K., Niiler N. 2010. Influence of warm SST anomalies formed in the eastern Pacific subduction zone on recent El Nino events. *Journal of Marine Research*, 68(3–4), 459–477.
- Lehmann A., Krauss W., Hinrichsen H.-H. 2002. Effects of remote and local atmospheric forcing on circulation and upwelling in the Baltic Sea. *Tellus A*, 54, 299–316.
- Lehmann A., Myrberg K., Höflich K. 2012. A statistical approach to coastal upwelling in the Baltic Sea based on the analysis of satellite data for 1990–2009. *Oceanologia*, 54, 369–393.
- Leichter J.J., Deane G.B., Stokes M.D. 2005. Spatial and temporal variability of internal wave forcing on a coral reef. *Journal of Physical Oceanography*, 35, 1945–1962.

- Lennert-Cody C.E., Franks P.J.S. 2002. Fluorescence patches in high-frequency internal waves. *Marine Ecology Progress Series*, 235, 29–42.
- Leppäranta M., Myrberg K. 2009. *The Physical Oceanography of the Baltic Sea*. Springer, Berlin Heidelberg, 378 pp.
- Levin S. 1994. Patchiness in marine and terrestrial systems: From individuals to populations. *Philosophical Transactions of the Royal Society*, B343, 99–103.
- Lilover M.J., Pavelson J., Kõuts T. 2011. Wind forced currents over shallow Naissaar Bank in the Gulf of Finland. *Boreal Environment Research*, 16(Suppl. A), 164–174.
- Liu S.-K., Leendertse J. 1978. Multidimensional numerical modelling of estuaries and coastal seas. *Advances in Hydroscience*, 11, 95–164.
- Liu Y., Weisberg R.H., Hu C., Zheng L. 2011. Tracking the Deepwater Horizon oil spill: A modeling perspective. *EOS Transactions*, 92(6), 45–46.
- Löptien U., Meier H.E.M. 2011. The influence of increasing water turbidity on the sea surface temperature in the Baltic Sea: A model sensitivity study. *Journal of Marine Systems*, 88, 323–331.
- Mallory M.L. 2008. Marine plastic debris in northern fulmars from the Canadian high Arctic. *Marine Pollution Bulletin*, 56, 1501–1504.
- Martín J., Puig P., Palanques A., Masqué P., García-Orellana J. 2008. Effect of commercial trawling on the deep sedimentation in a Mediterranean submarine canyon. *Marine Geology*, 252(3–4), 150–155.
- Maximenko N., Hafner J., Niiler P. 2012. Pathways of marine debris derived from trajectories of Lagrangian drifters. *Marine Pollution Bulletin*, 65, 51–62.
- Maximenko N., Lumpkin R., Centurioni L. 2013. Ocean surface circulation. *International Geophysics*, 103, 283–304.
- Meier H.E.M. 1999. *First Results of Multi-Year Simulations Using a 3D Baltic Sea Model*. SMHI Reports Oceanography, No. 27, Norrköping, Sweden, 48 pp.
- Meier H.E.M. 2001. On the parametrization of mixing in three-dimensional Baltic Sea models. *Journal of Geophysical Research–Oceans*, 106(C12), 30997–C31,016.
- Meier H.E.M., 2007. Modeling the pathways and ages of inflowing salt- and freshwater in the Baltic Sea. *Estuarine, Coastal and Shelf Science*, 74(4), 610–627.
- Meier H.E.M., Höglund A. 2013. Studying the Baltic Sea circulation with Eulerian tracers. In: Soomere T., Quak E. (eds.), *Preventive Methods for Coastal Protection*. Springer, Cham, Heidelberg, pp. 101–130.
- Meier H.E.M., Döscher R., Faxén T. 2003. A multiprocessor coupled ice-ocean model for the Baltic Sea: Application to salt inflow. *Journal of Geophysical Research–Oceans*, 108(C8), Art. No. 3273.
- Millero F., Kremling I. 1976. The densities of the Baltic Sea deep waters. *Deep Sea Research*, 23, 1129–1138.

- Mori, N., Takahashi, T., Yasuda, T., Yanagisawa, H. 2011. Survey of 2011 Tohoku earthquake tsunami inundation and run-up. *Geophysical Research Letters*, 38(18), Art. No. L00G14.
- Murawski J., Woge Nielsen J. 2013. Applications of an oil drift and fate model for fairway design. In: Soomere T., Quak E. (eds.), *Preventive Methods for Coastal Protection*. Springer, Cham, Heidelberg, pp. 376–415.
- Myrberg K., Andrejev O. 2003. Main upwelling regions in the Baltic Sea – a statistical analysis based on three-dimensional modelling. *Boreal Environment Research*, 8, 97–112.
- Myrberg K., Soomere T. 2013. The Gulf of Finland, its hydrography and circulation dynamics. In: Soomere T., Quak E. (eds.), *Preventive Methods for Coastal Protection*. Springer, Cham, Heidelberg, pp. 181–222.
- Myrberg K., Ryabchenko V., Isaev A., Vankevich R., Andrejev O., Bendtsen J., Erichsen A., Funkquist L., Inkala A., Neelov I., Rasmus K., Rodriguez M.M., Raudsepp U., Passenko J., Söderkvist J., Sokolov A., Kuosa H., Anderson T.R., Lehmann A., Skogen M.D. 2010. Validation of three-dimensional hydrodynamic models in the Gulf of Finland based on a statistical analysis of a six-model ensemble. *Boreal Environment Research*, 15, 453–479.
- Niros A., Vihma T., Launiainen J. 2002. Marine meteorological conditions and air-sea exchange processes over the northern Baltic Sea in 1990. *Geophysica*, 38(1/2), 59–87.
- Ollitrault M., Gabillet C., Colin de Verdiere A. 2005. Open ocean regimes of relative dispersion. *Journal of Fluid Mechanics*, 533, 381–407.
- Orlanski I. 1976. A simple boundary condition for unbounded hyperbolic flows. *Journal of Computational Physics*, 21, 251–269.
- Page B., McKenzie J. 2004. Entanglement of Australian sea lions and New Zealand fur seals in lost fishing gear and other marine debris before and after Government and industry attempts to reduce the problem. *Marine Pollution Bulletin*, 49(1–2), 33–42.
- Periáñez R. 2004. A particle-tracking model for simulating pollutant dispersion in the Strait of Gibraltar. *Marine Pollution Bulletin*, 49, 613–623.
- Perlekar P., Benzi R., Nelson D., Toschi F. 2010. Population dynamics at high Reynolds number. *Physical Review Letters*, 105(14), Art. No. 144501.
- Pichel W.G., Churnside J.H., Veenstra T.S., Foley D.G., Friedman K.S., Brainard R.E., Nicoll J.B., Zheng Q., Clemente-Colon P. 2007. Marine debris collects within the North Pacific subtropical convergence zone. *Marine Pollution Bulletin*, 54(8), 1207–1211.
- Powell T.M., Okubo A. 1994. Turbulence, diffusion and patchiness in the sea. *Philosophical Transactions of the Royal Society B*, 343(1303), 11–18.
- Rhines P. 1979. Geostrophic turbulence. *Annual Review of Fluid Mechanics*, 11, 401–441.

- Richards Z.T., Beger M. 2011. A quantification of the standing stock of macrodebris in Majuro lagoon and its effect on hard coral communities. *Marine Pollution Bulletin*, 62(8), 1693–1701.
- Richardson L.F. 1926. Atmospheric diffusion shown on a distance-neighbor graph. *Proceedings of the Royal Society A*, 110, 709–737.
- Samuelson A., Hjøllø S.S, Johannessen J.A., Patel R. 2012. Particle aggregation at the edges of anticyclonic eddies and implications for distribution of biomass. *Ocean Science*, 8(3), 389–400.
- Samuelsson P., Jones C.G., Willén U., Ullerstig A., Gollvik S., Hansson U., Jansson C., Kjellström E., Nikulin G., Wyser K. 2011. The Rossby Centre Regional Climate Model RCA3: Model description and performance. *Tellus A*, 63, 4–23.
- Schilling K., Zessner M. 2011. Foam in the aquatic environment. *Water Research*, 45(15), 4355–4366.
- Schumacher J, Eckhardt B. 2002. Clustering dynamics of Lagrangian tracers in free-surface flows. *Physical Review E*, 66, Art. No. 017303.
- Seifert T., Tauber F., Kayser B. 2001. A high resolution spherical grid topography of the Baltic Sea, revised edition. In: *Baltic Sea Science Congress, 25–29 November 2001*, Poster #147, Stockholm, [www.iowarnemuende.de/iowtopo\\_resampling.html](http://www.iowarnemuende.de/iowtopo_resampling.html).
- Simpson S.D., Harrison H.B., Claereboudt M.R., Planes S. 2014. Long-distance dispersal via ocean currents connects omani clownfish populations throughout entire species range. *PLoS ONE* 9(9), Art. No. e107610.
- Smagorinsky J. 1963. General circulation experiments with the primitive equations, I. The basic experiment. *Monthly Weather Review*, 91, 99–164.
- Soomere T., Keevallik S. 2003. Directional and extreme wind properties in the Gulf of Finland. *Proceedings of the Estonian Academy of Sciences, Engineering*, 9, 73–90.
- Soomere T., Quak E. 2007. On the potential of reducing coastal pollution by a proper choice of the fairway. *Journal of Coastal Research*, 50, 678–682.
- Soomere T., Quak E. (eds.) 2013. *Preventive Methods for Coastal Protection: Towards the Use of Ocean Dynamics for Pollution Control*. Springer, Cham, Heidelberg, 442 pp.
- Soomere T., Myrberg K., Leppäranta M., Nekrasov A. 2008. The progress in knowledge of physical oceanography of the Gulf of Finland: A review for 1997–2007. *Oceanologia*, 50, 287–362.
- Soomere T., Viikmäe B., Delpeche N., Myrberg K. 2010. Towards identification of areas of reduced risk in the Gulf of Finland. *Proceedings of the Estonian Academy of Sciences*, 59(2), 156–165.

- Soomere T., Delpeche N., Viikmäe B., Quak E., Meier H.E.M., Döös K. 2011. Patterns of current-induced transport in the surface layer of the Gulf of Finland. *Boreal Environment Research*, 16(Suppl. A), 49–63.
- Soomere T., Döös K., Lehmann A., Meier H.E.M., Murawski J., Myrberg K., Stanev E. 2014. The potential of current- and wind-driven transport for environmental management of the Baltic Sea. *Ambio*, 43, 94–104.
- Stevens D.P. 1991. A numerical ocean circulation model of the Norwegian and Greenland Seas. *Progress in Oceanography*, 27(3–4), 365–402.
- Strass V.H. 1992. Chlorophyll patchiness caused by mesoscale upwelling at fronts. *Deep Sea Research A*, 39, 75–96.
- Thorpe S.A. 2009. Spreading of floating particles by Langmuir circulation. *Marine Pollution Bulletin*, 58(12), 1787–1791.
- Torsvik T. 2013. Introduction to computational fluid dynamics and ocean modelling. In: Soomere T., Quak E. (eds.), *Preventive Methods for Coastal Protection*. Springer, Cham, Heidelberg, pp. 65–100.
- Uiboupin R., Laanemets J., Sipelgas L., Raag L., Lips I., Buhhalko N. 2012. Monitoring the effect of upwelling on the chlorophyll a distribution in the Gulf of Finland (Baltic Sea) using remote sensing and in situ data. *Oceanologia*, 54(3), 395–419.
- Uppala S.M., Kållberg P.W., Simmons A.J., Andrae U., da Costa B.V., Fiorino M., Gibson J.K., Haseler J., Hernandez A., Kelly G.A., Li X., Onogi K., Saarinen S., Sokka N., Allan R.P., Andersson E., Arpe K., Balmaseda M.A., Beljaars A.C.M., van de Berg L., Bidlot J., Bormann N., Caires S., Chevallier F., Dethof A., Dragosavac M., Fisher M., Fuentes M., Hagemann S., Hólm E., Hoskins B.J., Isaksen I., Janssen P.A.E.M., Jenne R., McNally A.P., Mahfouf J.-F., Morcrette J.-J., Rayner N.A., Saunders R.W., Simon P., Sterl A., Trenberth K.E., Untch A., Vasiljevic D., Viterbo P., Woollen J. 2005. The ERA-40 re-analysis. *Quarterly Journal of the Royal Meteorological Society*, 131, 2961–3012.
- Vandenbulcke L., Beckers J.-M., Lenartz F., Barth A., Poulain P.-M., Aidonidis M., Meyrat J., Arduin F., Tonani M., Fratianni C., Torrisi L., Pallela D., Chiggiato J., Tudor M., Book J.W., Martin P., Peggion G., Rixen M. 2009. Super-ensemble techniques: Application to surface drift prediction. *Progress in Oceanography*, 82, 149–167.
- Viikmäe B. 2014. *Optimising Fairways in the Gulf of Finland Using Patterns of Surface Currents*. PhD thesis. Tallinn University of Technology, 196 pp.
- Viikmäe B., Soomere T. 2014. Spatial pattern of hits to the nearshore from a major marine highway in the Gulf of Finland. *Journal of Marine Systems*, 129, 106–117.
- Viikmäe B., Torsvik T. 2013. Quantification and characterization of mesoscale eddies with different automatic identification algorithms. *Journal of Coastal Research*, Special Issue 65, 2077–2082.

- Viikmäe B., Torsvik T., Soomere T. 2013. Impact of horizontal eddy-diffusivity on Lagrangian statistics for coastal pollution from a major marine fairway. *Ocean Dynamics*, 63, 589–597.
- Visbeck M.H., Hurrell J.W., Polvani L., Cullen H.M. 2001. The North Atlantic oscillation: Past, present, and future. *Proceedings of the National Academy of Sciences of the United States of America*, 8(23), 12876–12877.
- Vucelja M., Falkovich G., Fouxon I. 2007. Clustering of matter in waves and currents. *Physical Review E*, 75(6), Art. No. 065301.
- Webb D.J., Coward A.C., de Cuevas B.A., William G.S. 1997. A multiprocessor ocean circulation model using message passing. *Journal of Atmospheric and Oceanic Technology*, 14, 175–183.
- Wilson R., Davenport C., Jaffe B. 2012. Sediment scour and deposition within harbors in California (USA), caused by the March 11, 2011 Tohoku-oki tsunami. *Sedimentary Geology*, 282, 228–240.
- Zaitseva-Pärnaste I. 2013. *Wave Climate and its Decadal Changes in the Baltic Sea Derived from Visual Observations*. PhD thesis. Tallinn University of Technology, 173 pp.
- Yun N.Y., Hamada M., 2014. Evacuation behavior and fatality during the 2011 Tohoku tsunami. *Science of Tsunami Hazards*, 33(3), 144–155.

## Acknowledgements

Thanks are due to a lot of people who have helped me during the course of my PhD study. Mere words mentioned here cannot possibly do them justice.

Professor Tarmo Soomere has been kind, patient and tolerant during countless occasions over the past four years, pointing out my errors, and inspiring me to always go forward in spite of the difficulties ahead. He is a man of vision and great modesty, and he wisely guided this project, from the inception to its conclusion. I am profoundly thankful to him.

I thank Professor Jaan Kalda for the help and supervision, especially during the first part of this work. Specifically, he envisioned the founding idea of the finite-time compressibility, guided me in the process of framing it mathematically, and greatly helped throughout the extension of my PhD studies: for this I am very grateful to him

I thank the Swedish Meteorological and Hydrological Institute for providing the Rossby Centre Ocean data. I also thank Prof. Kristofer Döös at the Department of Meteorology at Stockholm University for providing the TRACMASS trajectory model and a guided detail on its capabilities.

I am grateful to all the Laboratory of Wave Engineering staff's members, who often have gone out of their way for me, especially Dr. Nicole Delpeche, Maris Eelsalu, Katri Pindsoo, Artem Rodin, Dr. Tomas Torsvik, Dr. Bert Viikmäe, Dr. Maija Viška, and all whom I've inadvertently left out.

I am grateful to my all-time dearest friend Lieutenant Marco Berruti for helping me choose the right path and giving me perspective and valuable feedback, and the emotional support, comraderie and caring he provided.

I wish to acknowledge my parents, Walter Giudici and Renza Schreieder, who always let me chase my passions and encouraged me throughout my pitfalls, all while raising me, supporting me, teaching me, and loving me. To them I dedicate the entirety of this work.

\* \* \*

The studies were supported by DoRa scholarship funded from the European Social Fund.

## Abstract

The thesis makes an attempt at developing a technology that can be employed for identifying and quantifying areas of spontaneous patch formation in the marine surface layer. The main mechanism of the patch formation addressed in the thesis is the impact of three-dimensional downwelling motions in the water column on a two-dimensional field of substances that are concentrated in the surface layer or locked on the surface. The ability of patch formation can be quantified in terms of compressibility of the surface velocity field. The test area is the Gulf of Finland in the Baltic Sea.

A modified measure of surface flow compressibility, called finite-time compressibility, is introduced. This measure is evaluated by means of geometric properties of triangular elements of sea surface formed by triplets of floats that are passively carried by surface currents. It is designed to account for time correlations of the realistic flows on the sea surface and to directly relate these correlations with the ability of a region to form clusters of passive surface tracers. It is shown that a quadratic relationship between the classical flow compressibility and finite-time compressibility exists for ideal Kraichnan flows. Spontaneous clustering of passive surface tracers may occur if finite-time compressibility exceeds a critical value of  $\sqrt{1/2}$ .

Spatial maps of finite-time compressibility are calculated for the Gulf of Finland using Lagrangian trajectories of passive floating items or selected water parcels at the sea surface. The basic properties of this measure are established using velocity data of moderate resolution (2 nautical miles, Rossby Centre Ocean model) and enhanced resolution (1 nautical mile, OAAS model) across a time span of 5 years (1987–1991). The average instantaneous value of finite-time compressibility across the gulf is well below the threshold for clustering. The typical maxima of finite-time compressibility for single month-long batches are around 0.6 and are usually found in the nearshore of the southern coast of the Gulf of Finland and in the north-western and easternmost regions of the gulf. Only one offshore area in the widest part of the gulf shows large values of finite-time compressibility.

The regions where instantaneous values of finite-time compressibility often exceed the threshold for the clustering of surface floats correspond to the areas in which spontaneous patch formation is likely. Nine such regions of different size have been identified in the study area. Six of these are located near the southern coast of the gulf, two near the north-western coast and one region is found in the central part. The persistency of these regions is analysed by means of their appearance in different seasons and the average duration of over-threshold levels of finite-time compressibility. The areas showing a high count of over-threshold values of finite-time compressibility exhibit substantial seasonal variation. Most of these are present during spring, but they are relatively rare during summer. The average maximum duration of over-threshold levels of finite-time compressibility for single years is mostly between 2 and 3 days.

## Resüme

Töö keskseks eesmärgiks on arendada välja tehnoloogia, mis võimaldaks määratleda ja iseloomustada merealasad, millel võivad iseeneslikult moodustuda pinnakihis paiknevate ainete kõrged kontsentratsioonid (laigud). Fookuses on situatsioonid, kus ujuvad objektid või pinnakihis paiknevad lisandid kontsentreeruvad kolmemõõtmelise merehoovuste süsteemi konvergentsialadel esineva pealisveelange (downwelling) käigus. Laigu moodustumine on kõige intensiivsem siis, kui tekkiva laigu edasikandumine on sünkroniseeritud konvergentsiala liikumisega. Laikude tekkimise võimalus kvantifitseeritakse pinnahoovuste kahemõõtmelise süsteemi kiirusvälja kokkusurutavuse analüüsi alusel. Testalaks on valitud Soome laht.

Defineeritakse uus hoovuste kiirusvälja kokkusurutavust iseloomustav parameeter – lõpliku korrelatsiooniajaga kokkusurutavus (LKKS, finite-time compressibility), mis integreerib kiirusvälja ruumilised muutused teatava ajavahemiku vältel. Selle väärtuste arvutamiseks loodud meetodika tugineb hoovuste poolt edasi kantavate passiivsete ujuvate objektide kolmikute moodustatud kolmnurksete merepinna elementide deformatsiooni jälgimisele. LKKS peegeldab pinnahoovuste kiirusvälja korrelatsioone teatava aja vältel ning seob saadud suuruse võimalusega, et mingites piirkondades või mingitel ajavahemikel koonduvad hoovustega passiivselt edasi kanduvad ujuvad objektid tihedatesse parvedesse, teisisõnu, moodustuvad laigud. On demonstreeritud, et ideaalsete Kraichnani voolamiste puhul on klassikaline kiirusväljade kokkusurutavus ja LKKS seotud teatava ruutvõrrandiga. Selliste voolamiste puhul arenevad iseeneslikult parved, kui LKKS ületab kriitilise läve  $\sqrt{1/2}$ .

Soome lahe jaoks on arvatud LKKS ajalis-ruumilise muutlikkuse kaardid, mis tuginevad hoovustega passiivselt edasi kanduvate ujuvate objektide Lagrange'i trajektooride kolmikute analüüsi erinevate ajavahemike vältel. Arvutuste aluseks on 2-miilise sammuga pinnahoovuste kiirusväljad RCO mudelist ja 1-miilise sammuga kiirusväljad OAAS mudelist viie aasta jaoks (1987–1991). LKKS keskmised väärtused on kogu Soome lahel märksa väiksemad kui kriitiline lävi. Ühe kuu pikkuste ajavahemike jaoks leitud LKKS maksimaalsed väärtused on enamasti väiksemad kui 0,6. Suurimad väärtused paiknevad Soome lahe lõunaranniku lähistel, aga ka üksikutes lahe looderanniku lõikudes ja lahe idaosas. Suhteliselt suured LKKS väärtused esinevad ka lahe kõige laiema osa keskel.

Laikude tekkimine on kõige tõenäolisem kohtades, kus LKKS üksikväärtused regulaarselt või pikema aja vältel ületavad parvedesse koondumise läve. On identifitseeritud üheksa sellist kohta. Neist kuus paiknevad Soome lahe lõunaranniku lähistel, kaks lahe looderanniku lähistel ja üks lahe kõige laiemas osas avamerel. On analüüsitud laikude tekkimiseks soodsate tingimuste regulaarsust ja sesoonset muutlikkust. Enamus laikude tekkimiseks soodsaid alasid ilmneb kevadeti, kuid mitmeid neist ei avaldu suvel. Laikude tekkimiseks soodsad tingimused (LKKS üle kriitilise läve) püsivad üksikutel aastatel sageli 2–3 päeva vältel.

## Appendix A: Curriculum Vitae

### 1. Personal data

Name	Andrea Giudici
Date and place of birth	29.03.1985, Savona, Italy
Address	Akadeemia tee 21, 12618 Tallinn
Phone	(+372) 583 90 544
E-mail	andrea@cens.ioc.ee

### 2. Education

Educational institution	Graduation year	Education (field of study / degree)
Università degli Studi di Genova	2010	Computer Science / Master's Degree in Computer Science (MSCS)
Università degli Studi di Genova	2008	Computer Science / Bachelor's Degree in Computer Science (BSCS)

### 3. Language competence/skills

Language	Level
Italian	Native language
English	Fluent
French	Good working knowledge
Estonian	Basic skills

### 4. Special courses and further training

Period	Educational or other organisation
September 2011	International Summer School on <i>Preventive methods for coastal protection</i> (Klaipėda, Lithuania)

### 5. Professional employment

Period	Organisation	Position
Jan. 2011–to date	Tallinn University of Technology, Institute of Cybernetics	Technician, Engineer

### 6. Research activity

#### 6.1. Publications

*Articles indexed by the Web of Science database (1.1):*

**Giudici A.,** Soomere T. 2014. Finite-time compressibility as an agent of frequent spontaneous patch formation in the surface layer: a case study for the Gulf of Finland, the Baltic Sea. *Marine Pollution Bulletin*, 89(1–2), 239–249.

Kalda J., Soomere T., **Giudici A.** 2014. On the finite-time compressibility of the surface currents in the Gulf of Finland, the Baltic Sea. *Journal of Marine Systems*, 129, 56–65.

**Giudici A.**, Soomere T. 2013. Identification of areas of frequent patch formation from velocity fields. *Journal of Coastal Research*, Special Issue 65, vol. 1, 231–236.

*Peer-reviewed articles in other international journals (1.2) and collections (3.1):*

**Giudici A.**, Soomere T. 2014. Measuring finite time compressibility from large simulated datasets: towards identification of areas of spontaneous patch formation in the Gulf of Finland. In: Haav H.M., Kalja A., Robal T. (eds.) *Databases and Information Systems*, 8–11 June 2014, Tallinn, Estonia, Proceedings of the 11th International Baltic Conference, Baltic DB & IS 2014. Tallinn University of Technology Press, Tallinn, 441–446.

**Giudici A.**, Nikolkina I. 2014. Automated detection of crossing seas from simulated wave spectra. In: *2014 IEEE/OES Baltic International Symposium, 26–29 May 2014, Tallinn, Estonia*. Proceedings. IEEE.

**Giudici A.**, Soomere T. 2014. On the possibility of spontaneous patch formation in the Gulf of Finland. In: *2014 IEEE/OES Baltic International Symposium, 26–29 May 2014, Tallinn, Estonia*. Proceedings. IEEE.

**Giudici A.**, Kalda J., Soomere T. 2012. On the compressibility of surface currents in the Gulf of Finland, the Baltic Sea. In: *IEEE/OES Baltic 2012 International Symposium, 8–11 May 2012, Klaipėda, Lithuania*. Proceedings. IEEE, 7 pp.

*Articles published in other conference proceedings (3.4):*

**Giudici A.**, Soomere T. 2014. Highly persisting patch formation areas in the Gulf of Finland, the Baltic Sea. In: Witkowski A., Harff J., Reckermann M. (eds.), *2nd International Conference on Climate Change – The Environmental and Socio-Economic Response in the Southern Baltic Region, 12–15 May 2014, Szczecin, Poland. Conference Proceedings*. International Baltic Earth Secretariat Publication, Geesthacht, Germany, 2, 94–95.

*Abstracts of conference presentations (5.2):*

**Giudici A.**, Nikolkina I. 2014. Automated detection of crossing seas from simulated wave spectra. In: *Measuring and Modeling of Multi-Scale Interactions in the Marine Environment. IEEE/OES Baltic Symposium 2014, 26–29 May 2014, Tallinn, Estonia. Book of Abstracts*, 38.

**Giudici A.**, Soomere T. 2014. On the possibility of spontaneous patch formation in the Gulf of Finland. In: *Measuring and Modeling of Multi-Scale Interactions in the Marine Environment. IEEE/OES Baltic Symposium 2014, 26–29 May 2014, Tallinn, Estonia. Book of Abstracts*, 38.

**Giudici A.**, Soomere T. 2014. Quantification of spontaneous patch generation in marine surface layer. In: *MEME'2014 Mathematics and Engineering in Marine and Earth Problems, 22–25 July 2014, Aveiro, Portugal. Book of Abstracts*, 56–57.

**Giudici A.**, Soomere T. 2014. Finite-time compressibility as a measure of likelihood of spontaneous patch formation in the Gulf of Finland. In: Salupere A., Maugin G.A. (eds.), *IUTAM Symposium on Complexity of Nonlinear Waves, 8–12 September 2014, Tallinn 2014. Book of Abstracts*. Institute of Cybernetics at Tallinn University of Technology, Tallinn, 55–56.

**Giudici A.**, Soomere T. 2013. Identification of coastal areas of frequent patch formation from velocity fields. In: Russell P.E., Masselink G. (eds.), *ICS2013 International Coastal Symposium 2013, 8–12 April 2013, Plymouth, England. Book of Abstracts*. CERF, 105.

**Giudici A.**, Soomere T. 2013. In search for the areas of natural patch generation in the Gulf of Finland In: *9th Baltic Sea Science Congress: New Horizons for Baltic Sea Science, 26–30 August 2013, Klaipėda, Lithuania. Abstract Book*. Coastal Research and Planning Institute of Klaipėda University (KU CORPI), Klaipėda, 40.

**Giudici A.**, Kalda J., Soomere T. 2012. On the compressibility of surface currents in the Gulf of Finland, the Baltic Sea. In: *2012 IEEE/OES Baltic International Symposium "Ocean: Past, Present and Future Climate Change Research, Ocean Observation & Advances Technologies for Regional Sustainability", 8–11 May 2012, Klaipėda, Lithuania. Presentation Abstracts*. Baltic Valley, Klaipėda, 54.

**Giudici A.**, Kalda J. 2011. Compressibility of sea surface created by 3D current field. In: *BSSC 8th Baltic Sea Science Congress, 22–26 August 2011, Saint Petersburg, Russia. Book of Abstracts*. Russian State Hydrometeorological University (RSHU), Saint Petersburg, 57.

## Appendix B: Elulookirjeldus

### 1. Isikuandmed

Ees- ja perekonnanimi    Andrea Giudici  
Sünniaeg ja -koht        29.03.1985, Savona, Itaalia  
Aadress                      Akadeemia tee 21, 12618 Tallinn  
Telefon                      (+372) 583 90 544  
E-mail                        andrea@cens.ioc.ee

### 2. Hariduskäik

Õppeasutus	Lõpetamise aeg	Haridus (eriala / kraad)
Genua Ülikool (Università degli Studi di Genova)	2010	Arvutiteadus / magister
Genua Ülikool (Università degli Studi di Genova)	2008	Arvutiteadus / bakalaureus

### 3. Keelteoskus

Keel	Tase
itaalia	emakeel
inglise	kõrgtase
prantsuse	kesktase
eesti	algtase

### 4. Täiendõpe

Õppimise aeg	Täiendõppe läbiviija nimetus
September 2011	Rahvusvaheline suvekool <i>Preventive methods for coastal protection</i> (Klaipėda, Leedu)

### 5. Teenistuskäik

Töötamise aeg	Tööandja nimetus	Ametikoht
Jaauary 2011–tänaeni	Tallinna Tehnikaülikooli Küberneetika Instituut	Tehnik, insener

### 5. Teadustegevus

Avaldatud teadusartiklite ja konverentsiteeside loetelu on toodud ingliskeelse CV juures.

## Paper I

**Giudici A.**, Kalda J., Soomere T. 2012. On the compressibility of surface currents in the Gulf of Finland, the Baltic Sea. In: *IEEE/OES Baltic 2012 International Symposium, 8–11 May 2012, Klaipėda, Lithuania*. Proceedings. IEEE, 8 pp., doi: 10.1109/BALTIC.2012.6249178



# On the compressibility of surface currents in the Gulf of Finland, the Baltic Sea

A. Giudici<sup>a</sup>, J. Kalda<sup>a</sup>, T. Soomere<sup>a,b</sup>

<sup>a</sup>Institute of Cybernetics at Tallinn University of Technology, Akadeemia tee 21, 12618 Tallinn, Estonia

<sup>b</sup>Estonian Academy of Sciences, Kohtu 6, 10130 Tallinn, Estonia

*Abstract*—We address ways of quantification of the ability of different substances in the marine environment to form areas with high concentrations (patches) in the surface layer. This ability is usually linked with the so-called property of (flow) compressibility of sea surface (understood as the relative weight of the potential component of a velocity field). We analyze the potential of using for this purpose a modified measure – the Finite Time Compressibility (FTC) that is directly related to the ability of clustering of passive tracers in some regions of the sea surface and that can be calculated in a straightforward way from surface velocities. Shown is that under reasonable assumptions and short time intervals the FTC is a direct extension of the classical flow compressibility. An explicit relationship between the two definitions is derived under these assumptions. The two quantities are generally slightly different and coincide for a particular value of 0.781. The maps of FTC are evaluated for the Gulf of Finland based on 3D velocity fields obtained using the Rossby Centre Ocean Model (Swedish Meteorological and Hydrological Institute) for 1991 and the TRACMASS code for tracking Lagrangian trajectories.

## I. INTRODUCTION

The natural three-dimensional (3D) motions in the ocean generally scatter initially close clusters of particles [1,2]. Consequently, in fully 3D flow fields the density of adverse impacts rapidly decreases with the distance from their release site. The situation is fundamentally different for light particles (e.g., oil spill or plastic debris [3,4]) that float in surface currents. Persistent currents, such as the Gulf Stream or Kuroshio, carry large water masses and also floating pollutants across great distances. For example, debris originating from South America often reaches as far as remote Pacific Islands [5].

A remarkable property of particles floating in the surface layer is their ability to gather into patches in some regions of the open ocean. This usually occurs in major convergence or subduction zones [6,7] owing to specific 3D features of the ocean circulation. The presence of differently sized and shaped patches of a number of intrinsic properties of the marine environment such as salinity or temperature [8] is an inherent part of the functioning of the World Ocean. For example, filament generation in quasi-2D velocity fields [9] naturally leads to extremely complicated spatial structure of concentrations of various quantities [10]. Even frequently occurring phenomena like horizontal density gradient [11] or classical estuarine circulation [12] may lead to accumulation of sediment particles or well-defined turbidity maxima. The Langmuir circulation [13] mechanism may lead to similar

effects and operates at even smaller scales. All these phenomena are characterized by a substantial vertical component and therefore a 3D vertical structure of the motions.

In this paper, we continue the analysis of the ways of quantification of the potential of formation of patches (more generally, inhomogeneities in initially homogeneously distributed fields of passive tracers locked in the surface layer) on the sea surface [14]. The starting point is the so-called property of (flow) compressibility of sea surface. Differently from the classical definition of compressibility of the medium (understood as a measure of the relative volume change), our notion relies on the motion of water particles, and is a natural generalization of the divergence or convergence of the flow field. The flow compressibility  $C_c$  is usually defined using the Helmholtz decomposition of virtually any realistic field of motions into the sum of an irrotational (curl-free, also called potential) vector field and a solenoidal (divergence-free) components. A particular value of  $C_c$  is the relative weight of the potential component of the velocity field at a certain location. A fully solenoidal flow has compressibility  $C_c = 0$  and a potential flow has compressibility  $C_c = 1$ . In essence, the flow compressibility is a naturally normalized generalization of the divergence of this flow.

Different properties of the fluid motion and transport have been related to the effects of flow compressibility within various theoretical and experimental approaches [15–18]. The importance of these effects in marine environments is still unclear. A promising way forward is to interpret the compressibility of the sea surface as an indicator of the potential for the concentration of floaters at a particular position on the surface. If the overall surface of an enclosed sea area does not change in time (as is approximately the case in the World Ocean), the average flow divergence over the entire sea surface is strictly zero. Floaters though, tend to spend more time in contracting regions than in expanding ones: The expanding flows tend to push floaters away, while the contracting ones tend to attract and keep floaters within their areas of influence. Therefore, floaters or tracers tend to gather into patches within areas which systematically show nonzero compressibility.

The systematic formation of areas with high or low concentration of tracers is possible only if the potential flow component dominates. Moreover, it only happens if the value

of flow compressibility at each point of a certain area exceeds a particular threshold. For example, in ideal Kraichnan flows (which are delta-correlated in time), the crossover to clusterization takes place at the critical value of compressibility  $C_c = 0.5$  [15]. The presence of non-zero flow compressibility can affect dramatically the behavior of the tracers, giving rise to extensive clusterization and development of fractal structures [19–20]. High values of  $C_c$  can, thus, be naturally associated with areas prone to the development of patches of floaters. Such areas are inherent candidates for areas of reduced risk in terms of pollution transport towards the coasts [21]. Their use for environmental management could potentially affect both the probability and propagation time of adverse impacts from different offshore areas to the vulnerable regions.

The 3D atmospheric and ocean flows are usually almost incompressible in this framework, hence incapable of producing the patchiness of tracers [22]. The impact of (weakly) nonlinear waves in increasing the values of  $C_c$ , is almost negligible in the marine environment [23].

The most notable exception that may exhibit substantial flow compressibility is the marine surface layer that hosts an almost 2D velocity field. Here larger values of  $C_c$  are possible due to the capability of the particles floating on the surface to “dive” into the third dimension [24], for example, owing to upwelling or downwelling phenomena. Thus, the average flow compressibility of such a formally 2D velocity field on sea surface may largely exceed the analogous values for any other part of the overall 3D motion. This feature therefore could explain, at least partially, the development of patches of floaters in the marine environment. We specifically emphasize the importance of 3D effects on the large values of  $C_c$ : as mesoscale and large-scale flows in marine environments are often quasi-2D [25–26], the observed values of flow compressibility at the surface are usually relatively low.

In this paper, we focus on the possibility of the formation of high levels of flow compressibility of a 2D velocity field that may substantially affect the concentration of substances on the sea surface. The phenomenon of sea patchiness has been the object of many studies and applications in the Baltic Sea since the 1980s [27,28]. Our test area is the Gulf of Finland [29], the easternmost sub-basin of the Baltic Sea. This sea is characterized by particularly frequent occurrence of 3D dynamics [30]. The Gulf of Finland frequently hosts powerful up- and downwelling events [31,32] and thus is a natural example of a domain with substantial nonzero values of flow compressibility in the surface layer.

Both experimental and numerical results indicate that the time correlations (which are always present for real hydrodynamic flows) can either inhibit or catalyze the clusterization process [17]. For example, the free-slip surface of fully turbulent water volumes is characterized by  $C_c \approx 0.5$  [33]. For this reason we employ a modified measure of flow

compressibility that is directly related to the ability of some regions of the sea surface to shrink or expand and also accounts for finite-time correlations of the motions [14]. This measure, which we will refer to as the *finite-time compressibility* (FTC), will be shown to coincide with the classical flow compressibility at the limit of ideal Kraichnan flows [15] although the single values of these two measures may deviate from each other to some extent. For reference purposes we use an alternative definition of flow compressibility, the values of which coincides with the classical flow compressibility for ideal Kraichnan flows but which allows for a simple link with the actual behavior of floaters at sea surface.

Since the compressibility values of a velocity field coincide with those of the motion of fluid particles floating in it, we choose to study the compressibility of a velocity field through the displacement vector fields of simulated floater’s trajectories generated by that velocity field.

The structure of this paper is as follows. The pool of velocity data, models used for its calculation and for tracking the surface elements on the sea surface are described in Section 2. The definition of the finite-time compressibility and its calculation scheme are presented in section 3. Section 4 quantifies the relationship between the (classical) flow compressibility and the FTC. Section 5 depicts the spatial distribution of the FTC and the classical flow compressibility for the Gulf of Finland across selected periods. Section 6 contains some final conclusions.

## II. CIRCULATION MODEL AND LAGRANGIAN TRACKING CODE

We use velocity fields calculated for the year 1991 by the Rossby Centre Ocean Model (RCO) and provided by the Swedish Meteorological and Hydrological Institute in the framework of BONUS+ BalticWay cooperation. This year has been chosen in order for the results to be comparable with the outcome of the quantification of offshore areas in terms of their ability to serve as sources of environmental risk to the coastal areas in terms of current-induced transport [34]. The RCO model has been described in a number of sources [35–37]. Its particular realization has a spatial resolution of  $2 \times 2$  nautical miles and 41 vertical levels along the z-axis in the entire Baltic Sea. The thickness of the surface layer is 3 m. This model is based on a Bryan-Cox-Semtner primitive equation circulation model, coupled with a sea ice model, with a free surface and open boundary conditions in the northern Kattegat. The particular model run was forced with 10 m wind, 2 m air temperature, 2 m specific humidity, precipitation, total cloudiness and sea level pressure fields from a regionalization of the ERA-40 re-analysis over Europe using a regional atmosphere model with a horizontal resolution of 22 km during 1961–2007 [38]. For further details of the model set-up and an extensive validation of model input the reader is referred [35–37.]

The horizontal displacement of water particles, associated with tracers, has been calculated using their Lagrangian

trajectories found by the TRACMASS model [39–41] from the RCO velocity fields. The vertical motions of the particles were ignored. Owing to the relatively coarse resolution of the RCO velocity data, the analysis below ignores the diffusion of particles and most of the impact of subgrid-scale processes (only a part of which have been accounted for through various parameterizations in the RCO model). Also, the version of the TRACMASS model use in this study does not account for local turbulent diffusion. The results, therefore, only reflect the compressibility of relatively large-scale motions.

### III. FINITE-TIME COMPRESSIBILITY

As discussed in [14], the nonzero values of compressibility alone are unable to justify the development of patches on the sea surface for real time-correlated flows. Following the ideas developed in [14], we shall use a measure of compressibility that has a larger potential to describe the formation of patches. While the classical definition of flow compressibility relies on certain instantaneous properties of the flow field (and thus ignores any history of the flow field), our aim is to account for the properties of real flows with finite-time correlations. The key idea behind the definition of the FTC [14] is to relate the finite-time changes in the material volumes (e.g. surface areas in the case of 2D flows overlying 3D circulation) to the finite-time changes in the separation between material particles.

The formation of a patch of otherwise more or less homogeneously distributed tracers or particles on the sea surface is obviously associated with a substantial decrease in the distance between the particles or, equivalently, in the area that initially hosts these particles. Probably the simplest way to observe and track systematic changes to specific areas at the sea surface is to track the development of small elements of this surface. The simplest of these elements is a triangle whose vertices initially belong to adjacent grid cells forming an L-shaped pattern (Fig. 1). By definition, the area of such a triangle is initially nonzero.

The values of the FTC are calculated by means of tracking the displacement of its vertices over certain time intervals. The motion of vertices is equivalent to Lagrangian drift of particles at the locations of these vertices. This drift is also calculated using the trajectory simulation code TRACMASS.

Initially, one tracer is positioned at the center of every grid cell of the RCO model. The initial separation of two adjacent tracers along latitude and longitude is, therefore, the same as the resolution of the grid, approximately 2 nautical miles.

Let  $S_t/2$  be the instantaneous area of a triangle formed by a

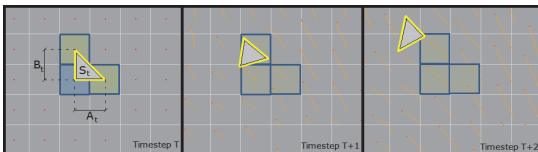


Figure 1. Scheme of the selection of surface elements and their distortions in time.

centre of a selected grid point and the centers of its immediate neighbors to the south and east at a (discrete) time instant  $t$  (Fig. 1). As the velocity information in use has been saved once in 6 hours, the natural time “step” in our calculations is 6 hours. We use below somewhat shorter step of 4 hours. The relative change over time of the area of the triangle is  $dS_t = (S_t - S_{t-1})/S_t$ . The other components of the definition of the FTC are the squared lengths  $A_t$  and  $B_t$  of two edges of the triangle that are initially parallel to the latitudes and longitudes, respectively. Their respective changes over time are  $dA_t = (A_t - A_{t-1})/A_t$  and  $dB_t = (B_t - B_{t-1})/B_t$ . The finite-time compressibility  $C_{fic}$  is calculated now from the changes to the three quantities in question at different time steps:

$$C_{fic} = \frac{2dS_{rms}}{dA_{rms} + dB_{rms}}, \quad (1)$$

where the components of the right-hand side of (1) have the meaning of rms (root mean square) values of the respective quantities; e.g.,

$$dS_{rms} = \sqrt{\frac{1}{n} \sum_i^n dS_t^2}, \quad (2)$$

where  $i$  indicates a particular realization of the flow (a calendar day in our simulations, see below). The rms in (2) is calculated on a number of samples that linearly depends on the length of the chosen time window.

From (1)–(2) it follows that for a purely incompressible flow  $dS_{rms} = 0$ , and hence the compressibility  $C_{fic} = 0$  in the entire area covered by such a flow. In the contrary, if the flow is purely contractive or expanding, the quantities  $A$  or  $B$  would change with the same relative rate as  $S$ , so that we would have  $C_{fic} = 1$ . The values of  $C_{fic}$  defined by (1) obviously are in the range  $[0,1]$ , with  $C_{fic} = 1$  implying a purely compressible flow. This measure of compressibility  $C_{fic}$  accounts for the finite-time correlations and its values are, by definition, directly related to the ability of gathering the tracer particle into patches [14].

The scheme of calculations of  $C_{fic}$  resembles a similar scheme used for the identification of semi-persistent circulation patterns [21]. A longer time interval  $t_D$  of interest (year 1991 in the calculations in this paper) is divided into time intervals (windows) with a length of  $t_W = 16\text{--}96$  hours

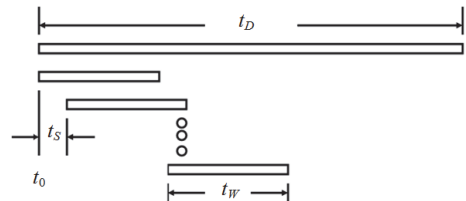


Figure 2. Definition sketch of splitting the simulation period into time windows.

(Fig. 2). As mentioned above, one tracer is placed at the center of each wet grid point of the RCO model and its displacement is traced over this window. The results form one realization of the changes to the area of surface elements. Every subsequent realization tracks the same pattern of tracers and surface elements but the TRACMASS simulations are restarted with a time lag of  $t_S = 1$  day (and thus use a new set of velocity data). An estimate of the value of  $C_{fic}$  for a particular time interval (day, week, season, etc.) is obtained by pointwise averaging the corresponding set of realizations.

The resulting spatial maps characterize the field of FTC for different time intervals. As discussed above, large values of compressibility show that large changes to the concentration of various tracers are expected. In other words, large values of  $C_{fic}$  indicate areas where high concentrations of floaters, garbage, adverse impacts, etc., are likely to be formed.

The described method for evaluating the FTC can be also used to calculate the classical flow compressibility  $C_c$ . This similarity allows us to provide direct comparisons between the two measures. At any step of a simulation, the floater, initially positioned at the center of the cell on the  $r^{\text{th}}$  row and  $c^{\text{th}}$  column, has coordinates  $(x'_{(r,c)}, y'_{(r,c)})$ . We define a displacement vector field  $\vec{D} = (Dx, Dy)$  of the motion of the tracer during a time step  $[t, t+1]$ :

$$Dx'_{(r,c)} = x'^{t+1}_{(r,c)} - x'^t_{(r,c)}, \quad Dy'_{(r,c)} = y'^{t+1}_{(r,c)} - y'^t_{(r,c)}. \quad (3)$$

This vector field is built from differences of subsequent positions within trajectories governed by the underlying velocity field. Therefore, the field  $\vec{D}$  is simply a discrete approximation of the velocity field and thus has the same flow compressibility

$$C_c = \frac{(u_x + v_y)^2}{u_x^2 + u_y^2 + v_x^2 + v_y^2} \quad (4)$$

as the underlying velocity field  $\vec{v} = (u, v)$ . Here subscripts indicate differentiation along the respective coordinate. This widely used alternative to the classical definition of the compressibility is provided by the squared ratio of the velocity divergence to the norm of the velocity gradient tensor. For ideal Kraichnan flows, this definition coincides with the classical one. The flow compressibility is evaluated using (4) and the finite difference representation of the velocity field in terms of the displacement vector field:

$$\begin{aligned} u_x &= \left( Dx'_{(r,c+1)} - Dx'_{(r,c)} \right) / \Delta t, \\ u_y &= \left( Dx'_{(r+1,c)} - Dx'_{(r,c)} \right) / \Delta t, \\ v_x &= \left( Dy'_{(r,c+1)} - Dy'_{(r,c)} \right) / \Delta t, \\ v_y &= \left( Dy'_{(r+1,c)} - Dy'_{(r,c)} \right) / \Delta t. \end{aligned} \quad (5)$$

Note that the results using this formula may slightly deviate from the theoretical values owing to the use of finite-difference representation of the velocity fields. An implicit checking of the accuracy of the results can be made using the

basin-wise average 2D flow divergence. This quantity should be exactly zero for enclosed sea areas. Its deviations from this value offer a way to judge to a certain degree about the correctness of the calculations. Many areas of the Gulf of Finland host quite large values of divergence, up to 0.80. The divergence, integrated over the entire area of the Gulf of Finland (calculated using the described technique with  $t_W = 4$  hours), shows very small values, typically of the order of 0.01, for every single day throughout the year 1991 (Fig. 3). Consequently, the approximation in use properly reflects not only the flow properties at single points but also its integrated properties. The small variations in the overall divergence reflect, additionally to inaccuracies of the discrete approximation, also to some extent the surface water exchange between the Gulf of Finland (over which the divergence is calculated) and the Baltic Proper. The mostly positive values apparently mirror the excess of fresh water inflow into this area while a few negative values evidently are connected with surface water inflow owing to specific wind events [32].

#### IV. COMPARISON WITH THE CLASSICAL DEFINITION OF FLOW COMPRESSIBILITY

The relationship between the two definitions of compressibility can be established in the following manner. Let us start from a single surface element, laying within a surface layer velocity field, at two infinitely close time instants  $t$  and  $t+1$  (Fig. 4). The flux of the vector field of velocity through the contour of the surface element is related to the behavior of the vector field inside this element by Ostrogradsky's theorem

$$\Delta S = \int_S \nabla \cdot \vec{v} \, dt. \quad (6)$$

Since we consider  $dt$  to be very small, we can assume that during that time interval, the surface does not change significantly, thus we can write the integral in (6) as  $\Delta S = \nabla \cdot \vec{v} (\Delta t)$ .

From this relation it follows that

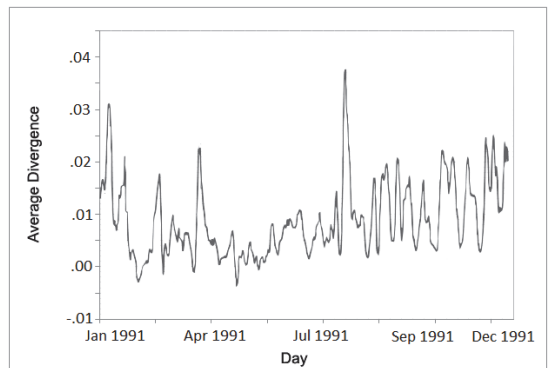


Figure 3. Divergence of the 2D flow on the sea surface, integrated over the entire Gulf of Finland throughout year 1991 [14].

$$dS = \frac{\Delta S}{S} = \nabla \cdot \vec{v} \Delta t \quad \text{or} \quad (dS_{rms})^2 = \langle (\nabla \cdot \vec{v})^2 \rangle (\Delta t)^2. \quad (7)$$

where the angle brackets denote an ensemble average (here understood as taking the rms).

Let us now consider a moving frame of reference  $(\xi, \eta)$ , centered at vertex  $(x'_1, y'_1)$ . One of its axes, let it be  $\xi$ , is parallel to vector  $\vec{a}'_3 = (x'_3 - x'_1, y'_3 - y'_1)$ . Then, within the moving frame of reference  $(\xi, \eta)$ , vector  $\vec{a}_3$  has components  $(L_B, 0)$  and represents the length  $|\vec{a}_3^t| = L_B$ , where  $L_B = \sqrt{B}$  of the relevant edge.

At the next time step  $t+1$ , vector  $\vec{a}_3^{t+1}$  becomes:

$$\vec{a}_3^{t+1} = (L_B + U_\xi L_B \Delta t, V_\xi L_B \Delta t), \quad (8)$$

where  $\vec{V} = (U, V)$  is the velocity in the  $(\xi, \eta)$ -coordinates. Therefore,

$$\Delta(\vec{a}_3)^2 = |\vec{a}_3^{t+1}|^2 - |\vec{a}_3^t|^2 \approx 2U_\xi L_B^2 \Delta t, \quad (9)$$

where the terms  $O((\Delta t)^2)$  have been ignored. This gives us an expression for  $d(L_B^2) = dB$ :

$$d(L_B^2) = \frac{\Delta(\vec{a}_3)^2}{(\vec{a}_3)^2} \approx 2U_\xi \Delta t. \quad (10)$$

By definition of the rms we have now:

$$dB_{rms} \approx 2\sqrt{\langle U_\xi^2 \rangle} \Delta t. \quad (11)$$

It is natural to assume that the vector fields of velocity are statistically isotropic. From this property it follows that

$$dB_{rms} \approx 2\sqrt{\langle U_\xi^2 \rangle} \Delta t = 2\sqrt{\langle u_x^2 \rangle} \Delta t = 2\sqrt{\langle v_y^2 \rangle} \Delta t. \quad (12)$$

Similarly, we can write

$$dA_{rms} \approx 2\sqrt{\langle u_x^2 \rangle} \Delta t. \quad (13)$$

At this point, we have all the elements to be plugged into the expressions for the classical flow compressibility (4) and for the FTC (1). The key point of the presented chain of derivation is the possibility to replace the sum  $dA_{rms} + dB_{rms}$  in (1) by certain quantities that can be expressed in terms of the classical flow compressibility. After substituting the

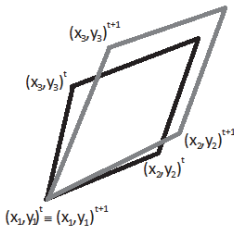


Figure 4. A surface element at two infinitely close time intervals.

derived expressions into (1) and (4) we have:

$$C_c = \frac{\langle (\nabla \cdot \vec{v})^2 \rangle}{2\langle u_x^2 \rangle + 2\langle u_y^2 \rangle}, \quad (14)$$

$$C_{ftc}^2 = \frac{4(dS_{rms})^2}{(dA_{rms} + dB_{rms})^2} = \frac{\langle (\nabla \cdot \vec{v})^2 \rangle}{4\langle u_x^2 \rangle}.$$

From (14) we get the following relationship between the flow compressibility and the FTC:

$$C_{ftc}^2 = \frac{\langle u_x^2 \rangle + \langle v_y^2 \rangle}{2\langle u_x^2 \rangle} C_c. \quad (15)$$

We can at this point recall the expressions for velocity components in terms of  $C_c$ , according to ([42], Eq. (58)) as follows:

$$\langle u_x^2 \rangle = K[(3 - 2C_c) + 2(2C_c - 1)] = K(2C_c + 1), \quad (16)$$

$$\langle v_y^2 \rangle = K(3 - 2C_c).$$

The factor  $K$  in these expressions involves some constant quantities which will cancel out after substitution of (16) into (15). This substitution gives us the final result:

$$C_{ftc}^2 = \frac{2C_c}{2C_c + 1}. \quad (17)$$

From (17) it is clear that the two measures (Fig. 5) simultaneously tend to zero. At the threshold  $C_c = 0.5$  for the process of clustering the finite-time compressibility is  $C_{ftc} = \sqrt{1/2}$ . For moderate levels of compressibility  $C_{ftc} > C_c$ . The two measures only coincide if  $C_{ftc} = C_c = \sqrt{(\sqrt{17} - 1)}/4 \approx 0.781$ . For larger values of  $C_c$  the FTC exceeds the flow compressibility. When  $C_c = 1$ , the FTC measures  $C_{ftc} = \sqrt{2/3}$ . This implies that for  $\sqrt{2/3} < C_{ftc} \leq 1$ , there are no corresponding values for flow compressibility.

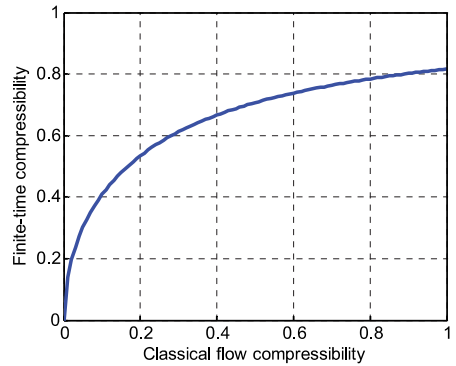


Figure 5. FTC as a function of classical flow compressibility.

It is, however, easy to show that there exist situations where the values of FTC may reach  $C_{ftc} = 1$ , which would be impossible in terms of the classical flow compressibility definition because of (17). Let us consider a patch, whose edges are orthogonal to each other, and whose vertices are moving apart from each other alongside its edges. Let the squared lengths of its edges  $A$  and  $B$  be respectively  $L_A^2$  and  $L_B^2$  at time step  $t$  and  $L_A^2(1-\varepsilon)^2$  and  $L_B^2(1-\varepsilon)^2$  at time step  $t+1$ , where  $\varepsilon$  is an arbitrarily small value. Further,  $S^t = L_A L_B$  at time step  $t$  and  $S^{t+1} = L_A L_B (1-\varepsilon)^2$  at time step  $t+1$ . Therefore,  $dS \approx -2\varepsilon L_A^2$  and  $dA \approx dB \approx -2\varepsilon L_A^2$  provided  $L_A \approx L_B$ . Substituting these values into the definition of FTC (1) gives:

$$C_{ftc} = \frac{2\langle dS \rangle}{\langle dA \rangle + \langle dB \rangle} = \frac{2 \cdot (-2\varepsilon)}{-2\varepsilon - 2\varepsilon} = 1. \quad (18)$$

## V. COMPRESSIBILITY MAPS

The produced maps clearly show that there exist areas characterized by high FTC in the Gulf of Finland. Many of these areas have elongated stripe-like shapes and are generally located close to the shore (Fig. 6). As expected, the regions frequently hosting up- or downwelling phenomena [30] exhibit large values of FTC. These phenomena might present also upwelling filaments, or divergence or convergence zones between coastal currents and offshore mesoscale circulation. For example, during the first week of November 1991, the highest compressibility is found in the vicinity of the mouth of the River Kymi, in the north-eastern part of the Gulf of Finland. This region is characterized by values of FTC up to 0.9. The probable reason for such high values is merging of voluminous amounts of waters coming from the River Neva and River Kymi.

In contrast with the classical flow compressibility, the FTC naturally depends on the length of the time window used for estimates of the change to the area of surface elements. As shown above, for short windows, the values of FTC almost coincide with those of the classical flow compressibility. Using longer time windows is helpful to track the distortions of the surface elements during their Lagrangian drift, and thus to identify areas over which the FTC increases cumulatively

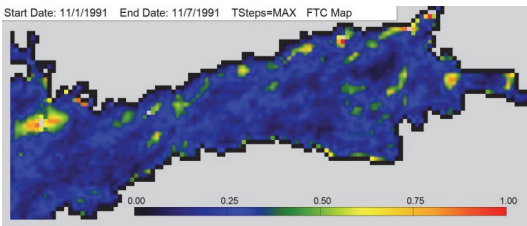


Figure 6. Average finite-time compressibility of water surface in the Gulf of Finland for one week in November 1991 calculated using the time window of 48 hours.

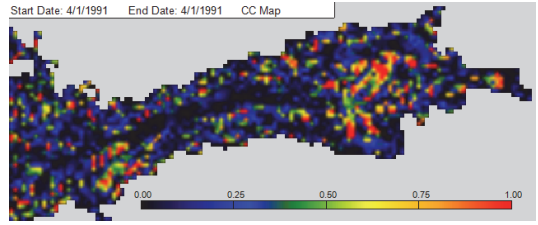


Figure 7. Classical flow compressibility of water surface in the Gulf of Finland on 1 April 1991.

over some time interval. These areas are the best candidates for gathering clusters of adverse impacts.

Similar observations become evident at the maps of the classical flow compressibility (Fig. 7). Its pointwise values offer some indication about areas where floaters are likely to gather into patches.

In fact, a grid cell characterized by high flow compressibility does not predict the likelihood of that cell to really develop patches of floaters during a longer time interval [14]. In essence, they mirror high instantaneous values of divergence or convergence, with essentially no correlation with the long-term flow properties. This explains why these maps look more pixelated and change in time much more rapidly than the maps of FTC. The maps of FTC account for changing flow properties over longer time windows and therefore are better candidates to indicate high compressibility in areas where the development of patchiness is likely from the physical point of view, such as coastal stripes or domains where usually up- and downwelling phenomena take place.

When using shorter time windows, resulting values of the FTC are generally below the critical threshold of  $\text{Sqrt}(0.5)$ . The threshold is usually crossed when the size of the time window is 12 hours or more (Fig. 8). When progressively increasing this length to 48–72 hours, the threshold is crossed at several locations (Fig. 8). Nevertheless, high compressibility areas remain the same, independently of the length of the chosen time window.

In many occasions the areas with high FTC form elongated patterns that may be interpreted as regions with increasing compressibility in the direction of some surface current. Some of these patterns are oriented across the Gulf of Finland (Fig. 8), close enough to intense transport pathways [21]. The resulting development of patches may be associated with simultaneous transport of the patches towards certain coastal section.

Recent simulations of spatial distributions of the FTC [14] indicate strong seasonal variability in the location of areas with high compressibility. The maximum values of the FTC are largest in autumn. Much smaller values, usually below the threshold value of  $\text{Sqrt}(0.5)$ , appear in other seasons. Several spots with high values of FTC (near the mouth of the River Neva and at the entrance to the Gulf of Finland) are present during longer time intervals. Their life-time seems not to exceed a few months

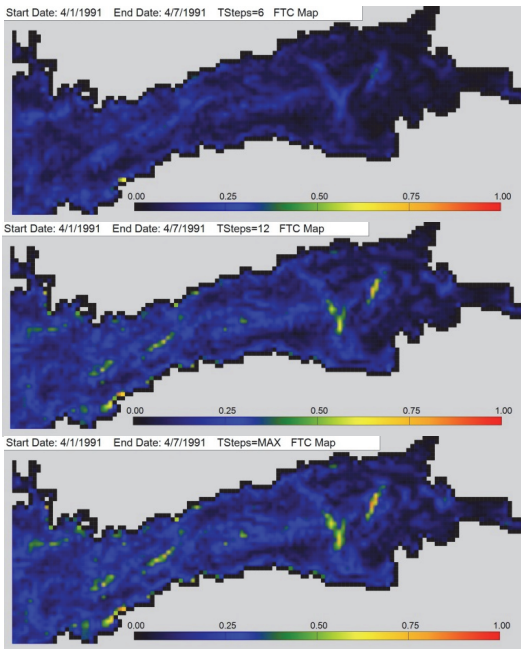


Figure 8. Average compressibility of water surface in the Gulf of Finland for one week in April 1991, calculated with the time window of 24 hours (upper panel), 48 hours (middle panel) and 72 hours (lower panel) [14].

Finally we underline that in this study we have used finite-difference representation of derivatives to calculate the maps of compressibility. This method may introduce some errors. The errors apparently do not distort the results as suggested by the analysis of Fig. 3. For the future, however, it is natural to avoid this type of numerical problems by means of calculating the classical flow compressibility through its original definition, using a direct decomposition of the underlying velocity field into its solenoidal and potential component.

## VI. CONCLUDING REMARKS

We have addressed the potential of the Finite Time Compressibility (FTC) for systematic quantification of the ability of different substances in the marine environment to form areas with high concentrations (patches) in the surface layer. The focus has been on a fundamental resource of patch development – the specific nature of the local 3D circulation that may give rise to systematic diving (e.g. downwelling) or uplift (e.g. upwelling) of water masses in certain sea areas. An interesting effect of these phenomena is the formation of potentially persistent patches of initially separated clusters of floaters. Understanding and quantification of the relevant mechanisms could shed more light to the behavior of potentially dangerous substances that are released into the sea.

This resource can be quantified using measures characterizing the persistence of convergence (or subduction)

areas. Several these measures (such as the flow compressibility of sea surface, understood as the relative weight of the potential component of a velocity field) have simple definitions but their analysis and especially their link with phenomena that occur at the sea surface is not always direct. In this sense, better understanding of the potential of using the FTC for this purpose would essentially clarify the situation as this measure can be directly related to the ability of clustering of passive tracers in some regions of the sea surface. Moreover, it can be calculated in a straightforward way from surface velocities.

Traditionally, flow compressibility is measured point-wise, and hence provides a measure of short-term processes. By definition, it does not take into account the time history of motions, and thus may fail to predict where and for how long clusters of floaters are more likely to form. The FTC tracks and accounts for local changes to the areas of basic sea-surface elements, over differently sized time frames. Its use may allow to more reliably highlighting the areas of the sea which systematically show a high likelihood in forming clusters of floaters.

The key outcome of this study is a simple proof that under reasonable assumptions and short time intervals the FTC is a direct extension of the classical compressibility. The FTC tends to behave qualitatively similarly to the classical flow compressibility, although the particular values of these two quantities are generally different.

Given the availability of high-resolution simulated 3D velocity fields for different sea domains, calculation of the maps of both classical (surface) flow compressibility and the FTC is a relatively simple exercise today. Our preliminary experiments suggest that there exist certain regions of the sea where patch formation occurs during a substantial time of the year. This process may take place not only in the coastal regions or in the well-documented regions of intense downwelling. Instead, it may become active at seemingly usual locations in the offshore. Generally, a better resolution of mesoscale variations than used in this study is necessary for reliable description of such sites in the Baltic Sea.

## ACKNOWLEDGMENT

The research was supported by the targeted financing by the Estonian Ministry of Education and Research (grant SF0140007s11), Estonian Science Foundation (grant No 9125 and 7909), and the European Union via a support to the Estonian Centre of Excellence CENS from the European Regional Development Fund. Andrea Giudici is supported by the framework of international PhD studentships (DoRa) in Estonia.

## REFERENCES

- [1] L.F. Richardson, "Atmospheric diffusion shown on a distance-neighbor graph," *Proc. Roy. Soc.*, vol. A110, pp. 709-737, 1926.
- [2] M. Ollitrault, C. Gabillet, and A. Colin de Verdiere, "Open ocean regimes of relative dispersion," *J. Fluid Mech.*, vol. 533, pp. 381-407, 2005.

- [3] A.L. Andrady, "Microplastics in the marine environment," *Mar. Pollut. Bull.*, vol. 62, pp. 1596-1605, 2010.
- [4] K. Schilling and M. Zessner, "Foam in the aquatic environment," *Water Res.*, vol. 45, 4355-4366, 2011.
- [5] Z.T. Richards and M. Beger, "A quantification of the standing stock of macro-debris in Majuro lagoon and its effect on hard coral communities," *Mar Pollut. Bull.*, vol. 62, pp. 1693-1701, 2011.
- [6] W.G. Pichel, J.H. Churnside, T.S. Veenstra, D.G. Foley, K.S. Friedman, R.E. Brainard, J.B. Nicoll, Q. Zheng, and P. Clemente-Colon, "Marine debris collects within the North Pacific Subtropical convergence zone," *Mar. Pollut. Bull.*, vol. 54, pp. 1207-1211, 2007.
- [7] D.K. Lee and N. Niiler, "Influence of warm SST anomalies formed in the eastern Pacific subduction zone on recent El Niño events," *J. Marine Res.*, vol. 68, pp. 459-477, 2010.
- [8] T.M. Powell and A. Okubo, "Turbulence, diffusion and patchiness in the sea," *Phil. Trans. Roy. Soc. London*, vol. 343, 11-18, 1994.
- [9] I.M. Held, R.T. Pierrehumbert, S.T. Garner, and K.L. Swanson, "Surface quasi-geostrophic dynamics," *J. Fluid Mech.*, vol. 282, pp. 1-20, 1995.
- [10] J. Kalda, "Simple model of intermittent passive scalar turbulence," *Phys. Rev. Lett.*, vol. 84, pp. 471-474, 2000.
- [11] H. Burchard, G. Floeser, J. V. Staneva, T.H. Badewien, and R. Riethmüller, "Impact of density gradients on net sediment transport into the Wadden Sea," *J. Phys. Oceanogr.*, vol. 38, 566-587, 2008.
- [12] H. Burchard, K. Bolding, and M.R. Villarreal, "Three-dimensional modelling of estuarine turbidity maxima in a tidal estuary," *Ocean Dyn.*, vol. 54, pp. 250-265, 2004.
- [13] S.A. Thorpe, "Spreading of floating particles by Langmuir circulation," *Mar. Pollut. Bull.*, vol. 58, pp. 1787-1791, 2009.
- [14] J. Kalda, T. Soomere, and A. Giudici, "On the compressibility of the surface currents in the Gulf of Finland, the Baltic Sea," submitted to *Journal of Marine Systems*.
- [15] G. Falkovich, K. Gawędzki, and M. Vergassola, "Particles and fields in fluid turbulence," *Rev. Mod. Phys.*, vol. 73, pp. 913-975, 2001.
- [16] J.R. Cressman, J. Davoudi, W.I. Goldburg, and J. Schumacher, "Eulerian and Lagrangian studies in surface flow turbulence," *New J. Phys.*, vol. 6, Art. No. 53, 2005.
- [17] G. Boffetta, J. Davoudi, B. Eckhardt, J. Schumacher, "Lagrangian tracers on a surface flow: The role of time correlations," *Phys. Rev. Lett.*, vol. 93, Art. No. 134501, 2004.
- [18] J. Kalda, "Sticky particles in compressible flows: aggregation and Richardson's Law," *Phys. Rev. Lett.*, vol. 98, Art. No. 064501, 2007.
- [19] J. Bec, K. Gawędzki, and P. Horvai, "Multifractal clustering in compressible flows," *Phys. Rev. Lett.*, vol. 92, Art. No. 224501, 2004.
- [20] P. Perlekar, R. Benzi, D. Nelson, and F. Toschi, "Population dynamics at high Reynolds number," *Phys. Rev. Lett.*, vol. 105, Art. No. 144501, 2010.
- [21] T. Soomere, B. Viikmäe, N. Delpeche, and K. Myrberg, "Towards identification of areas of reduced risk in the Gulf of Finland," *Proc. Estonian Acad. Sci.*, vol. 59, pp. 156-165, 2010.
- [22] R.A. Fine and F.J. Millero, "Compressibility of fluids as a function of temperature and pressure," *J. Chem. Phys.*, vol. 59, pp. 5529-5536, 1973.
- [23] M. Vucelja, G. Falkovich, and I. Fouxon, "Clustering of matter in waves and currents," *Phys. Rev. E*, vol. 75, Art. No. 065301, 2007.
- [24] T.S. Garrison, *Essentials of oceanography*, 5th ed. Pacific Grove: Brooks Cole, 2011.
- [25] P. Rhines, "Geostrophic turbulence," *Ann. Rev. Fluid Mech.*, vol. 11, pp. 401-441, 1979.
- [26] R.H. Kraichnan and D. Montgomery, "Two-dimensional turbulence," *Repts. Progr. Phys.*, vol. 43, pp. 548-619, 1980.
- [27] K. Kononen, S. Nömmann, G. Hansen, R. Hansen, G. Breuel, and E.N. Gupalo, "Spatial heterogeneity and dynamics of vernal phytoplankton species in the Baltic Sea in April-May 1986," *J. Plankton Res.*, vol. 14, pp. 107-125, 1992.
- [28] M. Granskog, H. Kaartokallio, H. Kuosa, D. Thomas, J. Ehn, and E. Sonninen, "Scales of horizontal patchiness in chlorophyll a, chemical and physical properties of landfast sea ice in the Gulf of Finland (Baltic Sea)," *Polar Biology*, vol. 28, pp. 276-283, 2005.
- [29] P. Alenius, A. Nekrasov, and K. Myrberg, "Physical oceanography of the Gulf of Finland: a review," *Boreal Environ. Res.*, vol. 3, pp. 97-125, 1998.
- [30] K. Myrberg and O. Andrejev, "Main upwelling regions in the Baltic Sea - a statistical analysis based on three-dimensional modeling," *Boreal Environ. Res.*, vol. 8, pp. 97-112, 2003.
- [31] A. Lehmann and K. Myrberg, "Upwelling in the Baltic Sea - a review," *J. Marine Sys.*, vol. 74, S3-S12, 2008.
- [32] M. Leppäranta and K. Myrberg, *The physical oceanography of the Baltic Sea*. Berlin Heidelberg: Springer, 2009.
- [33] J. Schumacher and B. Eckhardt, "Clustering dynamics of Lagrangian tracers in free-surface flows," *Phys. Rev. E*, vol. 66, Art. No. 017303, 2002.
- [34] T. Soomere, O. Andrejev, A. Sokolov, and K. Myrberg, "The use of Lagrangian trajectories for identification of the environmentally safe fairway," *Mar. Pollut. Bull.*, vol. 62, pp. 1410-1420, 2011.
- [35] H.E.M. Meier, R. Doscher, and T. Faxen, "A multiprocessor coupled ice-ocean model for the Baltic Sea: application to salt inflow," *J. Geophys. Res.*, vol. C106, C30,997-C31,016, 2003.
- [36] H.E.M. Meier, "Modeling the pathways and ages of inflowing salt- and freshwater in the Baltic Sea," *Estuar. Coast. Shelf Sci.*, vol. 74, pp. 610-627, 2007.
- [37] H.E.M. Meier, "On the parametrization of mixing in three-dimensional Baltic Sea models," *J. Geophys. Res.*, vol. C106, pp. 30,997-31,016, 2001.
- [38] P. Samuelsson, C.G. Jones, U. Willén, A. Ullerstig, S. Gollvik, U. Hansson, C. Jansson, E. Kjellström, G. Nikulin, and K. Wyser, "The Rossby Centre Regional Climate Model RCA3: Model description and performance," *Tellus A*, vol. 63, pp. 4-23, 2011.
- [39] B. Blanke and R. Raynard, "Kinematics of the Pacific Equatorial Undercurrent: an Eulerian and Lagrangian approach from GCM results," *J. Phys. Oceanogr.*, vol. 27, pp. 1038-1053, 1997.
- [40] K. Döös, "Inter-ocean exchange of water masses," *J. Geophys. Res.*, vol. C100, pp. 13499-13514, 1995.
- [41] P. de Vries and K. Döös, "Calculating Lagrangian trajectories using time-dependent velocity fields," *J. Atmos. Ocean. Techn.*, vol. 18, pp. 1092-1101, 2001.
- [42] G. Falkovich, K. Gawędzki, and M. Vergassola, "Particles and fields in fluid turbulence," *Rev. Modern Phys.*, vol. 73, pp. 913-975, October 2001.

## Paper II

**Giudici A.**, Soomere T. 2013. Identification of areas of frequent patch formation from velocity fields. *Journal of Coastal Research*, Special Issue 65, vol. 1, 231–236, doi: 10.2112/SI65-040.1



# Identification of areas of frequent patch formation from velocity fields



Andrea Giudici†, Tarmo Soomere†‡

† Institute of Cybernetics at Tallinn  
University of Technology, Akadeemia  
tee 21, Tallinn, EE-12618, Estonia  
andrea@cens.ioc.ee

‡ Estonian Academy of Sciences,  
Kohtu 6, 10130 Tallinn, Estonia  
soomere@cs.ioc.ee

[www.cerf-jcr.org](http://www.cerf-jcr.org)



[www.JCRonline.org](http://www.JCRonline.org)

## ABSTRACT

Giudici, A., Soomere, T., 2013. Identification of areas of frequent patch formation from velocity fields. In: Conley, D.C., Masselink, G., Russell, P.E. and O'Hare, T.J. (eds.), *Proceedings 12<sup>th</sup> International Coastal Symposium* (Plymouth, England), *Journal of Coastal Research*, Special Issue No. 65, pp. 231-236, ISSN 0749-0208.

We explore the ability of the formation of patches of substances floating on the sea surface owing to intrinsic features of ocean circulation associated with persistent flow convergence in areas characterised with strong vertical velocities (e.g. hosting downwelling). Their impact on the field of surface floaters can be quantified using so-called flow compressibility of a two-dimensional velocity field. Large values of this measure for idealized, delta-correlated-in-time flows are directly related to the tendency of floating tracers to gather into patches. We employ a modification of this measure, so called finite-time-compressibility to describe the real marine flows in a more consistent way, accounting for the match of areas with high convergence with the Lagrangian transport of the resulting patches. Analysis of this measure for the Gulf of Finland, the Baltic Sea, using surface velocity fields from the OAAS model with a resolution of 1 nm shows that domains where systematic development of patchiness is very likely occur either along straight sections of the coastlines that usually host downwelling. Surprisingly, high values of finite-time compressibility frequently occur throughout the year in two offshore locations and in the windy season near the centre of the widest part of the gulf.

**ADDITIONAL INDEX WORDS:** *flow compressibility, finite-time compressibility, patchiness.*

## INTRODUCTION

The probability of different coastal sections of being hit by high concentrations of adverse impacts (algal blooms, marine litter, oil pollution, etc.) is closely related to both the potential of the formation of patches of substances floating on the sea surface and the subsequent transport of these patches to the nearshore. The process of patchiness formation (Powell and Okubo, 1994), although not particularly well understood, reflects the ability of substances and tracers in the surface layer to naturally form areas with high concentrations. This process has been thoroughly examined for the nearshore areas and for semi-sheltered sea domains (e.g., Kononen *et al.*, 1992; Granskog *et al.*, 2005) where it is frequently driven either by local bathymetry, coastal jets and/or associated intense up- or downwelling events, or by anthropogenic intervention (dredging, dumping, etc.). It is frequently coupled with the generation of strong gradients in some domains and of a mixture of areas with highly different concentration of various substances (Kalda, 2000), which is another natural ocean process, basically driven by the inverse energy cascade of the almost two-dimensional (2D) large-scale motions (Cushman-Roisin and Beckers, 2011); however, this process only redistributes areas with high concentration of different substances and does not amplify the concentration.

There is increasing evidence that certain parts of open ocean that are located far from strong jets (e.g., so-called Great Pacific Ocean Garbage Patch (Pichel *et al.*, 2007) located in the North Pacific Subtropical Convergence Zone where marine litter has a tendency to gather) and several nearshore areas governed by essentially three-dimensional (3D) motions systematically develop

patches of high concentrations of certain substances. The formation of such areas is usually associated with large-scale convergence and subduction zones (Lee and Niiler, 2010) characterised by strong vertical velocities. Similar properties may have nearshore areas hosting up- or downwelling, or areas of interaction of jet-like currents and mesoscale vortices.

The potential impact of the velocity patterns towards the formation of patches of high concentration in the initially more-or-less homogeneous fields of surface floaters or tracers can be quantified using so-called flow compressibility  $C_c$  of a 2D velocity field on the sea surface, which lies over the 3D circulation. Differently from the compressibility of the medium, the flow compressibility reflects the divergence or convergence of the flow field. It is defined as the relative weight of the irrotational (curl-free or potential) component of the flow (which is generally composed of potential and solenoidal components). Large values of this measure are directly related to the tendency of floating tracers to gather into patches (Cressman *et al.*, 2004; Kalda, 2007) because of the capability of water particles to “dive” (Garrison, 2011) whereas the floating particles are locked at the surface and their concentration therefore increases. While spatio-temporal variations in the divergence field generally lead to a certain domination of the gathering of the floaters (see discussion of this effect in (Giudici *et al.*, 2012; Kalda *et al.*, 2012)), the areas hosting high values of  $C_c$  are inherent candidates for domains where the natural formation of patches of dangerous concentrations of pollution may occur. The presence of such areas could potentially affect both the probability and propagation time of adverse impacts from the offshore areas to the vulnerable regions (Chrastansky and Callies, 2009; Soomere *et al.*, 2010).

Systematic formation of areas with high concentration of tracers only happens for relatively high values flow compressibility. In

DOI: 10.2112/SI65-040.1 received 07 December 2012; accepted 06 March 2013.

© Coastal Education & Research Foundation 2013

ideal Kraichnan flows (which are delta-correlated in time), the clusterization starts only if  $C_c \geq 0.5$  (Falkovich *et al.*, 2001). Although for smaller values of  $C_c$  theoretical studies predict that there are no distinct patches of floaters but still there are regions of increased concentrations (Bec *et al.*, 2004; Boffetta *et al.*, 2004). It has been also shown that if the floater particles stick to each other (e.g. like pieces of plastic sheets do), the patch formation starts at considerably smaller values of flow compressibility (Kalda, 2007).

The presence of high values of  $C_c$  not necessarily leads to the increase in the concentration of particles. Samuelsen *et al.* (2012) demonstrated that particle aggregation systematically occurred in the rim of an anticyclonic eddy. The highest particle concentration coincided with the vorticity patterns, but not the divergence field. The spatial de-correlation between the divergence field and the areas of high concentration apparently occurred because the areas of strong convergence stayed fixed in space relative to the eddy, while the particles were advected with the currents. In other words, while areas of high convergence may impact the concentration field, the largest concentration anomalies occur if a set of particles stays in such areas for a longer time interval. Such areas are the most natural candidates for patch formation even if the instantaneous values of divergence remain relatively modest.

The classical definition of flow compressibility relies on certain instantaneous properties of the flow field and ignores its history. Both experimental and numerical results indicate that time correlations (which are always present for real hydrodynamic flows) can either inhibit or catalyze the clusterization process (Boffetta *et al.*, 2004). For this reason, Giudici *et al.* (2012) and Kalda *et al.*, (2012) employed a modified measure called finite-time compressibility. This measure is not only directly related to the ability of some regions of the sea surface to shrink or expand but also accounts for finite-time correlations (the history) of the motion, and thus has a larger potential to describe the formation of patches. It essentially relates the finite-time changes in the material volumes (e.g. surface areas in 2D flows overlying 3D circulation) to the finite-time changes in the separation between material particles.

Previous research (Giudici *et al.*, 2012; Kalda *et al.*, 2012) has established the basic relations between the classical flow compressibility and finite-time compressibility, and also demonstrated the link between the finite-time compressibility and divergence field. In this paper we focus on long-term spatial distributions of the finite-time compressibility in a particular sea domain that is famous for the high proportion of vertical motions of water masses—the Gulf of Finland, the easternmost sub-basin of the Baltic Sea (Leppäranta and Myrberg, 2009). This sea is characterized by frequent occurrence of 3D dynamics (Myrberg and Andrejev, 2003). The Gulf of Finland frequently hosts powerful up- and downwelling events (Lehmann and Myrberg, 2007) and thus is a natural example of a domain with substantial nonzero values of flow compressibility in the surface layer. The focus is on the identification of areas where the finite-time compressibility exceeds the threshold for the clusterization in terms of the classical flow compressibility.

## METHOD AND DATA

### Finite-time compressibility

As we are basically interested in changes in the concentration of substances or particles passively carried by the flow (below called simply (floating) particles) in the surface layer, we focus on the calculation of relative changes in the surface elements that are passively carried with the surface current. We track the displacement of and changes to triangles formed by a selected

point of the sea surface and its immediate neighbours to the north and east (Figure 1) to represent the change in the surface area at this point. This stencil is applied to the entire sea domain of interest. The values of the finite-time compressibility  $C_{fic}$  are calculated from the root-mean-square (rms) changes to such triangles (equivalently, from the separation between triplets of particles floating on the surface) over a certain time interval (Kalda *et al.*, 2012):

$$C_{fic} = \frac{2dS_{rms}}{dA_{rms} + dB_{rms}}. \quad (1)$$

Here  $S_t$  is the surface of such an initially right-angled triangular element at a time instant  $t$ ,  $dS_t = (S_t - S_{t-1})/S_t$  is the relative change of its area over one time step, and  $dA_t = (A_t^2 - A_{t-1}^2)/A_t^2$ ,  $dB_t = (B_t^2 - B_{t-1}^2)/B_t^2$  are changes to the squared length  $A_t^2$ ,  $B_t^2$  of its catheti. By definition, this measure characterises persistent changes in the surface of such elements that are carried with surface current and thus the "ability" of a tracer, substance or concentration field to develop extensive variations (patches) in some sea areas. For a purely incompressible flow  $dS_{rms}$  and hence  $C_{fic} = 0$ . If the flow is purely compressible (contractive or expanding), the quantities  $A$  or  $B$  would change with the same relative rate as  $S$  and  $C_{fic} = 1$ . The values of  $C_{fic}$  are expected to mostly lie in the range  $[0, 1]$ .

The classical flow compressibility  $C_c$  and the quantity  $C_{fic}$  are highly correlated but not equivalent (Giudici *et al.*, 2012). For delta-correlated, ideal Kraichnan flows the relation between the two quantities is:

$$C_{fic}^2 = \frac{2C_c}{2C_c + 1}. \quad (2)$$

The two measures simultaneously tend to zero. The threshold  $C_c = 0.5$  for the process of clustering (Falkovich *et al.*, 2001) corresponds to  $C_{fic} = \sqrt{1/2} \approx 0.7$ . For moderate levels of compressibility  $C_{fic} > C_c$ . The two measures only coincide if  $C_{fic} = C_c \approx 0.781$ . For larger values of  $C_c$  the  $C_{fic}$  exceeds the flow compressibility. The limiting value  $C_c = 1$  corresponds to  $C_{fic} = \sqrt{2/3}$ . This implies that for  $\sqrt{2/3} < C_{fic} \leq 1$ , there are no corresponding values for  $C_c$  (Giudici *et al.*, 2012).

### Velocity data for the Gulf of Finland

Since the flow compressibility values of a velocity field coincide with those of the motion of fluid particles floating in it, we study the compressibility of a velocity field through the

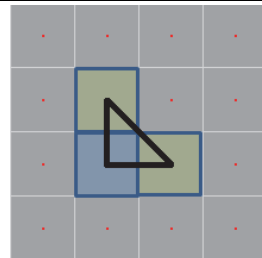


Figure 1. Elementary triangular set of floating particles used for the calculations.

displacement vector fields of simulated particles' trajectories generated by that velocity field. The previous studies in this test area (Giudici *et al.*, 2012; Kalda *et al.*, 2012) relied on velocity fields with a moderate spatial resolution of 2 nautical miles (nm), which only to some extent resolved the basic features of dynamics in this water body. In this study we use velocity fields with a resolution of 1 nm. This means a considerable improvement of the adequacy of the results as the 1 nm models are expected to properly resolve most of the mesoscale dynamics in the Gulf of Finland.

More specifically, 2D surface velocity fields were extracted from long-term numerical simulations using the OAAS hydrodynamic model (Andrejev and Sokolov, 1989; 1990) and performed in the framework of BONUS+ BalticWay cooperation. This time-dependent, free-surface, baroclinic model based on hydrostatic approximation has a vertical resolution of 1 m (and only the uppermost layer is assumed to be 2 m thick). It was specifically designed for areas characterized by complex hydrostatic and bathymetric structures, such as the Gulf of Finland. Its latest features and characteristics are presented in Andrejev *et al.* (2010). The particular model run (Andrejev *et al.*, 2011) was forced with meteorological data from a regionalization of the ERA-40 re-analysis over Europe using a regional atmosphere model with a horizontal resolution of 25 km (Höglund *et al.*, 2009; Samuelsson *et al.*, 2011). The velocity field covers the Gulf of Finland to the west of longitude 23°27'E during years 1987–1991, with a temporal resolution of 3 hours. As in the previous studies, we only used the velocity data in the uppermost layer.

### Set-up of numerical experiments

We developed a simulation environment (QTRAC) to calculate spatial distributions of  $C_{fc}$  from velocity fields. As the first step of the calculation pipeline, QTRAC loads the vector 2D velocity information and stores it in a staggered Arakawa B-grid (Arakawa and Lamb, 1977). An (offline) interpolation in time is then optionally performed to fit the data with any resolution chosen for the simulations. The velocity is assumed to vanish within dry grid cells and outside the boundaries of the model.

The scheme implied in the evaluation of the finite-time compressibility resembled the one used for the identification of semi-persistent surface flow patterns (Soomere *et al.*, 2010). The time interval  $t_D$  of interest (normally from a month up to first years) was divided into shorter (optionally overlapping) time spans of custom length (typically 4–96 hours in various experiments, 24 hours in the simulations used in this study). One particle was positioned at the centre of each wet grid cell of the model. The particles were thus separated by exactly 1 nm from their closest neighbours.

The displacement of all released particles was then tracked throughout the chosen time span using the assumption that the particles are passively carried by the modelled velocity field. No means to replicate the effect of subgrid-scale motions is used. The coordinates of the resulting set of trajectories are sampled at a custom rate (30 min in this paper). The position of the particles was then reset and a new set of trajectories was calculated over the next time span that started one day (24 hours) after the previous one.

The trajectories of floating particles are resolved through an Euler-type Runge-Kutta procedure, a first-order method that yields a global error which is proportional to its time step size (Kloeden and Platen, 1999). Whilst higher-order schemes would be definitely necessary to properly resolve the vertical component of the trajectories in strongly stratified environments such as the

Baltic Sea (Gräwe *et al.*, 2012), we limit our trajectories in the uppermost layer where the Euler scheme is commonly believed to give proper results.

We use the local velocity vector calculated via double linear interpolation from the modelled velocity components at four closest grid points to the instantaneous location of the trajectory. The next location of the particle along its trajectory is calculated component-wise. After each simulation over the chosen time span has completed, each batch of trajectories is stored. The trajectory of each floating particle is then linked with its two closest neighbours at the initial time step according to the stencil in Figure 1. This results in a set of triangular elements.

A value of the finite-time compressibility associated with each grid cell and the initial time of each time span is then evaluated using Eq. (1), the values of the catheti lengths and surface areas. While for low-vorticity flows in offshore domains the distortions to the triangles normally remain modest and the calculations are straightforward, several cases of realistic flows need particular attention (Figure 2). Firstly, if one or more particles forming a triangle gets stuck at the seashore (or drifts out of the model domain), the evolution of the triplet no more characterizes the compressibility of surface currents. To remove the associated non-physical values in Eq. (1), the further evolution of such triplets is discarded from when the trajectory of an element of the triplet lands on the shore.

Secondly (and usually more frequently) it may happen (especially in the Gulf of Finland that hosts strongly circularly polarised motions) that the three vertices of a triplet align along a straight line or coincide with each other. This would result in an attempt to divide by zero in Eq. (1). Physically, it means that very strong stretching occurs in the relevant area and the evolution of the triplet is no more able to properly characterise the flow compressibility. In order to avoid the resulting miscalculation, the evaluation according to Eq. (1) was stopped when the vertices became too closely aligned or nearly coincident. The further behaviour of such a triplet was ignored.

Although the final value of  $C_{fc}$  for each point must be  $\leq 1$  (Giudici *et al.*, 2012), there is still a possibility for single larger values of this measure at the first steps of calculation (Figure 3). Such values may appear in quite diverse locations (not shown) but they decrease rapidly, normally within one time step, into the expected range  $[0,1]$  (Figure 3). As a rule, the point-wise values of

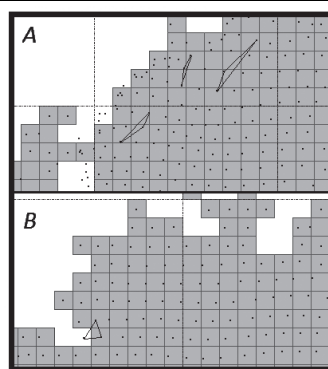


Figure 2. Potential failures of the calculation scheme in Eq. (1). (A): vertices of a triangular element tend to align, yielding a null area; (B): one of the vertices hits the coast.

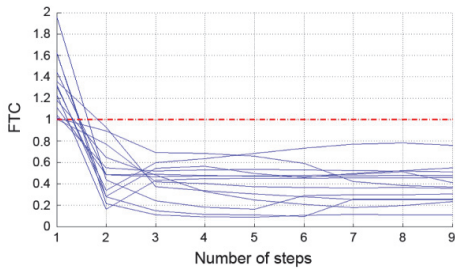


Figure 3. Dependence of finite-time compressibility (FTC) values initially  $>1$  on the number of time steps in a calculation that started on the 1<sup>st</sup> of January 1987. The time step is 30 min.

$C_{ftc}$  relax to the level close to their final values within 3–4 steps.

## RESULTS: SPATIAL DISTRIBUTIONS OF THE FINITE-TIME COMPRESSIBILITY

The single estimates of the finite-time compressibility for different time spans were used to construct various maps characterising this measure for different sea areas and time intervals.

The overall average level of  $C_{ftc}$  is around 0.4 during the windy season (October–March). Spatial distributions of the finite-time compressibility for single weeks (Giudici *et al.*, 2012) and months (Figure 4) reveal comparatively large variability of this measure both in space and time. While for some months these distributions are almost featureless (like December 1987 in Figure 4), some other months contain a number of clearly defined areas with high values of  $C_{ftc}$ . The typical maximum values of  $C_{ftc}$  for single months (like in February 1987 in Figure 4) are around 0.6, that is,

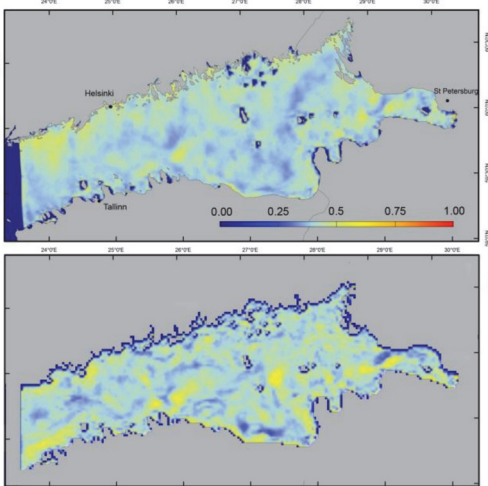


Figure 4. Spatial distribution of finite-time compressibility (colour code) for the Gulf of Finland in December 1987 (upper panel) and February 1988 (lower panel).

well below the threshold  $C_{ftc} = 0.7$  for the clustering process to become effective. The largest values of  $C_{ftc}$  usually occur (i) in the nearshore of the southern coast of the Gulf of Finland, (ii) in the north-western part and (iii) in the easternmost domain of the gulf.

Offshore areas hosting largest monthly average values of  $C_{ftc} > 0.5$  are normally different in different months (Figure 4). Only one area at the entrance to the River Neva estuary in the easternmost part of the gulf regularly hosts large values of finite-time compressibility. This domain hosts very small internal Rossby radius and contains an extremely complicated flow pattern driven by the interaction of basin-wide cyclonic circulation of the water masses and the optional anticyclonic gyre at the surface layer (Soomere *et al.*, 2011) with the voluminous runoff of River Neva (Leppäranta and Myrberg, 2009). Another relatively persistent area of high values of  $C_{ftc}$  is located in the middle of the widest part of the Gulf of Finland.

The seasonally averaged values of  $C_{ftc}$  (Figure 5) are generally flatter and normally do not exceed the level of about 0.5.

Although it is likely that changes in the concentration occur at the levels of  $C_{ftc}$  well below the threshold for clusterization (see above), systematic patch formation can only be expected when the threshold of  $C_{ftc} = 0.7$  is reached in some sea area for a relatively long time. The maps presented in Figures 4 and 5 give an overview of the spatial distribution of areas with high finite-time compressibility but they fail to deliver a good estimate of the likelihood of an area where clustering of particles or formation of high concentrations is likely to occur as the average  $C_{ftc}$  tends to fade towards lower values when considering longer intervals (Giudici *et al.*, 2012).

A more detailed insight into the temporal course of finite-time compressibility in selected domains (Figure 6) reveals that this measure normally fluctuates around its long-term value of  $\sim 0.4$ . Consistently with the information in Figures 4 and 5 it has more likely high values in the windy season than in the calm one. It exceeds the threshold for patch formation for many days in a row during several weeks (again more likely in the windy season). These weeks are, therefore, the most likely candidates for the patch formation process to become evident.

Given such an intermittent temporal behaviour of the finite-time compressibility, the temporal extent and spatial location of the areas prone to patch formation can be at best characterised using a method similar to the peak-over-threshold method used in many branches of physical oceanography, coastal engineering, and wave science (e.g., Holthuijsen, 2007). Following this idea, it was counted for each wet grid cell, how many instantaneous values of  $C_{ftc}$  exceeding the critical level of 0.7 occurred during a certain time interval. The resulting maps (Figure 7) spot all the areas

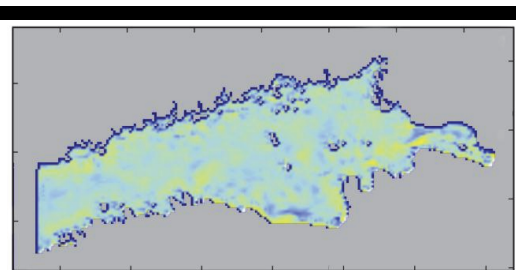


Figure 5. Spatial distribution of finite-time compressibility for the Gulf of Finland in the windy season October 1987–March 1988. The average value is  $C_{ftc} = 0.41$ . Colour code is the same as for Figure 4.

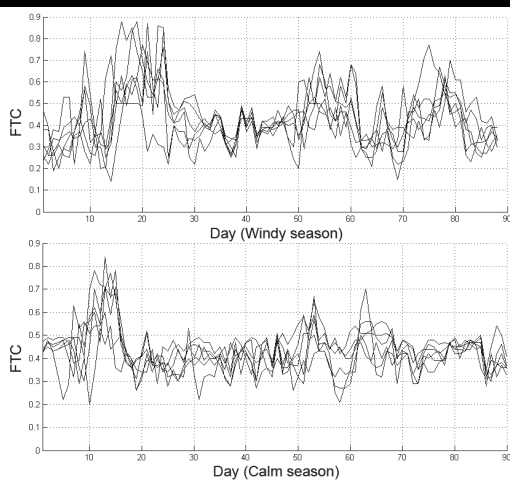


Figure 6. Temporal course of finite-time compressibility (FTC) at six grid cells in the area of relatively high values of  $C_{fte}$  located outside the Neva Bight, for the first three months of the windy season (October 1987–March 1988, upper panel) and the calm season (April–September 1987, lower panel).

which systematically show high  $C_{fte}$ , equivalently, the areas characterised by the frequent occurrence of favourable structures of currents for patch formation. The number of simulations (equivalently, days) in which the single values of  $C_{fte} > 0.7$  exceeds 50 (>30% of the full count of days) a season in the most pronounced areas. Not surprisingly, both the extension of such areas and the number of days in which this threshold was exceeded was larger in the windy season than in the calm one.

The majority of such areas are located in the nearshore. The largest area, characterised also by the largest amount of “days over threshold” stretches along the almost straight section of the southern coast of the Gulf of Finland. It is evident during both the windy and the calm season and very likely represents the presence of frequent downwelling owing to the predominant south-western winds (Lehmann and Myrberg, 2007). A similar area at the southern coast of Neva Bight in the easternmost domain of the gulf is located in very shallow waters and probably is not related to large-scale downwelling phenomena. Interestingly, it is present with more-or-less equal intensity in both calm and windy seasons. This feature suggests that it may be related with the interplay of the circulation in the gulf and the discharge from the River Neva. Several smaller nearshore areas located next to different peninsula may reflect zones of convergence of coastal currents with the basin-wide circulation.

Even more interesting is the presence of several offshore areas that frequently host high values of finite-time compressibility. Not unexpectedly, they are more evident during the windy season than in the calm period. Two areas are evident (with somewhat different percentage of cases with  $C_{fte}$  over threshold) in both seasons. One of them is an elongated area at the entrance to Neva Bight in the eastern Gulf of Finland. As it was also highlighted in earlier calculations with a modest resolution (2 nm) of the ocean model (Giudici *et al.*, 2012), it apparently reflects a very persistent feature of the dynamics of the Gulf of Finland (probably the presence of a more-or-less permanent convergence zone of the

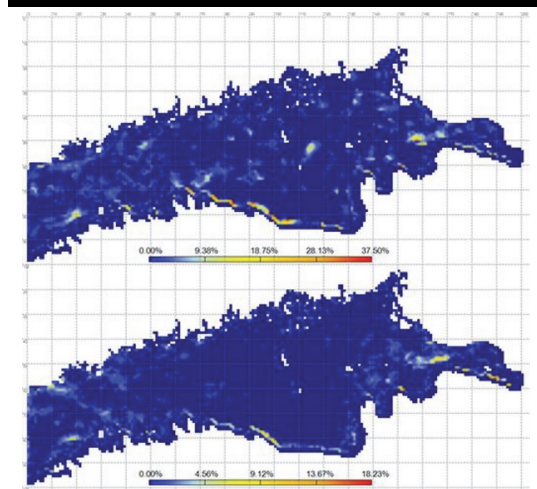


Figure 7. Spatial distribution of the number of days during which the finite-time compressibility exceeds the threshold for patch formation the windy season, from October 1987 to March 1988 (upper panel), and for the calm season, from April to September 1987 (lower panel).

overall cyclonic circulation of the Gulf of Finland and the runoff of River Neva) and is the most probably candidate to provide frequent generation of patches of high concentration of different substances. The background for the similar area in the south-western part of the gulf and for the one that becomes evident only in the windy season in the middle of the widest section of the gulf needs to be clarified in the future.

## CONCLUDING REMARKS

The concept of finite-time compressibility of flow on sea surface combines the “ability” of the classical compressibility of 2D flows overlying 3D dynamics to serve as an indicator of the potential of formation of patches of high concentration of different substances with the history of Lagrangian transport of the affected counterparts. The definition of this measure (Eq. (1)) not only relates it to physical deformations of the sea surface but also allows to simply calculating its values in a systematic and consistent manner whenever the properties of surface currents are available with an appropriate resolution.

The presence of areas with persistently high values of finite-time compressibility in the southern nearshore of the Gulf of Finland, albeit interesting, is not completely unexpected because the areas where floating objects tend to gather are commonly associated with convergence zones and downwelling phenomena (Pichel *et al.*, 2007; Samuelsen *et al.*, 2012). This feature, however, points to the possibility to apply the technique of the evaluation of finite-time compressibility to operationally highlight the areas of frequent and strong downwelling directly from the map of surface velocities.

The presence of offshore areas frequently hosting high values of finite-time compressibility (except for possibly the one near the eastern end of the Gulf of Finland) seem to be a new dynamic feature of the circulation in this water body. It is highly interesting to independently verify their “ability” to systematically build large concentrations of tracers or substances.

## ACKNOWLEDGEMENT

This study was supported by the Estonian Science Foundation (grant no. 9125), targeted financing by the Estonian Ministry of Education and Research (grant SF0140007s11), and through support of the European Regional Development Fund to the Centre of Excellence in Non-linear Studies. AG is supported by the DoRa programme for international doctoral studies in Estonia. The velocity data have been kindly provided by Dr. Oleg Andrejev (†2012) in the framework of the BONUS+ BalticWay cooperation. The authors thank Dr. Jaan Kalda for fruitful discussions of the material of this paper.

## LITERATURE CITED

- Andrejev O. and Sokolov, A., 1989. Numerical modelling of the water dynamics and passive pollutant transport in the Neva inlet. *Meteorologia i Hydrologia*, 12, 75-85 (in Russian).
- Andrejev O. and Sokolov, A., 1990. 3D baroclinic hydrodynamic model and its applications to Skagerrak circulation modelling. In: *Proc. 17<sup>th</sup> Conference of the Baltic Oceanographers*. Norrköping, Sweden, pp. 38-46.
- Andrejev, O., Sokolov, A., Soomere, T., Värvi, R. and Viikmäe, B. The use of high-resolution bathymetry for circulation modelling in the Gulf of Finland. *Estonian Journal of Engineering*, 16 (3), 187-210.
- Andrejev, O., Soomere, T., Sokolov, A. and Myrberg, K., 2011. The role of spatial resolution of a three-dimensional hydrodynamic model for marine transport risk assessment. *Oceanologia*, 53 (1-T1), 309-334.
- Arakawa, A. and Lamb, V.R., 1977. *Methods of Computational Physics*. New York: Academic Press, 17, pp. 173-265.
- Bec, J., Gawedzki, K. and Horvai, P., 2004. Multifractal clustering in compressible flows. *Physical Review Letters* 92 (22), Art. No. 224501.
- Boffetta, G., Davoudi, J., Eckhardt, B. and Schumacher, J., 2004. Lagrangian tracers on a surface flow: The role of time correlations. *Physical Review Letters*, 93 (13), Art. No. 134501.
- Chrastansky, A. and Callies U., 2009. Model-based long-term reconstruction of weather-driven variations in chronic oil pollution along the German North Sea coast. *Marine Pollution Bulletin*, 58, 967-975.
- Cressman, J.R., Davoudi, J., Goldberg, W.I. and Schumacher, J., 2004. Eulerian and Lagrangian studies in surface flow turbulence. *New Journal of Physics*, 6, Art. No. 53.
- Cushman-Roisin, B. and Beckers, J.-M., 2011. *Introduction to geophysical fluid dynamics*. Amsterdam: Elsevier, Academic Press.
- Falkovich, G., Gawedzki, K. and Vergassola, M., 2001. Particles and fields in fluid turbulence. *Reviews in Modern Physics*, 73 (4), 913-975.
- Garrison, T.S., 2011. *Essentials of oceanography*, 5th ed. Pacific Grove: Brooks Cole.
- Giudici, A., Kalda, J. and Soomere, T., 2012. On the compressibility of surface currents in the Gulf of Finland, the Baltic Sea. In: *Proceedings of the IEEE/OES Baltic 2012 International Symposium "Ocean: Past, Present and Future. Climate Change Research, Ocean Observation & Advanced Technologies for Regional Sustainability"* (May 8–11, Klaipėda, Lithuania). IEEE Conference Publications, 8 pp. doi: 10.1109/BALTIC.2012.6249178
- Granskog, M., Kaartokallio, H., Kuosa, H., Thomas, D., Ehn, J. and Sonninen, E., 2005. Scales of horizontal patchiness in chlorophyll a, chemical and physical properties of landfast sea ice in the Gulf of Finland (Baltic Sea). *Polar Biology* 28 (4), 276-283.
- Gräwe, U., Deleersnijder, E., Shah, S.H.A.M. and Heemink, A.W., 2012. Why the Euler scheme in particle tracking is not enough: the shallow-sea pycnocline test case. *Ocean Dynamics*, 62 (4), 501-514.
- Höglund, A., Meier, H.E.M., Broman, B. and Kriezi, E., 2009. *Validation and correction of regionalised ERA-40 wind fields over the Baltic Sea using the Rossby Centre Atmosphere Model RCA3.0*. Rapport Oceanografi No. 97. Norrköping, Sweden: Swedish Meteorological and Hydrological Institute.
- Holthuijsen, L.H., 2007. *Waves in oceanic and coastal waters*. Cambridge University Press, 387p.
- Kalda, J., 2000. Simple model of intermittent passive scalar turbulence. *Physical Review Letters*, 84 (3), 471-474.
- Kalda, J., 2007. Sticky particles in compressible flows: aggregation and Richardson's Law. *Physical Review Letters*, 98 (6), Art No. 064501.
- Kalda, J., Soomere, T. and Giudici, A., 2012. On the finite-time compressibility of the surface currents in the Gulf of Finland, the Baltic Sea. *Journal of Marine Systems*, <http://dx.doi.org/10.1016/j.jmarsys.2012.08.010>
- Kloeden, P.E. and Platen, E., 1999. *Numerical solution of stochastic differential equations*. Berlin: Springer, 632p.
- Kononen, K., Nömmann, S., Hansen, G., Hansen, R., Breuel, G. and Gupalo, E.N., 1992. Spatial heterogeneity and dynamics of vernal phytoplankton species in the Baltic Sea in April–May 1986. *Journal of Plankton Research*, 14 (1) 107-125.
- Lee, D.K. and Niiler, N., 2010. Influence of warm SST anomalies formed in the eastern Pacific subduction zone on recent El Niño events. *Journal of Marine Research*, 68 (3-4), 459-477.
- Lehmann, A. and Myrberg, K., 2007. Upwelling in the Baltic Sea - A review. *Journal of Marine Systems*, 74, S3-S12
- Leppäranta, M. and Myrberg, K., 2009. *The physical oceanography of the Baltic Sea*. Berlin Heidelberg: Springer.
- Myrberg, K. and Andrejev, O., 2003. Main upwelling regions in the Baltic Sea - a statistical analysis based on three-dimensional modelling. *Boreal Environment Research*, 8(2), 97-112.
- Pichel, W.G., Churnside, J.H., Veenstra, T.S., Foley, D.G., Friedman, K.S., Brainard, R.E., Nicoll, J.B., Zheng, Q., Clemente-Colon, P., 2007. Marine debris collects within the North Pacific Subtropical convergence zone. *Marine Pollution Bulletin*, 54 (8), 1207–1211.
- Samuelson, A., Hjøllo, S.S., Johannessen, J.A. and Patel, R., 2012. Particle aggregation at the edges of anticyclonic eddies and implications for distribution of biomass. *Ocean Science*, 8 (3), 389-400.
- Samuelsson, P., Jones, C.G., Willén, U., Ullerstig, A., Gollvik, S., Hansson, U., Jansson, C., Kjellström, E., Nikulin, G. and Wyser, K., 2011. The Rossby Centre Regional Climate Model RCA3: Model description and performance. *Tellus*, 63A (1), 4-23.
- Soomere, T., Viikmäe, B., Delpeche, N. and Myrberg, K., 2010. Towards identification of areas of reduced risk in the Gulf of Finland, the Baltic Sea. *Proceedings of the Estonian Academy of Sciences*, 59 (2), 156-165.
- Soomere, T., Delpeche, N., Viikmäe, B., Quak, E., Meier, H.E.M., Döös, K., 2011. Patterns of current-induced transport in the surface layer of the Gulf of Finland. *Boreal Environment Research*, 16 (Suppl. A), 49-63.

## Paper III

Kalda J., Soomere T., **Giudici A.** 2014. On the finite-time compressibility of surface currents in the Gulf of Finland, the Baltic Sea. *Journal of Marine Systems*, 129, 56–65, doi: 10.1016/j.jmarsys.2012.08.010





# On the finite-time compressibility of the surface currents in the Gulf of Finland, the Baltic Sea



Jaan Kalda<sup>a</sup>, Tarmo Soomere<sup>a,b</sup>, Andrea Giudici<sup>a,\*</sup>

<sup>a</sup> Institute of Cybernetics at Tallinn University of Technology, Akadeemia tee 21, 12618 Tallinn, Estonia

<sup>b</sup> Estonian Academy of Sciences, Kohtu 6, 10130 Tallinn, Estonia

## ARTICLE INFO

### Article history:

Received 29 November 2011

Received in revised form 22 August 2012

Accepted 27 August 2012

Available online 12 September 2012

### Keywords:

Compressibility

Time correlations

Finite-time compressibility

Lagrangian transport

Patchiness

Pollution control

Baltic Sea

Gulf of Finland

## ABSTRACT

We study the effects of flow compressibility of a two-dimensional (2D) velocity field on the transport and mixing of substances floating on the sea surface overlying 3D circulation. The test area is the Gulf of Finland, the Baltic Sea, where large variations in flow compressibility are likely. The key development is the introduction of a modified measure of finite-time compressibility that accounts for time correlations of realistic flows and is directly related to the ability of clustering of passive tracers in some regions of the sea surface. This measure is evaluated based on 3D velocity fields calculated using the Rossby Centre Ocean Model (Swedish Meteorological and Hydrological Institute) for 1991 and the TRACMASS code for tracking Lagrangian trajectories. The maps of finite-time compressibility are calculated using a variable integration time of 12–72 h and compared with a similar map of average surface divergence. The level of finite-time compressibility reaches the threshold of likely formation of patches usually in coastal regions but also in certain elongated offshore areas. The spatial distributions of this measure reveal extensive seasonal-scale variations, with the most persistent areas of high finite-time compressibility in the windy season (October–December) near the River Neva mouth.

© 2012 Elsevier B.V. All rights reserved.

## 1. Introduction

Knowledge of fundamental features of pollution behaviors and impacts on marine environment is crucial for sustainable management of vulnerable sea areas. This knowledge is of key importance not only for a better understanding of the environmental responses to pollutants but even more for the development of efficient prevention measures. This knowledge is still sparse, and many factors are yet to be taken into account (Andrady, 2011; Schilling and Zessner, 2011). One of the vital questions is how and where dangerous concentrations of adverse impacts (e.g. harmful algal blooms), frequently observed in natural conditions in the surface layer, develop from overall low readings of background fields.

The movement of different substances within the water column in the ocean is governed by the three-dimensional (3D) system of currents. Such motions generally result in spreading of initially closely located particles (Ollitrault et al., 2005; Richardson, 1926). Therefore, it is natural to expect that the concentration of different adverse impacts is the largest in the vicinity of their release site to the marine environment and that remote areas are safe. The situation is much more complicated for substances (such as oil pollution or plastic debris) that are locked in the surface layer. First of all, this layer is additionally affected by wind and waves. Both wind-

and wave-induced transport are highly anisotropic and mostly mimic the behavior of the wind and wave patterns, which can be forecast and hindcast with a reasonable accuracy nowadays. As the properties of both these fields usually vary quite slowly over the open sea areas, the related transport normally does not lead to substantial changes in the concentration of different substances in the surface layer.

It is well known that large intense currents such as the Gulf Stream or Kuroshio carry large water masses from coastal areas across oceans to a distance of many 1000s of km. This feature makes the pollution or litter propagation problem a fairly general and global one. Moreover, substances in the surface layer are carried to extremely remote locations over areas that do not host such strong currents. For example, debris originating from South America is frequently found as beach litter on remote Pacific Islands (Richards and Beger, 2011).

A fascinating property of marine debris is its ability to form areas with high concentrations in the open ocean, far from jet currents. Perhaps the most well-known such area is located in the North Pacific Subtropical Convergence Zone and is sometimes called the Great Pacific Ocean Garbage Patch (Pichel et al., 2007). Therefore, even remote offshore locations are certainly not immune from problems related to high readings of pollution or litter in the surface layer.

The existence of such areas is usually associated with specific three-dimensional (3D) features of the ocean circulation (Lee and Niiler, 2010). In essence, this feature can be interpreted as a particular realization of so-called patchiness of a number of different properties of the marine environment (Powell and Okubo, 1994). Many physical

\* Corresponding author. Tel.: +372 58390544.  
E-mail address: [andrea@cens.ioc.ee](mailto:andrea@cens.ioc.ee) (A. Giudici).

processes may be responsible for the presence of patches of different size and shape. For example, filament generation in quasi-two-dimensional velocity field (Held et al., 1995) naturally leads to extremely complicated spatial structure of concentrations of various properties (Kalda, 2000) and even such frequently occurring phenomena as horizontal density gradient (Burchard et al., 2008) or classical estuarine circulation (Burchard et al., 2004) may lead to accumulation of sediment particles or well-defined turbidity maxima. In the Baltic Sea patchiness has been subject to intense studies since the 1980s (Granskog et al., 2005; Kononen et al., 1992). In this area the phenomenon of patchiness is usually linked to various mesoscale hydrodynamic features such as eddies, frontal zones, or local jet currents. A similar mechanism, usually working at even smaller scales, is Langmuir circulation (Thorpe, 2009). All the listed phenomena normally have a substantial vertical component and, thus, an essentially 3D vertical structure.

In this paper, we make an attempt to link the potential of formation of patches (more generally, inhomogeneities in initially homogeneously distributed fields of passive tracers locked in the surface layer) on sea surface with so-called property of compressibility of sea surface. This property is one of important factors, which controls the behavior of the pollution spreading, and, if present, may naturally lead to the formation of high concentrations in different adverse impacts or marine garbage. We emphasize the substantial difference of this phenomenon from the more widely spread concept of compressibility of the entire medium (sea water or air) understood as a measure of the relative volume change owing to pressure variations. In this paper we use the notion of flow compressibility as the relative weight of the potential component of a velocity field. This definition relies on the motion of water particles. Three-dimensional atmospheric flows as well as the flows in the bulk of the water basins are usually almost incompressible; however, the two-dimensional (2D) velocity field at the water surface can be compressible even when water particles, initially located at the surface, are confined to stay at the surface. This happens because of the possibility of vertical motions of water masses (up- and down-welling in the marine environment) in the water column. In this sense, flow compressibility of sea surface can be interpreted as an indicator of the impact of 3D motions on the concentrations of different substances in a particular location of the surface. The highest values of flow compressibility can, thus, be naturally associated with areas prone to the development of well-defined patches.

While the effect of flow compressibility on different properties of the fluid motion and transport has been extensively studied both theoretically and experimentally (Boffetta et al., 2004; Cressman et al., 2004; Falkovich et al., 2001; Kalda, 2007), the evidence of its importance in the marine environment is still scarce. The most prominent consequence of large values of flow compressibility is the gathering of floating particles into patches. This feature is crucial in many environmental applications as it may substantially affect both the probability and propagation time of adverse impacts in different offshore areas to the vulnerable regions. For example, pollution is likely to stay for a long time in areas of high compressibility. Such areas can be interpreted as natural areas of reduced risk in terms of pollution transport from these to the coasts (Soomere et al., 2010).

In this paper, we study the effects of flow compressibility of a 2D velocity field on the transport and mixing of substances floating on the sea surface of the Baltic Sea, in the area of the Gulf of Finland, and overlying a 3D field of motions. Although the notion of divergence is used in the definition of the flow compressibility, these two quantities are not equal and, strictly speaking, not equivalent. The values of flow compressibility also depend on the solenoidal component of the velocity field whereas interrelations between these components may be extremely complicated. Furthermore, our goal is to develop a measure that accounts for time correlations of realistic flows. The reason for such an extension is that high values

of flow compressibility at certain locations are usually not enough for the formation of patches. The process of patch formation takes some time and ordinarily becomes effective only if the area of high flow compressibility (or divergence) moves together with the flow. Thus, we aim at the introduction of a measure that (i) has basically the same properties as flow compressibility at short-term limit but also (ii) is able to integrate the contributions of moving areas of high divergence to the patch-formation process (e.g. similarly to the generation of high waves by moving storms (Dysthe and Harbitz, 1987)). The key development is the introduction of a modified measure of flow compressibility (that is directly related to the ability of clustering of passive tracers in some regions of the sea surface) and a demonstration that its values may exceed the threshold for the formation of patches. We call this measure finite-time compressibility to distinguish it from the classical flow compressibility.

The structure of the paper is as follows. Section 2 gives a short insight into the general problem of compressibility of 2D and 3D flows. The pool of velocity data, models used for its calculation and for tracking the surface elements on sea surface are described in Section 3. The definition of a modified measure for compressibility of 2D flows and its calculation scheme from 2D velocity fields are presented in Section 4. Section 5 depicts the resulting spatial distribution of this measure for the Gulf of Finland. The basic message from the research to the marine science is formulated in Section 6.

## 2. Compressibility of 2D flows overlying almost incompressible 3D motions

The fundamental theorem of vector calculus, the Helmholtz's theorem, states that any sufficiently smooth, rapidly decaying vector field in three dimensions can be expressed as the sum of an irrotational (curl-free, also called potential) vector field and a solenoidal (divergence-free) vector field. This is known as the Helmholtz decomposition. Consequently, virtually every realistic field of motions in the ocean (formally, defined everywhere in space and vanishing at infinity together with its first derivatives) can be decomposed, to a first approximation, into its solenoidal and potential components (with zero divergence and curl, respectively). In this framework, flow compressibility is defined as the relative weight of the potential component of the velocity field. Its particular values, therefore, are in the range from 0 (fully solenoidal flow) to 1 (fully potential flow). In what follows, however, we adopt a slightly different definition of flow compressibility, which will be referred to as the *finite-time compressibility*. It coincides with the classical definition at the limit of ideal Kraichnan flows (Falkovich et al., 2001). The reasons for such an approach will be explained below.

There exists a direct link between the flow compressibility of a motion system (either 2D or 3D) and the possibility of formation of patches of concentration of passive tracers or particles injected into the fluid. Namely, systematic development of patches is only possible if the potential flow component dominates, that is, if the values of compressibility exceed the threshold of 0.5. Compressibility (both in terms of volume changes and flow compressibility) of a realistic fluid motion is generally nearly 0, hence fluids are incapable of producing the patchiness of tracers (Fine and Millero, 1973). The most important exception is the marine surface layer. Here large values of flow compressibility are possible due to the ability of the particles floating on it to "dive" into the third dimension (Garrison, 2011). Thus, the average flow compressibility of such a formally 2D velocity field on sea surface may largely exceed the analogous values for purely 2D. This property, in essence, is a generalization of several above-mentioned phenomena that lead to the development of inhomogeneities on the sea surface and can explain, at least partially, the patchiness of floats in the marine environment.

The presence of non-zero flow compressibility can affect dramatically the behavior of the tracers, giving rise to clusterization of the

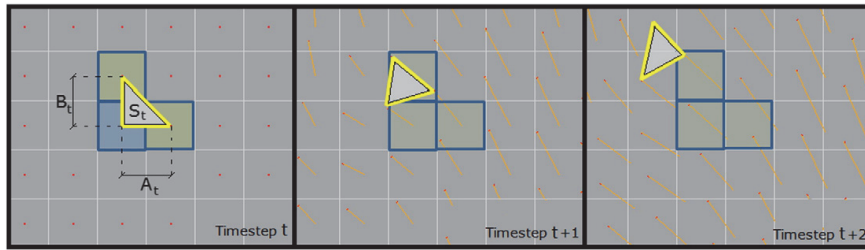


Fig. 1. Scheme of the selection of surface elements and their distortions in time. A color version of the figure is available in the online version of this manuscript.

tracer particles and fractal structures (Bec et al., 2004; Perlekar et al., 2010). Theoretically, non-linear waves may contribute to the increase in the surface compressibility. This effect apparently becomes evident, if at all, in quite specific conditions. For example, it has been shown that such an effect is negligible for weakly nonlinear waves (Vucelja et al., 2007). Therefore, the major source of sea surface compressibility evidently is the specific nature of the local 3D circulation that may give rise to systematic diving (e.g. downwelling) or uplift (e.g. upwelling) of water masses in certain sea areas.

According to the theoretical studies of ideal Kraichnan flows (which are delta-correlated in time), the crossover to clusterization takes place at the critical value of flow compressibility  $C=0.5$  (Falkovich et al., 2001). These and higher values of  $C$  are not very common at the sea surface. The free-slip surface of fully turbulent (that is, hosting essentially 3D motions) water volumes is characterized by  $C \approx 0.5$  (Schumacher and Eckhardt, 2002) but mesoscale and large-scale marine water flows are often quasi-2D (Kraichnan and Montgomery, 1980; Rhines, 1979). Weakening of the vertical flow component obviously leads to the reduction of the flow compressibility of the relevant surface velocity field.

Both experimental and numerical results indicate that the time correlations (which are always present for real hydrodynamic flows) can either inhibit or catalyze the clusterization process (Boffetta et al., 2004; Samuelsen et al., 2012). Theoretical analysis of the associated effects is extremely complicated and the results are not always directly applicable for the marine environment. For this reason we make an attempt to develop a measure that can be easily evaluated from the known properties of the surface flow and that can be directly related to the patch-formation processes. In doing so we note that the compressibility of a velocity field coincides with that of the motion of fluid particles floating in it. This feature makes it possible to quantify the compressibility of the particle field (in terms of classical volume/surface changes) at sea surface by means of addressing the flow compressibility of the vector field consisting of displacement vectors of simulated floats' trajectories.

If the overall surface area of the sea is constant in time, the average flow divergence over the entire surface is strictly zero. Surface floats (passive tracers, adverse impacts, plastic debris, oil pollution, etc.) though, tend to spend more time in contracting regions than in expanding ones: the expanding flows tend to push floats away, while the contracting ones tend to attract and keep floats within their areas of influence. Therefore, particles tend to gather into patches in areas that systematically reveal nonzero compressibility.

### 3. Circulation model and Lagrangian tracking code

We concentrate on the Gulf of Finland (Alenius et al., 1998), the easternmost sub-basin of the Baltic Sea. This water body frequently hosts long-term powerful upwelling and downwelling events (Lehmann and Myrberg, 2008; Leppäranta and Myrberg, 2009) and thus is a natural candidate for sea domains with substantial nonzero levels of surface compressibility. We employ surface

velocity fields calculated for 1991 in the Swedish Meteorological and Hydrological Institute using the Rossby Centre Ocean Model (RCO) and made available the framework of BONUS + BalticWay cooperation (Soomere et al., 2010). This year has been chosen in order to make our results at least partially comparable with those obtained in the framework of studies into the quantification of offshore areas in terms of their ability to serve as sources of environmental risk to the coastal areas in terms of current-induced transport of adverse impacts released at these areas to the near-shore (Soomere et al., 2011). The horizontal resolution of the model grid is  $2 \times 2$  nautical miles and the model uses 41 vertical levels in  $z$ -coordinates (Meier, 2007; Meier et al., 2003). The thickness of the vertical layers varies between 3 m close to the surface and 12 m in 250 m depth. The uppermost layer corresponds to water masses at depths 0–3 m.

The RCO model has been described in a number of sources (Meier, 2001; Meier et al., 2003). As we only use velocity fields produced using this model, we present here only shortly its key features. It is a Bryan-Cox-Semtner primitive equation circulation model following (Webb et al., 1997) with a free surface (Killworth et al., 1991) and open boundary conditions (Stevens, 1991) in the northern Kattegat. It is coupled to a Hibler-type sea ice model (Hibler, 1979) with elastic-viscous-plastic rheology (Hunke and Dukowicz, 1997). Subgrid-scale mixing is parameterized using a turbulence closure scheme of the  $k$ - $\epsilon$  type with flux boundary conditions to include the effect of a turbulence-enhanced layer due to breaking surface gravity waves (Meier, 2001). A flux-corrected, monotonicity-preserving transport scheme following (Gerdes et al., 1991) is embedded. No explicit horizontal diffusion is applied. The model run, data from which is used below, is forced with 10 m wind, 2 m air temperature, 2 m specific humidity, precipitation, total cloudiness and sea level pressure fields from a regionalization of the ERA-40 re-analysis over Europe using a regional atmosphere model with a horizontal resolution of 22 km (Samuelsson et al., 2011). As the atmospheric model tends to underestimate wind speed extremes, the wind is adjusted using simulated gustiness to improve the wind statistics (Samuelsson et al., 2011). Standard bulk formulae are used to calculate the air-sea fluxes over open water and over sea ice. A time step splitting is used, with the choice of 15 s for the barotropic and 150 s for the baroclinic timestep. The output is stored once in 6 h. For further details of the model set-up and an extensive validation of model output the reader is referred to Meier (2001) and Meier et al. (2003).

The displacement of water particles has been calculated using their Lagrangian trajectories found by the TRACMASS model (Blanke and Raynard, 1997; de Vries and Döös, 2001; Döös, 1995) using a linear interpolation of precomputed RCO velocity fields in space. The code used a variation of the adaptive time step. It was set equal to the temporal resolution of the stored output of the RCO model (6 h) when the particle stayed in a particular cell. Additionally, the interpolated velocity field was updated every time when the particle reached the boundary between the grid cells. Theoretically, using the TRACMASS model together

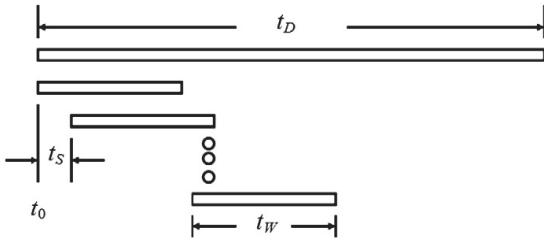


Fig. 2. Definition sketch of splitting the simulation period into time windows.

with the 3D velocity data, it would be possible to calculate the classical (flow) compressibility of the 3D velocity fields. As we are specifically interested in the properties of the surface flow, the test particles have been locked in the uppermost layer.

The use of a spatial resolution of 2 miles means that the RCO model is barely eddy-permitting in the Gulf of Finland and that a part of mesoscale features and all submesoscale features are not reproduced by the model. The version of the TRACMASS code does not account for subgrid-scale effects (such as turbulent diffusion) and the resulting trajectories follow (within approximation errors of the relevant differential equations) the RCO velocity field. In other words, displacement of particles calculated using this technique only experience relatively large-scale advection but no diffusion. Such reproduction of only mesoscale and larger-scale features generally suppresses the local 3D effects and decreases the level of surface compressibility as this measure is small for almost 2D fields. An inclusion of a parameterization of subgrid-scale features might be interpreted as more exact representation of certain properties of realistic flows such as spreading of initially closely located particles. In our case doing so would basically mean an addition of noise with certain spectral parameters to the velocity field.

As mentioned above, for real time-correlated flows, the non-zero values of flow compressibility alone are unable to describe the development of patches on the sea surface. The physical reason for that is most explicitly demonstrated when we consider a hypersonic gas flow which is compressible in terms of the volume change. In such flows, at any moment of time, the velocity field is also compressible, because the dynamic pressure exceeds the hydrostatic one. Meanwhile, this compressibility has long-term negative correlation. The volume growth rate can be quantified in terms of the sum of Lyapunov exponents. This sum is strictly zero for incompressible flows as demonstrated in (Falkovich et al., 2001, p. 919). It is possible to express Lyapunov exponents as functions of compressibility, and

their sum is strictly negative if the compressibility is non-zero (Falkovich et al., 2001, p. 928). Therefore, for delta-correlated flows, nonzero values of compressibility mean that material volumes contract exponentially in time. This contraction is actually the fundamental reason of the creation of patchiness owing to the presence of non-zero compressibility. However, the material volumes of hypersonic gas flow cannot contract exponentially: eventually the hydrodynamic pressure will play a role and stop the contraction. As a result, even though the classical compressibility of hypersonic flows can be considerable, the sum of the Lyapunov exponents remains strictly equal to zero. This property is equivalent to the absence of creation of long-term patchiness in 3D flows.

#### 4. Finite-time compressibility

Therefore, in order to reach a measure that is more directly related to the formation of patches, the definition of compressibility needs to be revised toward accounting for the properties of real flows with finite time-correlations. Following this line of thinking, we employ the modified definition of (finite-time) compressibility. The idea is to relate the finite-time changes in the material volumes (e.g., surface areas in the case of 2D flows overlying 3D circulation) with the finite-time changes in the separation between material particles. The modification is consistent in the sense that the introduced measure coincides with the values of the classical compressibility at the limit of infinitesimally small time windows and Kraichnan flows.

The basic idea in the calculations of this measure is to look at the changes in the surface of small elements of the surface. The simplest element is formed by three points at the surface, forming a triangle with nonzero area (Fig. 1). Let us consider a grid cell, at time step 0 for a given day. We choose a triangle consisting of this point and its immediate neighbors to the south and east (Fig. 1) to represent the change in the surface area at this point. This stencil is applied to the entire surface of the Gulf of Finland and its entrance area. More formally, let  $(x_1^t, y_1^t)$ ,  $(x_2^t, y_2^t)$  and  $(x_3^t, y_3^t)$  be the coordinates of the vertices of an element at time step  $t$ . It is convenient to consider twice the surface of an element  $S_t$ , expressed at time step  $t$  as follows:

$$2S_t = |(x_2^t - x_1^t) \cdot (y_3^t - y_1^t) - (x_3^t - x_1^t) \cdot (y_2^t - y_1^t)|. \tag{1}$$

The relative change over time of its area is  $dS_t = (S_t - S_{t-1})/S_t$ . Another component of our definition is the squared length of two edges of the element:

$$A_t = (x_1^t - x_2^t)^2 + (y_1^t - y_2^t)^2; B_t = (x_1^t - x_3^t)^2 + (y_1^t - y_3^t)^2. \tag{2}$$

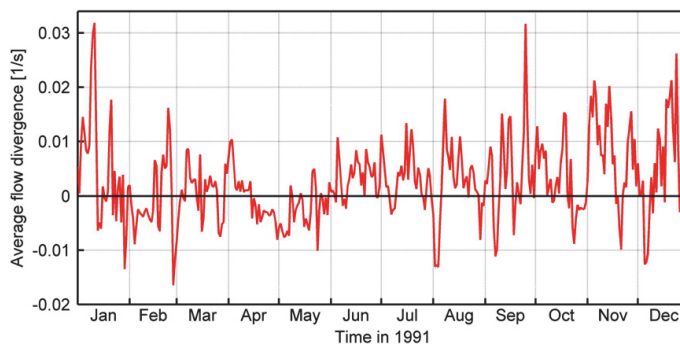


Fig. 3. Divergence of the 2D flow on the sea surface, integrated over the entire Gulf of Finland in 1991.



Fig. 4. Average finite-time compressibility of water surface in the Gulf of Finland for one week (01–07 November 1991) calculated using the time window of 48 h. A color version of the figure is available in the online version of this manuscript.

Their respective changes over time are obviously  $dA_t = (A_t - A_{t-1})/A_t$  and  $dB_t = (B_t - B_{t-1})/B_t$ . The finite-time compressibility is calculated now from the changes to the three quantities in question at different time steps as follows:

$$C = \frac{2dS_{rms}}{dA_{rms} + dB_{rms}}, \quad (3)$$

where the components of the right-hand side of Eq. (3) have the meaning of rms (root mean square) values of the respective quantities

$$dS_{rms} = \sqrt{\frac{1}{n} \sum_i^i dS_i^2}, dA_{rms} = \sqrt{\frac{1}{n} \sum_i^i dA_i^2}, dB_{rms} = \sqrt{\frac{1}{n} \sum_i^i dB_i^2} \quad (4)$$

and  $i$  indicates a particular realization of the flow. The rms in Eqs. (4) is calculated from a number of samples (realizations) that usually increases with the increase in the length of the time interval under consideration (see below). The values in Eq. (4) also depend on the length of tracking the elements in order to account for correlations over certain time intervals. It is, however, obvious that the limiting values of  $C$  in Eq. (3) do not

depend on the number of samples provided the velocity field is statistically stationary.

From Eqs. (1)–(4) it follows that if the flow is purely incompressible,  $dS_{rms} = 0$ , and hence the compressibility  $C = 0$  in the entire volume filled (or area covered) by such a flow. In the contrary, if the flow is purely contractive or expanding, the quantities  $A$  or  $B$  would change with the same relative rate as  $S$ , so that we would have  $C = 1$ . The values of  $C$  defined by Eq. (3) obviously lie in the range  $[0, 1]$ , with  $C = 1$  implying a purely compressible flow. The importance of the presented definition of the measure of compressibility  $C$  is that it accounts for the finite-time correlations and its values are directly related to the ability of gathering the tracer particle into patches.

The scheme of calculations of the finite-time compressibility resembles a similar scheme used for the identification of semi-persistent surface flow patterns (Soomere et al., 2010). A longer time interval  $t_D$  of interest (year 1991 in the calculations in this paper) was divided into time intervals (windows) with a length of  $t_W = 4–96$  h (Fig. 2). One tracer is placed at the center of each wet grid point of the RCO model. The initial separation of the neighboring tracers along latitudes and along longitudes is, therefore, about 2 nautical miles. The changes to their positions (locations of the

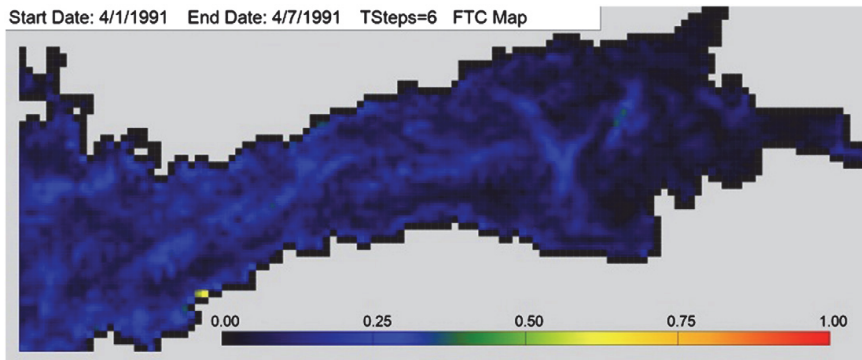


Fig. 5. Average finite-time compressibility of water surface in the Gulf of Finland for one week (01–07 April 1991) calculated using the time window of 24 h. A color version of the figure is available in the online version of this manuscript.

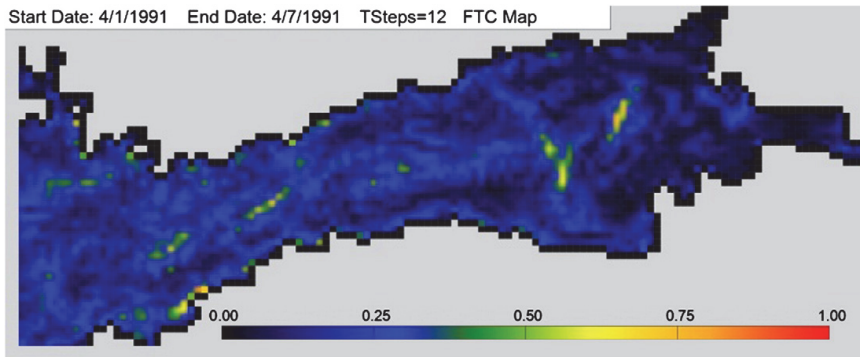


Fig. 6. Average finite-time compressibility of water surface in the Gulf of Finland for 01–07 April 1991 calculated with the time window of 48 h. A color version of the figure is available in the online version of this manuscript.

vertices) were obtained by running the TRACMASS code during the time window. From these simulations, we retrieved a displacement vector field of tracers' positions and the properties of the surface elements. They were used to calculate the divergence of surface velocity and finite-time compressibility value for each grid cell and particular realization. The results of calculations over a particular time window formed one realization of the changes to the area of surface elements. For subsequent realizations, the simulations of the same pattern of tracers and surface elements were restarted with a time lag  $t_s = 1$  day. The longer realizations thus overlap to some extent.

After performing simulations for such a pool of realizations, we averaged the value of  $C$  pointwise over different time spans: on daily, monthly, seasonal and yearly base. The resulting maps characterize the spatial variations in the field of compressibility for different time intervals over the Gulf of Finland. As discussed above, large values of finite-time compressibility in these maps highlight the likelihood of tracers inserted into various sea areas to gather into patches, equivalently, areas where high concentrations of floats, garbage, adverse impacts, etc., are likely.

The above-mentioned property (that the basin-wide average 2D flow divergence is zero for a sea area of constant size) offers an implicit way to judge to a certain degree about the correctness of the calculations. Fig. 3 presents the average divergence, integrated over the entire area of the Gulf of Finland, calculated for every day of year 1991 using the described technique of tracking of particles

using the TRACMASS code with  $t_w = 4$  h. The maximum absolute values of divergence are up to 0.8 1/s. In this sense the average values on the level of 0.01 1/s for single calendar days show that the technical side of calculations apparently is reliable. The small variations reflect the surface water exchange between the area over which the divergence is calculated and the Baltic Proper. The mostly positive values and the annual average of 0.0025 1/s apparently mirror the excess of fresh water inflow in this area (Leppäranta and Myrberg, 2009) while a few negative values evidently are connected with surface water inflow owing to specific wind events.

### 5. Spatial distributions of compressibility

The resulting maps vividly demonstrate that there exist areas with high finite-time compressibility values in the Gulf of Finland (Fig. 4). A part of these areas have an elongated stripe-like shape and are generally located close to the shore. Most likely the areas with high finite-time compressibility reflect regions hosting intense vertical motions (upwelling or downwelling) in coastal areas, possibly with upwelling filaments, or divergence or convergence zones between coastal currents and offshore mesoscale circulation. For example, during the first week of November 1991, the highest compressibility is found in the vicinity of the River Kymi mouth in the north-eastern part of the Gulf of Finland. This region, with local values of  $C$  up to 0.9, is also characterized by merging of the voluminous runoff of the

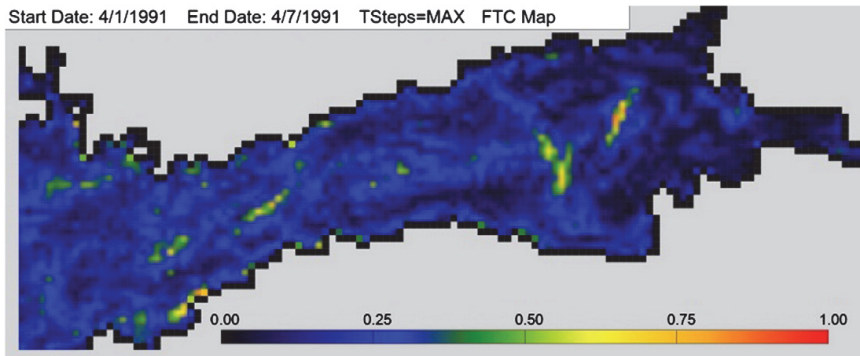


Fig. 7. Average finite-time compressibility of water surface in the Gulf of Finland for 01–07 April 1991 calculated with the time window of 72 h. A color version of the figure is available in the online version of this manuscript.

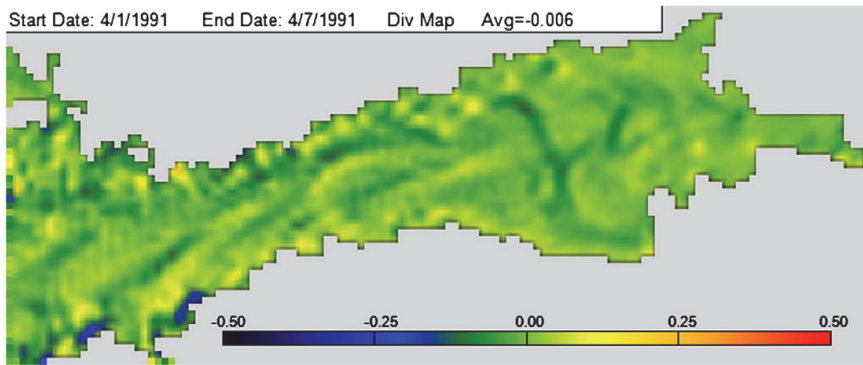


Fig. 8. Average divergence (1/s) of water surface in the Gulf of Finland for 01–07 April 1991. A color version of the figure is available in the online version of this manuscript.

River Neva with brackish waters of the Gulf of Finland and, thus, high values of  $C$  are not unexpected.

In contrast with the classical definition, our definition of finite-time compressibility makes it possible to calculate its dependence on the length of the time window used for the evaluation of the change to the area of surface elements. The use of very short time windows is equivalent to the calculation of the compressibility with a very small contribution of time correlations. Calculations using different lengths of  $t_w$  show that, for shorter time windows (0 to 24 h), the resulting values of  $C$  are relatively low and generally do not reach the critical value of 0.5 (Fig. 5).

The use of longer time windows makes it possible to track the distortions of the surface elements over a certain sea area during their Lagrangian drift. This option allows identifying areas over which the finite-time compressibility increases cumulatively over some time interval. Such areas are actually the best candidates for emerging high concentrations of adverse impacts. With an increase in the time window to 48–72 h, this threshold is reached at several locations (Figs. 6, 7).

The potential of the finite-time compressibility to reveal the areas with possible patch formation becomes evident from a comparison of distributions of this measure with similar distributions of divergence. A distribution of average sea surface divergence (Fig. 8) calculated for the same time interval as Figs. 5–7 and using a similar technique reveals certain qualitatively overlapping deviations from the zero mean similar to those in Fig. 8. Large absolute values of both the measures exist near a few locations of the north-western coast of Estonia

and the southernmost tip of Finland. The distribution of average divergence, however, is not able to highlight offshore areas of high finite-time compressibility. This feature has been vividly demonstrated in simulations of particle aggregation in the rim of an anticyclonic eddy. The highest particle concentration coincided with the vorticity patterns, but not the divergence field. The spatial de-correlation between the divergence field and the areas of high concentration apparently occurred because the areas of strong convergence stayed fixed in space relative to the eddy, while the particles were advected with the currents (Samuelsen et al., 2012).

In this context, it is natural to focus on the elongated areas of high  $C$  oriented across the gulf in its eastern as domains where Lagrangian surface transport is accompanied with more or less gradual contraction or stretching of the surface area. Such areas are the most natural candidates for patch formation. The key merit from the introduced technique of the finite-time compressibility is its ability to identify the areas which are likely to host patch formation phenomena in a systematic way, and to distinguish them from areas which only show short-time or pointwise expanding or shrinking.

This conjecture was checked by means of a comparison between the distributions of finite-time compressibility and density maps of floats calculated over the same time-interval and using the same scheme of calculations. The used model setup severely limits the number of independently propagating particles in each cell and for each time window. As the trajectories of initially closely located particles tend to stay close in the used version of the TRACMASS model (Döös and Engqvist, 2007), it was only reasonable to inject one

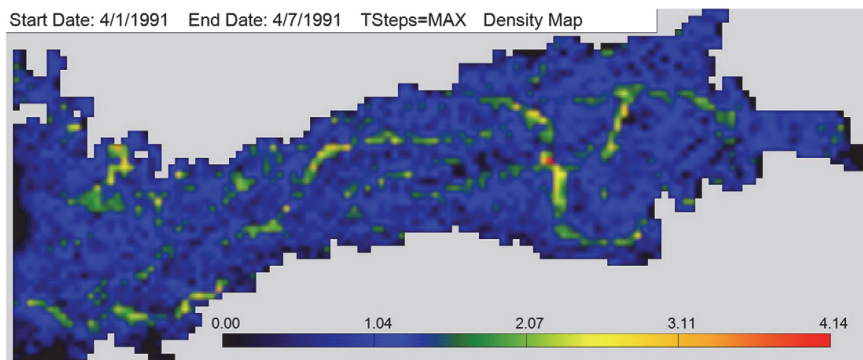


Fig. 9. Concentration of floats (per grid cell) in the Gulf of Finland for 01–07 April 1991. A color version of the figure is available in the online version of this manuscript.

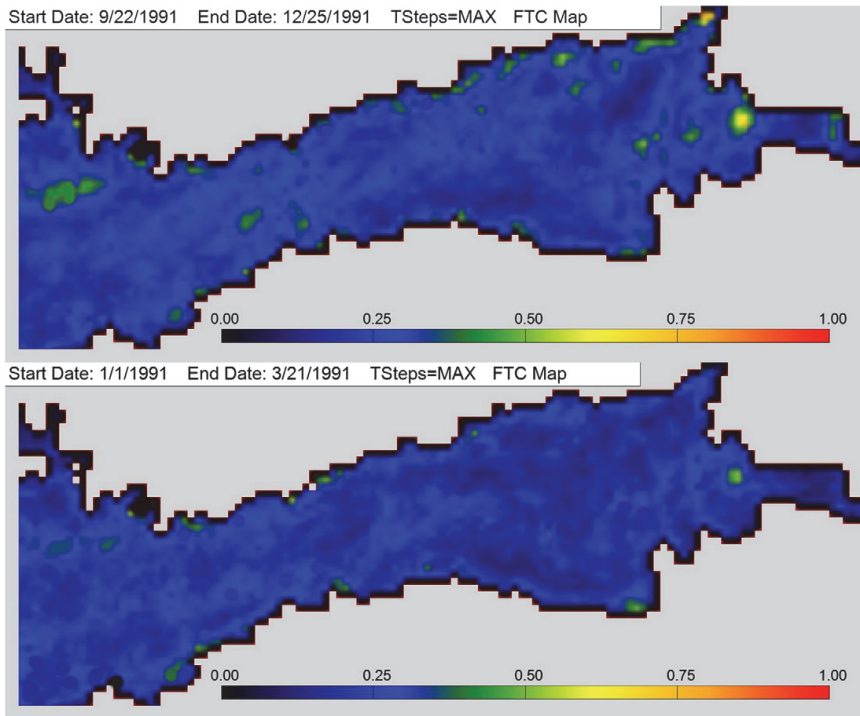


Fig. 10. Average compressibility of water surface in the Gulf of Finland in winter (lower panel, 01 January–21 March) and autumn (upper panel, 22 September–25 December) 1991. A color version of the figure is available in the online version of this manuscript.

particle into each cell. This limitation led to a high pixelization of the resulting fields in single realizations of the concentration. Still, already the results of simulations of the evolution of an ensemble of such small clusters validated these expectations. All the areas that were projected to host high finite-time compressibility also hosted a high density of floats (cf. Figs. 7 and 9).

A substantial level of noise in the spatial distribution of the concentration field (Fig. 9) apparently stems from a combination of the extremely discrete nature of the initial field of particles and the highly rotational character of the flow in the Gulf of Finland (Lilover et al., 2011). This combination often leads to a synchronous rotation and advection of particles in adjacent cells. Even if their distance does not change, they may show up within one grid cell, aligned along its diagonal, after some time as in the middle panel of Fig. 1. This process leads to large basically random local and short-time fluctuations of the gridded concentration field.

The presented results demonstrate that the locations of the high-value regions of  $C$  are qualitatively the same for all choices of the time window length. The elongated areas of high compressibility may be interpreted as regions in which the compressibility cumulatively increases in the direction of the surface current. The critical values in  $C$  are usually reached only if the time window is 12 h or longer. Remarkably, several elongated areas of high  $C$  are oriented almost across the gulf. Such areas may reflect relatively intense cross-gulf transport pathways (Soomere et al., 2010) which also demonstrate systematic contraction or expansion.

A comparison of Figs. 5–7 reveals that a sensible variation in the length of the time window allows highlighting the areas where the sea surface is characterized by high ( $>0.5$ ) cumulative values of  $C$

over a few days. Several such areas are missing in calculations with the time window below 48 h.

Further lengthening of the time window generally leads to a decay of the areas with high finite-time compressibility. Several patterns of high  $C$ , however, persist over a few months. The areas characterized by high values of  $C$  seem to be affected by a strong seasonal variability (Fig. 10). For the year 1991, the maximum values of the finite-time compressibility (Table 1) are the largest in autumn (October–December) whereas the average values of  $C$  exceed the patch-generation threshold of  $C = 0.5$  at several locations. It is remarkable that the highest values of  $C$  near the mouth of the River Neva and at the entrance to the Gulf of Finland occur almost at the same locations as in simulations for one week (Fig. 4). This feature suggests that the areas favorable for the generation of patches may persist over several months.

Other seasons have clearly less maximum values of  $C$  that are close to the threshold of  $C = 0.5$  and even remain below this threshold for the spring months (April–June). The qualitative appearance of the field of  $C$  is very much the same in different seasons (Fig. 10). The

Table 1  
Maximum values of finite-time compressibility  $C$  calculated using  $t_w = 4$  days for different seasons in the Gulf of Finland.

Season	Maximum compressibility
Spring 1991	0.4408
Summer 1991	0.5246
Autumn 1991	0.7634
Winter 1991	0.5072

life-time of high-value areas of finite-time compressibility seems to be limited to a few months: averaging over the entire year of 1991 leads to a substantial decrease in the local values of  $C$  which remained well below the threshold in question.

## 6. Conclusions

The property of compressibility of a 2D velocity field overlying 3D circulation is a natural generalization of the impact of various phenomena (such as upwellings, downwellings, convergence or divergence of ocean currents, Langmuir circulation, etc.) that may lead to the formation of inhomogeneities in otherwise smooth fields in the surface layer. In other words, such processes may cause contraction or extension of the sea surface, in this way affecting the behavior of different substances floating on the sea surface. Their obvious consequence is the formation of patches.

The traditional definition of (flow) compressibility basically relies on instantaneous velocity fields and does not account for the time history of motions and cumulative distortion of sea surface. The modified measure of finite-time compressibility, introduced in this paper through tracking the local changes to the area of surface elements, makes it possible to systematically quantify the impact of the listed processes, independently on their particular physical origin, on various fields on the sea surface. It allows for variable-length time window averaging for flows translating surface elements over the sea surface. This property makes it possible to calculate cumulative effects of local changes to the sea surface and, thus, to highlight sea regions characterized by large values of finite-time compressibility occurring during some finite time interval and which wouldn't have become evident using the classical definition. Another key feature of this measure is its tight relation with the ability of clustering of passive tracers in some regions of the sea surface, allowing hindcast and forecast of the domains in which the patch formation is most likely.

The particular value of finite-time compressibility naturally depends on the length of time slices over which it is calculated. The spatial variations of the finite-time compressibility are fairly high. While its values for short time slices are fairly low, for slices of quite reasonable length (48–72 h) its values reach and overshoot the threshold for the formation of extensive patches. Usually coastal regions are frequently characterized by significant finite-time compressibility values (above the critical level of 0.5) but comparable values are also found in elongated offshore areas. The spatial distributions of finite-time compressibility reveal extensive seasonal-scale variations. The performed simulations for one year (1991) suggest that several regions of high finite-time compressibility (equivalently, areas prone to the generation of surface patches) persist, at least, during a few months but apparently are smoothed out when averaged over an entire year.

Finally, we mention that this study only reflects mesoscale and basin-scale properties of the surface velocities. This fraction of the velocity fields generally exhibits much lower level of 3D effects compared with realistic flows in marine environment. In this light, the presented demonstration that the finite-time compressibility may reach the clusterization threshold under the given circumstances is even more significant. It is natural to assume that more realistic quantification of the compressibility by means of including realistic information about smaller-scale features of velocity (<2 nautical miles) could enhance the effect of patchiness (Granskog et al., 2005).

## Acknowledgments

This study was supported by the Estonian Science Foundation (grants no. 7909 and 9125), targeted financing by the Estonian Ministry of Education and Research (grant SF0140007s11), the BalticWay project, which was supported by funding from the European Community's Seventh Framework Program (FP/2007–2013) under

grant agreement no. 217246 made with the joint Baltic Sea research and development program BONUS, and by the European Union through support of the European Regional Development Fund to the Centre of Excellence in Non-linear Studies. AG is supported by the support program for international doctoral studies in Estonia DoRa.

## References

- Alenius, P., Nekrasov, A., Myrberg, K., 1998. Physical oceanography of the Gulf of Finland: a review. *Boreal Environ. Res.* 3 (2), 97–125.
- Andrady, A.L., 2011. Microplastics in the marine environment. *Mar. Pollut. Bull.* 62 (8), 1596–1605.
- Bec, J., Gawedzki, K., Horvai, P., 2004. Multifractal clustering in compressible flows. *Phys. Rev. Lett.* 92 (22) (Art. No. 224501).
- Blanke, B., Raynard, R., 1997. Kinematics of the Pacific equatorial undercurrent: an Eulerian and Lagrangian approach from GCM results. *J. Phys. Oceanogr.* 27 (6), 1038–1053.
- Boffetta, G., Davoudi, J., Eckhardt, B., Schumacher, J., 2004. Lagrangian tracers on a surface flow: the role of time correlations. *Phys. Rev. Lett.* 93 (13) (Art. No. 134501).
- Burchard, H., Bolding, K., Villarreal, M.R., 2004. Three-dimensional modelling of estuarine turbidity maxima in a tidal estuary. *Ocean Dyn.* 54 (2), 250–265.
- Burchard, H., Floeser, G., Staneva, J.V., Badewien, T.H., Riethmüller, R., 2008. Impact of density gradients on net sediment transport into the Wadden Sea. *J. Phys. Oceanogr.* 38 (3), 566–587.
- Cressman, J.R., Davoudi, J., Goldburg, W.J., Schumacher, J., 2004. Eulerian and Lagrangian studies in surface flow turbulence. *New J. Phys.* 6 (Art. No. 53).
- De Vries, P., Döös, K., 2001. Calculating Lagrangian trajectories using time-dependent velocity fields. *J. Atmos. Oceanic Technol.* 18 (6), 1092–1101.
- Döös, K., 1995. Inter-ocean exchange of water masses. *J. Geophys. Res. Oceans* 100 (C7), 13499–13514.
- Döös, K., Engqvist, A., 2007. Assessment of water exchange between a discharge region and the open sea — a comparison of different methodological concepts. *Estuarine Coastal Shelf Sci.* 74 (4), 585–597.
- Dysthe, K.B., Harbitz, A., 1987. Big waves from polar lows? *Tellus A* 39, 500–508.
- Falkovich, G., Gawedzki, K., Vergassola, M., 2001. Particles and fields in fluid turbulence. *Rev. Mod. Phys.* 73 (4), 913–975.
- Fine, R.A., Millero, F.J., 1973. Compressibility of fluids as a function of temperature and pressure. *J. Chem. Phys.* 59 (10), 5529–5536.
- Garrison, T.S., 2011. *Essentials of Oceanography*, 5th ed. Brooks Cole, Pacific Grove.
- Gerdes, R., Köberle, C., Willebrand, J., 1991. The influence of numerical advection schemes on the results of ocean general circulation models. *Clim. Dyn.* 5, 211–226.
- Granskog, M., Kaartokallio, H., Kuosa, H., Thomas, D., Ehn, J., Sonninen, E., 2005. Scales of horizontal patchiness in chlorophyll *a*, chemical and physical properties of landfast sea ice in the Gulf of Finland (Baltic Sea). *Polar Biol.* 28 (4), 276–283.
- Held, I.M., Pierrehumbert, R.T., Garner, S.T., Swanson, K.L., 1995. Surface quasi-geostrophic dynamics. *J. Fluid Mech.* 282, 1–20.
- Hibler, W., 1979. A dynamic thermodynamic sea ice model. *J. Phys. Oceanogr.* 9, 815–846.
- Hunke, E.C., Dukowicz, J.K., 1997. An elastic–viscous–plastic model for sea ice dynamics. *J. Phys. Oceanogr.* 27, 1849–1868.
- Kalda, J., 2000. Simple model of intermittent passive scalar turbulence. *Phys. Rev. Lett.* 84 (3), 471–474.
- Kalda, J., 2007. Sticky particles in compressible flows: aggregation and Richardson's Law. *Phys. Rev. Lett.* 98 (6) (Art. No. 064501).
- Killworth, P., Stainforth, D., Webb, D., Paterson, S., 1991. The development of a free-surface Bryan–Cox–Semtner ocean model. *J. Phys. Oceanogr.* 21, 1333–1348.
- Kononen, K., Nömmann, S., Hansen, G., Hansen, R., Breuel, G., Gupalo, E.N., 1992. Spatial heterogeneity and dynamics of vernal phytoplankton species in the Baltic Sea in April–May 1986. *J. Plankton Res.* 14 (1), 107–125.
- Kraichnan, R.H., Montgomery, D., 1980. Two-dimensional turbulence. *Rep. Prog. Phys.* 43 (5), 548–619.
- Lee, D.K., Niiler, N., 2010. Influence of warm SST anomalies formed in the eastern Pacific subduction zone on recent El Niño events. *J. Mar. Res.* 68 (3–4), 459–477.
- Lehmann, A., Myrberg, K., 2008. Upwelling in the Baltic Sea — a review. *J. Mar. Syst.* 74, S3–S12.
- Leppäranta, M., Myrberg, K., 2009. *The Physical Oceanography of the Baltic Sea*. Springer, Berlin Heidelberg.
- Lilover, M.-J., Pavelson, J., Kõuts, T., 2011. Wind forced currents over shallow Naissaar Bank in the Gulf of Finland. *Boreal Environ. Res.* 16 (Suppl. A), 164–174.
- Meier, H.E.M., 2001. On the parametrization of mixing in three-dimensional Baltic Sea models. *J. Geophys. Res.* 106 (C12), 30,997–31,016.
- Meier, H.E.M., 2007. Modeling the pathways and ages of inflowing salt- and freshwater in the Baltic Sea. *Estuarine Coastal Shelf Sci.* 74 (4), 610–627.
- Meier, H.E.M., Doscher, R., Faxen, T., 2003. A multiprocessor coupled ice-ocean model for the Baltic Sea: application to salt inflow. *J. Geophys. Res.* C106, C30,997–C31,016.
- Ollitrault, M., Gabillet, C., Colin de Verdière, A., 2005. Open ocean regimes of relative dispersion. *J. Fluid Mech.* 533, 381–407.
- Perlekar, P., Benzi, R., Nelson, D., Toschi, F., 2010. Population dynamics at high Reynolds number. *Phys. Rev. Lett.* 105 (14) (Art. No. 144501).
- Pichel, W.G., Churnside, J.H., Veenstra, T.S., Foley, D.G., Friedman, K.S., Brainard, R.E., Nicoll, J.B., Zheng, Q., Clemente-Colon, P., 2007. Marine debris collects within the North Pacific Subtropical convergence zone. *Mar. Pollut. Bull.* 54 (8), 1207–1211.

- Powell, T.M., Okubo, A., 1994. Turbulence, diffusion and patchiness in the sea. *Philos. Trans. R. Soc. London B* 343 (1303), 11–18.
- Rhines, P., 1979. Geostrophic turbulence. *Annu. Rev. Fluid Mech.* 11, 401–441.
- Richards, Z.T., Beger, M., 2011. A quantification of the standing stock of macro-debris in Majuro lagoon and its effect on hard coral communities. *Mar. Pollut. Bull.* 62 (8), 1693–1701.
- Richardson, L.F., 1926. Atmospheric diffusion shown on a distance-neighbor graph. *Proc. R. Soc. A* 110, 709–737.
- Samuelson, A., Hjøllø, S.S., Johannessen, J.A., Patel, R., 2012. Particle aggregation at the edges of anticyclonic eddies and implications for distribution of biomass. *Ocean Sci.* 8 (3), 389–400.
- Samuelsson, P., Jones, C.G., Willén, U., Ullerstig, A., Gollvik, S., Hansson, U., Jansson, C., Kjellström, E., Nikulin, G., Wyser, K., 2011. The Rossby Centre Regional Climate Model RCA3: model description and performance. *Tellus A* 63, 4–23.
- Schilling, K., Zessner, M., 2011. Foam in the aquatic environment. *Water Res.* 45 (15), 4355–4366.
- Schumacher, J., Eckhardt, B., 2002. Clustering dynamics of Lagrangian tracers in free-surface flows. *Phys. Rev. E* 66 (1) (Art. No 017303).
- Soomere, T., Viikmäe, B., Delpêche, N., Myrberg, K., 2010. Towards identification of areas of reduced risk in the Gulf of Finland. *Proc. Est. Acad. Sci.* 59 (2), 156–165.
- Soomere, T., Andrejev, O., Sokolov, A., Myrberg, K., 2011. The use of Lagrangian trajectories for identification of the environmentally safe fairway. *Mar. Pollut. Bull.* 62 (7), 1410–1420.
- Stevens, D.P., 1991. The open boundary condition in the United Kingdom fine-resolution-Antarctic-model. *J. Phys. Oceanogr.* 21 (9), 1494–1499.
- Thorpe, S.A., 2009. Spreading of floating particles by Langmuir circulation. *Mar. Pollut. Bull.* 58 (12), 1787–1791.
- Vucelja, M., Falkovich, G., Fouxon, I., 2007. Clustering of matter in waves and currents. *Phys. Rev. E* 75 (6) (Art. No. 065301).
- Webb, D.J., Coward, A.C., de Cuevas, B.A., Gwilliam, G.S., 1997. A multiprocessor ocean general circulation model using message passing. *J. Atmos. Oceanic Technol.* 14, 175–183.

## Paper IV

**Giudici A.**, Soomere T. 2014. Finite-time compressibility as an agent of frequent spontaneous patch formation in the surface layer: a case study for the Gulf of Finland, the Baltic Sea. *Marine Pollution Bulletin*, 89(1–2), 239–249, doi: 10.1016/j.marpolbul.2014.09.053





# Finite-time compressibility as an agent of frequent spontaneous patch formation in the surface layer: A case study for the Gulf of Finland, the Baltic Sea



Andrea Giudici<sup>a,\*</sup>, Tarmo Soomere<sup>a,b</sup>

<sup>a</sup> Institute of Cybernetics at Tallinn University of Technology, Akadeemia tee 21, 12618 Tallinn, Estonia

<sup>b</sup> Estonian Academy of Sciences, Kohtu 6, 10130 Tallinn, Estonia

## ARTICLE INFO

### Article history:

Available online 14 October 2014

### Keywords:

Pollution control  
Maritime pollution  
Patch formation  
Flow compressibility  
Lagrangian transport  
Baltic Sea

## ABSTRACT

We explore the possibilities for spontaneous formation of surface patches with high concentrations of contaminants through time correlations of the convergence field and the Lagrangian transport. The test area is the Gulf of Finland, the Baltic Sea, where surface velocity fields show extensive convergence. The flow properties are extracted from 3D velocity fields simulated for 1987–1991 using the OAAS model with a resolution of 1 mile. The focus is on the spatial distribution of the areas in which the values of finite-time flow compressibility of surface velocity fields exceed the threshold for clustering of floats. The distribution of such areas is asymmetric, with likely areas of patch formation located predominantly in the southern and eastern regions of the gulf. Out of nine areas of likely patch formation, six are located along the coast in regions of frequent downwelling, while three are identified in the central region of the gulf.

© 2014 Elsevier Ltd. All rights reserved.

## 1. Introduction

The marine surface layer is normally highly heterogeneous across a wide range of temporal and spatial scales. Such variations of any of key biogeochemical variables (such as salinity, temperature, oxygen, nutrients, optically active substances) can positively impact the ecosystem (e.g., providing more oxygen, or light) while others (such as pollution, microplastic, litter) may completely destroy it. In the literature, for any of these variables, any localised increase or decrease in concentration from ambient measures, are referred to as *patches*. On the one hand, their presence, termed *patchiness* (Brentnall et al., 2003) or more frequently *patchiness* (e.g., Kononen et al., 1992; Levin, 1994; Grünbaum, 2012), is not only just a feature of the marine environment (Kononen et al., 1992; Granskog et al., 2005) but also a key driver of ecological interactions and a basic ground to maintenance of ecological productivity of the marine environment (Levin et al., 2001; Chelton et al., 2011; Gruber et al., 2011; Grünbaum, 2012). On the other hand, patches of adverse impacts (e.g., oil or radioactive pollution) may completely destroy the parts of vulnerable ecosystem hit by such patches (Kachel, 2008). An increasing number of patches with

negative impact are of anthropogenic origin, created via, e.g., dredging, dumping, land reclamation, or aqua farming; also through river discharge of nutrients and chemicals, or release of oil.

Patches of various biogeochemical variables, pollution or contaminants may emerge in the open ocean because a multitude of mechanisms, including but not limited to mesoscale eddies, up/downwelling, the internal dynamics of the ocean currents and surface and internal waves, or interplay between waves and currents (Kahru, 1983; Powell and Okubo, 1994; Lennert-Cody and Franks, 2002; Leichter et al., 2005; Vucelja et al., 2007, among others). Even a horizontal density gradient (Burchard et al., 2008), classical estuarine circulation (Burchard et al., 2004), or Langmuir circulation (that collects surface floats into long windrows) (Allredge et al., 2002; Dethleff et al., 2009; Thorpe, 2009; Akan et al., 2013) may lead to the accumulation of particles or to well-defined turbidity maxima. Furthermore, some patches such as 'hot spots' of bioproduction (Strass, 1992; Calil and Richards, 2010) that stem from interactions within the ecosystem express the properties of the ocean as an excitable medium (Brentnall et al., 2003), in which the signal or wave may propagate only once and which cannot support the passing of another signal until a certain amount of time has passed. The nearshore area has often patches of different origin such as filaments of almost fresh water due to river inflow or inhomogeneities of water masses in

\* Corresponding author.

E-mail address: [andrea@cens.ioc.ee](mailto:andrea@cens.ioc.ee) (A. Giudici).

nearshore areas with different properties of bottom sediments owing to different exposure to hydrodynamic activity (Abraham, 1998), etc.

A frequent agent for the patch-generation process, often overlooked in the analysis of patchiness formation, is a system of three-dimensional (3D) motions in the water column affecting a two-dimensional (2D) field of items or substances that are concentrated at the sea surface (Lee and Niiler, 2010). This mechanism most strongly affects stratified environments such as microtidal shelf seas where the buoyancy keeps many substances and contaminants in the surface layer. The surface layer (of varying thickness) may exhibit extensive contraction or expansion (more generally, extensive compressibility), depending on the sign of divergence of the surface velocity field. The resulting effect becomes evident, e.g., as a fascinating ability of marine debris to form patches (Pichel et al., 2007) in the open ocean.

It is likely that the most systematic and rapid impact among such features provides a mechanism of generation of patches by localised convergence zones that move together with the surface current (Samuelson et al., 2012). This mirror phenomenon to a transient upwelling (Fennel et al., 2010) affects surfactant films (similarly to extreme events of edge waves, Averbukh et al., 2014) and substances (e.g., litter, biomass) that are floating on the sea surface or are concentrated in the uppermost layer. Very little is known about spatio-temporal distribution and magnitude of this effect although this and similar mechanisms are apparently very often active in strongly stratified environments (Giudici et al., 2012; Kalda et al., 2014).

In this paper, we employ the concept of finite-time compressibility (FTC) (Giudici et al., 2012) to study the location and temporal persistence of areas that may regularly exhibit high chances for a spontaneous increase in the surface concentrations of various items and substances. The results are first of all relevant for understanding how pollution, adverse impacts or contaminants that are either floating on the sea surface or are locked in the surface layer by e.g., buoyancy effects may spontaneously form dangerously high concentrations. The impact of finite-time compressibility on the concentration of floats resembles a similar impact of convergence fields that move over the sea surface synchronously with Lagrangian transport of the surface layer (Samuelson et al., 2012). In other words, this measure offers a possibility to systematically account for the long-term correlations between an emerging patch, its Lagrangian transport and relocation of the convergence field.

The test area is the Gulf of Finland (Fig. 1) in the easternmost Baltic Sea, a vulnerable region under extremely strong anthropogenic pressure (Leppäranta and Myrberg, 2009). The dynamics of a thin uppermost layer of this water body is often almost decoupled from the motions in the deeper layers (Myrberg and Soomere, 2013) and at times contains an anticyclonic gyre (Fig. 2) (Soomere et al., 2011). This gulf has been recently shown to frequently host areas of high (classical) compressibility of surface velocities as well as areas with high values of FTC (Kalda et al., 2014).

As a basis of the study, we use 3D velocity fields simulated using the OAS (Andrejev and Sokolov, 1989, 1990) ocean model with a spatial resolution of 1 nautical mile (NM). Our focus is on the spatial distribution of the areas in which the values of FTC exceed the threshold for clustering of floats (Falkovich et al., 2001), equivalently, for intense patch formation. This distribution is studied by means of counting the time during which the FTC exceeds the threshold in question during certain longer time intervals. The main development is the identification of nine clearly localised areas where the FTC often exceeds this threshold. While most of such areas are can be associated with coastal regions of frequent downwelling, intriguingly, three such areas are located in central part of the gulf.

We start from a short presentation of the basic idea of the FTC, a simple method for evaluation of its short-term values based on tracking of clusters of water or pollution parcels that are passively advected by modelled surface currents and the scheme for evaluation of spatial variations of FTC. As the OAS model has been widely discussed in international literature, we only provide the basic information about this circulation model and calculations. Some examples of spatial distribution of high-FTC areas are provided next. The main outcome of the work is a map of sea areas where areas with high FTC regularly occur.

## 2. Methods and data

### 2.1. Finite time compressibility: definition and basic properties

The classical notion of compressibility of a velocity field (called flow compressibility below) relies on the (Helmholtz) decomposition of realistic fields of ocean currents into their solenoidal (with zero divergence) and potential (with zero curl) components. Flow compressibility  $C_c$  is the relative weight of the potential component of the velocity field. Therefore, although the notion of divergence is used in the definition of the flow compressibility, these two quantities are not equivalent.

This decomposition and definition rely on instantaneous properties of the flow field and ignore its history. In reality, the history of the (interrelations) of the divergence field and Lagrangian transport of the parcels of a medium do play a large role as demonstrated, for example, by Samuelson et al. (2012). To account for the interplay of these two drivers, we adopt a slightly different definition of (surface) flow compressibility called finite-time compressibility and denoted as FTC. This measure integrates a certain section of the history of the surface flow. The reader is referred to Giudici et al. (2012) and Kalda et al. (2014) for an extended discussion of the origin of this measure and its interrelations with classical notions of compressibility of medium and flow compressibility. While these above studies have demonstrated the existence of spots with very high instantaneous values of FTC, we focus here on the areas where such high values may regularly occur in a longer time scale. Heuristically, such areas should often host downwelling. During strong downwelling events water parcels systematically sink into deeper layers whereas lighter additives (debris, microplastic, oil spills, polluted or nutrient-rich fresh water from rivers) stay at the surface. This process naturally leads to an increase in the concentration of additives. It may be particularly rapid if the flow compressibility exceeds a certain value, after which rapid and spontaneous clustering of floats may start (Falkovich et al., 2001). Our goal is to highlight the areas where the phenomenon of such spontaneous increase in surface concentrations is frequent, that is, frequently hosting values of FTC that exceed a certain important threshold. We use precomputed velocity fields and certain easily computable quantities for this task.

To reach this goal, it is necessary to properly quantify changes to the concentrations of floating matter (e.g., contaminants) and associated patch-formation process at the sea surface. For this reason we employ a definition of FTC that relies on the tracking of Lagrangian transport of single water parcels that are locked at the sea surface and represent passively carried floats (Giudici et al., 2012; Kalda et al., 2014). The compressibility of sea surface is evaluated semi-locally, by observing the relative changes in surface elements surrounded by such parcels that are passively carried by surface currents during a certain time interval. The method is implemented by grouping together triplets of simulated parcels and tracking the geometrical properties of resulting triangular elements through time (Fig. 3).

The compressibility of sea surface is evaluated using the ratio of the relative changes of the surface area of these elements over the

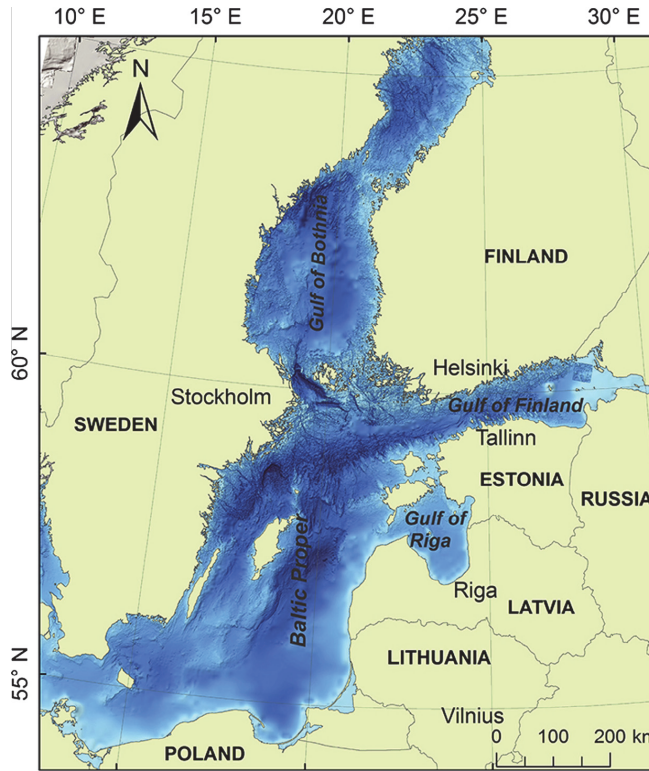


Fig. 1. Location scheme of the Baltic Sea and the test area Gulf of Finland.

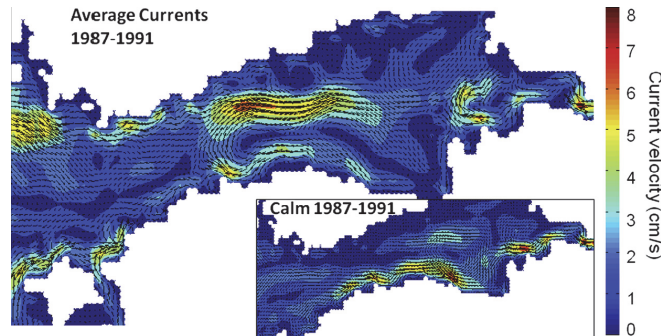


Fig. 2. Average velocity field in the uppermost layer of the Gulf of Finland in 1987–1991 and during calm seasons (May–August, inset) in these years (Soomere et al., 2011). The underlying velocity data are calculated using the Rossby Centre Ocean model RCO (Meier et al., 2003).

similar changes to their edges. The relative change  $dS_t$  of the area  $S_t$  of such an element over one time step is  $dS_t = (S_t - S_{t-1})/S_t$ . The relative changes to the squared lengths of two of its edges  $A_t$  and  $B_t$  (Fig. 3) are  $dA_t = (A_t^2 - A_{t-1}^2)/A_t^2$  and  $dB_t = (B_t^2 - B_{t-1}^2)/B_t^2$ . The approximate values of FTC over a certain time interval are calculated as follows (Giudici et al., 2012):

$$C_{FTC} = \frac{2dS_{rms}}{dA_{rms} + dB_{rms}}, \quad (1)$$

where  $dS_{rms}$ ,  $dA_{rms}$  and  $dB_{rms}$  stand for the root mean square of the instantaneous values of  $dS_t$ ,  $dA_t$  and  $dB_t$  over the time interval

during which the motion of the element is tracked. The resulting values of  $C_{FTC}$ , although related to the initial location of the element, actually characterise the motions over a certain wider sea area and implicitly involve a time scale that has the meaning of correlation length.

We are specifically interested in the identification and quantification of situations corresponding to high values of the classical flow compressibility, under which clustering phenomenon of surface floats may occur. This phenomenon may happen for the limit of ideal Kraichnan flows if the classical flow compressibility exceeds the value  $C_c = 0.5$  (Vucelja et al., 2007).

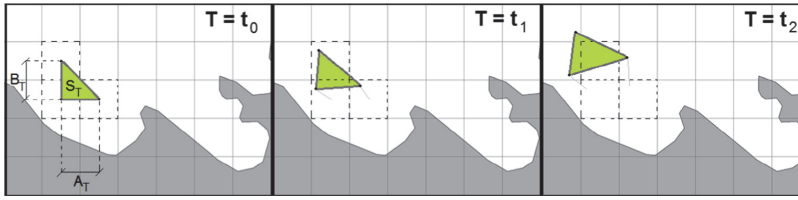


Fig. 3. Triangular elements used to evaluate finite-time compressibility.

For ideal Kraichnan flows and small values of compressibility (e.g., for almost rectilinear flows) the relationship between the classical flow compressibility  $C_c$  and  $C_{FTC}$  is described by the formula (Giudici et al., 2012):

$$C_{FTC}^2 = \frac{2C_c}{2C_c + 1}. \quad (2)$$

In this case the two measures simultaneously tend to zero and have often comparable values but coincide only when  $C_c = C_{FTC} = \sqrt{(\sqrt{17} - 1)}/4 \approx 0.781$ . They describe highly compressible flows in a somewhat different manner: when  $C_c$  reaches its maximum value of 1,  $C_{FTC} = \sqrt{2/3}$ . It is straightforward to demonstrate that values  $C_{FTC} > \sqrt{2/3}$  are physically feasible. For example, the process  $C_{FTC} \rightarrow 1$  corresponds to the plausible condition of a triangular patch, whose edges are orthogonal to each other, and whose vertices are moving in opposite directions alongside the edges. Therefore, a certain range of possible values of  $C_{FTC}$  corresponds to impossible values of  $C_c$ . The threshold  $C_c = 0.5$  for the classical flow compressibility, which coincides with the threshold for clustering phenomena to appear, corresponds to somewhat larger values of the finite-time compressibility  $C_{FTC} = \sqrt{1/2} \approx 0.7$ .

## 2.2. Numerical setup

The previous studies of this concept (Giudici et al., 2012; Giudici and Soomere, 2013; Kalda et al., 2014) relied on the output of an ocean circulation model with a modest resolution (2 NM) that was barely eddy-permitting in the Gulf of Finland and thus only conditionally represented the surface dynamics in this basin. The surface 2D velocity fields used in this paper are derived from numerical simulations of the hydrodynamic model OAAS (Andrejev and Sokolov, 1989, 1990), carried out in the framework of BONUS + BalticWay cooperation (Soomere et al., 2014) with a spatial resolution of 1 NM.

As the model and the runs, results of which are employed in this paper, are extensively described in the international literature (Andrejev et al., 2010, 2011; Soomere et al., 2014), we only bring here the key features of the model, its setup and forcing data. The OAAS model is a primitive-equation, time-dependent, free-surface, baroclinic model based on hydrostatic approximation. It is specifically designed for simulation of ocean circulation in basins with complicated geometry. The vertical resolution is 1 m (except for the uppermost layer that is 2 m thick). The model run, the velocities from which are used for this study, was forced with the river runoff data from Bergström and Carlsson (1994) and meteorological data from a regionalization of the ERA-40 re-analysis over Europe. The forcing data were prepared using a regional atmosphere model with a spatial horizontal resolution of 25 km in which wind gustiness was adjusted to match modelled and measured wind statistics (Höglund et al., 2009; Samuelsson et al., 2011). The model was run for the interior of the Gulf of Finland to the east of longitude 23°27'E. At this boundary, the

OAAS model uses 3D information about hydrographic and hydrodynamic fields calculated using the RCO model for the entire Baltic Sea (Rossby Centre Ocean Model, Meier et al., 2003; Meier, 2007). The modelled velocity data cover the entire Gulf of Finland for 1987–1991, with a temporal resolution of 3 h, thus leading to 161,600 information vectors for each day.

The simulation environment QTRAC (Giudici and Soomere, 2013) was extended to deal with the higher-resolution velocity dataset and to produce the “climatology” for highly persistent high- $C_{FTC}$  areas. The calculation pipeline (Fig. 4) resembles the scheme used in (Soomere et al., 2011) to highlight semi-persistent patterns of Lagrangian transport.

The calculation pipeline begins with loading the surface velocity information, out of which here the 2D horizontal velocity components at sea surface are used for a certain sea area and a longer time interval  $[START_{TOT}, END_{TOT}]$  with a temporal resolution of the available velocity fields  $SIM_{Step}$ . One fluid parcel is then positioned at the centre of each wet grid cell of the OAAS model and triangular elements are composed from these as indicated in Fig. 3. As the OAAS model uses regular rectangular grid with an almost equal step along latitudes and longitudes (Andrejev et al., 2010, 2011), the selected parcels are uniformly distributed over the study area.

The entire simulation interval  $[START_{TOT}, END_{TOT}]$  is divided into time windows, over which the motion of the selected parcels is tracked. The length of the time window  $SIM_{Length}$  has the meaning of the correlation length during which the local properties of flow convergence and underlying Lagrangian transport are tracked. Some advanced techniques of building Lagrangian trajectories from precomputed velocity data (e.g., TRACMASS; Döös, 1995; de Vries and Döös, 2001) use internal interpolation of the trajectories within the time step  $SIM_{Step}$  of velocity data. As several key statistical properties of the resulting sets of trajectories are almost invariant with respect to variations in the method of their calculation (Viikmäe et al., 2013) we use the simplest first order Euler method (with a step  $SIM_{Step}$ ) to construct the trajectories. The quantities  $dS_r$ ,  $dA_r$  and  $dB_r$  are evaluated for each time step of the saved velocity data according to the stencil shown in Fig. 3. From these instantaneous values, the quantities at the right-hand side of Eq. (1)  $dS_{rms}$ ,  $dA_{rms}$  and  $dB_{rms}$  are evaluated for each triangular element. The product of each calculation over a time window  $SIM_{Length}$  for the entire set of elements is a spatial distribution (map) of  $C_{FTC}$ , similar to those described in (Kalda et al., 2014). For simplicity, these distributions are called instantaneous maps of  $C_{FTC}$  in this paper (Fig. 5).

Similar calculations, performed for a number of different starting instants ( $START$  for  $SIM1$ ,  $SIM2$ , etc. in Fig. 4) for the same selection of fluid parcels and triangular elements, result in a number of  $C_{FTC}$  maps, each representing the chosen time window (correlation length) and starting instants of calculations.

These calculations and resulting maps are grouped together in so-called batches (FTC1, FTC2, etc. with a length of  $\delta_{FTC}$  in Fig. 4) that usually represent months or seasons. There are several options for further handling of the instantaneous maps of  $C_{FTC}$  that belong

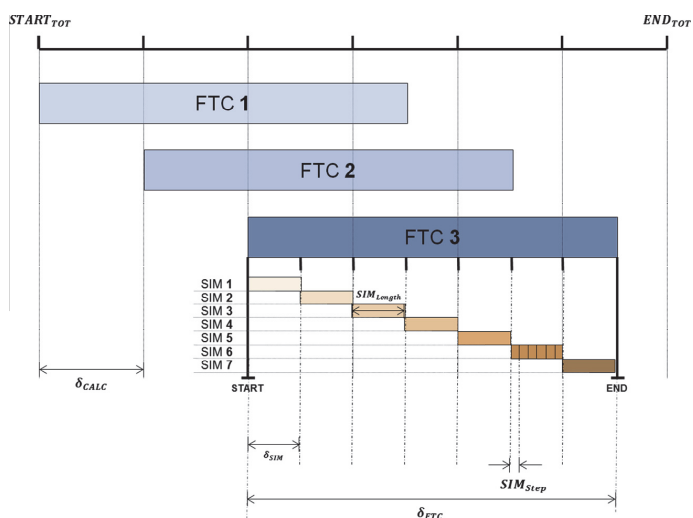


Fig. 4. Sketch of the calculation pipeline.

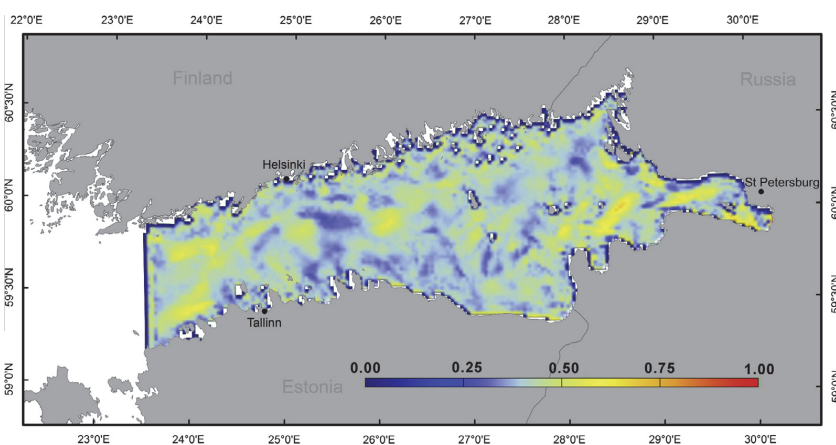


Fig. 5. An instantaneous FTC map calculated for 01 March 1987 with  $SIM_{Length} = 24$  hours.

to a certain batch. As the resulting maps for a single time window are quite noisy and pixelated, studies of semi-persistent patterns of Lagrangian transport (Soomere et al., 2011) and fairway design (Andrejev et al., 2011; Lu et al., 2012) use pixelwise (cell-wise) averaging of the values in similar distributions over a certain set of time intervals.

We are specifically interested in the quantification of the frequency of appearance of the spontaneous clustering phenomenon of surface floats. Following this goal, the focus is on the values of  $C_{FTC}$  that exceed the threshold for clustering. This information is likely to be smoothed out if a pixelwise average is taken over a large number of instantaneous maps. For this reason we choose another way to extract information from the instantaneous maps of  $C_{FTC}$ . The temporal behaviour of the FTC field within each batch (say, FTC3 in Fig. 4) is analysed using a method similar to peak-over-threshold approach often used elsewhere in physical oceanography (e.g., Holthuijsen, 2007). Namely, we count for each wet grid

cell of the OAS model, how many instantaneous values of  $C_{FTC}$  exceed the critical threshold of  $\sqrt{1/2}$  for the clustering phenomenon during the time interval (or a selection of seasons) covered by the batch. This algorithm produces a map of the count (equivalently, the frequency of occurrence) of over-threshold values of  $C_{FTC}$  during the batch (Fig. 6). Finally, the total number of such values is counted for each wet grid point of the OAS model over all batches of a fixed length. Doing so is equivalent to the calculation of an average number of occasions of  $C_{FTC} \geq \sqrt{1/2}$  in each model grid cell.

The potential impact of the listed parameters on the results of calculations is similar to the impact of equivalent parameters on the statistics of Lagrangian transport (Viikmäe et al., 2010). The “external” parameters  $START_{TOT}$ ,  $END_{TOT}$  and  $SIM_{Step}$  reflect the entire time interval for which velocity data are available and the temporal resolution of the velocity data, and can be only adjusted by rerunning the ocean circulation model. The calculations involve also several adjustable parameters. The key quantities, to be

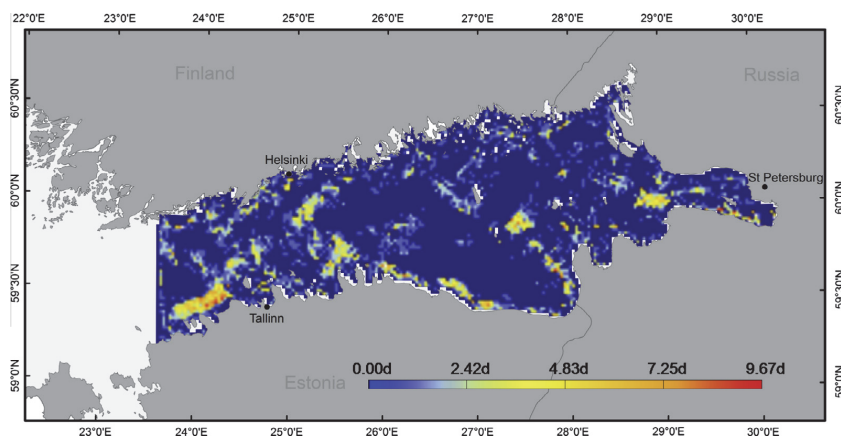


**Fig. 6.** A map of the count of days during which the values of  $C_{FTC}$  in single cells exceeded the clustering threshold  $\sqrt{1/2}$  in batch with a length of  $\delta_{FTC} = 30$  days. The map is calculated using the following parameters: start instant = 01 December 1987,  $SIM_{Step} = 3$  h.

chosen properly to highlight phenomena with specific time scales, are the batch length  $\delta_{FTC}$  and  $SIM_{Length}$ . The choice of batch lengths  $\delta_{FTC}$ , their time lag  $\delta_{SIM}$  and the set of batches with this length are determined by the particular research question. The batch length defines the characteristic time scale (e.g., whether seasonal, inter-annual or long-term phenomena are under consideration), during which a certain regularly present or semi-persistent structure may appear. The parameter  $SIM_{Length}$  (the length of each particle tracking simulation) specifies the time interval, over which the correlation between the convergence field and Lagrangian transport of the emerging patch is accounted for. A discussion of the reasonable choice of these parameters in the Gulf of Finland is presented in (Viikmäe et al., 2010; Soomere et al., 2011) in the context of semi-persistent patterns of Lagrangian transport.

The main effect of variations of  $SIM_{Step}$  on the results is that high  $C_{FTC}$  values tend to be smoothed out as this parameter increases. This is because the longer  $SIM_{Step}$  is, the greater are the chances to overlook or smooth out the effect of small-scale or short-lived features with high  $C_{FTC}$  values. Although the measure of  $C_{FTC}$  is highly dependent on time correlations, we do not know beforehand for how long such correlations persist. As discussed above, whenever a domain of convergence of surface velocity field moves together with the underlying current (Samuelson et al., 2012), patch formation becomes stronger and more evident, and thus leads to a higher level of  $C_{FTC}$ . It is therefore natural to assume that the time scale during which patch formation occurs to some extent reflects the persistency of the local Lagrangian transport. It has been recently shown that the Gulf of Finland hosts semi-persistent patterns of Lagrangian flows, which can be highlighted using time windows of a length of few days (Soomere et al., 2011).

The role of the temporal distance (time lag)  $\delta_{SIM}$  between two consecutive calculations of  $C_{FTC}$  that characterizes the shift in time between the starting instant of subsequent time windows is less obvious. Together with  $SIM_{Length}$  it defines the total number of single calculations of the  $C_{FTC}$  values to be performed. Following the analysis in (Viikmäe et al., 2010), we choose always  $\delta_{SIM} \geq SIM_{Length}$  to avoid serial correlations of the calculation results. It is, however, possible to formally increase the temporal resolution of  $C_{FTC}$  calculations for each batch within the dataset by using overlapping time windows, that is, by setting  $\delta_{SIM} < SIM_{Length}$  (cf. Viikmäe et al., 2010).

The calculations of instantaneous maps of  $C_{FTC}$  were performed repeatedly using different values for the discussed parameters

(Table 1). The combinations of these parameters resulted in 1215 different maps. In this paper, we focus on the frequency of occurrence of over-threshold values of  $C_{FTC}$  in all batches of the entire interval of simulations (1987–1991). The results characterise long-term properties of potential spontaneous patch formation in the Gulf of Finland. The counts of instantaneous high values of  $C_{FTC}$  over the entire calculation interval are evaluated pointwise for each wet grid cell of the OAAS model from the entire set of instantaneous maps for a fixed duration. This procedure is equivalent to a two-step averaging. In the first step (counting the over-threshold values for each batch, Fig. 6) the variations within large (over-threshold)  $C_{FTC}$  values are ignored. This is meant to reduce the numerical noise associated with relatively moderate spatial and temporal resolution of the velocity data. The second step is equivalent to averaging of the pointwise results of the above count over the entire simulation time interval. If the batch length does not exceed  $\delta_{CALC}$ , this procedure reduces to the calculation of the sum (or average) of over-threshold values on single instantaneous  $C_{FTC}$  maps. If the batches overlap, these maps in the first and last batches have lower weights. The resulting maps of average counts of over-threshold  $C_{FTC}$  values for different batch lengths eventually make it possible to identify the set of the most frequently occurring high  $C_{FTC}$  areas.

### 3. Results

#### 3.1. Frequently occurring areas of high finite-time compressibility

The areas with high FTC in instantaneous maps (Fig. 5) and the counts of over-threshold values of  $C_{FTC}$  in single batches (Fig. 6) usually vary strongly in time and space. As explained above, the process of constructing the maps of frequency of occurrence of over-threshold FTC values ignores part of this variability in a single

**Table 1**  
Main parameters of calculations in Fig. 4.

Parameter	Description	Value(s)
$\delta_{FTC}$	FTC batch length	30, 90, 180 (days)
$SIM_{Step}$	Simulation step	3 (h)
$SIM_{Length}$	Length of time window	6, 12, 18 (h)
$\delta_{CALC}$	Consecutive FTC batch offset	24, 48 (h)
$\delta_{SIM}$	Time lag between calculations	6, 12, 18 (h)

cell and only accounts for whether the  $C_{FTC}$  exceeds the clustering threshold  $\sqrt{1/2}$ . Therefore, already in single relatively short batches (Fig. 6) the presence of even very large instantaneous values of  $C_{FTC}$  is smoothed out.

Further averaging of the count of over-threshold values over several subsequent 90 and 180-days long batches, not unexpectedly, further smoothens out many features of relevant single maps. The resulting average maps however show remarkably how certain areas of the Gulf of Finland often (albeit not continuously) host above-clustering-threshold values of the finite-time compressibility (Fig. 7). While the average count of  $C_{FTC} \geq \sqrt{1/2}$  is around 0.93 days and 1.91 days (for 90 and 180 day long batches, respectively), certain easily identifiable regions show such counts of up to 30 and 60 days, respectively. Therefore in such regions in the Gulf of Finland the spontaneous patch formation phenomenon is likely to happen for over one third of the time. It is to be expected that the results averaged over 180 days exhibit clearly less spatial variability of the high- $C_{FTC}$  count. Is it however remarkable that the relative frequency of occurrence of such values is almost the same for 90-day and 180-day long batches. This feature signals that some areas of the Gulf of Finland may often almost continuously host intense patch generation.

There areas where over-threshold values of FTC often occur are mostly concentrated in coastal regions, predominantly along the southern coast of the Gulf of Finland (Fig. 7). The most remarkable areas of this type are found in a certain section of the north-eastern coast of Estonia and in a slightly more offshore area between the islands of Naissaar and Pakri. Similar areas near the northern coast of the gulf are smaller and weaker. Importantly, a few such areas are located in the open part of the gulf. Among these, the strongest

and most persistent is an area in the easternmost part of the gulf at the entrance to the Neva Bight. Another clearly defined region hosting frequently over-threshold FTC values is located in the widest part of the gulf. Note that the areas located in the easternmost part of the Neva Bight next to Saint Petersburg may reflect the inability of the model to properly resolve dynamics in this shallow-water region. Moreover, the model evidently does not correctly replicate the impact of the Saint Petersburg Flood Protection Facility.

### 3.2. Asymmetry of areas of likely spontaneous patch formation

Another perspective on the location and magnitude of areas frequently hosting high FTC values provide meridional and zonal averages of the maps in Fig. 7. The average level of the time during which the FTC exceeds the clustering threshold for 90-day long batches is about 0.97 days and 1.49 days for the zonal and meridional profiles, respectively. For the 180-day long batches these values are about 2.2 days and 3.1 days for the zonal and meridional profiles, respectively. The standard deviation of the pointwise values from the overall mean is 2.06 days and 2.09 days for the 90-day batches and 3.91 days and 3.97 days for the 180-day batches and zonal/meridional average, respectively. These values indicate that the pointwise values of frequent occurrence of over-threshold levels of FTC vary moderately across the Gulf of Finland but considerably more extensively along the gulf (in the east–west direction).

The zonally averaged values of these maps (the average over rows of the underlying data of Fig. 7) reveal strong asymmetry of the regions with the frequent occurrence of over-threshold levels

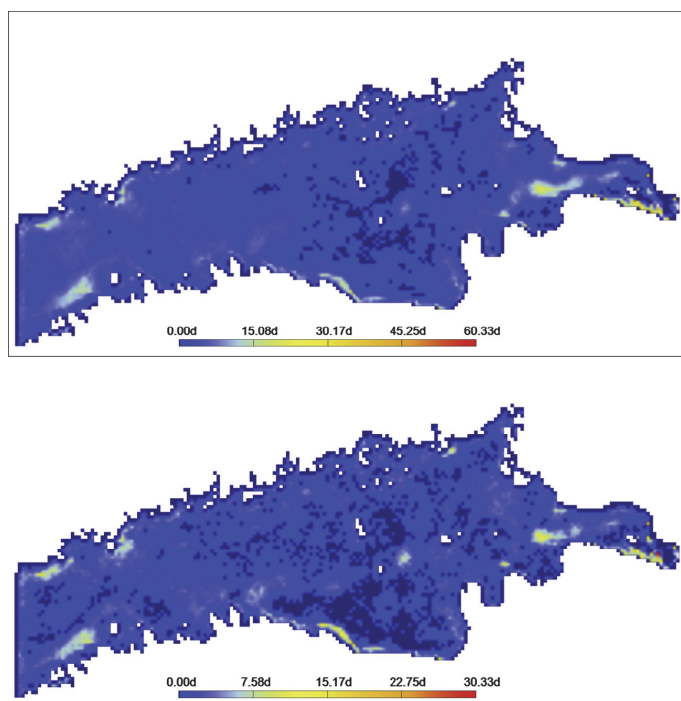


Fig. 7. Maps of the average count of the over-threshold FTC values for 180 and 90 day long batches calculated using the following parameters:  $\delta_{SIM} = 24$  h,  $SIM_{Length} = 12$  h,  $SIM_{Step} = 1.5$  h. The colour coding shows how many times in total the values of  $C_{FTC}$  exceed the clustering threshold 0.7 in total 16 or 8 similar maps for 90 or 180-day long batches.

of FTC values in the north–south direction, equivalently, across the Gulf of Finland (Fig. 8). Namely, the southern parts of the gulf host systematically more frequent occurrence of  $C_{FTC} \geq \sqrt{1/2}$  than the northern parts. Thus, the patch-formation process can be expected to be generally more likely along the southern coast of the gulf. The largest zonally averaged values in Fig. 7 at the southern coast by more than a factor of two exceed the overall average level of the measure in question.

Meridionally averaged values of the fields represented in Fig. 7 show much larger variation in the east–west direction (Fig. 8). The central part of the Gulf of Finland has an overall low level of this measure. Clearly higher values are found in the western part of the gulf. These values, especially close to the boundary of the simulation area, may be caused by boundary effects. Several high peaks in the easternmost part of the gulf evidently reflect an important feature of the dynamics of the gulf that may reflect frequent convergence of the overall cyclonic circulation with the voluminous discharge from three major rivers (Narva, Neva and Kymi) into this part of the gulf. Although some of the magnitude of these peaks may be related with a smaller number of samples used for their calculations in the narrow Neva Bight, their maxima by several times exceed the average for the given latitude. As mentioned above, the highest peak in the Neva Bight (that reaches values of 10.2 days and 8.3 days, respectively for 180- and 90-day averages) probably reflects the inability of the ocean model to replicate the field of motions in this area.

### 3.3. Persistency of potential regions of spontaneous patch formation

From the described procedure of construction of maps in Fig. 7 it follows that the maxima of the frequency of occurrence of over-threshold values of FTC are the most likely areas of spontaneous patch formation, equivalently, of spontaneous increase in the concentration of surface floats, pollution or contaminants locked in the surface layer. The persistency of such areas can be evaluated to a certain extent by means of an analysis of the regions of frequent occurrence of over-threshold values of FTC for single batches (cf. Fig. 6). We have associated each such area within a single batch with an oval-shaped region roughly matching the orientation and appearance of each area and with the centre of the oval matching the maximum of the relevant count of over-threshold values of FTC. The centroid's position, the size and the shape of each area of high count of over-threshold FTC values vary for single batches. The criterion used to select areas of likely and

frequent patch generation was that a clearly identifiable local maximum, with characteristic geometrical properties, was present within at least 80% from the total amount of single batches. Given the duration of the batches (90 and 180 days), this criterion means that a high count of over-threshold FTC values is present in such areas in all seasons.

This procedure resulted in nine distinctly distinguished and clearly separated from each other areas of where high values of  $C_{FTC}$  regularly occur, equivalently, areas with high potential for patch generation (Fig. 9). Two areas (1 and 2 in Fig. 9) were found near the northern Finnish coast, between longitudes 23°30' E and 24°30' E. Five such areas (3, 4, 5, 7) were found near the southern coast of the gulf, spanning across all its relatively wide part, between longitudes 24° E and 28° E. Area 9 is located near Saint Petersburg, to the east of its flooding protection facility, where the OAAS model has insufficient resolution to replicate the flow properties. Area 8 coincides with the region where the voluminous runoff of River Neva merges with the overall cyclonic circulation in the gulf (Leppäranta and Myrberg, 2009) and where convergent flow is likely. Area 6 was found in the middle of the widest part of the gulf between the islands of Gogland, Moshchny and Bolshoy Tyuters. Note that areas 5, 8 and 9 were also highlighted in previous studies using velocity fields with a spatial resolution of 2 NM and temporal resolution of 6 hours (Giudici et al., 2012; Kalda et al., 2014).

The persistency of these areas over the entire simulation interval of 1987–1991 can be to some extent quantified using the relevant values of the maxima in the count of over-threshold FTC values for single batches (Table 2). The standard deviation of the maxima for each of selected areas (except for area 6) is well below than half of the relevant average value and often on the level of 20–30% of this average. This feature can be interpreted as showing relatively high persistency of the selected areas. In terms of maxima over all maps, the area with the smallest count of over-threshold FTC values (area 6) has a value about 50% from the overall maximum. In terms of the average “strength” (average of the maxima for each selected area and all maps for single batches) this area shows 3–4 times lower values. This difference signals that this area (and possibly some other areas) may be present during specific seasons or years. The relevant analysis is in progress and will be presented elsewhere.

The above results have been presented in terms of simple count of the number over-threshold values of FTC from single 3-h intervals. As the spatial resolution of the velocity data (1 NM) is modest,

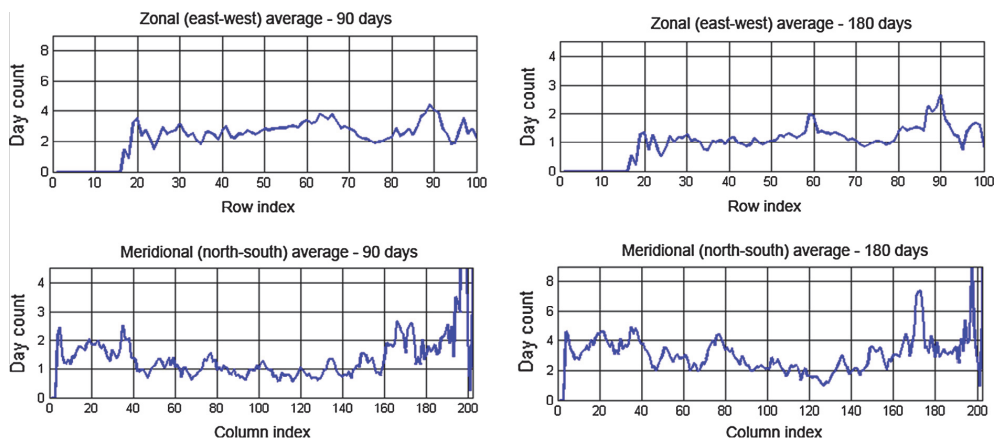


Fig. 8. Meridional and zonal averages of the average count of the over-threshold FTC values for 90 and 180 day long batches in Fig. 7. The row and column indices express the distance (in nautical miles) from the entrance of the Gulf of Finland or from its northern coast, respectively.

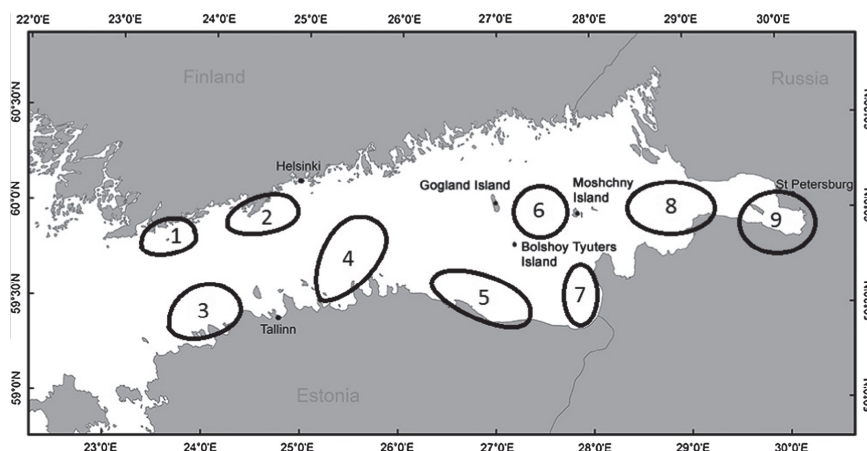


Fig. 9. The set of persistent high- $C_{FTC}$  regions in the Gulf of Finland in 1987–1991.

Table 2

Maximum levels (overall maximum Abs Max and average maximum Avg Max) and standard deviations (Std Dev) of these maxima of the count of over-threshold values of FTC in areas 1–9 of Fig. 8 for single 90-day and 180-day long batches.

Area	90-day long batches			180-day long batches		
	Abs Max	Avg Max	Std Dev	Abs Max	Avg Max	Std Dev
Area 1	15	10.3	3.1	31	23.3	6.4
Area 2	15	11.4	3.6	34	19.4	9.6
Area 3	15	9.1	3.4	35	24.2	6.4
Area 4	19	12.1	5.5	36	19.8	9.0
Area 5	17	14	3	45	32.2	6.8
Area 6	15	7.3	3.6	29	12.9	8.8
Area 7	19	11.3	4.5	29	16.3	6.6
Area 8	22	15.6	3.5	37	29.1	5.8
Area 9	30	22.2	3.9	60	46.5	7.1

the presence of high FTC values during one such interval not necessarily leads to the formation of a noticeable deviation in the concentration of surface floats. In general, several days of consecutive match of the convergence field with the underlying Lagrangian transport may be necessary to form substantial patches. To characterise the persistency of the events with over-threshold values of FTC, we singled out the longest continuous time interval during which  $C_{FTC} \geq \sqrt{1/2}$  for each batch in a selected location in each of areas 1–9 in Fig. 9. The average value of this time interval for single years and areas was mostly between 2 and 3 days (Fig. 10). The smallest values of this “index of persistency” were found for area 6.

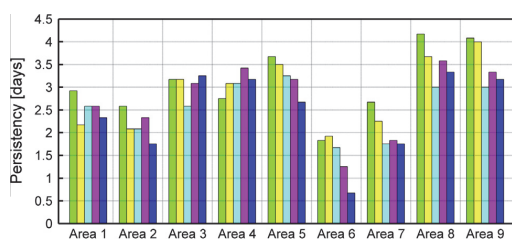


Fig. 10. Annual average of the maximum duration of consecutive events of  $C_{FTC} \geq \sqrt{1/2}$  within single 30-day batches in locations of the highest counts of the over-threshold FTC values in areas 1–9 (Fig. 9) in the Gulf of Finland in 1987–1991.

This feature signals (quite expectedly) that the dynamics of currents in this offshore region is more variable than in other areas in question that are located much closer to the coasts. This “index of persistency” of over-threshold values of FTC varied less than by 25% for different years for all areas (except for area 6). The time interval of a few days is apparently sufficient for the formation of noticeable patches.

#### 4. Discussion and conclusions

The presented approach to quantify the long-term potential of different sea areas to serve as locations of spontaneous patch formation of substances locked in the uppermost layer of the sea relies exclusively on the standard output of contemporary 3D ocean models and uses a set of simple geometric elements to estimate areas where high flow compressibility is synchronised with the local Lagrangian transport. The discussed material demonstrates that this essentially elementary approach has the capacity to highlight clearly defined areas where the joint impact of convergence of surface flow and Lagrangian transport of the emerging patches may often (albeit not continuously) lead to considerable increase in concentrations of surface floats, contaminants or pollution in the surface layer, surfactant films, or other items of substances that are locked in the water column near the sea surface.

This effect of synchronisation of high flow compressibility and underlying Lagrangian transport has been quantified in terms of frequent occurrence of large values of finite-time compressibility that exceed the threshold for the phenomenon of clusterisation of surface floats to occur. This result is universal and apparently works for any substances (contaminants, pollution, nutrients, etc.) that are locked in the uppermost layer by some reason and mostly affected by surface currents. Note that the described mechanism, strictly speaking, is only relevant for their concentration per unit area, which not necessarily means changes to their concentration per unit volume in the water column. This approach ignores the potential direct wind impact and wave-driven effects and is thus only conditionally applicable for floating items and substances directly at the surface. These impacts, however, can be easily incorporated into the model similarly to the recent work of (Murawski and Woge Nielsen, 2013).

Our analysis highlighted nine clearly distinguishable areas where the clusterisation phenomenon and associated spontaneous

patch-formation process, according to the model in use, is relatively frequent. We stress that the processes in the area at the River Neva mouth may be resolved inadequately and models with much higher spatial and temporal resolution are necessary to adequately evaluate the properties of both flow and patch-formation in this region.

The presence of other areas is consistent with the current understanding of the circulation patterns of the Gulf of Finland. The presence of one of the strongest of such areas in a region of the gulf where the voluminous runoff of the Neva River (and possibly of the Narva River) merges with the overall circulation pattern of waters of the Gulf of Finland is not unexpected because convergent flow patterns, one of the reasons of persisting high  $C_{FTC}$  values, evidently are frequent there. This area has been highlighted as often hosting downwelling (Myrberg and Andrejev, 2003). Also, all identified areas of potential spontaneous patch formation along the southern coast of the gulf (especially areas 3 and 7) exhibit frequent downwelling according to the model results of Myrberg and Andrejev (2003).

The presence of areas that may often host conditions of spontaneous patch formation in the northern part of the gulf may be related with the quite persistent inflow of fresh waters present in the surface-layer (0–2.5 m) near the northern coast (Andrejev et al., 2004), which is thought to play a major role in the functioning of the gulf. The most interesting in this context are the areas located near the north-western coast of the gulf and in the middle of the widest part of the gulf. Their existence is somewhat surprising. Although their presence may be seasonal or limited to a few years, it still signals the possible presence of frequent and long-term convergence areas of surface currents and calls for further studies into the discussed phenomenon.

Finally, it is important to emphasize that the presented approach to highlight the areas potentially prone to patch formation is based on counting the number of days during which the finite-time compressibility exceeds the level for clustering. This is, strictly speaking, only a necessary condition for an actual patch formation to occur. If the days with over-threshold values of finite-time compressibility are interspersed with days when this quantity is lower, the emerging patch may simply drift out of the region in question and no substantial increase in the concentration occurs. This feature may limit the possibilities to detect the presence of intense clustering of surface floats in some of the indicated areas from *in situ* experiments or remote measurements. Also, a detectable (or potentially dangerous) increase in the concentrations only occurs if the background concentrations are high enough. This feature calls for further research into pathways of contaminants and potentially dangerous substances in the surface layer from their release spots (river mouths, wastewater releases) to the areas of likely patch formation.

## Acknowledgements

This study was supported by the Estonian Science Foundation (Grant No. 9125), targeted financing by the Estonian Ministry of Education and Research (Grant SF0140007s11), and by the European Union through support of the European Regional Development Fund to the Mobilitas project MTT63 and Centre of Excellence in Non-linear Studies. AG is grateful to the support program for international doctoral studies in Estonia DoRa.

## References

Akan, C., Tejada-Martinez, A.E., Grosch, C.E., Martinat, G., 2013. Scalar transport in large-eddy simulation of Langmuir turbulence in shallow water. *Cont. Shelf Res.* 55, 1–16.

Aldredge, A.L., Cowles, T.J., MacIntyre, S., Rines, J.E.B., Donaghay, P.L., Greenlaw, C.F., Holliday, D.V., Deksheniaks, M.M., Sullivan, J.M., Zaneveld, J.R.V., 2002.

Occurrence and mechanisms of formation of a dramatic thin layer of marine snow in a shallow Pacific fjord. *Mar. Ecol. Prog. Ser.* 233, 1–12.

Andrejev, O., Sokolov, A., 1989. Numerical modelling of the water dynamics and passive pollutant transport in the Neva inlet. *Meteorol. Hydrol.* 12, 75–85 (in Russian).

Andrejev, O., Sokolov, A., 1990. 3D baroclinic hydrodynamic model and its applications to Skagerrak circulation modelling. In: *Proceedings 17th Conference of the Baltic Oceanographers*. Norrköping, Sweden, pp. 38–46.

Andrejev, O., Myrberg, K., Alenius, P., Lundberg, P.A., 2004. Mean circulation and water exchange in the Gulf of Finland – a study based on three dimensional modelling. *Boreal Environ. Res.* 9 (1), 1–16.

Andrejev, O., Sokolov, A., Soomere, T., Värvi, R., Viikmäe, B., 2010. The use of high-resolution bathymetry for circulation modelling in the Gulf of Finland. *Estonian J. Eng.* 16, 187–210.

Andrejev, O., Soomere, T., Sokolov, A., Myrberg, K., 2011. The role of spatial resolution of a three-dimensional hydrodynamic model for marine transport risk assessment. *Oceanologia* 53, 309–334.

Averbukh, E., Kurkina, O., Kurkin, A., Soomere, T., 2014. Edge-wave-driven durable variations in the thickness of the surfactant film and concentration of surface floats. *Phys. Lett. A* 378, 53–58.

Bergström, S., Carlsson, B., 1994. River runoff to the Baltic Sea: 1950–1990. *Ambio* 23, 280–287.

Brentnall, S.J., Richards, K.J., Brindley, J., Murphy, E., 2003. Plankton patchiness and its effect on larger-scale productivity. *J. Plankton Res.* 25, 121–140.

Burchard, H., Bolding, K., Villarreal, M.R., 2004. Three-dimensional modelling of estuarine turbidity maxima in a tidal estuary. *Ocean Dyn.* 54, 250–265.

Burchard, H., Floeser, G., Staneva, J.V., Badewien, T.H., Riethmueller, R., 2008. Impact of density gradients on net sediment transport into the Wadden Sea. *J. Phys. Oceanogr.* 38, 566–587.

Calil, P.H.R., Richards, K.J., 2010. Transient upwelling hot spots in the oligotrophic North Pacific. *J. Geophys. Res. Oceans* 115, C02003.

Chelton, D.B., Gaube, P., Schlax, M.G., Early, J.J., Samelson, R.M., 2011. The influence of nonlinear mesoscale eddies on near-surface oceanic chlorophyll. *Science* 334, 328–332.

de Vries, P., Döös, K., 2001. Calculating Lagrangian trajectories using time-dependent velocity fields. *J. Atmos. Oceanic Technol.* 18, 1092–1101.

Dethleff, D., Kempema, E.W., Koch, R., Chubarenko, I., 2009. On the helical flow of Langmuir circulation – approaching the process of suspension freezing. *Cold Reg. Sci. Technol.* 56, 50–57.

Döös, K., 1995. Inter-ocean exchange of water masses. *J. Geophys. Res. Oceans* 100, C13499–C13514.

Falkovich, G., Gawedzki, K., Vergassola, M., 2001. Particles and fields in fluid turbulence. *Rev. Mod. Phys.* 73, 913–975.

Fennel, W., Radtke, H., Schmidt, M., Neumann, T., 2010. Transient upwelling in the central Baltic Sea. *Cont. Shelf Res.* 30, 2015–2026.

Giudici, A., Soomere, T., 2013. Identification of coastal areas of frequent patch formation from velocity fields. *J. Coast. Res. Special Issue* 65, 231–236.

Giudici, A., Kalda, J., Soomere, T., 2012. On the compressibility of surface currents in the Gulf of Finland, the Baltic Sea. In: *Proceedings of the IEEE/OES Baltic 2012 International Symposium “Ocean: Past, Present and Future, Climate Change Research, Ocean Observation & Advanced Technologies for Regional Sustainability” (May 8–11, Klaipėda, Lithuania)*. IEEE Conference Publications, p. 8. doi: <http://dx.doi.org/10.1109/BALTIC.2012.6249178>.

Granskog, M., Kaartokallio, H., Kuosa, H., Thomas, D., Ehn, J., Sonninen, E., 2005. Scales of horizontal patchiness in chlorophylla, chemical and physical properties of landfast sea ice in the Gulf of Finland (Baltic Sea). *Polar Biol.* 28 (4), 276–283.

Gruber, N., Lachkar, Z., Frenzel, H., Marchesiello, P., Münnich, M., McWilliams, J.C., Nagai, T., Plattner, G.-K., 2011. Eddy-induced reduction of biological production in eastern boundary upwelling systems. *Nature Geosci.* 4, 787–792.

Grünbaum, D., 2012. The logic of ecological patchiness. *Interface Focus* 2, 150–155.

Höglund, A., Meier, H.E.M., Broman, B., Kriezi, E., 2009. Validation and correction of regionalised ERA-40 wind fields over the Baltic Sea using the Rossby Centre Atmosphere Model RCA3.0. *Rapport Oceanografi No. 97*. Norrköping, Sweden: Swedish Meteorological and Hydrological Institute.

Holthuijsen, L.H., 2007. *Waves in Oceanic and Coastal Waters*. Cambridge University Press, p. 387.

Kachel, M.J., 2008. Particularly sensitive sea areas: the IMO's role in protecting vulnerable marine areas. *Hamburg Studies on Maritime Affairs*, vol. 13, Springer, Berlin, p. 376.

Kahr, M., 1983. Phytoplankton patchiness generated by long internal waves – a model. *Mar. Ecol. Prog. Ser.* 10, 111–117.

Kalda, J., Soomere, T., Giudici, A., 2014. On the finite-time compressibility of the surface currents in the Gulf of Finland, the Baltic Sea. *J. Mar. Syst.* 129, 56–65.

Kononen, K., Nömmann, S., Hansen, G., Hansen, R., Breuel, G., Gupalo, E.N., 1992. Spatial heterogeneity and dynamics of vernal phytoplankton species in the Baltic Sea in April–May 1986. *J. Plankton Res.* 14, 107–125.

Lee, D.K., Niiler, N., 2010. Influence of warm SST anomalies formed in the eastern Pacific subduction zone on recent El Niño events. *J. Mar. Res.* 68, 459–477.

Leichter, J.J., Deane, G.B., Stokes, M.D., 2005. Spatial and temporal variability of internal wave forcing on a coral reef. *J. Phys. Oceanogr.* 35, 1945–1962.

Lennert-Cody, C.E., Franks, P.J.S., 2002. Fluorescence patches in high-frequency internal waves. *Mar. Ecol. Prog. Ser.* 235, 29–42.

Leppäranta, M., Myrberg, K., 2009. *Physical Oceanography of the Baltic Sea*. Springer, Chichester, UK, p. 378.

- Levin, S., 1994. Patchiness in marine and terrestrial systems: from individuals to populations. *Philos. Trans. R. Soc. Lond. A* B343, 99–103.
- Levin, L.A., Boesch, D.F., Covich, A., Dahm, C.N., Erseus, C., Ewel, K.C., et al., 2001. The function of marine critical transition zones and the importance of sediment biodiversity. *Ecosystems* 4, 430–451.
- Lu, X., Soomere, T., Stanev, E.V., Murawski, J., 2012. Identification of the environmentally safe fairway in the South-Western Baltic Sea and Kattegat. *Ocean Dyn.* 62, 815–829.
- Meier, H.E.M., 2007. Modeling the pathways and ages of inflowing salt- and freshwater in the Baltic Sea. *Estuarine Coast. Shelf Sci.* 74, 610–627.
- Meier, H.E.M., Döscher, R., Faxén, T., 2003. A multiprocessor coupled ice-ocean model for the Baltic Sea: application to salt inflow. *J. Geophys. Res. – Oceans* 108 (C8), 32–73.
- Murawski, J., Woge Nielsen, J., 2013. Applications of an oil drift and fate model for fairway design. In: Soomere, T., Quak, E. (Eds.), *Preventive Methods for Coastal Protection: Towards the Use of Ocean Dynamics For Pollution Control*. Springer, Cham, pp. 367–415.
- Myrberg, K., Andrejev, O., 2003. Main upwelling regions in the Baltic Sea – a statistical analysis based on three-dimensional modelling. *Boreal Environ. Res.* 8, 97–112.
- Myrberg, K., Soomere, T., 2013. The Gulf of Finland, its hydrography and circulation dynamics. In: Soomere, T., Quak, E. (Eds.), *Preventive Methods for Coastal Protection: Towards the Use of Ocean Dynamics for Pollution Control*. Springer, Cham, pp. 181–222.
- Abraham, E.R., 1998. The generation of plankton patchiness by turbulent stirring. *Nature* 391, 577–580.
- Pichel, W.G., Churnside, J.H., Veenstra, T.S., Foley, D.G., Friedman, K.S., Brainard, R.E., Nicoll, J.B., Zheng, Q., Clemente-Colon, P., 2007. Marine debris collects within the North Pacific subtropical convergence zone. *Mar. Pollut. Bull.* 54, 1207–1211.
- Powell, T.M., Okubo, A., 1994. Turbulence, diffusion and patchiness in the sea. *Philos. Trans. R. Soc. Lond. A* B 343 (1303), 11–18.
- Samuelsen, A., Hjøllø, S.S., Johannessen, J.A., Patel, R., 2012. Particle aggregation at the edges of anticyclonic eddies and implications for distribution of biomass. *Ocean Sci.* 8, 389–400.
- Samuelsson, P., Jones, C.G., Willén, U., Ullerstig, A., Gollvik, S., Hansson, U., Jansson, C., Kjellström, E., Nikulin, G., Wyser, K., 2011. The Rossby centre regional climate model RCA3: model description and performance. *Tellus* 63A, 4–23.
- Soomere, T., Delpeche, N., Viikmäe, B., Quak, E., Meier, H.E.M., Döös, K., 2011. Patterns of current-induced transport in the surface layer of the Gulf of Finland. *Boreal Environ. Res.* 16 (Suppl. A), 49–63.
- Soomere, T., Döös, K., Lehmann, A., Meier, H.E.M., Murawski, J., Myrberg, K., Stanev, E., 2014. The potential of current- and wind-driven transport for environmental management of the Baltic Sea. *Ambio* 43, 94–104.
- Strass, V.H., 1992. Chlorophyll patchiness caused by mesoscale upwelling at fronts. *Deep Sea Res. A* 39, 75–96.
- Thorpe, S.A., 2009. Spreading of floating particles by Langmuir circulation. *Mar. Pollut. Bull.* 58, 1787–1791.
- Viikmäe, B., Soomere, T., Viidebaum, M., Berezovski, A., 2010. Temporal scales for transport patterns in the Gulf of Finland. *Est. J. Eng.* 16, 211–227.
- Viikmäe, B., Torsvik, T., Soomere, T., 2013. Impact of horizontal eddy-diffusivity on Lagrangian statistics for coastal pollution from a major marine fairway. *Ocean Dyn.* 63, 589–597.
- Vucelja, M., Falkovich, G., Fouxon, I., 2007. Clustering of matter in waves and currents. *Phys. Rev. E* 75, Art. No. 065301.



## Paper V

**Giudici A.**, Soomere T. 2014. On the possibility of spontaneous patch formation in the Gulf of Finland. In: *IEEE/OES Symposium "Measuring and Modeling of Multi-scale Interactions in the Marine Environment," 26–29 May 2014 Tallinn, Estonia*. Proceedings. IEEE, accepted, ISBN: 978-1-4799-5707-1



# On the possibility of spontaneous patch formation in the Gulf of Finland

A. Giudici, T. Soomere

Institute of Cybernetics at Tallinn University of Technology, Akadeemia tee 21, 12618 Tallinn, Estonia

**Abstract**—We address a novel option to identify areas of spontaneous patch formation using the concept of finite-time compressibility (FTC) of surface velocity fields. This concept makes it possible to systematically account for the correlations of convergence of surface velocity fields and the underlying Lagrangian transport in the surface layer. Areas with high levels of FTC naturally arise if a transient localized convergence area (e.g. downwelling) moves synchronously with the surface current. We evaluate the FTC levels in the Gulf of Finland by means of tracking changes to the geometry of a large set of triplets of passively advected water parcels by surface currents extracted from 3D simulations for the period 1987–1991 using the OAS model with a spatial resolution of 1 nautical mile. The focus is on seasonal variations of areas in which the FTC regularly exceeds the threshold for clusterization of surface floats in ideal Kraichnan flows. Six such areas are located along the coast and roughly coincide with frequent downwelling areas whereas three are located in the central region of the gulf. The areas near the southern coast of the gulf and at the entrance to the Neva Bight are present all year round whereas other areas only emerge during certain seasons.

## I. INTRODUCTION

Under normal conditions, the sea surface layer is extremely heterogeneous across a broad range of spatial and temporal scales. The underlying ecosystems may be deeply influenced by variations of any of the natural biogeochemical variables or substances of anthropogenic origin. Such variations in concentrations, referred to as patches [1,2], may impact the ecosystem in a positive or negative way. Negative impact is often associated with factors of anthropogenic origin and substances released into the environment through e.g. dredging, dumping, aquafarming or discharge of (micro)plastic, chemicals or pollutants.

An important role in the formation of such patches of floating substances may play three-dimensional motions (in which water parcels may dive) underlying the two-dimensional surface layer that hosts lighter floats, films or substances that are locked in this layer by other constraints [3]. Surface velocity fields of such systems may often host long-living convergence areas. Items and substances that are either floating on the sea surface or are locked in the surface layer (e.g. radioactive substances in a thin layer of fresher water, [4]) tend to gather in such areas. This property can be quantified in terms of the classical notion of compressibility of a velocity field [5] (called flow compressibility below). Such an increase in the concentration is usually relatively modest as surface currents are not necessarily correlated with the convergence field and thus tend to carry the emerging patch

away from the convergence region. The concentration, however, may explosively accelerate if the flow compressibility exceeds a certain threshold, after which rapid and spontaneous clustering of floats may start [5]. This process may naturally happen when the convergence field and the underlying current are correlated during a longer time interval; for example, when an area of intense convergence moves synchronously with the Lagrangian transport of the gradually forming patch [6]. Therefore, an analysis of the history of correlation (finite-time correlations) is necessary to identify such phenomenon rather than looking at a sequence of instantaneous correlations of convergence and Lagrangian transport.

We explore a simple method for identification of such areas of natural increase in the concentration of items on sea surface by means of the recently developed measure of finite-time compressibility (FTC, [7,8]). As we are interested in the possibilities of spontaneous patch generation in realistic conditions, we evaluate the FTC levels in the Gulf of Finland, the Baltic Sea, using only surface velocity fields. This is done by tracking changes to the geometry of a large set of triplets of water parcels that are passively advected by surface currents. This water body often hosts downwelling [9–11] and has been shown to frequently host regions of high FTC [8]. These areas are generally prone to changes in concentrations of floating matter and the associated patch-formation process in the surface layer. With this measure, we illustrate the presence and seasonal variability within the years 1987–1991 of single regions in which the FTC often exceeds the threshold for clusterization of surface floats in ideal Kraichnan flows [12].

Recent studies [7,8] have demonstrated the existence of spots with very high instantaneous values of FTC in semi-enclosed sea areas as the Gulf of Finland. Similarly to [12], we focus here on the areas where such high values may regularly occur in a longer time scale. Our goal is to highlight the areas where the phenomenon of such spontaneous increase in surface concentrations is frequent, that is, frequently hosting values of FTC that exceed a certain important threshold. The areas are the most likely candidates for rapid and spontaneous patch formation.

We use precomputed velocity fields and certain easily computable quantities for this task. The focus is on seasonal variations of areas in which the FTC regularly exceeds the threshold for clusterization of surface floats in ideal Kraichnan flows.



Figure 1. Location scheme of the Baltic Sea and the test area Gulf of Finland.

## II. METHODS AND DATA

### 1. Quantification of finite-time compressibility

The concept of FTC and its interrelations with the classical compressibility of a medium and with flow compressibility (of surface velocity field) have been extensively described in [7,8] and we present here only the most important aspects. The classical notion of flow compressibility employs the (Helmholtz) decomposition of velocity fields into their solenoidal (with zero divergence) and potential (with zero curl) components. Flow compressibility  $C_C$  is the relative weight of the potential component and thus is a normalized quantity that substantially differs from the notion of divergence. This definition ignores the history of the velocity field. In many occasions, though, long-term interrelations of the divergence (or flow compressibility) field and Lagrangian transport of the parcels of the medium are decisive [6]. The FTC provides an option to account for the interplay of these two drivers by integrating in some sense their joint impact over a certain (finite-time) section of their history.

Theoretically, it is possible to start from the 3D velocity fields, to split them into solenoidal and potential components, and to analyze these components. This process, however, is not straightforward and, given the approximate nature and relatively low spatio-temporal resolution of numerically simulated velocity fields, may contain extensive uncertainties. For this reason we employ a definition of FTC that relies on the tracking of changes to certain elements of the sea surface that are formed by triplets of water parcels (Fig. 2) that are

locked at the sea surface and passively advected by horizontal components of surface currents [7,8]. The finite-time compressibility of each point of the sea surface is evaluated semi-locally, by observing the relative changes in the geometrical properties of these surface elements during a certain time interval (Fig. 2).

To evaluate this measure, we calculate the ratio of the relative changes  $dS_i$  of the surface area of these elements  $S_i$  over the similar changes to their edges. The relative change of the area  $S_i$  of such an element over one time step is  $dS_i = (S_i - S_{i-1})/S_i$ . The relative changes to the squared lengths of two of its edges  $A_i$  and  $B_i$  (Fig. 2) are  $dA_i = (A_i^2 - A_{i-1}^2)/A_i^2$  and  $dB_i = (B_i^2 - B_{i-1}^2)/B_i^2$ . The approximate values of FTC over a certain time interval are calculated as follows [7]:

$$C_{FTC} = \frac{2dS_{rms}}{dA_{rms} + dB_{rms}}, \quad (1)$$

where  $dS_{rms}$ ,  $dA_{rms}$ ,  $dB_{rms}$  stand for the root mean square of the instantaneous values of  $dS_i$ ,  $dA_i$  and  $dB_i$  over the time interval during which the motion of the element is tracked. The resulting values of  $C_{FTC}$ , although related to the initial location of the element, actually characterize the motions over a certain wider sea area. This method of calculations implicitly involve a time scale over which  $dS_{rms}$  etc. are calculated and that has the meaning of correlation length accounted for in the calculations.

As mentioned above, spontaneous patch generation is most likely if the classical flow compressibility exceeds a certain threshold, over which clustering phenomenon of surface floats may occur. For the idealized Kraichnan flows such a clustering is expected if the classical flow compressibility exceeds the value  $C_C = 0.5$  [13]. For such flows the relationship between the classical flow compressibility  $C_C$  and  $C_{FTC}$  has been obtained in [7]:

$$C_{FTC}^2 = \frac{2C_C}{2C_C + 1}, \quad (2)$$

Equation (2) confirms that these two measures behave

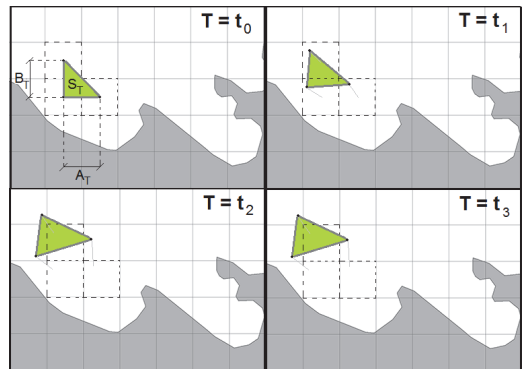


Figure 2. Triplets of simulated floating particles used to calculate Finite-Time Compressibility.

similarly (e.g., they simultaneously tend to zero) but their single values are normally different. They only coincide at  $C_C = C_{FTC} \approx 0.781$ .

## 2. Numerical setup

The surface 2D velocity fields used in this paper are derived from simulations of the hydrodynamic model OAAS (see [14–16] and references therein) with a spatial resolution of 1 nautical mile and a vertical resolution of 1 m (except for the uppermost layer that is 2 m thick). The OAAS model is specifically designed for simulation of ocean circulation in basins with complicated geometry such as the Gulf of Finland [14]. The model run, the velocities from which are used for this study, was forced with the river runoff data from [17] and meteorological data from a regionalization of the ERA-40 re-analysis over Europe with a spatial horizontal resolution of 25 km [18,19]. The model was run for the interior of the Gulf of Finland to the east of longitude 23°27' E. At this boundary, the OAAS model uses 3D information about hydrographic and hydrodynamic fields calculated using the RCO model [20] for the entire Baltic Sea [16]. The modeled velocity data cover the entire Gulf of Finland for 1987–1991, with a temporal resolution of 3 hours.

The calculations employ 2D horizontal velocity components at sea surface for a certain sea area and a longer time interval  $[START_{TOT}, END_{TOT}]$  with a temporal resolution of the available velocity fields  $SIM_{Step}$ . (Fig. 3) One fluid parcel then positioned at the center of each wet grid cell of the circulation model and triangular elements are composed from these as indicated in Fig. 2. As the OAAS model uses regular rectangular grid with an almost equal step along latitudes and longitudes [16,21], the selected parcels are uniformly distributed over the study area.

The interval  $[START_{TOT}, END_{TOT}]$  is divided into time windows with an equal length of  $SIM_{Length}$ , over which the motion of the selected parcels is tracked (cf. [22]). In essence, this parameter indicates the time over which the possible correlation between the local properties of flow convergence and underlying Lagrangian transport are tracked accounted for.

There exist many technologies for building Lagrangian trajectories from precomputed velocity data. The methods that work with relatively low temporal resolution of the data (e.g., TRACMASS, [23,24]) or methods that are applied in environments with strong gradients [25] use internal interpolation of the trajectories within the time step  $SIM_{Step}$  of velocity data and/or higher-order numerical schemes for solving the advection of selected parcels. As several key statistical properties of the resulting sets of trajectories of passively advected parcels on the sea surface have been shown to be almost invariant with respect to variations in the method of their calculation [26] we use the simplest first order Euler method (with a step  $SIM_{Step}$ ) to construct the trajectories.

The quantities  $dS_i$ ,  $dA_i$  and  $dB_i$  are evaluated for each time step of the saved velocity data according to the stencil

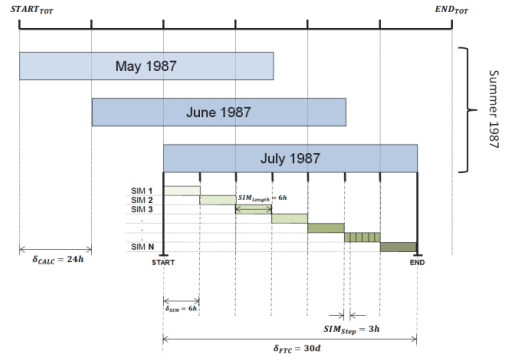


Figure 3. Calculation scheme for season-long batches.

shown in Fig. 2. From these instantaneous values, the quantities at the right-hand side of Eq. (1)  $dS_{rms}$ ,  $dA_{rms}$  and  $dB_{rms}$  are evaluated for each triangular element and the set of used times instants within the time window  $SIM_{Length}$ . The product of each calculation over a time window for the entire set of elements is a spatial distribution (map) of  $C_{FTC}$ , similar to those described in [8]. For simplicity, these distributions are called instantaneous maps of in this paper (Fig. 4).

The calculations involve several adjustable parameters. The key quantities, to be chosen properly to highlight phenomena with specific time scales, are the batch length  $\delta_{FTC}$  and  $SIM_{Length}$ . In this paper they are chosen as 30 days and 6 hours, respectively, in order to highlight phenomena on a seasonal scale. A discussion of the reasonable choice of these parameters in the Gulf of Finland is presented in [27] in the context of semi-persistent patterns of Lagrangian transport.

The resulting maps are grouped together in so-called season-long batches. In this paper we consider batches corresponding to a calendar map (“June”, “July”) with a length of 1 month (Fig. 3). As our focus is on the spontaneous increase in surface concentrations, we identify pixel-wise the cases when  $C_{FTC}$  exceeds the critical threshold of  $\sqrt{1/2}$  for the clustering phenomenon in each instantaneous map. Doing so is similar to the peak-over-threshold approach often used

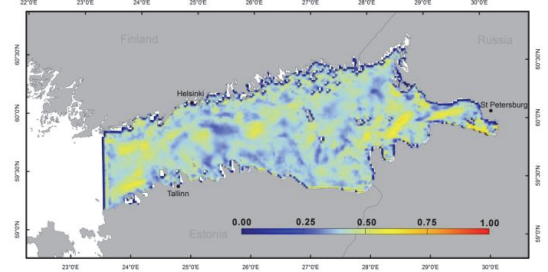


Figure 4. An instantaneous FTC map calculated for 01 March 1987 with  $SIM_{Length} = 24$  hours.

elsewhere in physical oceanography (e.g., [28]) and in extreme value analysis [29]. For each batch and pixel (wet grid cell of the circulation model) we count next how many times the values of  $C_{FTC}$  exceeded this threshold in all maps belonging to this batch. This algorithm produces a map of the count (equivalently, the frequency of occurrence) of over-threshold values of  $C_{FTC}$  during single months.

Variations in the properties of Lagrangian transport in the study area usually have no distinguishable pattern on monthly scale but reveal clear seasonal patterns [26,30]. To properly reproduce the reaction of the FTC on seasonal variations of the driving forces, we rely the seasonal course of wave heights in the Gulf of Finland [31] and choose the following representation of seasons: calm spring-summer season: May, June and July; transitional autumn season: August, September October; windy autumn-winter season: November, December, January; transitional spring season: February, March, April. For each season, we count pixel-wise for each wet grid point how many times the instantaneous values of  $C_{FTC}$  have exceeded the clusterization threshold. This procedure is equivalent to simple averaging of the number of over-threshold values of  $C_{FTC}$  in instantaneous FTC maps within each season in the sense of the above definition.

Similar counts for the entire five-year interval 1987–1991 were recently analyzed from the viewpoint of the existence of single areas where the over-threshold  $C_{FTC}$  values often occur in all seasons using types and spatio-temporal resolutions of the ocean model [7,8,12]. This analysis resulted nine distinct areas of where high values of  $C_{FTC}$  may regularly occur (Fig. 5).

Two such areas were found near the northern coast of the gulf and four areas near the southern coast of the gulf,

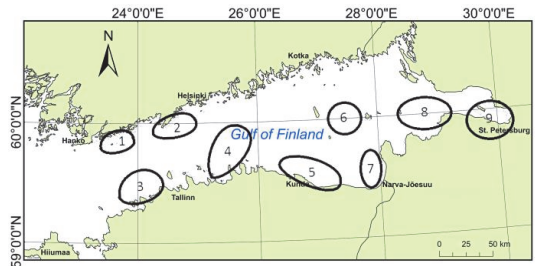


Figure 5. Location scheme of regions where over-threshold values of  $C_{FTC}$  often occur in the Gulf of Finland in 1987–1991.

spanning across all its relatively wide part. One area was identified at the entrance to the Neva Bight where the runoff of River Neva merges with the cyclonic circulation in the gulf [10]. Somewhat surprisingly, one such area was found in the middle of the widest part of the gulf. The area near Saint Petersburg is probably not realistic as the circulation model evidently had insufficient resolution to replicate the flow properties in this region.

### III. RESULTS

The described areas not only reveal extensive pattern of seasonal variations (Fig. 6) but also some interesting features that were smoothed out when considering the entire five-year time interval. We do not discuss here area 9 in the immediate vicinity of Saint Petersburg because it is located in a region where the OAAS model is probably not capable of adequately representing the flow field.

First of all, all areas where the count of over-threshold values exceeds about 10% of the time in a particular season

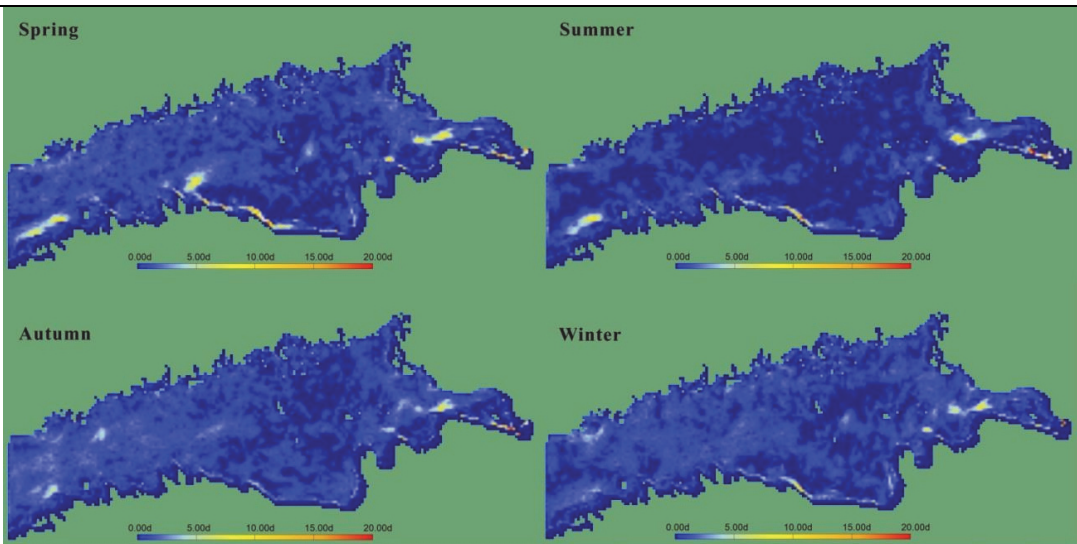


Figure 6. Maps of the average count of the over-threshold FTC values for season-long batches.

are much more concentrated in single seasons. Several areas are clearly present only in a specific season: area 4 in spring and area 2 in autumn. Moreover, areas 1 and 2 near the northern coast are relatively weak and thus spontaneous patch generation is not generally unlikely in their locations. Area 6 is distinguishable in spring and winter and thus may be to some extent related to the presence of ice cover.

Other areas are evident in most of seasons. Among these, the number of over-threshold counts in area 3 at the southern coast of the gulf near its entrance is very large in spring and summer but much smaller in autumn and almost zero in winter. This count in area 7 in Narva Bay also substantially varies in different seasons but the area itself has an almost constant size and location. Similarly, this count in the elongated and quite narrow area 5 that stretches over almost 100 km long segment of the north-eastern coast of Estonia varies almost three times in different season but the area itself almost does not vary. The most persistent in all seasons is a relatively large area 8 in the eastern gulf. The permanent presence of large number of over-threshold values of  $C_{FTC}$  in this region is characteristic also to earlier simulations [12] and apparently is a long-term feature of the dynamics of the Gulf of Finland.

The schematic presentation of the seasonal presence areas in question (Fig. 7) in different years confirms that some areas (e.g., areas 3 or 8) are present in almost all seasons (except in autumn for area 3) of the five-year interval in question. The most frequent presence is found for the spring season and the most fragmentary for the summer season. This difference may reflect the seasonal variations of the directional structure of winds (and also distribution of downwelling areas) in the Gulf of Finland [11] but no clearly defined relationship seems to exist.

It is to be expected that using a longer duration of the time windows reduce the count of over-threshold values of FTC. This feature evidently reflects the loss of correlation between the convergence field and the underlying Lagrangian transport of the emerging patch after some time

#### IV. DISCUSSION

The performed analysis of seasonal variations of the frequency of occurrence of over-threshold values of the finite-time compressibility of surface flows highlights three areas where such values are not only frequent but occur almost all-year round. Specifically, the nearshore of the southern coast of the entrance to the Gulf of Finland, an almost 100 km long segment of the north-eastern coast of Estonia and the easternmost part of the Gulf of Finland near the entrance to the Neva Bight apparently are the most likely regions of spontaneous increase in the concentrations of various floats on the sea surface and substances locked in the uppermost layer of the sea.

The first two are located in regions that often host downwelling [9]. During strong downwelling events water parcels systematically sink into deeper layers whereas lighter

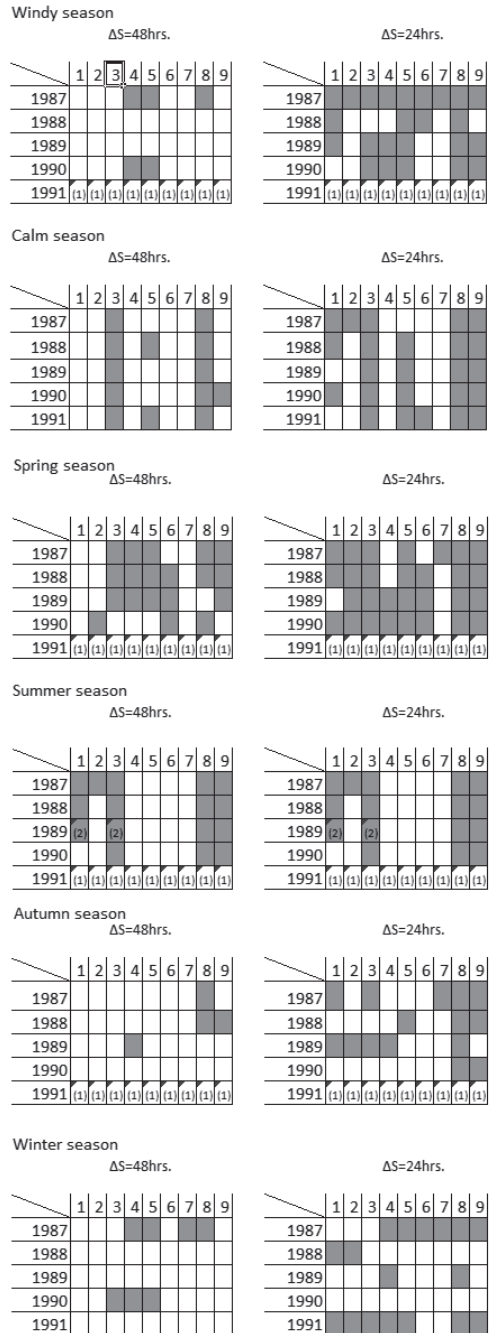


Figure 7. The presence of areas with often occurring over-threshold values of FTC in different seasons in the Gulf of Finland. (1) Data not available.

additives (debris, microplastic, oil spills, polluted or nutrient-rich fresh water from rivers) stay at the surface. Therefore, this process naturally leads to an increase in the concentration of additives. The areas in question are natural candidates for spontaneous patch formation. Also, the area at the entrance to the Neva Bight where the runoff of River Neva merges with the cyclonic circulation in the gulf [10] naturally hosts frequent convergence zones that may be at times synchronized with the surface currents.

The frequency of occurrence of high values of finite-time compressibility is quite sensitive with respect to the time interval during which the correlation of the convergence and Lagrangian transport is calculated. The presented material suggests that this correlation substantially weakens already within about two days. The temporal resolution of the velocity data used in this study (3 hours) is insufficient for a detailed analysis of the sensitivity of the results with respect to the correlation length. However, such a study is highly desirable as it would shed much more light to the structure of flow fields in the selected areas.

#### ACKNOWLEDGMENT

This study was supported by the Estonian Science Foundation (grant no. 9125), targeted financing by the Estonian Ministry of Education and Research (grant SF0140007s11), and by the European Union through support of the European Regional Development Fund to the Mobilitas project MTT63 and Centre of Excellence in Non-linear Studies. AG is grateful to the support program for international doctoral studies in Estonia DoRa.

#### REFERENCES

- [1] S.J. Bretnall, K.J. Brindley, and E. Murphy, "Plankton patchiness and its effect on larger scale productivity," *J. Plankton Res.*, vol. 25, pp. 121-140, 2003.
- [2] K. Kononen, S. Nömmann, G. Hansen, R. Hansen, G. Breuel, and E.N. Gupalo, "Spatial heterogeneity and dynamics of vernal phytoplankton in the Baltic Sea in April-May 1986," *J. Plankton Res.*, vol. 14, pp. 107-125, 1992.
- [3] D.K. Lee and N. Niiler, "Influence of warm SST anomalies formed in the eastern Pacific subduction zone on recent El Nino events," *J. Mar. Res.*, vol. 68, pp. 459-477, 2010.
- [4] R. Periañez, "A particle-tracking model for simulating pollutant dispersion in the Strait of Gibraltar," *Mar. Pollut. Bull.*, vol. 49, pp. 613-623, 2004.
- [5] G. Falkovich, K. Gawedzki, and M. Vergassola, "Particles and fields in fluid turbulence," *Rev. Mod. Phys.*, vol. 73, pp. 913-975, 2001.
- [6] A. Samuelsen, S.S. Hjøllo, J.A. Johannessen, and R. Patel, "Particle aggregation at the edges of anticyclonic eddies and implications for distribution of biomass," *Ocean Sci.*, vol. 8(3), pp. 389-400, 2012.
- [7] A. Giudici, J. Kalda, and T. Soomere, "On the compressibility of the surface currents in the Gulf of Finland, the Baltic Sea," in *Proceedings of the IEE/OES Baltic 2012 International Symposium "Ocean: Past, Present and Future. Climate Change Research, Ocean Observation & Advanced Technologies for Regional Sustainability."* IEEE Conference Publications, 8 pp. doi: 10.1109/BALTIC.2012.6249178
- [8] J. Kalda, T. Soomere, and A. Giudici, "On the finite-time compressibility of the surface currents in the Gulf of Finland, the Baltic Sea," *J. Mar. Syst.*, vol. 129, pp. 56-65, 2014.
- [9] K. Myrberg and O. Andrejev, "Main upwelling regions in the Baltic Sea - A statistical analysis based on three-dimensional modelling," *Boreal Environ. Res.*, vol. 8(2), pp. 97-112, 2003.
- [10] M. Leppäranta and K. Myrberg, *Physical Oceanography of the Baltic Sea*, Chichester, UK: Springer, 2009, 378 pp.
- [11] A. Lehmann and K. Myrberg, "Upwelling in the Baltic sea - a review," *J. Mar. Syst.*, vol. 74(Suppl. 1), pp. S3-S12, 2008.
- [12] A. Giudici and T. Soomere, "Finite-time compressibility as an agent of frequent spontaneous patch formation in the surface layer: a case study for the Gulf of Finland, the Baltic Sea," submitted to *Mar. Pollut. Bull.*, 2014.
- [13] M. Vucelja, G. Falkovich, and I. Fouxon, "Clustering of matter in waves and currents," *Phys. Rev. E*, vol. 75, art. no. 065301, 2007.
- [14] O. Andrejev and A. Sokolov, "Numerical modeling of the water dynamics and passive pollutant transport in the Neva inlet," *Meteorol. Hydrol.*, vol. 12, pp. 75-85, 1989 (in Russian).
- [15] O. Andrejev, and A. Sokolov, "3D baroclinic hydrodynamic model and its applications to Skagerrak circulation modeling," in *Proc. 17<sup>th</sup> Conference of the Baltic Oceanographers, Norrköping, Sweden, 1990*, pp. 38-46.
- [16] O. Andrejev, A. Sokolov, T. Soomere, and K. Myrberg, "The role of spatial resolution of a three-dimensional hydrodynamic model for marine transport risk assessment," *Oceanologia*, vol. 53, pp. 309-334, 2011.
- [17] S. Bergström and B. Carlsson, "River runoff to the Baltic Sea 1950-1990," *Ambio*, vol. 23, pp. 280-287, 1994.
- [18] A. Höglund, H.E.M. Meier, B. Broman, and E. Kriezī, *Validation and Correction of Regionalised ERA-40 Wind Fields over the Baltic Sea using the Rossby Centre Atmosphere Model RCA3.0*, Rapport Oceanografi vol. 97, Norrköping, Sweden: Swedish Meteorological and Hydrological Institute, 2009.
- [19] P. Samuelsson, C.G. Jones, U. Willén, A. Ullerstig, S. Gollvik, U. Hansson, C. Jansson, E. Kjellström, G. Nikulin, and K. Wyser, "The Rossby Centre Regional Climate Model RCA3: Model description and performance," *Tellus A*, vol. 6, pp. 4-23, 2011.
- [20] H.E.M. Meier, "On the parameterization of mixing in three-dimensional Baltic Sea models," *J. Geophys. Res.-Oceans*, vol. 106, pp. 30,997-31,016, 2001.
- [21] O. Andrejev, A. Sokolov, T. Soomere, R. Värvi, and B. Viikmäe, "The use of high-resolution bathymetry for circulation modeling in the Gulf of Finland," *Estonian J. Eng.*, vol. 16, pp. 187-210, 2010.
- [22] T. Soomere, K. Döös, A. Lehmann, H.E.M. Meier, J. Murawski, K. Myrberg, and E. Stanev, "The potential of current- and wind-driven transport for environmental management of the Baltic Sea," *Ambio*, vol. 43, pp. 94-104, 2014.
- [23] K. Döös, "Inter-ocean exchange of water masses," *J. Geophys. Res.-Oceans*, vol. 100, pp. C13,499-C13,514, 1995.
- [24] P. de Vries and K. Döös, "Calculating Lagrangian trajectories using time-dependent velocity fields," *Atmos. Oceanic Technol.*, vol. 18, pp. 1092-1101, 2001.
- [25] U. Gräwe, E. Deleersnijder, S.H. Ali Muttaqi Shah, and A.W. Heemink, "Why the Euler scheme in particle tracking is not enough: The shallow-sea pycnocline test case," *Ocean Dyn.*, vol. 62(4), pp. 501-514, 2012.
- [26] B. Viikmäe, T. Torsvik, and T. Soomere, "Impact of horizontal eddy-diffusivity on Lagrangian statistics for coastal pollution from a major marine fairway," *Ocean Dyn.*, vol. 63, pp. 589-597, 2013.
- [27] T. Soomere, N. Delpeche, B. Viikmäe, E. Quak, H.E.M. Meier, and K. Döös, "Patterns of current-induced transport in the surface layer of the Gulf of Finland," *Boreal Environ. Res.*, vol. 16 (Suppl. A), pp. 49-63, 2011.
- [28] L.H. Holthuijsen, *Waves in Oceanic and Coastal Waters*, Cambridge University Press, 2007, 387 pp.
- [29] A. Arns, T. Wahl, I.D. Haigh, J. Jensen, and C. Pattiaratchi, "Estimating extreme water level probabilities: A comparison of the direct methods and recommendations for best practice," *Coast. Eng.*, vol. 81, pp. 51-66, 2013.
- [30] B. Viikmäe and T. Soomere, "Spatial pattern of hits to the nearshore from a major marine highway in the Gulf of Finland," *J. Mar. Syst.*, vol. 129, pp. 106-117, 2014.
- [31] I. Zaitseva-Pärnaste, *Wave Climate and its Decadal Changes in the Baltic Sea Derived from Visual Observations*. PhD thesis. Tallinn University of Technology, 2013, 173 pp.

**DISSERTATIONS DEFENDED AT  
TALLINN UNIVERSITY OF TECHNOLOGY ON  
CIVIL ENGINEERING**

1. **Heino Mölder.** Cycle of Investigations to Improve the Efficiency and Reliability of Activated Sludge Process in Sewage Treatment Plants. 1992.
2. **Stellian Grabko.** Structure and Properties of Oil-Shale Portland Cement Concrete. 1993.
3. **Kent Arvidsson.** Analysis of Interacting Systems of Shear Walls, Coupled Shear Walls and Frames in Multi-Storey Buildings. 1996.
4. **Andrus Aavik.** Methodical Basis for the Evaluation of Pavement Structural Strength in Estonian Pavement Management System (EPMS). 2003.
5. **Priit Vilba.** Unstiffened Welded Thin-Walled Metal Girder under Uniform Loading. 2003.
6. **Irene Lill.** Evaluation of Labour Management Strategies in Construction. 2004.
7. **Juhan Idnurm.** Discrete Analysis of Cable-Supported Bridges. 2004.
8. **Arvo Iital.** Monitoring of Surface Water Quality in Small Agricultural Watersheds. Methodology and Optimization of Monitoring Network. 2005.
9. **Liis Sipelgas.** Application of Satellite Data for Monitoring the Marine Environment. 2006.
10. **Ott Koppel.** Infrastruktuuri arvestus vertikaalselt integreeritud raudtee-ettevõtja korral: hinnakujunduse aspekt (Eesti peamise raudtee-ettevõtja näitel). 2006.
11. **Targo Kalamees.** Hygrothermal Criteria for Design and Simulation of Buildings. 2006.
12. **Raido Puust.** Probabilistic Leak Detection in Pipe Networks Using the SCEM-UA Algorithm. 2007.
13. **Sergei Zub.** Combined Treatment of Sulfate-Rich Molasses Wastewater from Yeast Industry. Technology Optimization. 2007.
14. **Alvina Reihan.** Analysis of Long-Term River Runoff Trends and Climate Change Impact on Water Resources in Estonia. 2008.
15. **Ain Valdmann.** On the Coastal Zone Management of the City of Tallinn under Natural and Anthropogenic Pressure. 2008.
16. **Ira Didenkulova.** Long Wave Dynamics in the Coastal Zone. 2008.
17. **Alvar Toode.** DHW Consumption, Consumption Profiles and Their Influence on Dimensioning of a District Heating Network. 2008.
18. **Annely Kuu.** Biological Diversity of Agricultural Soils in Estonia. 2008.

19. **Andres Tolli.** Hiina konteinerveod läbi Eesti Venemaale ja Hiinasse tagasisaadetavate tühjade konteinerite arvu vähendamise võimalused. 2008.
20. **Heiki Onton.** Investigation of the Causes of Deterioration of Old Reinforced Concrete Constructions and Possibilities of Their Restoration. 2008.
21. **Harri Moora.** Life Cycle Assessment as a Decision Support Tool for System optimisation – the Case of Waste Management in Estonia. 2009.
22. **Andres Kask.** Lithohydrodynamic Processes in the Tallinn Bay Area. 2009.
23. **Loreta Kelpšaitė.** Changing Properties of Wind Waves and Vessel Wakes on the Eastern Coast of the Baltic Sea. 2009.
24. **Dmitry Kurennoy.** Analysis of the Properties of Fast Ferry Wakes in the Context of Coastal Management. 2009.
25. **Egon Kivi.** Structural Behavior of Cable-Stayed Suspension Bridge Structure. 2009.
26. **Madis Ratassepp.** Wave Scattering at Discontinuities in Plates and Pipes. 2010.
27. **Tiia Pedusaar.** Management of Lake Ülemiste, a Drinking Water Reservoir. 2010.
28. **Karin Pachel.** Water Resources, Sustainable Use and Integrated Management in Estonia. 2010.
29. **Andrus Räämet.** Spatio-Temporal Variability of the Baltic Sea Wave Fields. 2010.
30. **Alar Just.** Structural Fire Design of Timber Frame Assemblies Insulated by Glass Wool and Covered by Gypsum Plasterboards. 2010.
31. **Toomas Liiv.** Experimental Analysis of Boundary Layer Dynamics in Plunging Breaking Wave. 2011.
32. **Martti Kiisa.** Discrete Analysis of Single-Pylon Suspension Bridges. 2011.
33. **Ivar Annus.** Development of Accelerating Pipe Flow Starting from Rest. 2011.
34. **Emlyn D.Q. Witt.** Risk Transfer and Construction Project Delivery Efficiency – Implications for Public Private Partnerships. 2012.
35. **Oxana Kurkina.** Nonlinear Dynamics of Internal Gravity Waves in Shallow Seas. 2012.
36. **Allan Hani.** Investigation of Energy Efficiency in Buildings and HVAC Systems. 2012.
37. **Tiina Hain.** Characteristics of Portland Cements for Sulfate and Weather Resistant Concrete. 2012.
38. **Dmitri Loginov.** Autonomous Design Systems (ADS) in HVAC Field. Synergetics-Based Approach. 2012.
39. **Kati Kõrbe Kaare.** Performance Measurement for the Road Network: Conceptual Approach and Technologies for Estonia. 2013.

40. **Viktorija Voronova**. Assessment of Environmental Impacts of Landfilling and Alternatives for Management of Municipal Solid Waste. 2013.
41. **Joonas Vaabel**. Hydraulic Power Capacity of Water Supply Systems. 2013.
42. **Inga Zaitseva-Pärnaste**. Wave Climate and its Decadal Changes in the Baltic Sea Derived from Visual Observations. 2013.
43. **Bert Viikmäe**. Optimising Fairways in the Gulf of Finland Using Patterns of Surface Currents. 2014.
44. **Raili Niine**. Population Equivalence Based Discharge Criteria of Wastewater Treatment Plants in Estonia. 2014.
45. **Marika Eik**. Orientation of Short Steel Fibres in Concrete: Measuring and Modelling. 2014.
46. **Maija Viška**. Sediment Transport Patterns Along the Eastern Coasts of the Baltic Sea. 2014.
47. **Jana Pöldnurk**. Integrated Economic and Environmental Impact Assessment and Optimisation of the Municipal Waste Management Model in Rural Area by Case of Harju County Municipalities in Estonia. 2014.
48. **Nicole Delpeche-Ellmann**. Circulation Patterns in the Gulf of Finland Applied to Environmental Management of Marine Protected Areas. 2014.